



School of Technology and Architecture
Department of Architecture and Urbanism

Origami Surfaces for Kinetic Architecture

Filipa Peres Frangolho Crespo Osório

Thesis specially presented for the fulfillment of the degree of
Doctor in Architecture and Urbanism
Specialization in Digital Architecture

Supervisor:

Doctor Alexandra Paio, Assistant Professor
ISTAR-IUL, ISCTE-Instituto Universitário de Lisboa

Co-supervisor:

Doctor Sancho Oliveira, Assistant Professor
IT-IUL, ISCTE-Instituto Universitário de Lisboa

December, 2019

IUL School of Technology and Architecture
Department of Architecture and Urbanism

Origami Surfaces for Kinetic Architecture

Filipa Peres Frangolho Crespo Osório

Thesis specially presented for the fulfillment of the degree of
Doctor in Architecture and Urbanism
Specialization in Digital Architecture

Jury:

Doctor João Pedro Sampaio Xavier, Associate Professor,
Faculdade de Arquitectura da Universidade do Porto
Doctor Gonçalo Lencastre Torres de Castro Henriques, Assistant Professor,
Faculdade de Arquitectura e Urbanismo da Universidade Federal do Rio de Janeiro
Doctor Pedro Miguel Gomes Januário, Assistant Professor,
Faculdade de Arquitectura da Universidade de Lisboa
Doctor Vasco Nuno da Ponte Moreira Rato, Associate Professor),
Departamento de Arquitectura e Urbanismo do ISCTE-Instituto Universitário de Lisboa

December, 2019

Agradecimentos/Acknowledgements

Em primeiro lugar, quero deixar um enorme agradecimento aos meus orientadores pelo apoio, discussão construtiva e orientação ao longo dos cinco anos de desenvolvimento da tese.

Um agradecimento muito especial aos Professores e colegas da Università di Roma - La Sapienza, nomeadamente Graziano Mario Valenti, Andrea Casale, Michele Calvano e Maurizio Giodice, pelos encontros anuais nas Summer Schools, recheados de conversas sobre origami, e pela amizade desenvolvida.

Este agradecimento estende-se aos restantes professores e tutores das Summer Schools de 2015 e 2016 especificamente Sancho Oliveira, Antonino Ciuro, Davide Ventura, Luca Frogheri, Ramona Feriozzi, João Sousa, João Ventura, Maria João Oliveira, Susana Neves e Vasco Craveiro Costa. E também aos alunos com quem desenvolvemos os protótipos, nomeadamente Bogdan-Dragos Munteanu, Caterina Reccia, Francesca Mangione, Gabriele Firmiano, Gea Ferrone, Gianluca Rodonò, Marco Cuccuru, Marco Guarany, Maurizio Giodice, Onur Hic, Roberta Pari, Sahand Riahi, Vipul Verma, Daniela Nóbrega, Denton Fredrickson, Federico Galizi, Inês Caetano, Ioanna Mitropoulou, Jan Broux, Maia Zheliazkova, Maria Bezzone, Pedro Januário e Ronaldo Barbosa.

Quero agradecer também à Professora Eliana Pinho e ao Professor Vasco Rato pela amizade e disponibilidade para discutir a tese, clarificar dúvidas e discutir opções, o que levou a um enriquecimento da dissertação. Na mesma linha quero deixar um agradecimento aos arquitectos e colegas de Doutoramento João Ventura e Filipe Brandão.

Agradeço à Lucy Adamson pela celeridade e sugestões na revisão de Inglês.

Quero agradecer também à Arquitecta Emília Lima por me ter despertado para a existência do origami, através dos seus inúmeros presentes na minha infância, que levaram a uma “quase” obsessiva necessidade de dobrar papel.

Um enorme obrigado à Doutora Arquitecta Maria José Bento e ao Arquitecto Pedro Mendonça pela oportunidade de leccionar na Lisbon School of Design, e mais ainda pela compreensão, apoio e sugestões nos últimos 5 anos, sem eles não teria sido possível concluir a tese.

Aos grandes amigos que acompanharam a tese de muito perto e estiveram presentes e disponíveis para a construção do protótipo final do KOS, João Sousa e Vasco Craveiro Costa um gigante obrigado!

Muito obrigada à Maria João Oliveira, parceira permanente nesta aventura! Obrigada pela amizade, pela partilha de trabalho, desesperos e alegrias. Pela sua típica honestidade e companheirismo em todo este percurso.

Um enorme agradecimento à Sílvia Costa e à Joana Fonseca, por serem como são, pela amizade e presença durante os últimos 20 anos, e especialmente pelo interesse e força que me deram para o desenvolvimento e conclusão da tese.

Quero agradecer ao Gustavo Cachudo, companheiro perfeito, pela incrível paciência, apoio incondicional e ajuda, especialmente importantes na recta final.

Um profundo agradecimento aos meus pais e irmãos por estarem sempre presentes, acreditarem em mim e apoiarem tudo o que me proponho fazer.

Finalmente gostaria de deixar um agradecimento muito especial a toda a minha família Frangolho e Crespo, e aos amigos, por me fazerem rir e me lembrarem que há vida para além do doutoramento.

Por último, gostaria de agradecer à Fundação para a Ciência e Tecnologia pelo apoio financeiro através da bolsa com referência SFRH/BD/100818/2014, sem o qual não teria sido possível realizar esta investigação.

Contents

Agradecimentos/Acknowledgements	i
Contents	iii
Abstract	vii
Resumo	ix
List of Acronyms and Abbreviations	xi
List of Tables	xiii
List of Equations	xiii
List of Images	xiv
Chapter 01 Introduction	1
1.1 Motivation	4
1.2 Hypothesis of the Thesis, Questions and Objectives	5
1.3 Methodology	7
1.4 Scope	8
1.5 Contributions	10
1.6 Structure of the Thesis	12
Chapter 02 Framework	15
2.1 Kinetic Architecture	17
2.1.1 Definitions	21
Zuk and Clark, 1970	22
Frei Otto, 1971	23
Merchan, 1987	24
Hanaor and Levy, 2001/Hanaor, 2009	26
Gantes, 2001	28
Pellegrino, 2001	29
Korkmaz, 2004	31
Schumacher, Schaeffer, Vogt, 2010	32
Stevenson, 2011	34
Del Grosso and Basso, 2013	37
Rivas Adrover, 2015	39
2.1.2 Mechanisms	41
Kinematic Joints	42
Simple Mechanisms	45

Pantographic Systems	48
Planar Double Chain Linkages	49
Straight SLEs	49
Angulated SLEs	51
Other possibilities for Double Chain Linkages	56
Hoberman's Iris Dome	56
Pantographic Plates	58
Origami as Spherical Mechanisms	59
Smart Materials as Mechanisms	62
Actuators	64
Control	66
2.2 Origami Geometry and Foldability	67
2.2.1 Origami Geometry	68
2.2.2 Origami Foldability	72
Rigid-Foldability	73
Strategies to Transform Non-Rigidly Folding Vertices	74
Flat-Foldability	77
Strategies to Transform Non-Flat-Foldable Vertices	79
Non-crossing Conditions	81
Origami Tessellations	82
Degree-2 Crease Patterns	84
Degree-4 Crease Patterns	85
Degree-6 Crease Patterns	86
Thick Origami	88
2.2.2 Origami in Architecture	94
2.3 Computational Design	101
2.3.1 Folding Algorithms and Simulators	101
Origami Design	103
Origami Foldability - Final Folded State	103
Origami Foldability - Folding Process	104
Chapter 03 Reaching KOS	107
3.1 Proposed Classifications	110
3.1.1 Demountable and Transportable Structures	111
3.1.2 Kinetic Architecture	114

3.2 Mechanisms	120
3.3 Origami Geometry	125
3.3.1 Crease Patterns	125
Degree-2 Crease Patterns	129
Degree-4 Crease Patterns	133
Degree-6 Crease Patterns	138
3.3.2 Proposed Origami Folding Simulations	145
Folding Simulator for degree-4 Tessellations	147
Folding Simulator for degree-6 Tessellations	157
3.3.3 Origami Thickness	168
3.4 Materials	171
3.5 Analysis of Experiments	176
3.5.1 Experiment 01	179
3.5.2 Experiment 02	187
Experiment 02 – Group A	190
Experiment 02 – Group B	192
Experiment 02 – Group C	194
Experiment 02 – Group D	196
3.5.3 Experiment 03	198
Experiment 03 – Group A	203
Experiment 03 – Group B	205
Experiment 03 – Group C	208
Experiment 03 – Group D	210
Experiment 03 – Group E	213
3.5.4 Conclusions of the Experiments	215
Chapter 04 Workflow and KOS Proof-of-Concept Prototype	219
4.1 Proposed Workflow	221
4.2 Prototype Development	227
4.2.1 Spatial Objectives and Constraints – Step 01	227
4.2.2 Crease Pattern and Digital Simulation – Steps 02 and 03	228
4.2.3 Rigid Materials, Thickness and Structural Testing – Steps 04 and 05	232
4.2.4 Thickness Method and Redesign – Steps 06 and 07	237

4.2.5 Interaction and Kinetic Response – Step 08	239
4.2.6 Mechanical System – Step 09	241
4.2.7 Small-Scale Prototypes for Testing – Steps 10 and 11	243
4.2.8 Design for Fabrication – Step 12	250
4.2.9 Assembly and Testing – Steps 13 and 14	252
4.2.10 Computational Control and Actuators – Steps 15 and 16	256
4.2.11 Final Assembly – Step 17	258
4.3 Evaluation and Results	261
Chapter 05 Conclusions and Future Work	267
5.1 Conclusions	269
5.2 Future Work	276
References	279
Annexes	293

Abstract

Title: Origami Surfaces for Kinetic Architecture

Name: Filipa Peres Frangolho Crespo Osório

PhD: PhD Program in Architecture of Contemporary Metropolitan Territories,
Specialization in Digital Architecture

Supervisor: Doctor Alexandra Paio

Co-Supervisor: Doctor Sancho Oliveira

This thesis departs from the conviction that spaces that can change their formal configuration through movement may endow buildings of bigger versatility. Through kinetic architecture may be possible to generate adaptable buildings able to respond to different functional solicitations in terms of the used spaces.

The research proposes the exploration of rigidly folding origami surfaces as the means to materialize reconfigurable spaces through motion. This specific kind of tessellated surfaces are the result of the transformation of a flat element, without any special structural skill, into a self-supporting element through folds in the material, which gives them the aptitude to undertake various configurations depending on the crease pattern design and well-defined rules for folding according to rigid kinematics.

The research follows a methodology based on multidisciplinary, practical experiments supported on digital tools for formal exploration and simulation. The developed experiments allow to propose a workflow, from concept to fabrication, of kinetic structures made through rigidly folding regular origami surfaces. The workflow is a step-by-step process that allows to take a logical path which passes through the main involved areas, namely origami geometry and parameterization, materials and digital fabrication and mechanisms and control.

The investigation demonstrates that rigidly folding origami surfaces can be used as dynamic structures to materialize reconfigurable spaces at different scales and also that the use of pantographic systems as a mechanism associated to specific parts of the origami surface permits the achievement of

synchronized motion and possibility of locking the structure at specific stages of the folding.

Keywords: Kinetic Architecture; Rigid Origami Surfaces; Parametric Design; Pantographic Systems; Digital Fabrication; Workflow.

Resumo

Título: Origami Surfaces for Kinetic Architecture

Nome: Filipa Peres Frangolho Crespo Osório

Doutoramento: Arquitetura dos Territórios Metropolitanos Contemporâneos
Especialidade em Arquitectura Digital

Orientadora: Prof. Doutora Arquitecta Alexandra Paio

Co-Orientador: Prof. Doutor Sancho Oliveira

A presente tese parte da convicção de que os espaços que são capazes de mudar a sua configuração formal através de movimento podem dotar os edifícios de maior versatilidade. Através da arquitectura cinética pode ser possível a geração de edifícios adaptáveis, capazes de responder a diferentes solicitações funcionais, em termos do espaço utilizado.

Esta investigação propõe a exploração de superfícies de origami, dobráveis de forma rígida, como meio de materialização de espaços reconfiguráveis através de movimento. Este tipo de superfícies tesselladas são o resultado da transformação de um elemento plano, sem capacidade estrutural que, através de dobras no material, ganha propriedades de auto-suporte. Dependendo do padrão de dobragem e segundo regras de dobragem bem definidas de acordo com uma cinemática rígida, a superfície ganha a capacidade de assumir diferentes configurações.

A investigação segue uma metodologia baseada em experiências práticas e multidisciplinares apoiada em ferramentas digitais para a exploração formal e simulação. Através das experiências desenvolvidas é proposto um processo de trabalho, desde a conceptualização à construção, de estruturas cinéticas baseadas em superfícies dobráveis de origami rígido de padrão regular. O processo de trabalho proposto corresponde a um procedimento passo-a-passo que permite seguir um percurso lógico que atravessa as principais áreas envolvidas, nomeadamente geometria do origami e parametrização, materiais e fabricação digital e ainda mecanismos e controle.

A dissertação demonstra que as superfícies de origami dobradas de forma rígida podem ser utilizadas como estruturas dinâmicas para materializar

espaços reconfiguráveis a diferentes escalas. Demonstra ainda que a utilização de sistemas pantográficos como mecanismos associados a partes específicas da superfície permite atingir um movimento sincronizado e a possibilidade de bloquear o movimento em estados específicos da dobragem.

Palavras Chave: Arquitectura Cinética; Superfícies em Origami Rígido; Desenho Paramétrico; Sistemas Pantográficos; Fabricação Digital; Processo de Desenho.

List of Acronyms and Abbreviations

2D – Two-Dimensional

3D – Three-Dimensional

AI - Artificial Intelligence

ASM – Axis Shift Method

BYU – Brigham Young University, Provo, Utah, United States of America

CEAAD – Curso de Estudos Avançados em Arquitectura Digital (Advanced
Studies Course in Digital Architecture)

CNC – Computer Numeric Control

CP – Crease Pattern

DDC – Developable Double Corrugation

DLG – Double Layer Grid

DoF – Degrees of Freedom

FEA – Finite Element Analysis

FPM – Foldable Programmable Matter

GH – Grasshopper

ILS – Institute for the Lightweight Structures, Stuttgart, Germany

ISCTE-IUL – Instituto Universitário de Lisboa, Lisbon, Portugal

KOS – Kinetic Origami Surface

MDF – Medium-Density Fiberboard

MEMS – Micro-Electro-Mechanical Systems

MFM – Membrane Folds Method

MFT – Metalized Folding Textile

MIT – Massachusetts Institute of Technology, Cambridge, Massachusetts,
United States of America

MoMa – Museum of Modern Art

MSE – Mutually Supported Elements

MV – Mountain-Valley

NASA – National Aeronautics and Space Administration, Washington, D.C.,
United States of America

OPT – Offset Panel Technique

OSB – Oriented Strand Board

OSME – Origami in Science, Mathematics and Education

PoC – Proof-of-Concept

PP – Polypropilene

PVC – Polyvinyl Chloride

SLE – Scissor-Like Elements

SLG – Single Layer Grid

SMA – Shape Memory Alloys

SS – Summer School

STEM – Storable Tubular Extendible Member

TPM – Tapered Panels Method

VGS – Variable Geometry Structures

List of Tables

Number	Caption	Page
2.1	Comparison between Fox, Moloney and Schumacher for Ways and Means in kinetic architecture	42
3.1	Summary table for kinetic architecture structures with examples	119
3.2	Kinematic joints	121
3.3	Mechanisms comparison table for architectural applications	122
3.4	Mechanisms for kinetic architecture	123
3.5	Resch Family CPs with Degree-6 and Degree-5 vertices	126
3.6	Maekawa and Kawasaki Theorems for degree-2 vertices	129
3.7	Patterns with degree 2 vertices analysis	132
3.8	Maekawa- Justin and Kawasaki-Justin Theorems for degree-4 vertices	133
3.9	Patterns with degree-4 vertices analysis on type of vertices and folding forms	136
3.10	Patterns with degree-4 vertices analysis	137
3.11	Maekawa- Justin and Kawasaki-Justin Theorems for degree-6 vertices	138
3.12	Relation between α , β and Ω angles for Regular Yoshimura CPs and generated cylinders	142
3.13	Patterns with degree-6 vertices analysis	143
3.14	Patterns with degree 6 vertices analysis	144
3.15	Criteria for the analysis of experiments	177
4.1	Values for area and free height for the folding states	240
4.2	Summary of mechanisms described in Section 3.2	241

List of Equations

Number	Caption	Page
2.1	Equation by You and Chen, 2012	52
2.2	Maekawa-Justin Theorem	78
2.3	Kawasaki-Justin Theorem	78
3.1	Proposed Equation for the relation between angles for regular Yoshimura	142

List of Figures

Number	Caption	Page
1.1	Main areas involved on the investigation and their connections	8
1.2	Diagram of the followed methodology	8
1.3	Structure of the Thesis	13
2.1	Contributions for the classification of kinetic structures	18
2.2	Distinction between demountable/transportable structures vs. kinetic structures	19
2.3	Kinetic typologies in architecture	20
2.4	Relation between Fox and Yeh's categories and demountable/transportable structures vs. kinetic structures	21
2.5	Relation between Korkmaz's categories and demountable/transportable structures vs. kinetic structures	21
2.6	Classification by Zuk and Clark, 1970	22
2.7	Otto's matrix for the opening and closing of roof membranes, ILS 1971	23
2.8	Otto's classification, 1971	24
2.9	Merchan's classification, 1987	25
2.10	Hanaor's classification, 2009	27
2.11	Hanaor's classification, 2009, updated from Hanaor and Levy's, 2001	28
2.12	Gantes' classification, 2001	29
2.13	Pellegrino's listing, 2001	30
2.14	Korkmaz's classification, 2004	31
2.15	Movements of rigid building elements	32
2.16	Movements of deformable building elements	33
2.17	Schumacher's et al. typologies of movement	33
2.18	Stevenson's classification, 2011	35
2.19	Morphological aspects and transformation strategies in kinetic architectural structures	36
2.20	Del Grosso and Basso's classification, 2013	38
2.21	Rivas Adrover's classification, 2015	40
2.22	Lower pair joints	43
2.23	Hinges examples	43
2.24	Two examples of higher pair joints	44

2.25	Rope winches	46
2.26	Bands and belts	46
2.27	Gears	46
2.28	Rods	46
2.29	Translation bearings	47
2.30	Rotary bearings	47
2.31	Rotary bearings	47
2.32	Straight and angulated scissor-like elements	48
2.33	Double chain linkage composed of four translational SLEs and two deployment positions	49
2.34	Double chain linkage composed of three polar SLEs and two deployment positions	50
2.35	Closed loop with zero mobility formed by eight polar SLEs	50
2.36	Intermediate ties as proposed by You and Chen, 2012.	50
2.37	Double chain linkage composed of three basic angulated SLEs and two deployment positions	51
2.38	Hoberman sphere	52
2.39	Expanding helicoid	52
2.40	Geometric relations for the design of generalized angulated SLEs	52
2.41	Addition of non-symmetric SLEs using symmetry	53
2.42	Closed double chain linkage with parallelograms between SLEs in grey and light grey	53
2.43	Connection of non-similar SLEs	53
2.44	Addition of planar closed loop chains	54
2.45	Yar et al.'s proposed kite and anti-kite units	54
2.46	Deployment of kite loop structures	55
2.47	Deployment of anti-kite loop structures	55
2.48	Iris dome, MoMa, 1994	56
2.49	Iris dome, Hanover, 2000	56
2.50	Winter Olympics Arch, Salt Lake City, USA, 2002	56
2.51	Relations for drawing and assembly of angulated SLEs for curved surfaces	57
2.52	Hoberman's proposal for the cover of the structures with rigid panels	57
2.53	Kassabian et al.'s proposal for the covering of pantographic structures, 1999	58

2.54	Model of planar expandable structure with rigid plates as pantographs	59
2.55	Cardboard model of non-circular plate structure	59
2.56	Cardboard model of the assembly of modular hexagonal structures	59
2.57	Comparison between 4R spherical linkage and an Origami vertex with four creases	59
2.58	Spherical mechanisms in open chains	60
2.59	Spherical mechanisms in networks	61
2.60	Crease patterns of the bases	61
2.61	Kinematic equivalents for each base	61
2.62	Hygroscope, Achim Menges in collaboration with Steffen Reichert, Centre Pompidou, Paris, 2012	63
2.63	Bloom, Doris Sung, M&A Gallery, Silver Lake, CA, 2011	63
2.64	Axioms 1 and 2	69
2.65	Axioms 3 and 4	70
2.66	Axiom 5	70
2.67	Axioms 6 and 7	71
2.68	Examples of rigid and flat foldability	73
2.69	Three examples of the diagram method	74
2.70	Two strategies proposed by Tachi to transform a closed vertex	75
2.71	Corner gadget	76
2.72	Triple parallel gadget	76
2.73	Level shifters	76
2.74	Graphic representation of the two-colourability rule	77
2.75	Graphic representation of Maekawa-Justin and Kawasaki-Justin Theorems	78
2.76	Example of a vertex that obeys the three rules but is not flat foldable	78
2.77	(a) Disk-packing example (b) Induced triangles and quadrilaterals	79
2.78	Example of quadrilaterals that are good flat quads, a convex one and another with a re-entrant angle	80
2.79	Justin's non-crossing conditions	81
2.80	Huffman's design with circles	82
2.81	Square twisted tessellation	82
2.82	The Resch Family patterns	83

2.83	Degree-2 CPs	84
2.84	Degree-4 CPs	86
2.85	Degree-6 CPs	87
2.86	Hoberman's method for symmetric degree-4 vertices. Three states of folding	88
2.87	Trautz and Kunstler example	89
2.88	One example of the non-generality of the Slidable Hinges Method	89
2.89	Tapered panels method	90
2.90	Existing methods for thick origami and proposed offset panel technique by Edmondson et al.	90
2.91	Thickening on both sides of the origami surface. a) Section diagram b) Plane CP c) Folded CP	91
2.92	Deployable ballistic barrier by Seymour et al., 2018	92
2.93	Kinematic diagram for patterns with two degree-4 vertices by Wang et al., 2018	92
2.94	Physical prototype folding sequence by Wang et al., 2018	92
2.95	Joseph Albers playing with Miura-Ori	94
2.96	Origami model from Joseph Albers' course, 1927-28	94
2.97	Origami model from Joseph Albers' course, 1927-28	94
2.98	Groups of origami in architecture	95
2.99	Auxetic Origami	96
2.100	Versus	96
2.101	Al Bahr Towers	97
2.102	Origami Kinetic Sculpture	97
2.103	Tachi's rigid thick origami prototype	98
2.104	Wallbot	98
2.105	Tunable Sound Cloud	99
2.106	Tessel	99
2.107	Ressonant Chamber	99
2.108	Cerebral Hut	99
2.109	Blumen Lumen	99
2.110	Atom Flower 2004	100
2.111	Atom Flower 2005	100

2.112	Oribotics evolution	100
2.113	2007 and 2010 versions	100
2.114	Origami simulators diagram	102
3.1	Relation between the criteria used by each author for the kinetic structures definitions	111
3.2	General proposed classification for demountable/transportable structures	112
3.3	Deployable Structures' proposed classification for demountable/transportable structures	114
3.4	Deployable structures' categories for kinetic structures	115
3.5	Kinetic structures' proposed classification	116
3.6	Schematic description of bar structures	116
3.7	Resch Family CPs, base faces and respective tessellations	127
3.8	Resch Family CPs compression faces	128
3.9	Degree-2 CPs	129
3.10	Degree-2 Vertex	129
3.11	Regular accordion transitional folding state and heights	130
3.12	Maximum height for each degree-2 CP	130
3.13	Simulation of radial accordion pattern, two folding states	130
3.14	Simulation of Yoshimura strip pattern, one folding state	131
3.15	Plan and sections of the folding states of the accordion pattern with irregular MV assignment	131
3.16	Simulation of the helicoidal pattern, three folding states	131
3.17	Typical degree-4 vertex	133
3.18	Degree-4 vertex inflexion examples for $\beta=45^\circ$ and 53°	133
3.19	Degree-4 CPs	135
3.20	Base faces of degree-4 CPs	135
3.21	Two flat foldable vertices with a VMMMM arrangement	138
3.22	Fuse's whirlpool spiral geometric relations	139
3.23	CPs with degree-6 vertices	140
3.24	Examples of folded models and volumes' section	140
3.25	Base faces for degree-6 CPs	141
3.26	Yoshimura vertex inflexion examples for $\beta=15^\circ$ and 30°	141

3.27	Methodology for the development of the simulators	146
3.28	Cluster of degree-4 base faces	147
3.29	Base faces geometry and nomenclature	148
3.30	First step for the definition of the base faces' geometry – GH definition	148
3.31	First step for the definition of the base faces' geometry – graphical representation	149
3.32	Second Step for the definition of the base faces' geometry – graphical representation of two options	149
3.33	Second Step for the definition of the base faces' geometry – GH definition	150
3.34	Third step, folding of the base faces – graphical representation of two options with correspondent circles to define point D	151
3.35	Third step, folding of the base faces – GH definition	151
3.36	Mirrored faces and points for orientation operation. Exemplification with the Miura and quadrilateral meshed patterns	152
3.37	Fourth step, mirrored base faces and columns on the first line of the tessellation – GH definition	152
3.38	Four steps of folding and correspondent circles defined by points DA, AB and moved AB, vectors from centre of the circle	153
3.39	Fifth step, copy of first line of the tessellation through linear or polar copies – GH definition	154
3.40	Examples of base faces for simulations on the four patterns	154
3.41	Four folding states of Miura pattern through D4 simulator	155
3.42	Four folding states of stretched Miura pattern through D4 simulator	155
3.43	Four folding states of irregular Miura pattern through D4 simulator	155
3.44	Four folding states of quadrilateral meshed pattern through D4 simulator	156
3.45	Interface appearance to the user	156
3.46	Cluster of degree-6 base faces	157
3.47	Cluster of degree-6 base faces	158
3.48	Additional base faces for irregular Yoshimura	158
3.49	Definition of points A, B, C and D, faces and mirrored faces	159
3.50	Intersection between circles O1 and O2 to find point D	160
3.51	Surface for regular Yoshimura	161
3.52	Four folding states of regular Yoshimura	161
3.53	Points definition for irregular Yoshimura	162
3.54	Four sets of base faces for irregular Yoshimura	162
3.55	States of folding for each of the four sets of base faces	163

3.56	Folding of first set of base faces	163
3.57	Folding of second set of base faces	163
3.58	Folding of third set of base faces	163
3.59	Folding of fourth set of base faces	163
3.60	Alignment of base faces and copies for irregular Yoshimura surface	164
3.61	Folding of irregular Yoshimura surface	164
3.62	Definition of points A, B and C for skewed Yoshimura or double helicoidal	165
3.63	Definition of base faces for skewed Yoshimura or double helicoidal	165
3.64	Surface for skewed Yoshimura or double helicoidal	166
3.65	Folding of double helicoidal	166
3.66	Folding of skewed Yoshimura	167
3.67	Relationship between every step of the folding simulator for degree-6 CPs	167
3.68	Dimension alteration through axis shift method	168
3.69	Valley folding restriction through axis shift method	168
3.70	Miura tessellation with plywood rigid faces using the axis shift method	169
3.71	Yoshimura tessellation with plywood rigid faces using the axis shift method	169
3.72	Gaps for valley folds and rotation movement on hinges on the membrane folds method	170
3.73	Materials' Families	172
3.74	Young's Modulus and Density	173
3.75	Young's Modulus and Strength	173
3.76	Fracture Toughness and Strength	174
3.77	Fracture Toughness and Strength	174
3.78	Spider scheme	178
3.79	Fujimoto and Nishiwaki paper model	179
3.80	Miura with regular tessellation paper models	179
3.81	Miura with irregular tessellation paper model	180
3.82	Intended geometry with non-parametric simulation	180
3.83	Digital fabrication, faces under compression and fastening of the sheets	181
3.84	Mechanical system movement scheme	182

3.85	Steps of motion	183
3.86	Summary of grades for the evaluation of experiment 01	185
3.87	Workflow for experiment 01	186
3.88	Workflow for experiment 02	188
3.89	CPs geometry and movement schemes	188
3.90	Final prototypes	189
3.91	Group A - prototype and movement scheme	190
3.92	Summary of grades for the evaluation of experiment 02 - A	191
3.93	Group B - prototype and movement scheme	192
3.94	Summary of grades for the evaluation of experiment 02 - B	193
3.95	Group C - prototype and movement scheme	194
3.96	Summary of grades for the evaluation of experiment 02 - C	195
3.97	Group D - prototype and movement scheme	196
3.98	Summary of grades for the evaluation of experiment 02 - D	197
3.99	Workflow for experiment 03	198
3.100	INPLAY's digital simulations	199
3.101	Movement schemes	200
3.102	Experiment 03, Group C - Plywood Stitching	202
3.103	Final prototypes	202
3.104	Group A, prototype and movement scheme	203
3.105	Summary of grades for the evaluation of experiment 03 - A	205
3.106	Group B - prototype and movement scheme	205
3.107	Summary of grades for the evaluation of experiment 03 - B	207
3.108	Group C - prototype and movement scheme	208
3.109	Summary of grades for the evaluation of experiment 03 - C	210
3.110	Group D - prototype and movement scheme	210
3.111	Summary of grades for the evaluation of experiment 03 - D	212
3.112	Group E - prototype and movement scheme	213
3.113	Summary of grades for the evaluation of experiment 03 - E	215

3.114	Comparison between experiments' analysis	215
4.1	Proposed workflow	222
4.2	Overview of the workflow and location of step 01	227
4.3	Overview of the workflow and location of steps 02 and 03	228
4.4	Choice for CP - step 02	229
4.5	First crease pattern experiment for KOS PoC using the degree-6 simulator – step 03	230
4.6	Crease pattern for KOS PoC	230
4.7	Rigidly folding states simulated for KOS PoC using the degree-6 simulator	231
4.8	Overview of the workflow and location of steps 04 and 05	232
4.9	Van Mises Stresses for KOS PoC 35° folding angle	233
4.10	Van Mises Stresses for KOS PoC 55° folding angle	234
4.11	Van Mises Stresses for KOS PoC 76° folding angle	234
4.12	Utilization for KOS PoC 35° folding angle	235
4.13	Utilization for KOS PoC 55° folding angle	235
4.14	Utilization for KOS PoC 76° folding angle	235
4.15	Displacement for KOS PoC 35° folding angle	236
4.16	Displacement for KOS PoC 55° folding angle	236
4.17	Displacement for KOS PoC 76° folding angle	237
4.18	Overview of the workflow and location of steps 06 and 07	237
4.19	Displacement of faces on an MMVMMV vertex of a thick surface	238
4.20	Redesign of the surface - step07	238
4.21	Overview of the workflow and location of step 08	239
4.22	Movement and its implications on KOS PoC	239
4.23	Area and free height changing values for motion range between 35° and 76°	240
4.24	Overview of the workflow and location of step 09	241
4.25	Lines of similar movement between CP and pantographs	242
4.26	Overview of the workflow and location of steps 10 and 11	243
4.27	Prototype A folding states	244
4.28	Prototype B fabrication pieces	244

4.29	Prototype B assembling of base faces, pantographic system and hinges	245
4.30	Prototype B folded columns	245
4.31	Prototype B detail of a folded vertex	245
4.32	Prototype C pieces for fabrication	246
4.33	Prototype C folding states for scissor elements design	246
4.34	Prototype B pantograph design and scheme attachment to faces	247
4.35	Maximum and minimum folding states with new scissor elements	248
4.36	Relation between folding angles and faces angles	248
4.37	Prototype C assembling	249
4.38	Prototype C assembling	249
4.39	Prototype C folded states	249
4.40	Overview of the workflow and location of step 12	250
4.41	Pieces for fabrication for the final prototype	250
4.42	Faces for the final prototype	251
4.43	Voids for screws and bolts and low relief for piano hinges	251
4.44	Overview of the workflow and location of steps	252
4.45	Faces attached through piano hinges	252
4.46	Assembly of pantograph system	252
4.47	Assembly of pantograph system	253
4.48	Closed structure, two views	253
4.49	Movement tests	253
4.50	SLE collapse	254
4.51	Round foot for ground supporting	254
4.52	Actuator's open and closed positions	255
4.53	Final pantograph pieces	255
4.54	Adjustments to the structure	256
4.55	Overview of the workflow and location of steps 15 and 16	256
4.56	Positioning of the actuators on the structure	257
4.57	Overview of the workflow and location of step	258

4.58	Suspended structure	258
4.59	Movement tests supported on the ground structure	259
4.60	Supported structure, breaking point	260
4.61	Broken bars of the pantographs	260
4.62	Spider scheme for KOS PoC prototype	264

01 | INTRODUCTION

01 | Introduction

“In an evolutionary sense, architecture appears to be going kinetic of necessity, in order to adapt more quickly and efficiently to man’s ever-changing needs.” (Zuk and Clark, 1970, pp.34)

Nowadays society is rightfully demanding, always looking for new and better answers to every problem, with constantly changing wills and needs that have a reflection on spatial requirements. Architecture should be capable of providing solutions that respect the users’ intentions and concerns through design exploration and the use of the available technological options.

This thesis proposes the use of kinetic architecture as a possible way to address society’s demands through reconfigurable spaces. Adaptable spaces allow the same space to shelter different functions with diverse geometrical configuration demands and/or their adaptation to changing conditions.

This idea is not new, in the 60’s and 70’s computation and technology took a leap that found eco in Architecture (Negroponte, 1973). Groups like Archigram, or Cedric Price’s Fun Palace, took this new kind of knowledge and used it in Architecture so spaces could be changed in order to fit the user’s wills and needs as they changed in time. The exponential growth of technology since the 80’s allowed the economic and technological feasibility for kinetic and responsive architecture ideas (Fox and Kemp, 2009).

Also, kinetic elements, as doors, windows or shutters or, the movable walls on the traditional domestic Japanese architecture, have always been used as simple systems to improve the use of the interior space by allowing the control of insulation, privacy and formal configuration of spaces and are nowadays considered essential on any building.

Even though kinetic systems are being used since ever, and with several recent examples, they are not yet an obvious choice for the common architectural practice and seem to have potential for exploration and investigation.

Although kinetic architecture is still not a common choice, experiments are being developed in the academic world, in big scale operable roofs or in smaller scale buildings, such as art installations, scenography or publicity stands. These last kinds of experiments are interesting cases to test kinetic ideas because the scale is often small, and thus more controllable, and usually these types of buildings come with greater freedom for creativity without the constraints of a building that must stand permanently.

The present investigation aims at exploring the potential of kinetic architecture as a possible answer for the transformation of spaces that may respond better to the needs of nowadays society. The research intends to develop a multidisciplinary workflow supported on the digital tools available to the architect today, such as simulation and parametric design, in order to explore a specific kind of foldable structures, rigidly folding origami tessellated surfaces to be used as kinetic structures.

1.1 | Motivation

“The motivation for advanced kinetic architectural systems lies in creating spaces and objects that can physically reconfigure themselves to meet changing needs with an emphasis on the dynamics of architectural space.”
(Fox, 2003, pp. 163)

This investigation is motivated by the opportunity to add to the current kinetic architecture options by proposing the utilization of tessellated surfaces as a specific kind of kinetic structures that can reconfigure themselves for the generation of dynamic spaces.

Tessellated surfaces, particularly rigidly folding origami surfaces, result from the transformation of a flat element, without any special structural ability, into a self-supporting element through folds in the material. These surfaces depart from a planar, rigid material, without elastic properties, that through a tessellated Crease Pattern (CP) acquires the power to grow, shrink and adapt to many configurations. The origami tessellations can transform into simple planar corrugated surfaces or singularly or doubly curved surfaces, in consequence of their CP and specific kinematics. Some of these tessellations can fold through rigid kinematics, where the faces act as rigid planar panels attached to each other through straight hinges.

The belief that this type of surfaces has potential to be used in kinetic architecture is a major motivator for the present investigation. It is intended to demonstrate that rigidly folding origami surfaces can be used as dynamic structures leading to reconfigurable spaces.

It is also a conviction of this investigation that the use of rigidly folding origami surfaces for kinetic architecture is underexplored. Most of the found examples, demonstrate only the use of symmetric modules with a small amount of faces. The suspicion that so much may be found if one looks at origami from the “tessellated surface perspective”, instead of the “module perspective” leads to

the belief that investigating this subject deeper can bring an important contribution to architecture, more specifically to kinetic architecture.

The possibility to use the current parametric design tools, such as Grasshopper for Rhinoceros, for the form-finding process and to test the geometries and folding movement based on rigid kinematics, is another motivator for the investigation. These tools are believed to be helpful for the design and real-time changing and adaptation of the CPs to fold, since they allow for the creation of a set of geometric rules that can fold a determined range of origami models. This way is believed to be possible the definition of the CP that will guide the construction of physical prototypes and used in conjunction with digital fabrication tools.

Finally, another motivator is the possibility to create a multidisciplinary workflow that can consequently order several steps, from concept to construction, passing through the definition of mechanisms, interaction and computational control, making possible a comprehensive investigation, from theory to practice. The workflow is intended to incorporate knowledge from other disciplines besides architecture, such as mathematics, parametric design, mechanics, computation and digital fabrication. The acquired knowledge is to be used in practical case studies which may allow to observe directly issues to correct, help to strategize for subsequent experiments and establish a “way of doing” to be used in the development of rigidly folding origami surfaces to be used in kinetic architecture.

1.2 | Hypothesis of the thesis, Questions and Objectives

From the described motivational context, it seems to be possible to establish several questions for investigation. This thesis tries to solve one main question, from which derived other, more specific, questions. The questions (Q) and corresponding objectives (O) will followingly be enumerated from bigger to smaller. From the determined questions and objectives can be articulated the main hypothesis of the dissertation.

Q1 – Can rigidly folding origami surfaces be used for the creation of adaptable spaces, thus representing a real contribution for kinetic architecture?

Is it possible to establish a way of doing for the conceptualization and construction of such surfaces that includes steps for each involved discipline?

O1 – Utilization of Kinetic Origami Surfaces (KOS) to create foldable surfaces to be used in reconfigurable spaces. This type of surfaces has a very adaptable geometry, with self-supporting abilities, that have the power to

grow, shrink and assume several geometric configurations. Additionally, these surfaces depart from planar materials which make them easy to construct, since each face is simply a 2D polygon.

In that sense this objective intends to develop a comprehensive workflow, from concept to fabrication, that permits the design, construction and action of kinetically reconfigurable rigidly folding origami surfaces. Construction of a Proof-of-Concept prototype as a physical proof of the validity of the workflow and of the utility of such surfaces for kinetic architecture.

Q2 – Origami surfaces are not yet seen as a specific category for kinetic architecture for the wide architecture community.

O2 – Critical analysis of existing kinetic architecture definitions and classifications to find their criteria, points of contact and disagreement, to develop a comprehensive kinetic architecture taxonomy where origami surfaces have a distinct and justified category.

Q3 – How do rigid origami tessellations fold and which serve kinetic architectural purposes? How to predict the formal and structural behaviour of a folding surface as well as its motion path?

O3 – Analysis of a wide *corpus* of existing origami tessellations through literature, physical folding and digital simulation. Utilization of digital simulation for form-finding, folding, kinematic analysis and structural analysis.

Establishment of CPs families through their geometry analysis and assumed configurations while folding. Development of simulation definitions for degree-4 and degree-6 families that allow to change the CP and include their kinematic behaviour, folding process and geometry export for structural analysis simulation.

Q4 – Can the architect be the central player of a multidisciplinary method to develop rigidly folding origami surfaces with thickness? In order to build physical objects, the origami surface cannot be a pure mathematical surface with zero-thickness. Surfaces with thickness may generate geometric problems throughout the folding process that are not perceivable on the kinematic simulations.

O4 – Development of physical architectural prototypes through multidisciplinary teams. Definition of ways of doing, through the analysis of the developed experiments. Analysis of existing strategies to generate thick origami surfaces to understand which are applicable when. Testing the strategies on small scale prototypes as well as on the final prototype.

Q5 – Rigidly folding origami surfaces have specific kinematics that do not oblige for synchronicity during folding and do not have locked states. The inexistence of synchronicity may lead to unpredictable movements by the faces which can provoke instability when using rigidly folding origami surfaces in large scale objects. Additionally, a folding structure must have the ability of being locked at specific stages for static utilization.

O5 – Analysis of existing mechanisms, experimentation on constructed prototypes and demonstration of the validity of the utilization of pantographic systems embedded on specific locations of the surfaces.

From the laid-out Questions and Objectives can be formulated the main hypothesis of this thesis. The dissertation hypothesizes that rigidly folding origami surfaces may be valuable for the utilization by kinetic architecture either in small or large-scale structures. If the architectural object has a large scale it becomes particularly important the possibility of locking folding stages and the generation of a smooth and well synchronised motion that can be achieved through pantographic mechanisms.

The conceptualization, construction and actuation of rigidly folding origami surfaces for kinetic architecture demands for multidisciplinary processes that must include paper modelling, knowledge on origami geometry and the forms into which regular tessellations fold, digital simulation, computational control and fabrication. Therefore, the thesis proposes a comprehensive workflow achieved through physical experiments from concept to construction that combine all the acting areas in order to achieve functional rigid and flat-foldable thick kinetic surfaces.

1.3 | Methodology

The methodology followed by this thesis is based on research followed by practical experimentation and observation for conclusions. It cannot be described through a linear flow were every subject has its bounds completely defined and separated from the others. It is rather a process of interconnection between the four main areas involved (**Figure 1.1**) which are kinetic architecture, origami geometry, materials and digital fabrication and mechanisms and control.

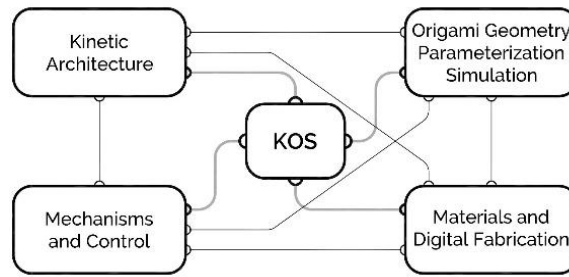


Figure 1. 1.
 Main areas involved on the investigation and their connections

The research on each subject happens at the same time as the others so each one helps to limit the scope of the others, they all inform and feed each other. It is the contribute of each area, all with an equally important role, that shapes the final contribution for Kinetic Origami Surfaces (KOS) and the establishment of the workflow through a cyclic process of researching, understanding, experimenting, as proposed by Schön (1984). The experiments are based on the construction of prototypes for observation and conclusions as defended by Burry and Burry (2012).

The cyclic process and the chronological placement of experiments can be described as shown on the diagram on **Figure 1.2.**

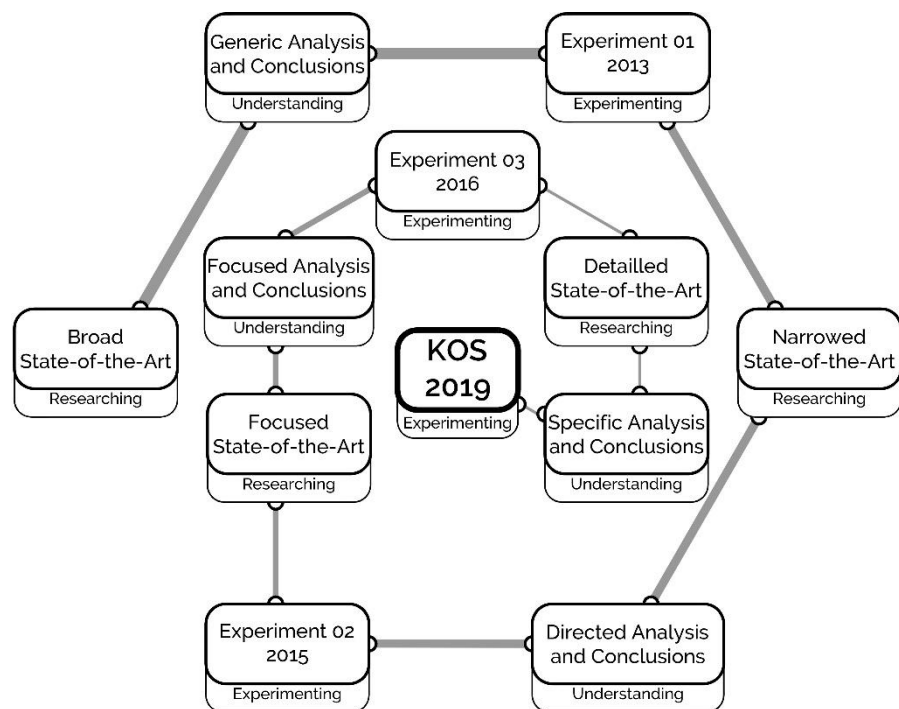


Figure 1. 2.
 Diagram of the followed methodology

The applied methodology focuses on every area at the same time, but it is guided by a progressive top-down approach. First is defined a general

background for kinetics, origami, mechanisms and materials, and from there the focus turns to the specifics of kinetic origami, mechanisms and materials. The thesis starts by trying to understand if rigid origami surfaces can be considered a branch for kinetic architecture from the review of the work by other authors. From there it is tried to determine which experiments have already been made with kinetic origami. The existing experiments along with the state-of-the-art on origami tessellations allow to determine which may serve kinetic architecture. At this point the thesis proposes two algorithms for the folding of rigidly folding regular origami tessellations for degree-4 and degree-6 CPs clusters which are intended to aid in the exploration of origami geometries with regular CPs through parametric tools.

From the state-of-the-art on mechanisms this investigation tries to understand which are most applicable to every kinetic architecture branch and particularly to rigidly folding origami.

Finally, is explored the use of digital fabrication as a way to physically test the geometries along with mechanisms, actuation and control.

This thesis has an heuristic and tangible approach, and in this way, the methodology is guided by experiments along with the theoretical work. The experiments are often done in the context of Summer Schools, which allow for very productive work. In the Summer Schools is possible to bring into the research the opinions of other designers and experts on parametric design, mechanics and computation while the work is being developed.

The method undertaken by the research includes also the writing of papers on international and national conferences, which provides valuable feedback from other researchers, experts on specific areas, and a way of consolidating knowledge and creating intermediary steps for balance and reflexion about the path followed by the research.

1.4 | Scope

The scope of the present research should be defined for each of the four areas involved, which are kinetic architecture, origami geometry, mechanisms and materials.

The **kinetic architecture** categories considered by this thesis are the ones where the architectural structure is able to reconfigure its geometry through movement, generating different formal spaces.

As a definition, it could be said that a structure is considered kinetic, by this thesis, when there are points of the structure, or architectural object, that

change their relative distance to other points of the same structure through the action of mechanisms, which may happen often and during their utilization. Throughout the related literature, different terms are used to refer to architecture and movement and many times different concepts are used as synonyms and the scope of each one gets blurred and confusing.

For the present thesis, alive or transformable architectures that do not use true, physical movement of elements will not be considered, these unconsidered interventions would include alterations in colour and/or light on static architectural elements, without movement or mechanisms.

El Razaz (2010) includes movement in the design phase as a type of static moving architecture, that is buildings that transmit a sense of movement due to their formal aspects, this kind of movement in architecture will not be considered either because there is no movement in a physical sense.

Structures that are movable to different places and settled there without any kind of kinetic mechanism will also be disregarded. As well as modular or incremental architecture, that is often considered dynamic because it allows for flexibility through time and as the needs of the user change. However, and even though there might be travelling of the modules from one location to another, the structure itself does not include movement or mechanisms on its body.

In what relates to **origami geometry** this thesis intends to investigate regular origami tessellations which may fold rigidly.

The thesis does not concern the traditional origami models of animals, flowers, etc. It is not intended to study either curved creased tessellations and tessellations that have overlaps or tucks, since these do not have a rigid behaviour during folding and often block the possibility of continuous movement.

The considered **mechanisms** on this thesis are the ones that might have a direct contribution for kinetic architecture and especially for folding and unfolding rigid origami surfaces.

The analysis on **materials** relates to planar materials that have potential to be used for rigidly folding origami surfaces due to their mechanical properties. These properties are the Young's Modulus and resistance to bending, tension and compression. It will not be an exhaustive analysis on every type of materials.

1.5 | Contributions

The contributions that this thesis intends to offer can be divided into practical and theoretical contributes and are directly related to the objectives defined on **Section 1.2**.

Contribution 1 – is a practical contribute and consists on the development, from concept to fabrication, of a justified and demonstrated workflow that may allow other designers to be able to create functional prototypes by using rigidly folding origami surfaces able to reconfigure themselves through movement. The workflow comprises every step needed for a trustable, functional, rigidly folding surface to be used for kinetic structures. It starts with the analysis of the space where the surface will be used and with the definition of the intended objectives for the surface, regarding geometry and behaviour. From that step is provided the needed knowledge for the choice of the most applicable origami pattern along with the simulation tools for the CP design and folding simulation. Then the workflow has steps for analysis of the stability of the structure, the definition of materials and mechanisms along with the options for control. It ends with the digital fabrication and construction of the kinetic origami surface and has several evaluation points and chances to correct previous steps.

Through this contribution is aimed to prove the possibility of a multidisciplinary investigation applied to architecture, specifically on the development of foldable surfaces capable of full compactness that may be used on new or existing buildings to give them the versatility and ability to better serve their users on a variety of situations and conditions.

Contribution 2 – is a theoretical contribution that encompasses the development of an exhaustive and updated taxonomy for kinetic architecture where origami surfaces are proven to constitute a distinct and defensible category.

Since the developed work allowed also for the determination of a distinction between Kinetic Structures for Architecture and the Demountable and Transportable Structures, it will also be provided a classification for these last ones since it helps understanding the similarities and differences between them.

Contribution 3 – is a theoretical/practical contribution. It has a theoretical part that encompasses the establishment of CPs families regarding their geometry and assumed configurations while folding.

Through this part of the contribution is intended to narrow the choice for CPs applicable to architecture and to flat-foldable rigidly folding surfaces, at the same time that is provided a deep understanding on the implications that the specific design of a CP has on the assumed geometries and folding path.

The practical part of the contribution follows the theoretical one and concerns the elaboration of rigid kinematics simulators for CPs families. The simulators allow for adjustments to the CP on any step of the folding, and also to assess their kinematic behaviour, folding process and geometry export for structural analysis simulation or implementation on 3D models.

With this contribution are provided two simulators, developed on Grasshopper for Rhinoceros, for crease patterns with degree-4 and degree-6 vertices. The simulators are intended to help designers to test quickly the geometry and rigid folding motion of the CPs and to export the generated surfaces to structural analysis simulators.

This way is intended to provide a tool that may save much time on the design process, specifically on the choice of the pattern and its geometric optimization, on the stability analysis and finally as a way to foresee problems with collisions within the surface itself and with surrounding objects and/or buildings.

Contribution 4 – is a practical contribution through the demonstration and analysis of experiments developed by multidisciplinary teams which helped to shape the workflow described on Contribution 1. The experiments followed different paths, different scales and used diverse simulation methods, materials, mechanisms and control. These experiments allowed also to use existing thickness methods, analyse them and draw conclusions.

Through the analysis of experiments on determined criteria are believed to be given important contributes that may guide designers on the choices to develop kinetic foldable surfaces to be used in architecture.

Contribution 5 – is a practical contribution that regards the choice of particular mechanisms to use in rigidly folding origami surfaces. Through this contribution is intended to prove the pertinence of using pantographic systems embedded on the rigidly folding surfaces because both systems have analogous kinematics. Additionally, the pantographic systems allow to control

the folding angles of the surface, introduce synchronicity on the general folding and are able to lock the structure on any folding step.

1.6 | Structure of the Thesis

This dissertation intends to create a smooth and well linked description of the developed research, constantly supported by illustrations and diagrams to better clarify the text. As described in **Section 1.3**, it has a top-down approach. The thesis starts by introducing the reader to the literature review about each of the areas involved (kinetic architecture, origami geometry, mechanisms and control, materials and digital fabrication). It continues with analysis on the laid-out aspects and tries to explain how each area connects to the other until they all fuse in one specific workflow to prototype KOS (**Figure 1.3**).

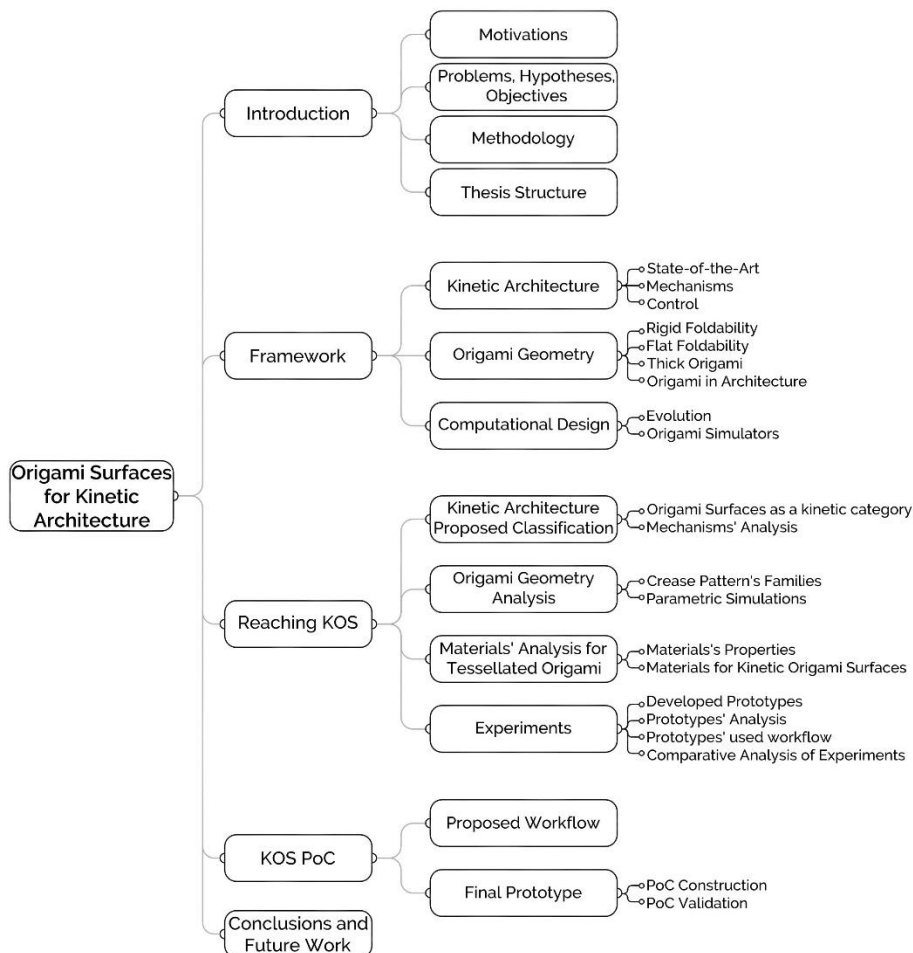


Figure 1.2.
Structure of the Thesis

The first chapter of this thesis introduces the study, describes the main problems that it tries to solve, clarifies the scope and presents the hypotheses and aimed contributions.

Chapter 2 is the framework of the research, a review of the literature on three of the main areas, kinetic architecture, which includes mechanisms, origami geometry, with examples of origami in architecture, and computational design specific for origami folding simulations.

Chapter 3 narrows the scope of the framework through analysis and comparison between key aspects on the main subjects described in the previous chapter.

This chapter introduces the classifications for kinetic architecture and demountable and transportable structures. It also presents the analysis on mechanisms to be used in kinetic architectural structures.

Subsequently, origami geometry is analysed and are determined the CPs families regarding their geometry and assumed configurations while folding. Next are analysed the existing origami simulators and are proposed two rigidly folding simulators for degree-4 and degree-6 CP clusters.

Finally, this chapter describes the analysis on materials to be used for rigidly folding origami surfaces and the developed experiments. The experiments are described, analysed, evaluated and compared, in what respects to the used workflow and criteria evaluation concerning Origami Geometry, Materials and Fabrication, Mechanisms and Control.

Chapter 4 presents the step-by-step workflow, from concept to construction. The validity of the workflow is proven at this chapter through the construction of the KOS PoC prototype which is made with an origami surface that is able to rigidly fold and reconfigure itself synchronously, aided by the utilization of a pantographic system embedded on the surface.

On **Chapter 5** are presented the conclusions and results achieved by the thesis as well as the possible future work.

02 | FRAMEWORK

02 | Framework

2.1 | Kinetic Architecture

“Freedom and flexibility are integral aspects of human existence.”

Kronenburg, 2015, pp. 33

Humankind has always used shelters that could be assembled and disassembled, for example the tents used by nomad cultures as homes or the tents for mobile events such as circuses and fairs. There has been always an interest in transformable and flexible spaces, like the movable interior walls used by Japanese traditional construction, or the well-known *vela* (or *velarium*), inspired by ships' sails and assembled by sailors, to provide sunshade for the audience in theatres and coliseums during the Roman Empire (Zuk and Clark, 1970) (Stevenson, 2011) (Kronenburg, 2015).

After the Industrial Revolution, with the emergence of new materials and the rising of a “pro-machine” culture, kinetic devices started to be used on buildings mainly for sun protection and to allow flexibility in interior partitions, but also on temporary buildings that had to be assembled and disassembled quickly and in different locations (Zuk and Clark, 1970) (Stevenson, 2011).

Even though there are several examples of constructed kinetic devices since the Industrial Revolution, it seems that it was only at the end of the 60's and beginning of the 70's that transformable architecture, and the possibilities that kinetics could offer to static and permanent common buildings, started to be a matter of research and experimentation for architects.

The “Movable Cities” proposed by Archigram and the “Conversation Theory” by Gordon Pask are some of the earliest evidence of the beginning of a new perspective for the possibilities of the “Architecture of Change” (Stevenson, 2011) (Kolarevic, 2015).

Cedric Price, and Nicholas Negroponte and MIT's architecture Machine Group challenged the mainstream notions of architectural processes by using the computational paradigms, including cybernetics, artificial intelligence (AI), and computer science. Their work manifests the use of computational logics with the objective of producing intelligent systems that would develop along with their users, to build a symbiotic relationship between user and system. Cybernetics is the generation of interdependent relationships between user, computer, and space (Ahlquist and Menges, 2011). As Ahlquist and Menges (2011, pp. 11) point out "*Cybernetics advanced the notion of systems theory to address the new existence of the man-machine relationship stimulating the notion of how computers may be utilised to expand (...) the complex*

interrelation of materials parts, and social engagement, shaping form, space and structure".

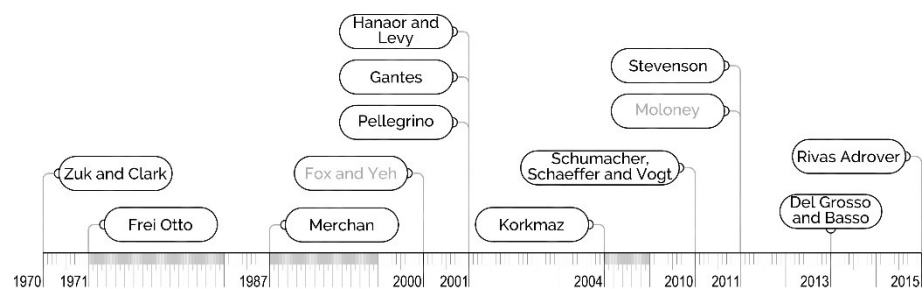
At the same time as these new ideas were finding their way into architecture William Zuk and Roger Clark (1970) published the first book that proposed definitions and fundamentals for architectural design and the application of kinetics. The authors define kinetic architecture as one “*which can adapt to a changing set of pressures which mould form*” (Zuk and Clark 1970, pp. 12)

In the beginning of the 70’s Frei Otto conducted similar research within his Institute for Lightweight Structures, at the University of Stuttgart, which produced annual or bi-annual publications on lightweight deployable structures, convertible roofs and other research themes that are not within the scope of this research.

During the 30 years that followed, kinetic and/or deployable structures continued to be constructed, explored and investigated. Examples relate mainly to retractable roofs for sport facilities, deployable tents for temporary events, collapsible shelters for military purposes or to use in disaster areas, experimentations on flexible interior spaces with movable or sliding walls, deployable structures to be used in space, and kinetic façades like the Institut du Monde Arabe by Jean Nouvel in 1989 (Stevenson, 2011) (Kolarevic, 2015). Before the XXI century, and after Zuk and Clark (1970) and Frei Otto (1971), another important contribution was the one by Carlos Merchan, in 1987.

In **Figure 2.1** are chronologically presented the main contributions over the last 45 years. The authors that provide classifications based on specific types of structures are in black, and the authors that describe more generic, or macro definitions, are in grey.

Figure 2.1.
Contributions for the
classification of
kinetic structures



Kinetic architecture seems to have gained more attention during the present century where is possible to see the increased amount of studies and attempts to define a taxonomy for kinetic architecture. Nevertheless, it was not yet reached a comprehensive classification able to group the diverse types of

structures in exclusive groups (Stevenson, 2011) (Megahed, 2017) (Fenci and Currie, 2017).

During the XXI century the most relevant contributions seem to be those by authors like Fox and Yeh (2000), Hanaor and Levy (2001, 2009), Gantes and Pellegrino (2001), Korkmaz (2004), Schumacher, Schaeffer and Vogt (2010), Moloney (2011), Stevenson (2011), Del Grosso and Basso (2013) and Rivas Adrover (2015). Not all of these authors provide detailed classifications and the criteria used are different, however all of them offer important definitions and insights that must be accounted for in the creation of a general taxonomy for kinetic structures for architecture.

As Stevenson (2011) and Megahed (2017) point out, one of the issues relating to the difficulty of achieving a classification is the wide available terminology that introduces blurred limits within each term. Terms such as adaptable, alive, collapsible, demountable, deployable, dynamic, flexible, foldable, movable, portable, retractable or transformable, can be used regarding several architectural types, different elements within a building, and also different kinds of movement.

In order to better understand the literature and place the definitions, it is followed a distinction between demountable/transportable structures and kinetic structures.

These two groups are often spoken about as if they were the same but critical requirements make them different (**Figure 2.2**) as argued by Korkmaz (2004) and Del Grosso and Basso (2013).

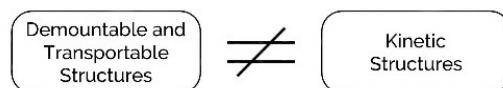


Figure 2. 2.
Distinction between demountable/transportable structures vs. kinetic structures

Buildings that are transportable and erected through deployment, and which have mechanisms associated with that deployment, are directly related to kinetic structures, as often the mechanisms are exactly the same in both groups. Nevertheless, the demountable/transportable structures only use their kinetic potential twice during each usage, one for erection and one for retraction and transportability. Deployable structures have “*two different uses in two different contexts, the first being the transportation or erection of the structure and the latter its static and functional behaviour when deployed*” (Del Grosso and Basso, 2013, pp. 122).

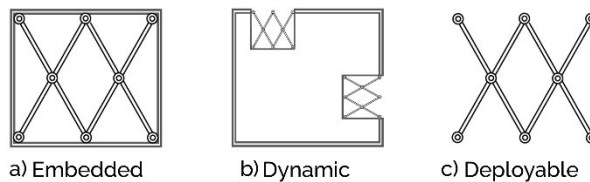
On the other hand, kinetic structures are expected to move often in their lifetime while maintaining their location. The most common time spans for movement, are daily or annually. These structures can move several times in

one day, depending on the specific function for which were designed, expanding and contracting everytime determined conditions change, or they can move a few times during the year which often means that their function is season dependable. These remarks introduce two key factors for the taxonomy of these structures which are the **location** of the structure and the **time** at which movement occurs (Korkmaz, 2004),

Fox and Yeh's (2000) general classification is defined by the function or location of the element within the architectonic whole and does not refer to geometry, structure or type of movement.

The authors divided the kinetic structures in three main groups: a) Embedded; b) Dynamic; c) Deployable (**Figure 2.3**).

Figure 2.3.
kinetic Typologies
in architecture
Source: Fox and
Yeh, 2000



The **embedded kinetic structures** are systems that are integrated in an architectonic whole at a fixed location. Their function is to help control the whole in response to changing conditions like retractable roofs, transformable façades, deployable structures that increase the buildings usable area, etc (Fox and Yeh, 2000).

The **dynamic systems** act independently of the architectural whole, like doors, louvers, partitions, or modular components. The authors consider these structures as mobile, transformable and incremental kinetic systems (Fox and Yeh, 2000).

The **deployable kinetic systems** are systems that are easily constructed and deconstructed, usually used for buildings in a temporary location, like pavilions for travelling exhibitions or events, and shelters for disaster areas (Fox and Yeh, 2000).

According to the distinction supported by Korkmaz (2004) and Del Grosso and Basso (2013), Fox and Yeh's *deployable kinetic systems* would belong to the demountable/portable structures and the *embedded*, as well as the *dynamic structures* would be included in kinetic structures (**Figure 2.4**). Korkmaz (2004) also divides movement in architecture into two main groups that follow the same distinction. The author argues that there are two types of buildings: a) Buildings with Variable Geometry or Movement; b) Buildings with Variable Location or Mobility (**Figure 2.5**) (Korkmaz, 2004).

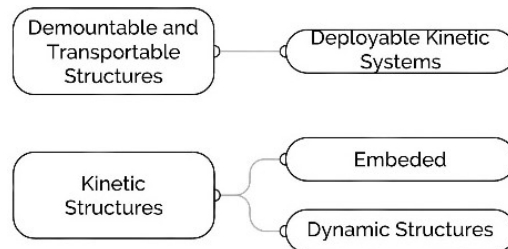


Figure 2. 4.
Relation between Fox and Yeh's categories and demountable/transportable structures vs. kinetic structures

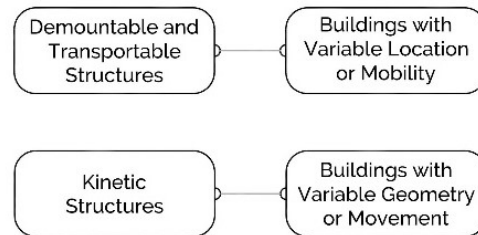


Figure 2. 5.
Relation between Korkmaz's categories and demountable/transportable structures vs. kinetic structures

2.1.1 | Definitions

From the first established distinction between kinetic structures and demountable/transportable structures it is going to be followed the work by Fenci and Currie (2017) and Megahed (2017) which analyse the contributions by the authors mentioned in the previous section for the definition of kinetic architecture. Two different approaches amongst the authors have been noticed by Fenci and Currie, while some authors try to provide classifications and/or definitions, others limit themselves to list distinct types of structures (Fenci and Currie, 2017).

Fenci and Currie (2017) provide several tree diagrams of each author's classification. The same strategy will be used in this section to facilitate the understanding of the classes of structures, and the relations between them, as proposed by each author.

Throughout the section each contribution will be analysed and diagrammed along with the specification of the criteria used by each author, in order to better understand the reasoning behind each approach.

Many of the contributions refer to deployable structures, not exactly to kinetic structures, but often the structural and mechanic aspects used to conduct movement can be used in both categories, thus it seems important to define them and find the points of contact and disagreement.

Zuk and Clark, 1970

In 1970 Zuk and Clark published the first book on kinetic architecture. This book is the first to define kinetic related concepts for architecture through explained experiments and built examples existing at the time. It was the first taxonomy for kinetic architecture, and the arguments used then remain valid 50 years later (**Figure 2.6**).

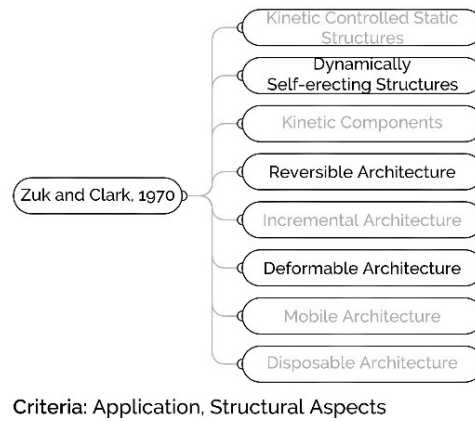


Figure 2. 6.
Classification by Zuk
and Clark, 1970
Source: Wener, 2013,
adapted

The authors divide the categories for kinetic architecture through their structural aspects and application into eight general groups:

- **Kinetic controlled static structures:** This considers that all structures move, even the static ones, due to loads, wind, vibrations, etc. To this group belong static buildings, and thus will not be considered for the final classification.
- **Dynamically self-erecting structures:** the authors describe these structures as those ones that can be brought to a site and there, through an energy input, automatically open into a stable expanded form. These would be the structures to which most of the deployable structures belong to; buildings that have joints and connections within their structure, which can be erected without auxiliary support.
- **Kinetic components:** these are components inside buildings that help to regulate the functioning of the building, such as doors, windows, elevators or escalators. As the name suggests these are “merely” components and not structures and thus will not be considered for the final classification.
- **Reversible architecture:** structures that can be erected and collapsed in the same, but reverse, manner. The buildings that belong to this category are much as the “Dynamically self-erecting structures”.
- **Incremental architecture:** buildings that are composed of addition, subtraction and/or substitution of modules in order to create combined configurations. According to the distinction by Korkmaz (2004) and Del

Grosso and Basso (2013) this group would belong to static structures, and thus will not be considered for the classification of kinetic architecture.

- **Deformable architecture:** buildings in which all parts are connected and continuous, hence change affects the whole form and the individual parts remain connected and continuous before and after change.
- **Mobile architecture:** buildings that move as a total unit and may be settled anywhere. The authors refer that this class is directly related to the classes of Incremental and reversible architecture. In this way, this group would belong to the demountable/transportable structures and will not be considered for the final classification.
- **Disposable architecture:** buildings, or parts of buildings that can be substituted when they are no longer a “good fit”. It can be seen as the recycling of components and materials for new and better ones (Zuk and Clark, 1970).

Frei Otto, 1971

Frei Otto’s classification focused on the application of deployables for convertible roofs. Although his reasoning is application oriented, it is important to consider, since it was one of the first contributions on the theme of movement and structures and because his considerations are also relevant to other applications.

Otto distinguishes between rigid constructions and flexible membrane constructions. For the membranes the author considers two distinct groups; the ones whose supporting structure remains static during movement and the ones whose structure moves alongside with the membrane. Otto also creates a matrix for the methods of opening and closing membrane structures which includes drawn examples and the directions of movement (Jensen, 2004) (Stevenson, 2011). (**Figures 2.7 and 2.8**)










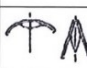


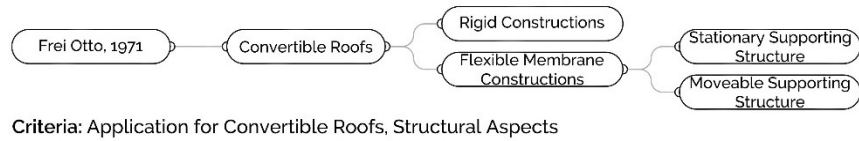
Construction system	Type of movement	Parallel	Central	Circular	Peripheral
Stationary supporting structure	Membrane				
	Membrane				
Moveable supporting structure	Supporting structure				
	Supporting structure				
	Supporting structure				

Figure 2.7. Otto’s matrix for the opening and closing of roof membranes, ILS 1971
Source: Jensen, 2004

Figure 2. 8.
Otto' classification,
1971
Source: Jensen,
2004, adapted



Merchan, 1987

Carlos H. H. Merchan, in his master thesis for the MIT, “Deployable Structures”, frames the applications of existing deployable structures in 1987, which still remains valid still at the present time:

- a) A situation in which there is a need to create enclosed or protected space for a short period of time and then to move that space to another location for erection or storage.
- b) Difficult places to access, and/or lack of labour.
- c) Special applications equipment and shelters for special equipment which cannot be transported in full open size and need to be erected in a very quick way.
- d) Need to enclose space due to variable weather conditions.
- e) Locations of high risk with elevated labour costs, hostile environments, costly transportation.
- f) Construction aid, deployable structures can provide a reusable, easy to erect scaffolding.
- g) As a construction method that consists of bringing the complete structure to the site in some compact configuration and deploying it there for permanent use (Merchan, 1987).

After the definition of applications for deployable structures, Merchan proposes a general classification that distinguishes between strut and surface structures.

In the **strut structures** the author includes *scissor-hinged mechanisms* (pantographs), *sliding or umbrella mechanisms*, that some authors disregard but that in fact have characteristics that do not allow them to be contained in other groups (Megahed, 2017) and *hinged-collapsible-strut* mechanisms. The latter group is different from the pantograph system because the bars are connected to each other by joints at the end of the struts and not somewhere in the middle as happens in pantographs. When the deployment form is reached the bars are locked through brakes, cables, or other restraints, maintaining it in a stable form (Megahed, 2017). This group could also be

referred to as bar linkages (Demaine and O'Rourke, 2007) (You and Chen, 2012).

For the **surface structures** Merchan defines three categories; the **inflatable or pneumatic structures**, the **telescopic structures** and the **folded structures**. this last group is subdivided into **rigid panels** and **continuous flexible material**. Merchan finishes his thesis with comprehensive examples, supported by images, of all the structures mentioned (Merchan, 1987).

Fenci and Currie (2017) contradict some of Merchan's conclusions. The authors note that Merchan does not make any distinction between air-inflated or air-supported when referring to the inflatable or pneumatic structures. They also point out that when Merchan divides the folded structures into Rigid Panels and Continuous Flexible Material (membranes), he should add if the membranes are connected to struts or cables and if they interact with them or are just supported by them (Fenci and Currie, 2017) as has been done by Frei Otto in 1971.

Regarding the telescopic structures, Fenci and Currie argue that Merchan neglects to clarify that telescopic structures can either be made up of open or closed section segments and refers only to the closed ones (Fenci and Currie, 2017).

Finally, they state that Merchan did not consider some deployable structures that existed at the time, such as tensegrities, air-supported structures and sliding structures. On the other hand, Merchan himself states at the beginning of his thesis that he would only consider those relevant to his research (Merchan, 1987) (Fenci and Currie, 2017).

The scheme for Merchan's classification is shown in **Figure 2.9**.

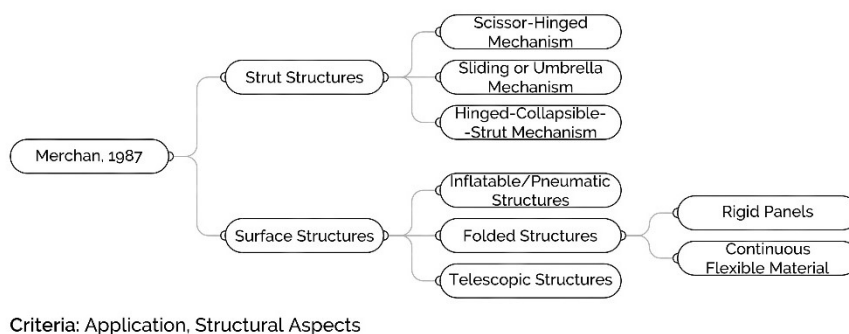


Figure 2.9.
Merchan's
classification, 1987
Source: Fenci and
Currie, 2017, adapted

Hanaor and Levy, 2001/Hanaor, 2009

In 2001, Hanaor and Levy published a comprehensive classification for deployable structures that has been referred to and used by several researchers since then due to their rigorous approach. Their considerations were later republished in another article by Hanaor in 2009, this is the article that this research will consider because it provides an update on the 2001 version.

The table classifies deployable typologies primarily regarding their morphological and kinematic properties, “*which are of primary significance in the context of deployable structures*” (Hanaor, 2009, pp. 84).

Hanaor defines two main groups, **rigid links** and **deformable**. for each of these two groups another two subcategories are defined, the **lattice or skeletal structures** and the **continuous or stressed-skin structures**. The difference between these two subcategories is the way in which the load bearing is made. Skeletal structures bear the load through discreet members while in the continuous structures, is the cover surface itself that carries the main load. The author refers to a third class, **hybrid structures** which combine skeletal and stressed skin elements and through which both types of elements have an equal role in the load-bearing function, but this third class is not present on the table (**Figure 2.10**) where the author deals separately with the two components (Hanaor, 2009).

The Lattice and Skeletal structures from the Rigid Links main group are divided by the authors into three groups, **double layer grid (DLG)**, **single layer grid (SLG)** and **spine**. Each of these three groups is further subdivided into pantographic and bars and examples of each category are provided by the authors.

The continuous or stressed skin structures from the rigid links main group are divided into two groups, **folded plates** (further subdivided into linear or radial deployment) and **spine**.

The lattice and skeletal structures from the deformables main group have only one extension, the **strut-cable systems**, which include tensegrities.

The continuous or stressed skin structures from the deformables main group also have only one extension, the **tensioned membranes** that are then subdivided into fabrics (tents and ribbed) or pneumatics (low pressure and high pressure).


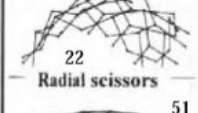

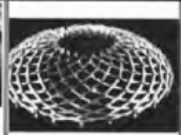
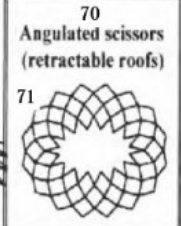

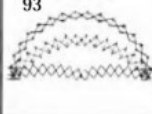

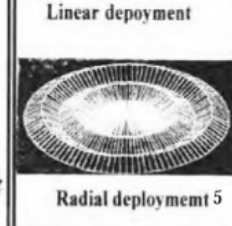
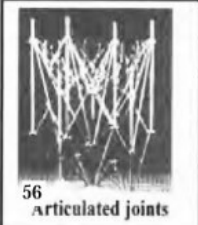
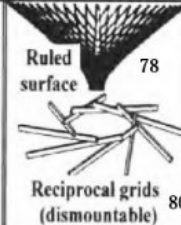
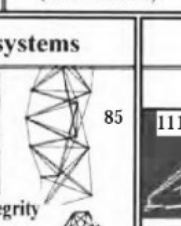
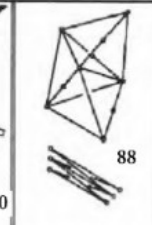
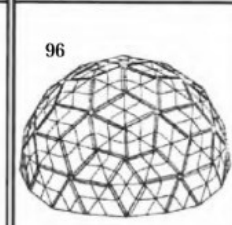
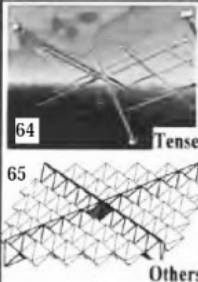
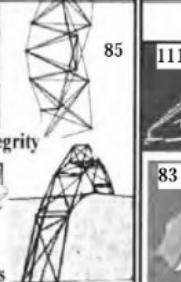

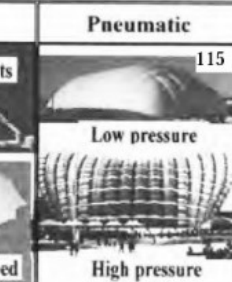
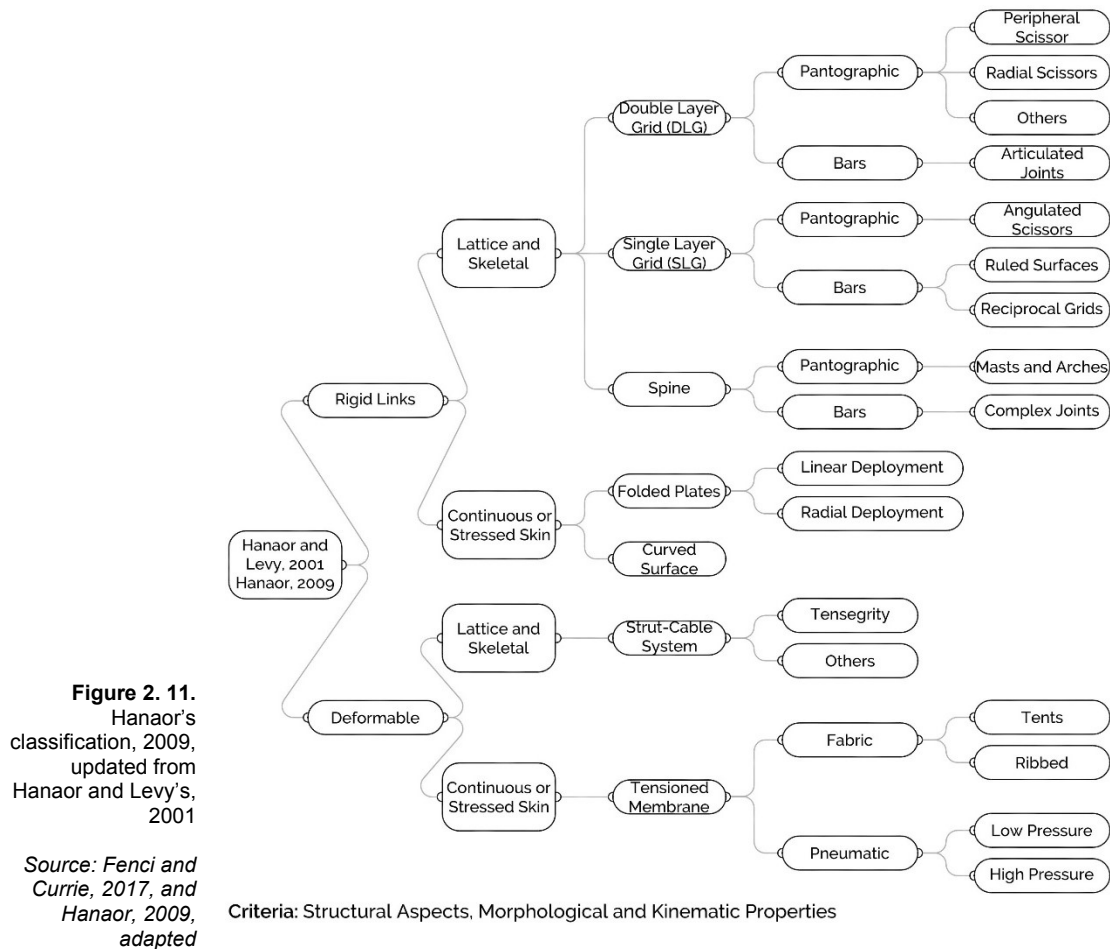
		Structural Morphology			
		Lattice			Continuous
		DLG	SLG	Spine	Plates
Kinematics	Rigid links	Pantographic (scissors)			Folded Plates
		 19 Peripheral scissors  22 Radial scissors  51 Others	 70 Angulated scissors (retractable roofs)  71 Others	 16 Masts and arches  93 Others	 101 Linear deployment  5 Radial deployment
		Bars			Curved surface
		 56 Articulated joints	 78 Ruled surface  80 Reciprocal grids (dismountable)	 88 Others  96 Curved surface	
Deformable	Strut-cable systems		Tensioned membrane		
	 64 Tensegrity 65 Others	 85 Tensegrity	 111 Fabric 83 Tents 83 Ribbed	 115 Pneumatic 115 Low pressure 115 High pressure	

Figure 2. 10. Hanaor's classification, 2009
 The numbers next to the images correspond to the references of the article written by Hanaor in 2009
 Source: Hanaor, 2009

The table from Hanaor (2009) is followingly diagrammed in **Figure 2.11**.



Gantes, 2001

Gantes makes a first distinction amongst deployable structures based on their application either on Earth or in Space. For the author several assumptions must be made about the design of these structures depending on their application (Earth or Space), such as the self-weight of the structure, the loading type, factors of safety, reliability and the degree of automation. Fenci and Currie, 2017, argue that even though these factors may vary between Earth and Space applications the kinematics and morphology “are not different enough to justify such a clean-cut distinction” (Fenci and Currie, 2017, pp. 115).

Despite this first division, Gantes does not pursue further categorization of Space structures and classifies only Earth based structures. Earth-based structures are analysed based on their morphology and are subdivided into: pantographs, two-dimensional panels, cable and membrane structures,

pneumatic structures, tensegrities and retractable roofs (Fenci and Currie, 2017).

Fenci and Currie argue that the last group (retractable roofs) should not exist since it is “*an application of deployable structures, rather than a particular structural shape or form*” (Fenci and Currie, 2017, pp. 115), and because the proposed examples use mechanisms that also apply to other deployable structures making this category inappropriate (Fenci and Currie, 2017).

In fact, Gante’s taxonomy cannot be really considered a taxonomy on deployable structures. The nominated groups should come from more specific categories instead of coming directly from “Earth Based Deployable Structures”. However, the mentioned groups (**Figure 2.12**) cover a wide range of the existing deployable structures and will be considered for the final proposed table.

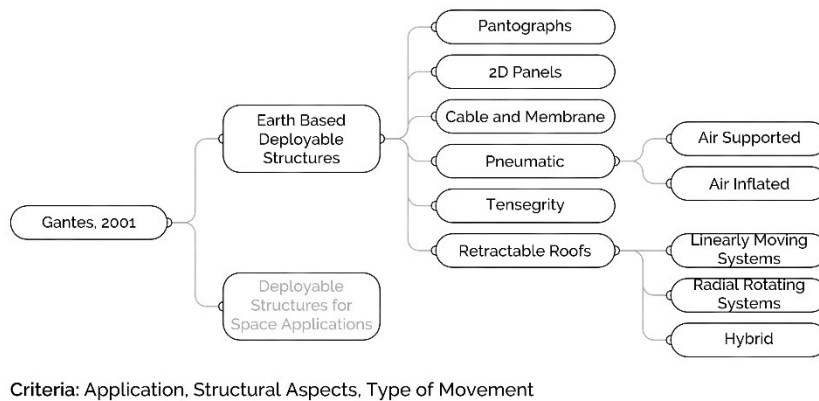


Figure 2. 12.
Gantes' classification,
2001
Source: Fenci and
Currie, 2017, adapted

Pellegrino, 2001

Sergio Pellegrino is an expert on deployable structures and founded the Deployable Structures Laboratory at the University of Cambridge in 1990.

In 2001, Pellegrino provided not a taxonomy but a listing of deployable structures, some of them innovative, to be used in Space but that might also be used on Earth (Pellegrino, 2001).

Even though Pellegrino does not offer an explicit classification, neither tries to mention all existing types of deployable structures, he approaches the structural form from a motion perspective and provides examples for each referred type, some of them never mentioned before by other authors, such as coilable masts, bi-stable structures or the mirror membrane developed for the Znamya-2 experiment (Fenci and Currie, 2017).

In the course lecture “Deployable Structures in Engineering”, 2001, Pellegrino defines **deployment** as the transformation from a compact (or bundle) state to an open state, and the reverse transformation as **retraction**.

The author presents examples of deployable structures made with deformable materials such as **coiled rods**, **flexible shells** and **membranes**. He also states that there are deployable structures that belong to the category “mechanism” as “assemblies of *rigid* parts connected by movable joints (Pellegrino, 2001, pp. 16)”. The chosen examples are those whose structure is at the same time a mechanism and load bearing structure, *i.e.* **structural mechanisms**. The examples presented are four-bar linkages with simple hinges or spherical joints, pantographs with straight and angulated bars that deploy synchronously, ring-like pantographs and 3D mechanisms. The author also considers structures such as the Tension Truss Antenna, Rigid Panels Structure and the Retractable Dome, that could also be considered a structural mechanism (Pellegrino, 2001).

The listing by Pellegrino (2001) is diagrammed in **Figure 2.13**.

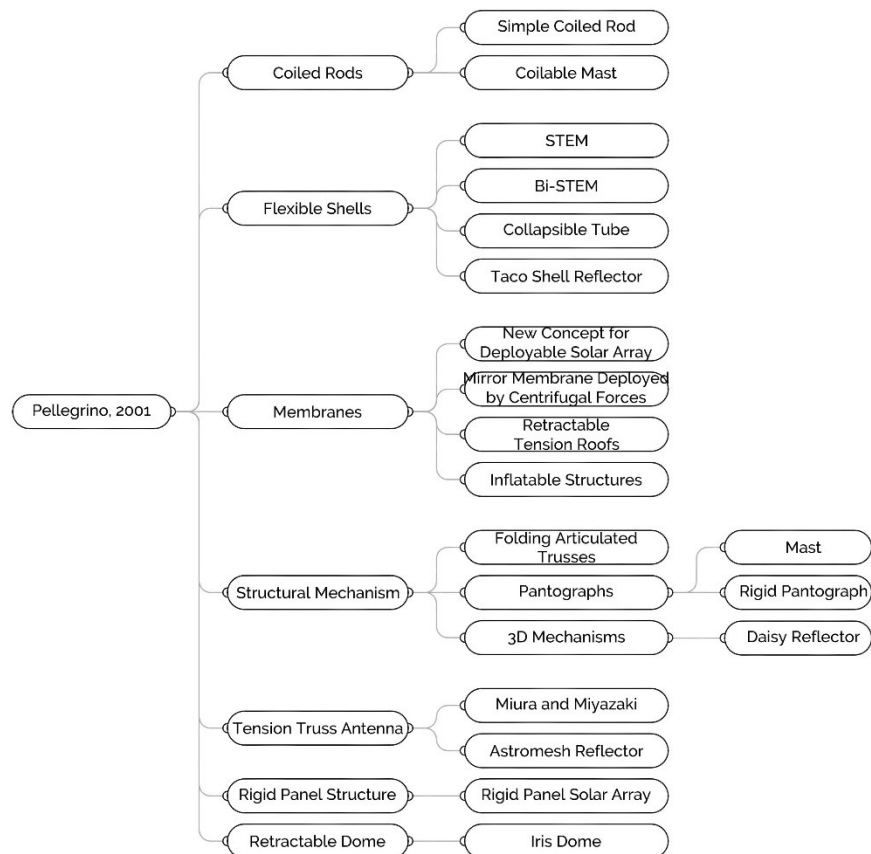


Figure 2.13.
 Pellegrino's listing,
 2001
 Source: Fenci and
 Currie, 2017, adapted

Criterion: Structural Aspects

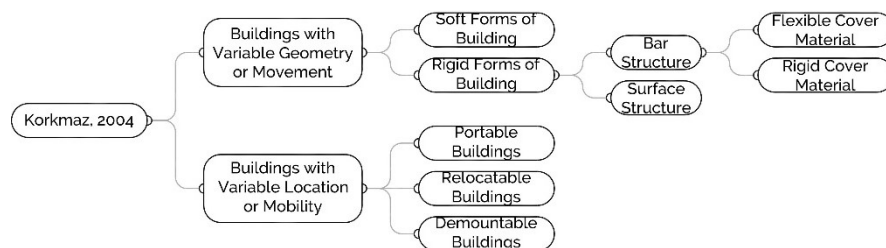
Korkmaz, 2004

In his PhD Thesis, Koray Korkmaz (2004), proposes a classification for deployable structures from an architectural perspective. His first division follows Fox and Yeh's (2000) classification of kinetic typologies in architecture and considers the **time** for movement and **location** as key parameters for the classification of kinetic structures. Korkmaz divides kinetic structures into **buildings with variable geometry or movement** and **buildings with variable location or mobility** (Korkmaz, 2004).

The author subdivides the group of buildings with variable location or mobility through Kronenburg's classification¹ into **portable**, **relocatable** and **demountable buildings** (Fenci and Currie, 2017).

In regard to buildings with variable geometry or movement, Korkmaz focuses on kinetic movement and material to further classify this group. He subdivides the group into **soft forms** and **rigid forms**. The author argues that the soft forms buildings can actuate diverse types of movements without the need for hinges or substructures because movement is achieved directly through the specificities of the material. Rigid form structures can move in different ways, for example sliding, folding or rotating, through joints connecting the members of the structure. These structures are subdivided into **bar** or **surface structures** depending on the geometry of the structural members that conduct movement (Korkmaz, 2004) (Fenci and Currie, 2017). In **Figure 2.14** is depicted the overview of the classes proposed by Korkmaz (2004).

Fenci and Currie, 2017, consider that Korkmaz fails by not including tensegrities within his classification and does not pursue a more profound classification for soft form buildings.



Criteria: Movement, Structural Aspects, Material

Figure 2. 14.
Korkmaz's
classification, 2004
Source: Fenci and
Currie, 2017, adapted

¹ Kronenburg, R.; Houses in motion: the genesis, history and development of the portable building. London: Academy Editions, 1995.

Schumacher, Schaeffer, Vogt, 2010

Schumacher, Schaeffer and Vogt, in their book *Move: Architecture in Motion*, 2010, classify kinetic structures with regard to their type of movement, and argue that there are different types of movement depending on the type of material, that can be rigid or deformable, in the same manner as Korkmaz (2004) does. This approach is different from most authors and departs from the same kind of reasoning of Frei Otto and Korkmaz, where the material is considered the main actor for movement.

For the **rigid materials**, Schumacher *et al.* start by defining the basic types of movement (as in robotics and mechanics) as Translation, Rotation and these two combined (Translation+Rotation). The authors consider that this definition should be further categorized for architectural application since the location of joints and gravity are not considered within the first division of movement types. They further classify rotation movements as swivel, rotate or flap, translation movements as slide parallel or vertically and the combined movements as fold and scissor-fold, and provide a schematic explanation of each type of movement for surfaces and volumes, as shown in **Figure 2.15** (Schumacher et.al, 2010).

Mechanical concept		Rotation	Rotation and translation	Translation				
Architectural type		Swivel alternately	Rotate	Flap	Fold	Scissor-fold	Slide parallel	Slide vertically
Simple movements of surfaces	Horizontal							
	Vertical							
	Level							
Simple movements of volumes	Horizontal							
	Vertical							
	Level							

Figure 2.15.
 Movements of rigid building elements
 Source: Schumacher et al., 2010

Regarding **deformable materials**, the authors consider that there are three types; flexible, elastic and pneumatic. For the types of movement, pneumatic materials are not considered by the authors since constructions with this type

of materials are usually not able to change form elastically, and have only two stable states, inflated or deflated. The authors also argue that elastic materials are not usually used in architecture but rather in smaller scale designs. Therefore, for the soft and flexible materials the types of movement defined are stretch, roll, bend, shear, flutter, free and gather. In **Figure 2.16** it is possible to see diagrams for each type of movement and for materials with one, two or three dimensions (Schumacher et.al, 2010).

The diagram for Schumacher *et al.* (2010) movement typologies is shown in **Figure 2.17**.

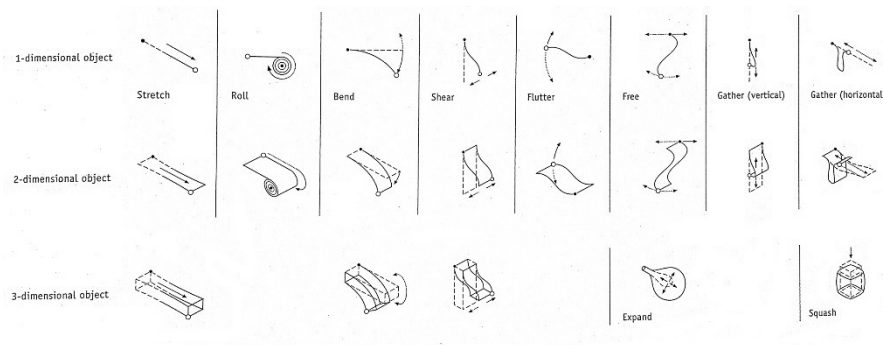
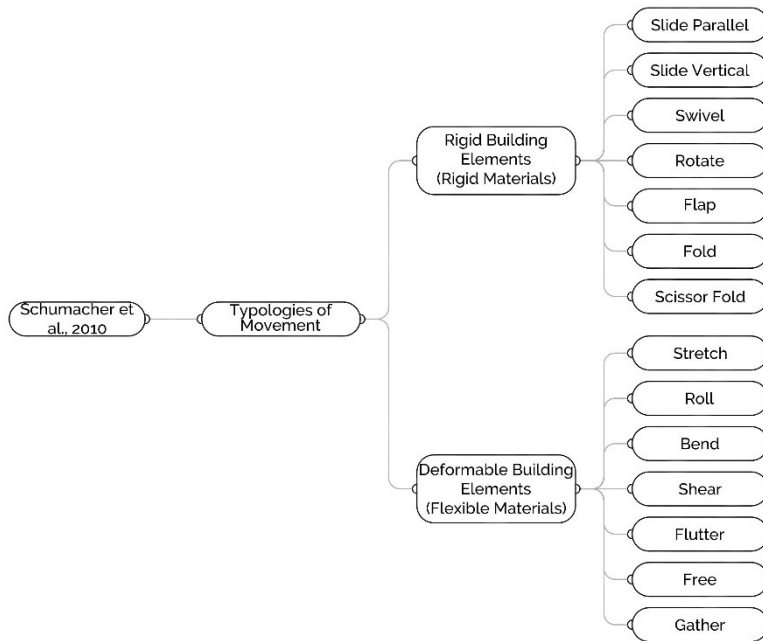


Figure 2. 16. Movements of deformable building elements
Source: Schumacher et al., 2010



Criteria: Structural Aspects, Materials, Type of Movement

Figure 2. 17. Schumacher's *et al.* typologies of movement

Stevenson, 2011

Carolina Stevenson, in her paper Morphological Principles of Kinetic Architectural Structures in 2011, tries to identify morphological characteristics of kinetic architectural structures. The author's aim is not to classify the typologies but rather to "*understand the broadest possible nature of kinetic architecture as well as making distinctions and establishing relationships between existing models* (Stevenson 2011, pp. 3)".

Stevenson makes a morphological analysis of the changes in the form of a building during the process of movement. She considers the combined action of all of the architectural components instead of focusing on the operation of single parts, which she calls "kinetic devices", in order to analyse the overall transformation of the global form (Stevenson 2011).

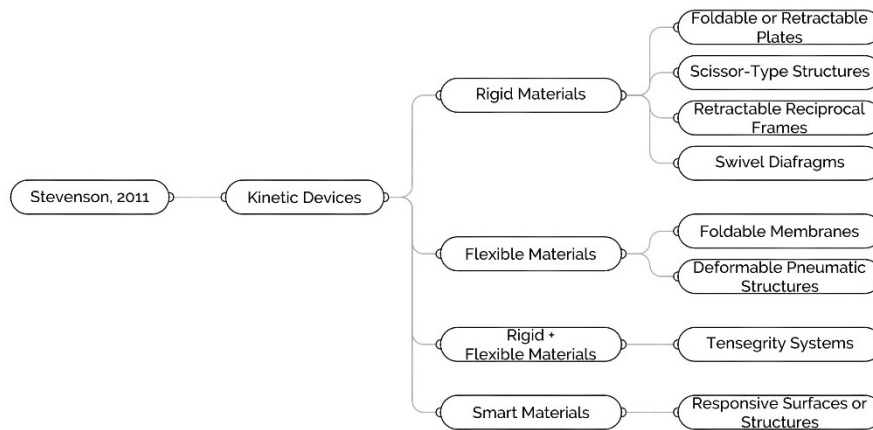
Despite the fact that her aim is not a general, comprehensive classification, Stevenson classifies the kinetic devices. The author argues that the modularity of these single parts is fundamental in kinetic architecture "*due to the pragmatic need of movement being transmitted from one element to the next* (Stevenson, 2017, pp. 4)" and divides them into three groups: **rigid**, **flexible** or **smart**.

For the **rigid materials** group, the author considers devices that act as mechanisms and are made of solid metals, plastics or timber. The type of structures in which these mechanisms can be used are foldable or retractable plates, scissor-type structures, retractable reciprocal frames and swivel diaphragms.

For the **flexible materials** group, Stevenson considers textiles or cables that transmit movement through folding, creasing, bending, stretching and/or inflating and that can be part of foldable membranes or deformable pneumatic structures.

The author also considers a combination of these two groups, rigid and flexible materials, and demonstrates this with composite structures such as deployable tensegrity systems.

Regarding the **smart materials**, Stevenson considers materials that transmit movement by changing their physical properties, their structure or composition and/or their functions in a controlled manner and can be used in responsive surfaces or structures in particular (Stevenson 2011). **Figure 2.18** presents the scheme for Stevenson's (2011) classification.



Criteria: Structural Aspects, Materials, Morphological Aspects, Type of Movement

Figure 2. 18. Stevenson's classification, 2011

Regarding the morphological analysis, Stevenson suggests that most kinetic architectural structures have centric or linear configurations. The **centric structures** usually have forms that can be inscribed in circular or spherical shapes, such as polygons, polyhedrons and organic loops and blobs. The movement in these structures is ruled from the centre or the periphery, with central masts or supporting elements on the border of the structures. **Linear structures** usually involve forms that are organized along an axis (that can be straight or curved), and often are used grids that develop around the axis and the movement is governed in parallel directions to that axis (Stevenson 2011).

Stevenson provides a two-way table (**Figure 2.19**) that places the studied kinetic structures in accordance with their **position in space and direction of transformation** and their **physical transformation**. Regarding the position in space and direction of transformation, the author subdivides the structures according to their configuration, whether it is **centric** or **linear**, and further subdivides these according to the type of movement of the structures that can be: **spherical**; **circular-tangential**; **radial**; **pivoting**; **monoaxial**; **biaxial** or **multi-axial**. Regarding the physical transformation, Stevenson subdivides this into changes in **shape**, **size** or **position** that can be further subdivided into **deform**, **fold**, **deploy**, **retract**, **slide** and **revolve** (Stevenson 2011).

Fenci and Currie argue that the transformations defined by Stevenson (deform, fold, deploy, retract, slide and revolve) are not completely correct since deployable structures often use a combination of transformations and thus cannot unequivocally be placed under only one. The authors also note that there are no structures with prestressed cables and nets in Stevenson's table, although there are several deployable structures that use them. Finally,

Fenci and Currie suggest that Stevenson neglects pneumatic structures, that have such a significant role in the deployables family. Stevenson only presents one example for pneumatic structures and leaves no space for the distinction between air-supported and air-inflated structures, making it very difficult to place other pneumatic structures within the table (Fenci and Currie, 2017).

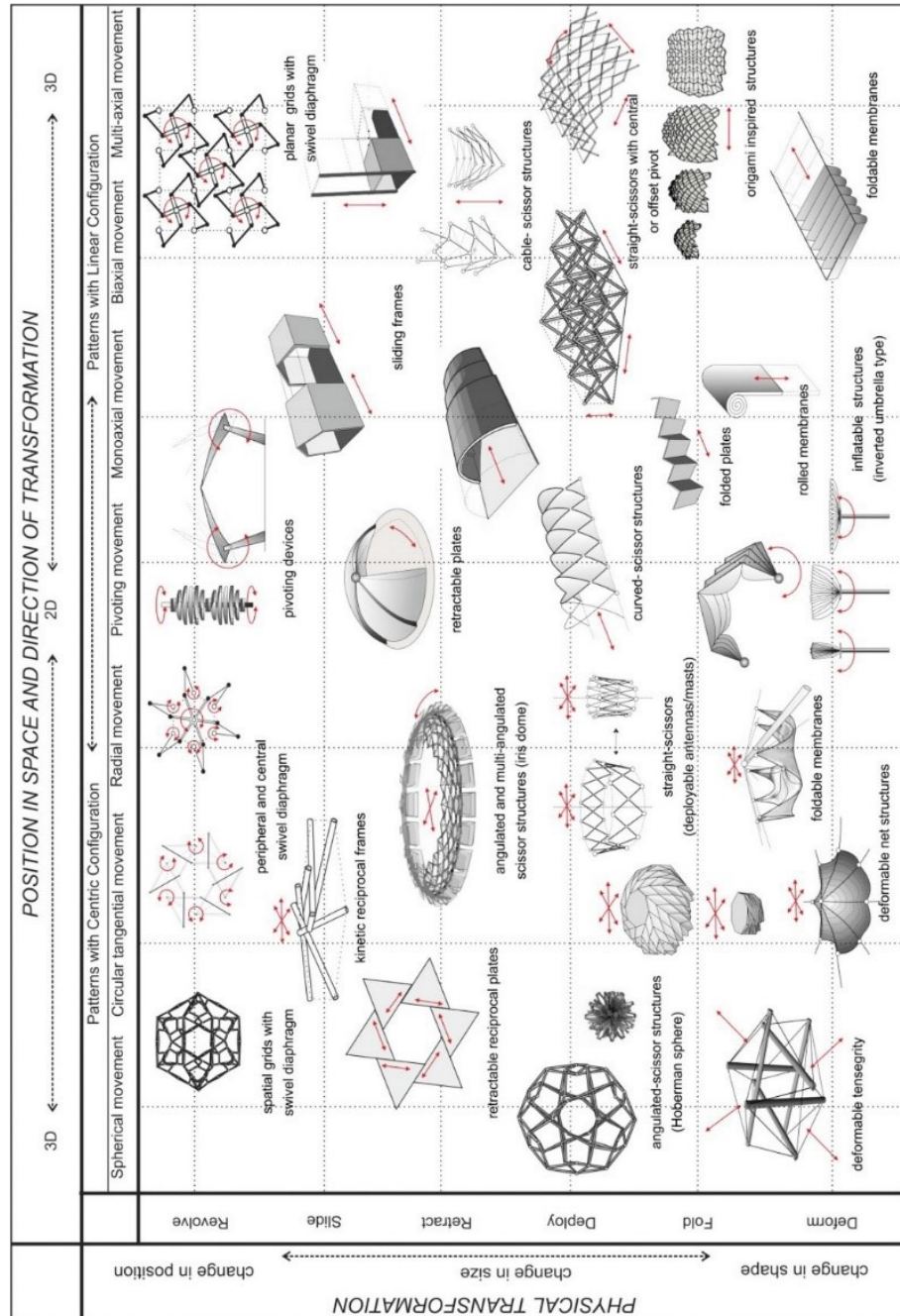


Figure 2.19.
 Morphological aspects and transformation strategies in kinetic architectural structures
 Source: Stevenson, 2011

Del Grosso and Basso, 2013

In 2013, Del Grosso and Basso developed a classification for deployable structures, which they call variable geometry structures (VGSs). They base their classification on Hanaor and Levy's work (2001) but extend it by adding structures that were not considered in 2001, such as compliant mechanisms for **deformable structures** and morphing truss structures for **rigid link structures** (Del Grosso and Basso, 2013) (Fenci and Currie, 2017).

For the **rigid links** group, Del Grosso and Basso consider four subdivisions; mutually supported elements, rigid foldable origami, morphing truss and scissor like structures.

The **mutually supported elements (MSE)**, also known as reciprocal frames or nexorade fans, are different from common truss assemblies because the rigid elements that compose the structure can be joined at the end points or at intermediate points. These structures eliminate the need for spherical joints and have the ability to change their supporting points.

These authors are the first to create a category named **Rigid Foldable Origami**, which they define as “*a piecewise linear developable surface that can realize a deployment mechanism if its facets and fold lines are substituted with rigid panels and hinges, respectively* (Del Grosso and Basso, 2013, pp. 126)”. Other authors have mentioned these kinds of structures as folded structures > rigid panels (Merchan, 1987), folded plates (Hanaor and Levy, 2001) and origami inspired structures (Stevenson, 2011), however Del Grosso and Basso are the first to define them as a mechanism.

The authors also consider **morphing truss structures**, which are similar to the traditional truss structures but have linear displacement actuators strategically placed on specific bars that allow for shape morphing.

The **scissor like mechanisms** considered by the authors include projects and developments by Pinero (1962), Hoberman (1993), and You and Pellegrino (1997). These were also considered by previously described contributions, but Del Grosso and Basso introduce a new one, the contributions by Akgun *et al.* in 2007 and 2010.

For the **deformable structures**, the authors divide them into compliant mechanisms, tensegrity and pneumatic structures.

Del Grosso and Basso argue that **compliant mechanisms** can offer great advantages, when compared to traditional mechanisms, because they do not have hinges and have the ability to store strain energy, which removes the need for return springs, further, they do not develop the backlash typical of kinematic joints and so are perfect to be used in contexts that need precision

and repeatable motion. These mechanisms have mainly been used for small scale displacements (usually put into motion with smart actuators) in precision engineering and aircraft engineering, but until now there are no relevant studies on an architectural scale (Del Grosso and Basso, 2013).

Regarding **tensegrity structures** the authors consider that these structures can often become unstable and difficult to control and suggest that it can be solved by using active control. This can be achieved, for example, by using a system of rods and wires controlled by pneumatic muscles, as has been studied and tested for application in architecture, but “*no significant realizations have been performed to date* (Del Grosso and Basso, 2013, pp. 125).”

Regarding the **pneumatic structures** the authors consider that air-inflated structures are more suitable to be used in an architectural context than air-supported structures. Air-supported structures must deal with problems such as large volumes of air and continuous control of air pressure. Air-inflated structures are easier to erect and control since the volume of air that must be under higher pressure is enclosed between two membranes, which also leaves the interior space, were people are located, under regular air pressure (Del Grosso and Basso, 2013). **Figure 2.20** summarizes the relations between the classes determined by Del Grosso and Basso (2013).

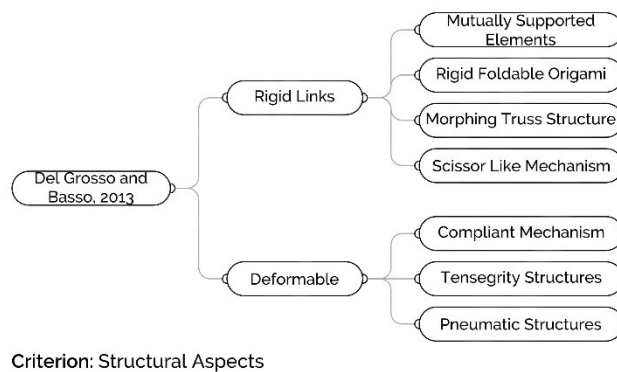


Figure 2.20.
 Del Grosso and Basso's classification, 2013
 Source: Fenci and Currie, 2017, adapted

Fenci and Currie, 2017, state that the category of compliant mechanism is relevant when referring to the way in which motion is achieved, however they consider that it does not constitute a category for classifying deployable structures because it is focused on the micro-aspects of deployment and not on the overall morphological aspect (Fenci and Currie, 2017).

The same argument is used regarding the morphing truss structures; Fenci and Currie consider these to be structures where some trusses are replaced with linear displacement actuators that act as hinged-collapsible-strut mechanisms, the category proposed by Merchan in 1987 (Fenci and Currie, 2017).

Rivas Adrover, 2015

Esther Rivas Adrover (2015) defined the typologies of deployable structures in architecture by placing thirty examples of such structures in specific categories. The author starts this classification by dividing deployable typologies into two main groups, **structural components** and **generative technique**. For the structural components group, deployables that were developed with a structural approach are considered. For this group the structural components of the deployable mechanism are its essence and base of design. For the generative technique, Rivas Adrover considers structures that were developed focusing on movement and form inspired by origami and biomimetics, and not the kinematics and morphology of the deployable structures. Rivas Adrover proceeds by dividing structural components into four subgroups, **rigid deployable components**, **deformable deployable components**, **flexible** and **combined deployables**, and the group of generative technique into two main subgroups, **biomimetics** and **origami paper pleat** (Rivas Adrover, 2015).

Fenci and Currie disagree with some points within Rivas Adrover's classification. First of all, they disregard the generative technique group since this group is developed from an inspirational source "*rather than focusing on their kinematics and morphology* (Fenci and Currie, 2017, pp. 123)". The origami pleat group in particular could be placed under the rigid structural components as suggested by Del Grosso and Basso, 2013, and the biomimetics group is too loosely defined by Rivas Adrover (Fenci and Currie, 2017).

Inside the structural components, Fenci and Currie argue that Rivas Adrover's classification has some conflicting information in relation to previous classifications by other authors, such as tensegrities, which are placed under combined deployables. These typologies would be more accurately placed simply under deformable deployable components, as argued by Hanaor and Levy, 2001. Fenci and Currie also suggest that deformable structural components should only include the inflatables, since nets and fabrics can only be stable with the aid of compression elements or anchored positions. This is a fact that Rivas Adrover herself mentions and refers these structures to the combined deployables but does not present examples (Fenci and Currie, 2017).

The authors consider that some examples are individually presented in such a specific way that other structures, that are based on the same principle, cannot be included. In the case of the NASA (National Aeronautics and Space

Administration) Type Cube, classified under latticework but equally could be classified as non-self-crossing linkages, so other structures could be included (Fenci and Currie, 2017).

Regarding flexible deployables, the presented examples are STEMs (storable tubular extendible member) and folding articulated trusses. The first should be placed under the deformable group, and the second under rigid components and latticework, making the category of flexible deployables irrelevant (Fenci and Currie, 2017).

The combined deployables section has examples of folding roof structures that include fabrics, however the fabric only helps to stabilize the structure in the fully deployed state as the loadbearing and the deployment are made by the grids. These structures would be better categorised as the rigid deployable components – grids section (Fenci and Currie, 2017). **Figure 2.21** resumes Rivas Adrover’s (2015) classification.

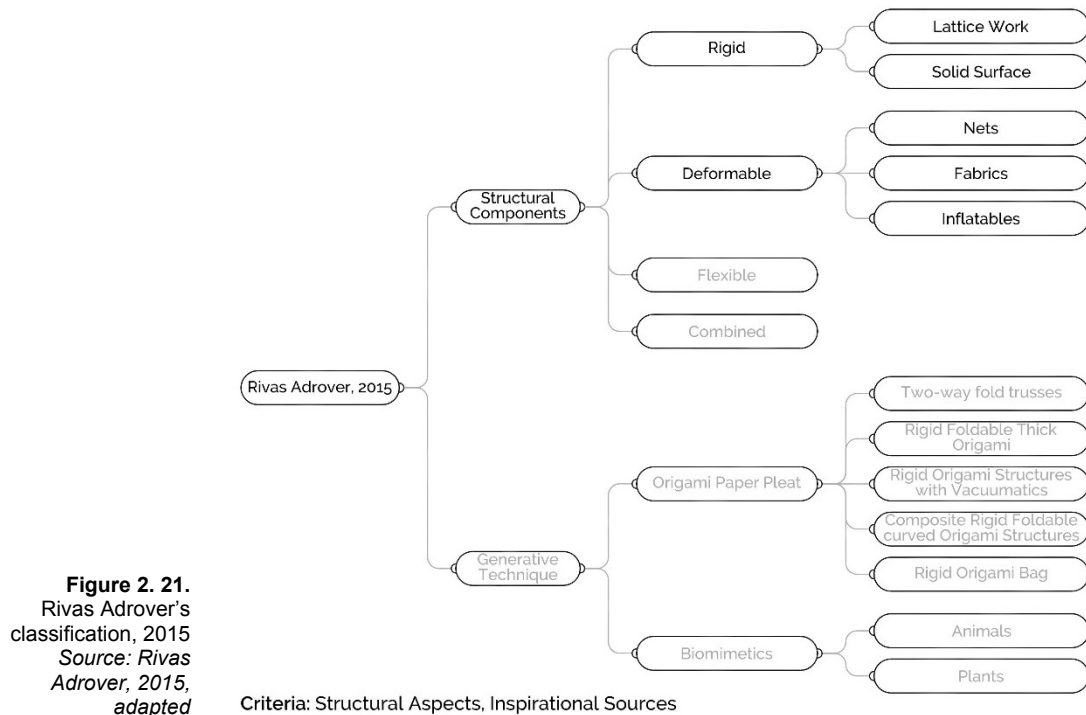


Figure 2. 21.
 Rivas Adrover’s classification, 2015
 Source: Rivas Adrover, 2015, adapted

Fenci and Currie also provide some clarification in regard to specific examples used by Rivas Adrover, such as the usual misunderstanding between the concepts of portable and deployable structures, or the wrong classification of deployables that use smart materials. As Fenci and Currie (2017, pp. 124) point out “*it can be said that Rivas Adrover provides specific examples in certain circumstances but then misses out on concentrating the attention on their common morphological characteristics and neglects some other structures belonging to that morphological and/or kinetic group*”

2.1.2 | Mechanisms

In 2009, Fox and Kemp made the distinction between Ways and Means in kinetic architecture. The authors consider that **Ways** are the geometric transformations that occur in the kinetic element like folding, sliding, expanding, shrinking and transforming. **Means** refer to the mechanisms or chemical transformations in the materials that are behind the movement (Fox and Yeh, 2000) (Fox and Kemp, 2009).

Jules Moloney (2011) makes a different distinction and argues that there are four building blocks for kinetics, three geometric transformations, translation, rotation and scaling and a fourth building block that is movement via material deformation through chemical transformations (Moloney, 2011).

There are valid points in both perspectives. There is definitely a distinction between Ways and Means, and the chemical transformations that occur in a material should be placed under the Means category, as Fox and Kemp (2009) suggest, instead of belonging to geometric transformations (Ways) as proposed by Moloney (2011). In addition, folding should not be considered a geometric transformation, since folding is a sub product of translating and rotating (Schumacher *et al.*, 2010). Finally expanding and shrinking may be put together as a scaling transformation, which can only happen with the deformation of materials or with the movement of a rigid element from a compacted state to an expanded state, which refers again to the basic movements.

In 2010, Schumacher *et al.* make the same distinction and define the possible movements (Ways) of rigid elements as; Swivel, Rotate, Flap, Slide, Fold, Expand and Contract. These can be summarized as three types of movements, Translation, Rotation and a combination of the two (Translation + Rotation), following the same basilar movements considered in mechanics and robotics. In order for the movements to happen, the Means described by Schumacher *et al.* are several mechanisms, chemical transformations of materials and material states and physical properties change (Schumacher *et al.*, 2010).

The approach of this research is to follow Fox's distinction between Ways and Means, Moloney and Schumacher's definition of translation and rotation for the Ways and Fox and Schumacher's characterisation for the possible Means in kinetic architecture as depicted in **Table 2.1**.

	Fox and Yeh, 2000 Fox and Kemp 2009	Moloney, 2011	Schumacher et al., 2010
WAYS	Folding	Translation	Translation
	Sliding	Rotation	Rotation
	Expanding	Scaling	Rotation + Translation
	Shrinking	Material deformation (through chemical transformations)	
	Transforming		
MEANS	Mechanisms		Mechanisms
	Chemical Transformations		Chemical Transformations
			Physical properties change

Table 2.1.
 Comparison between
 Fox, Moloney and
 Schumacher for
 Ways and Means in
 kinetic architecture

Kinematic Joints

You and Chen (2012) state that, from the perspective of kinematics, joints are the central pieces of a mechanism. A kinematic joint allows for relative motion, in certain directions, between the two rigid elements that it connects, while constraining motions in other directions. The number of Degrees of Freedom (DoF) of a joint is “*equal to the minimum number of independent coordinates needed to uniquely specify the position of a link relative to the other constrained by the joint*” (You and Chen, 2012, pp. 4) (Zuk and Clark, 1970). Releaux (1875) called a kinematic joint a **pair** and divided the types of joints into **lower pair** and **higher pair** joints. Lower pair joints are those in which there is contact at every point of one or more surface segments between two rigid members. Higher pair joints are those in which contact exists only at isolated points or along line segments (You and Chen, 2012). Due to these requirements there are only six essential types of lower pair joints differentiated by the types of relative motions that they permit, shown in **Figure 2.22** (Kolovsky *et al.*, 2000) (You and Chen, 2012).

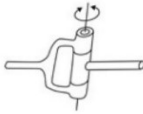
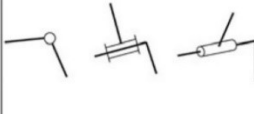
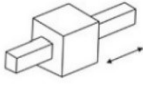
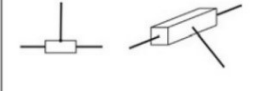
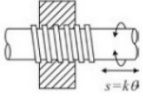
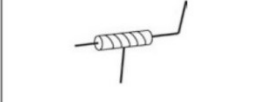
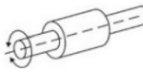
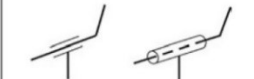

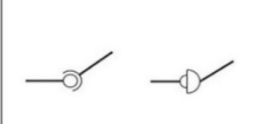
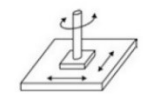
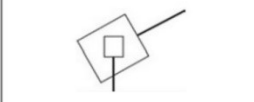
Joint name	Letter symbol	Number of degrees of freedom	Typical form	Sketch symbol
Revolute joint (hinge, turning pair or pin)	R	1		
Prismatic joint (slider or sliding pair)	P	1		
Screw joint (helical joint or helical pair)	H	1		
Cylindrical joint (cylindrical pair)	C	2		
Spherical joint (ball joint or spherical pair)	S	3		
Planar joint (planar pair)	P_L	3		

Figure 2. 22.
Lower pair joints
Source: You and Chen, 2012

Hinges are the simplest example of a device that is a revolute joint. They are the most common form of connecting and rotating flat elements, generally used on doors, windows and gates. Depending on the design of the hinge and on the point of connection between the hinge and the flat element, they can be constricted to rotating within a determined angle and direction or can be able to rotate on both directions, 180° or infinite turns of 360°. Some examples of hinges, by Schumacher *et al.*, are shown in **Figure 2.23**.

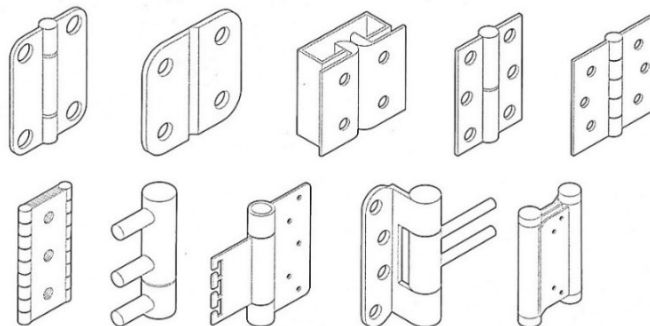


Figure 2. 23.
Hinges examples
Source: Schumacher et al. 2010

Unlike lower pair joints, there are an infinite number of higher pair joints, the two most common examples are shown in **Figure 2.24** (Kolovsky *et al.*, 2000) (You and Chen, 2012).

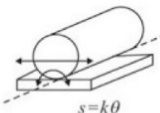
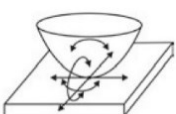
<i>Joint names</i>	<i>Number of degrees of freedom</i>	<i>Typical form</i>	<i>Comments</i>
Cylindrical roller	1		Roller rotates about the instantaneous contact line and does not slip on the surface.
Spatial point contact	5		Body can rotate about any axis through the contact point and slide in any direction in the tangent plane.

Figure 2. 24.
 Two examples of higher pair joints
 Source: You and Chen, 2012

The lower and higher pair joints described are perfect, theoretical mathematical models used to describe and calculate the kinematics of mechanisms. Kinematics only considers the position of elements during movement by constraints in the system itself and disregards any other kind of force such as gravity, friction between elements, wear, temperature, or geometric errors made in the design, as can occur in real constructed mechanisms (Kolovsky *et al.*, 2000).

A mechanism can also be called a kinematic chain, since “*any assemblage of links connected by kinematic pairs constitutes a kinematic chain* (Kolovsky *et al.*, 2000, pp. 10)”. A kinematic chain is a **linkage** if it is constituted by rigid links connected **only by lower pair joints** (Kolovsky *et al.*, 2000) (You and Chen, 2012).

The DoF of a mechanism can also be called its *mobility* and, similar to the DoF of a joint, it is the number of inputs required to determine the position of all the links in relation to a fixed reference, also called ground² (Kolovsky *et al.*, 2000) (You and Chen, 2012).

You and Chen (2012) provide a very comprehensive state-of-the-art, starting from the 19th century, of the first invented linkages and evolutions of these with four, five or six rigid members connected by revolute joints. These are the Myard, Goldberg, Altmann, Dietmaier, Goldberg, Sarrus, Schatz, Waldron,

² For more information on how to calculate the DoF's of a mechanism and the Kutzbach Criterion, please refer to You and Chen (2012) pp. 5-8.

Wohlhart and Chen and You Linkages that proceed, almost in every case, from the Bennett and Bricard Linkages³ (You and Chen, 2012).

Simple Mechanisms

You and Chen, 2012, define a mechanism, in machine theory, as “a set of moving or working parts used essentially as a means of transmitting motions or controlling movement of one part relative to another (You and Chen, 2012, pp. 1).”

Schumacher *et al.* (2010) define four basic types of simple machines that date back to Antiquity. The first are mechanical devices that allow for objects to be pushed or pulled using a rigid bar or a rope; these simple mechanisms apply the same force in the same direction but at a different point. The second is a combination of a rope and a pulley that allow a change in direction of the force. The third is the lever, that permits a change in the magnitude of the applied force, as the two forces are connected by a stiff bar that has a fixed point of rotation. Depending on the length of the arm and the distance of the applied force to the rotation point, it is possible to apply a small force at one end which causes a larger effect at the other.

The fourth principle is the inclined plane. Depending on the inclination of the plane, the magnitude of the force required to move an object changes. The relation is that the smaller the angle α the smaller the force that must be made to move the object but greater is the distance needed to achieve a determined height (Schumacher *et al.*, 2010).

The authors continue by stating that if one extends these basic principles, it is possible to create machines that allow for more complex movements. For example, the winch that combines the principles of the lever and the rope and pulley, or a screw, whose basic principle is the same as the inclined plane wrapped around an axis, that can convert rotational movement into linear (Schumacher *et al.*, 2010).

Figures 2.25, 2.26, 2.27 and 2.28 present the possibilities of a combination of simple machines (or mechanisms) as rope winches, bands and belts, gears and rod systems, by Schumacher *et al.*, 2010.

³ For more information on these types of linkages, please refer to You and Chen (2012) pp. 17-33.

Figure 2. 25.
 Rope winches
 Source: Schumacher
 et al. 2010

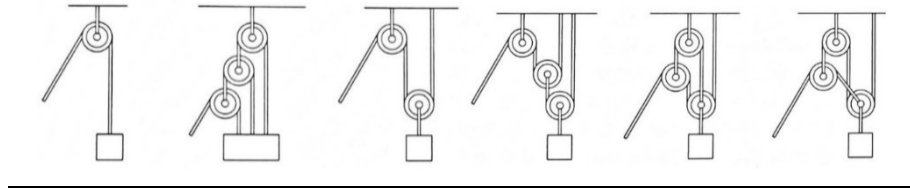


Figure 2. 26.
 Bands and belts
 Source: Schumacher
 et al. 2010

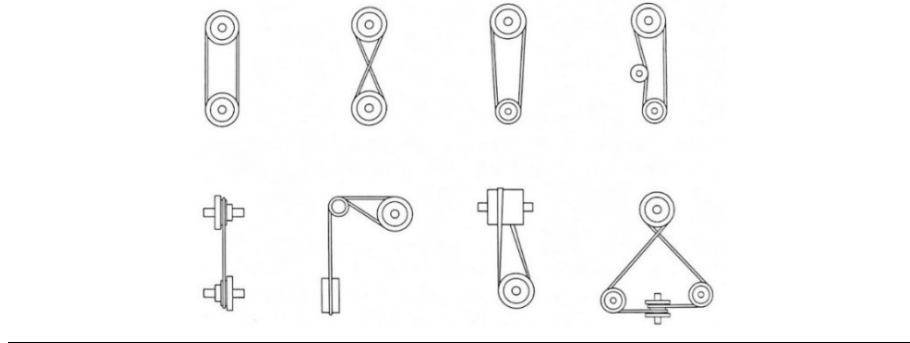


Figure 2. 27.
 Gears
 Source: Schumacher
 et al. 2010

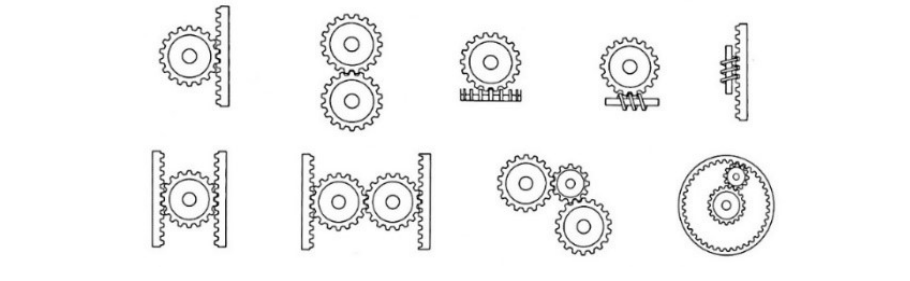
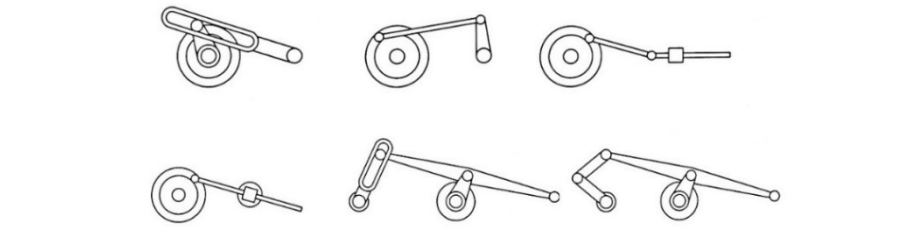


Figure 2. 28.
 Rods
 Source: Schumacher
 et al. 2010



You and Chen (2012) state that there are similarities between a **motion structure** and a **mechanism** but there are also significant differences. The first difference relates to the function of each one as the function of a motion structure is to change its shape due to practical requirements instead of transmitting or controlling motions. Secondly, a motion structure is usually composed of many more parts than a conventional mechanism. The third reason is that, generally, motion structures use less different types of joints, but these must be much more robust than in common mechanisms (You and Chen, 2012).

In the case of kinetic structures, the load bearing elements must be able to transfer loads at the same time as allowing the element to move. To facilitate movement between two load-bearing elements, independent components are used such as bearings, that can accommodate rotation, translation or a combination of both (Schumacher *et al.*, 2010).

Whenever there are two building elements in contact through a movable connection there is friction, so sliding and roller bearings are used to reduce this effect as much as possible. Sliding bearings are able to support high loads, high speeds of revolution and are impact-resistant, noise-absorbent and highly durable. The only limitation of using these bearings for architecture is that it is necessary to use lubricants which requires periodic maintenance. Better suited for architectural applications are the **sliding bearings** that are lubricant-free and require almost no maintenance, as are sliding bearings made of PTFE (Teflon) that in combination with steel surfaces have a very low coefficient of friction (Schumacher *et al.*, 2010).

Roller bearings use an intermediary element (balls or cylindrical bearings) that transfer forces from one contact surface to the other. These two types of bearings are the most commonly used in architecture but, for particular applications, floating bearings that employ water baths, electromagnetic forces, air cushions or air film systems can also be used (Schumacher *et al.*, 2010).

When the building elements are larger, and consequently heavier, there is often the need to use pre-mounted roller bearings that can be divided into radial or axial, depending on whether the load distributions are perpendicular or parallel to the axis of rotation. These are divided into **linear translation bearings** (mounted on rails), presented in **Figure 2.29**, and **rotary bearings** depicted in **Figures 2.30** and **2.31** (Schumacher *et al.*, 2010).

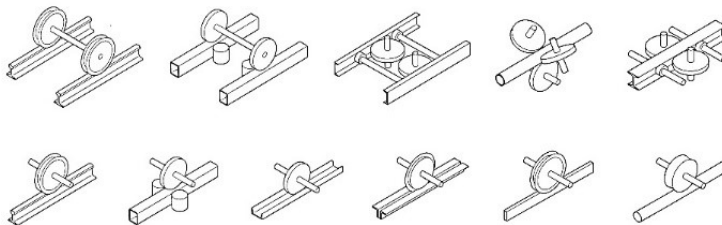


Figure 2.29.
Translation bearings
Source: Schumacher *et al.* 2010

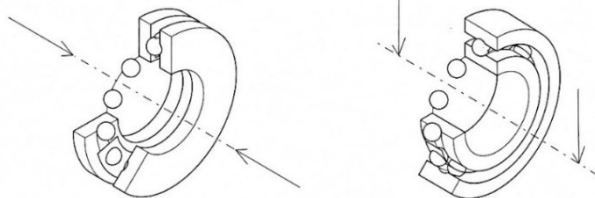


Figure 2.30.
Rotary bearings
Source: Schumacher *et al.* 2010

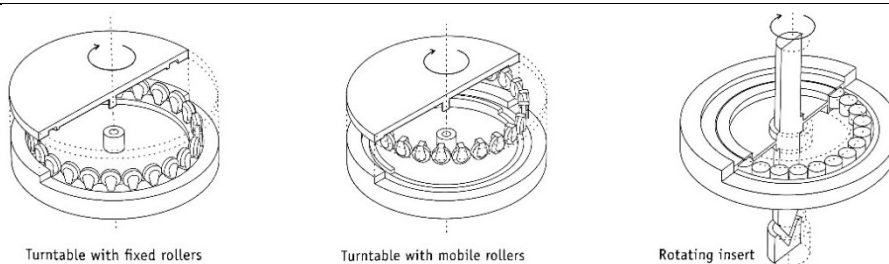


Figure 2.31.
Rotary bearings
Source: Schumacher *et al.* 2010

Pantographic Systems

Pantographic systems are linkages, since they only consist of rigid bars and revolute joints (lower pair joints), as defined by You and Chen (2012). The first known experiments with scissor mechanisms for architectural structures were those developed by Emilio Perez Piñero in 1961 (Válcárcel and Escrig, 1992), being further developed by Theodore Zeigler (1977), Escrig and Valcárcel (1993), and Chuck Hoberman (1991), as stated by Jensen (2004) and Yar *et al.* (2017). Following the work of the above-mentioned authors, important developments were achieved by You and Pellegrino (1997), Akgun *et al.* (2011), Li *et al.* (2016) and Yar *et al.* (2017).

Pantographic, scissor-systems or double chain linkages (You and Chen, 2012) are all names for the same systems that are composed of basic units, the Scissor-Like Elements (SLE). SLEs consist of two straight or angulated struts that are connected to each other at their midpoint, or not, by a revolute joint, so that the free rotation of one rod in relation to the other is allowed but any other relative motions are prevented (You and Chen 2012).

It is the shape of the bars (straight or angulated) and the position of the joint that determines the geometric path the system undertakes during deployment (You and Chen 2012) (Maden *et al.*, 2011) (Jensen, 2004).

You and Chen (2012) refer to the pantograph systems as double chain linkages, due to their appearance of two interwoven individual chains, and state that these linkages can be either planar or spherical. In the **planar double chain linkages**, the movement of all of the rigid elements happens on the same plane and the axis of the revolute joints are always perpendicular to that plane (You and Chen, 2012).

Depending on the design of the SLE, linear or radial movements can be achieved. The movements allowed by the units can be analysed through their **unit lines** (Figure 2.32). These lines are drawn between the endpoints of the two different bars on each side of the units (Yar *et al.*, 2017).

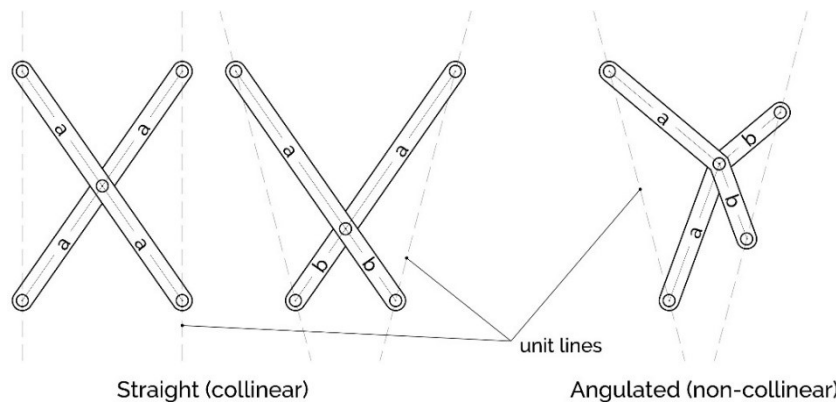


Figure 2.32.
Straight and
angulated scissor-
like elements

You and Chen (2012) defined two types of SLEs based on the location of the central revolute joint and its distance to the points of connection with subsequent units, collinear and non-collinear SLEs. The SLEs are collinear when the three points of each bar exist on the same line, or non-collinear when the bars are not straight but angulated, and the revolute joint that connects the two bars of the unit is on the kink. These two types are commonly referred as **straight** (collinear) and **angulated** (non-collinear) (You and Chen, 2012) (Yar *et al.*, 2017).

Planar Double Chain Linkages

Straight SLEs

Straight SLEs can be one of two types, **translational** or **polar**, depending on their deployment path, which is defined by the position of the pivot along the bars of each unit.

The **translational units** (Figure 2.33) have a connecting revolute joint at the midpoint of both rods. The most remarkable characteristic of this unit is that its unit lines remain parallel during the deployment and retraction processes (Maden *et al.*, 2011) (You and Chen 2012) (Yar *et al.*, 2017).

This feature is the base of the well-known Lazy-Tong System that has been widely used on elevator doors, mirrors, retractable closure systems for windows, etc, for which rails are often used as a materialization of the unit lines (You and Chen 2012) (Yar *et al.*, 2017).

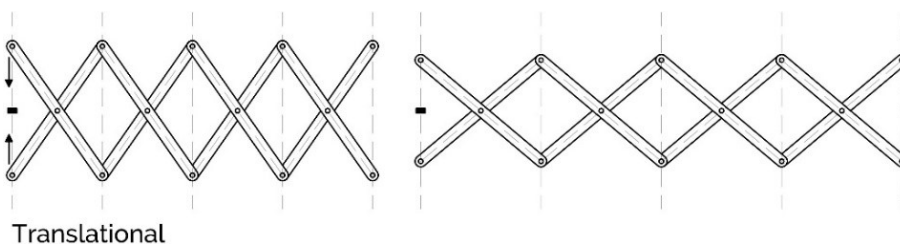


Figure 2.33. Double chain linkage composed of four translational SLEs and two deployment positions

The **polar units** (Figure 2.34) are created when the revolute joint is not at the middle point of the straight bars. In this case the unit lines are no longer parallel but radial. The angle between them varies during deployment, and consequently the curvature of the system that draws concentric circles while expanding (Yar *et al.*, 2017).

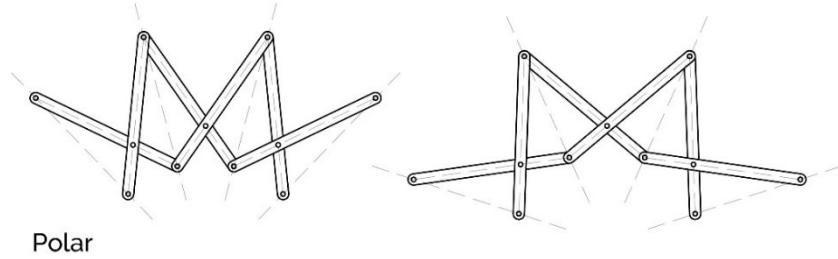


Figure 2.34.
 Double chain linkage
 composed of three
 polar SLEs and two
 deployment positions

These units are not suited to construct mobile planar **closed** double chains (**Figure 2.35**) because the mechanism loses its mobility; it transforms itself into a simple structure⁴ (Maden *et al.*, 2011) (You and Chen, 2012).

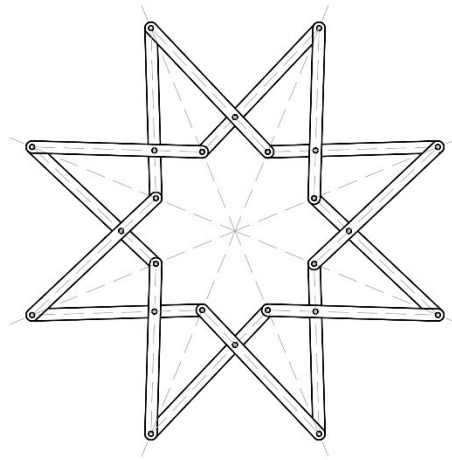


Figure 2.35.
 Closed loop with zero
 mobility formed by
 eight polar SLEs

You and Chen (2012) also demonstrate ways of connecting polar units to achieve translational movements or how to use special units as a connection between other types of SLEs (**Figure 2.36**), which they call the **alternative intermediate tie** (You and Chen, 2012). These elements can connect rings of other elements as long as they maintain relations of parallelism between the connected SLEs.

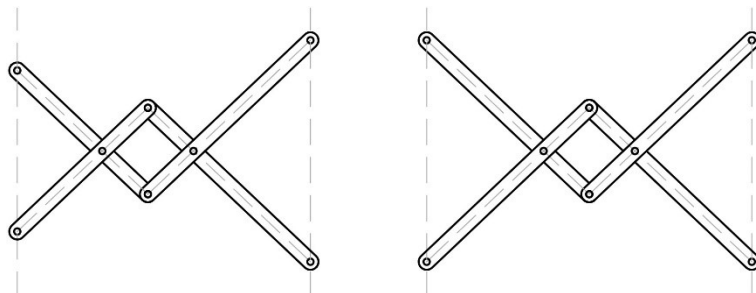


Figure 2.36.
 Intermediate Ties as
 proposed by You and
 Chen, 2012.

⁴ Proof at You and Chen 2012, pp. 38.

Angulated SLEs

The **basic angulated scissor unit**, invented by Hoberman in 1990, “can be used to form planar double chains where the mobility of individual elements is retained (You and Chen 2012, pp. 38).”

This unit is composed of two identical angulated bars, that is, with the same kink angle and the same lengths on each arm of the angulated rods (**Figure 2.37**). These units allow for deployment to occur in a permanent radial direction, which means that the unit lines do not change during the deployment process. As the structure expands, the two layers of angulated struts rotate in equal but opposite directions, one layer (that corresponds to all of the above or below struts, which must be placed in the same direction) rotates clockwise as the other rotates counter-clockwise (Maden *et al.*, 2011) (Jensen, 2004).

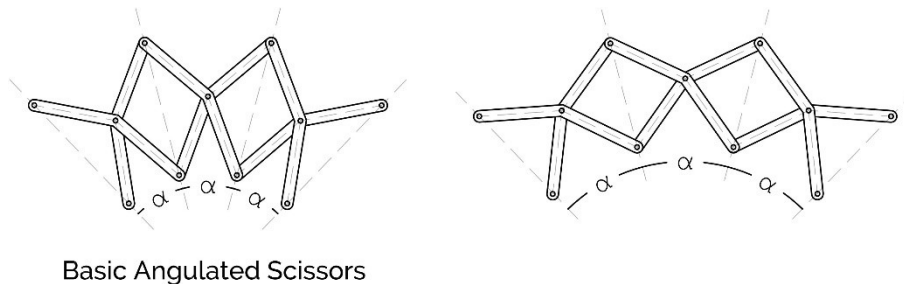


Figure 2.37. Double Chain Linkage composed of three Basic Angulated SLEs and two deployment positions

This was the principle used by Hoberman to create the Expanding Sphere. It was created in 1992 to be the centerpiece of the atrium in New Jersey’s Liberty Science Centre, which led to the creation of the Hoberman Sphere (**Figure 2.38**), a well-known toy that started to be sold in 1999. As stated by Zuk and Clark (1970, pp.51) “toys are not to be discounted as generators of ideas, for many profound principles of dynamics can be found in them.”

In the Hoberman Sphere, closed loops are created along the large circles of the sphere, so Hoberman relates the unit lines of pantographic elements to the normal elements of a 3D surface. “Basically, the process involves moving from surface properties in their pure mathematical form and translating them into linkage properties (Hoberman, 2015, pp. 110)”. He used this reasoning for other three-dimensional surfaces such as the Expanding Helicoid, 1997, shown in **Figure 2.39**. The principle behind these designs is that the form is always similar, only changing in size. Hoberman called this kind of structures as **shape-invariant expanding structures** (Hoberman, 1991) (You and Chen 2012) (Hoberman, 2015).

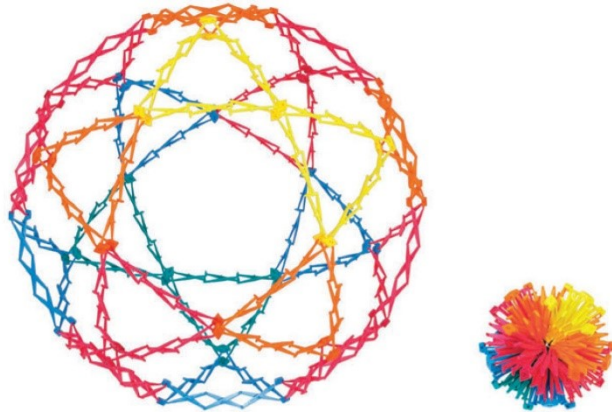


Figure 2.38.
 Hoberman Sphere
 Source: Hoberman,
 2012

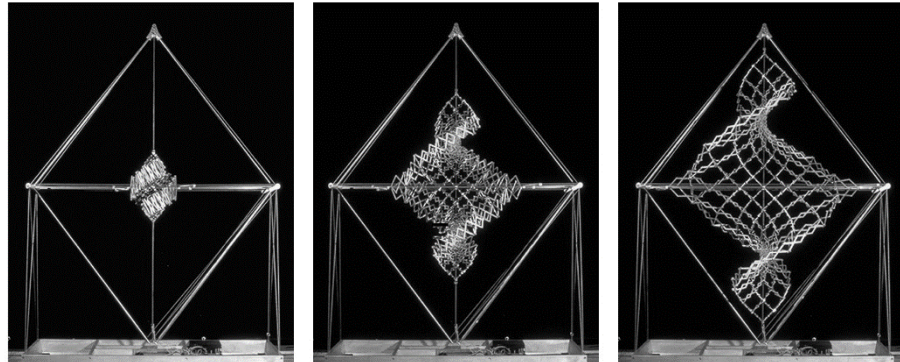


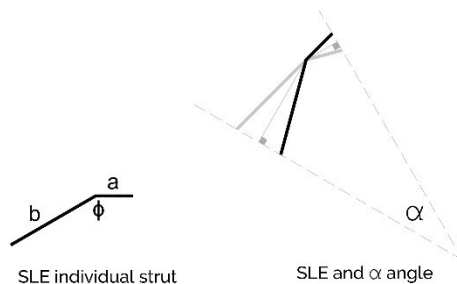
Figure 2.39.
 Expanding Helicoid
 Source: Hoberman,
 2012

To design this basic unit of shape-invariant expanding structures, You and Chen (2012) provide all of the necessary geometric relations. In addition to the similarity of the struts that make the unit, the pivot point must be placed at the intersection of two perpendiculars to the unit lines and the α angle between the unit lines is given by the difference between π and the kink angle ϕ (**Equation 2.1** and **Figure 2.40**).

Equation 2.1.
 Source: You and
 Chen, 2012

$$\alpha = \pi - \phi$$

Figure 2.40.
 Geometric relations
 for the design of
 generalized
 angulated SLEs



You and Chen (2012), propose a way to connect these generic units in a closed loop when it is not possible to simply translate the SLEs for connection, due to the α angle or the semi-lengths of the rods that do not allow for direct connection. The authors propose the use of symmetry (**Figure 2.41**) as a

possible strategy to create a functional, movable closed loop (You and Chen 2012).

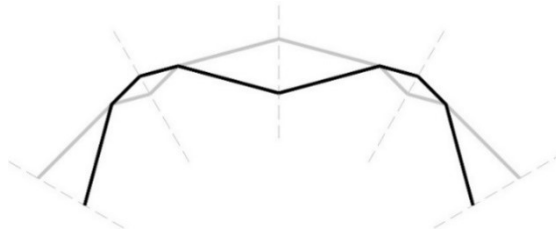


Figure 2. 41.
Addition of non-symmetric SLEs using symmetry

You and Chen (2012) also define the **Loop Parallelogram Constraint**⁵ for the creation of mobile closed loops with angulated SLEs. The authors prove that, for a **closed loop** to be mobile, the space between connected SLEs must be a parallelogram (**Figure 2.42**), otherwise the system will have no mobility (You and Chen 2012).

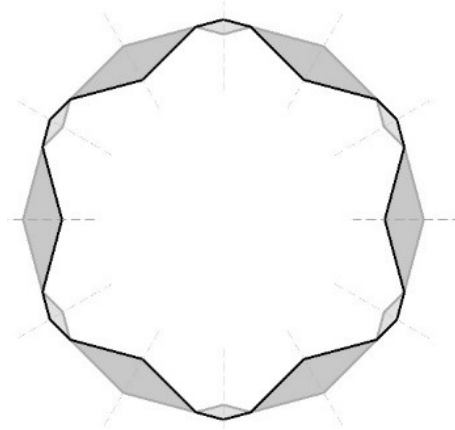


Figure 2. 42.
Closed double chain linkage with parallelograms between SLEs in grey and light grey

SLEs with different characteristics can also be combined (**Figure 2.43**) if the connection points are assured and if the **parallelogram constraint** is guaranteed (You and Chen 2012) (Yar *et al.*, 2017).

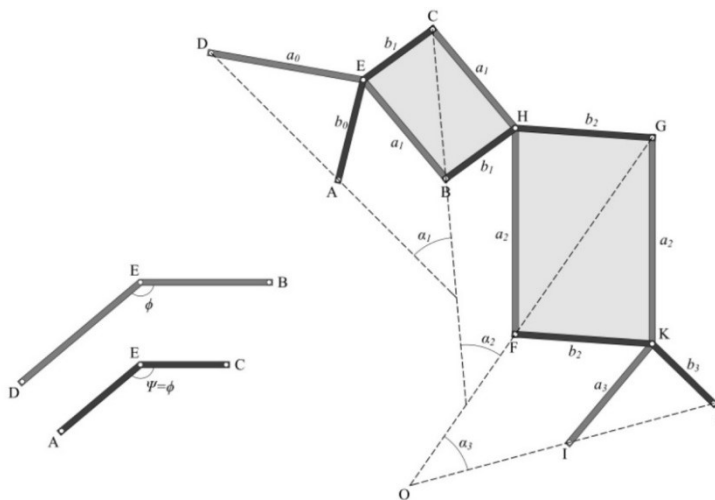


Figure 2. 43.
Connection of non-similar SLEs
Source: Yar *et al.*, 2017

⁵ For further explanations and Proof of the Loop Parallelogram Constraint please refer to You and Chen, 2012, pp. 42-58.

Hoberman, in his 1991 patent, proposes the addition of planar closed loop chains (**Figure 2.44**) by connecting the upper ends of one ring to the lower ends of another. The units of the subsequent rings have the same kink angle, naturally, since the α angle is maintained, but the lengths of the arms are consecutively smaller.

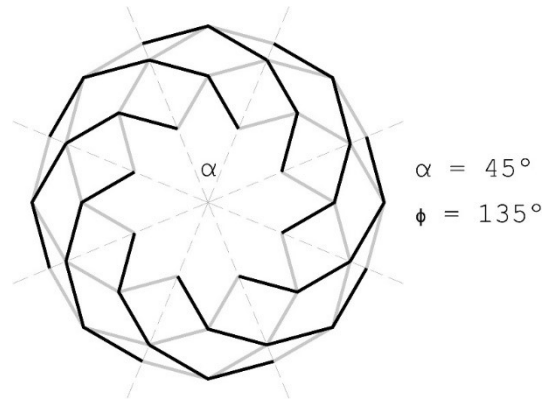


Figure 2.44.
 Addition of Planar
 Closed Loop Chains

You and Pellegrino (1997) found that, in fact, this assembly maintains a constant angle in the strut connection of each ring and thus they can be rigidly connected to each other, consequently forming single multi-angulated elements with more than one kink (You and Pellegrino, 1997) (Jensen, 2004) (Maden *et al.*, 2011).

Additionally, You and Pellegrino (1997) defined two **generalized angulated elements** from Hoberman's invention, for open systems. The first is the **equilateral angulated element**, in which semi-lengths of the rods are equal, but the kink angles do not have necessarily to be. The second is the **Similar angulated element** where the struts have proportional semi-lengths and equal kink angles (You and Pellegrino, 1997) (Yar *et al.*, 2017).

Yar *et al.* (2017), based on Hoberman's and You and Pellegrino's work, developed two other types of SLEs (**Figure 2.45**). The authors call them the **kite** and **anti-kite** units due to the form generated by the assembly of units (Yar *et al.*, 2017).

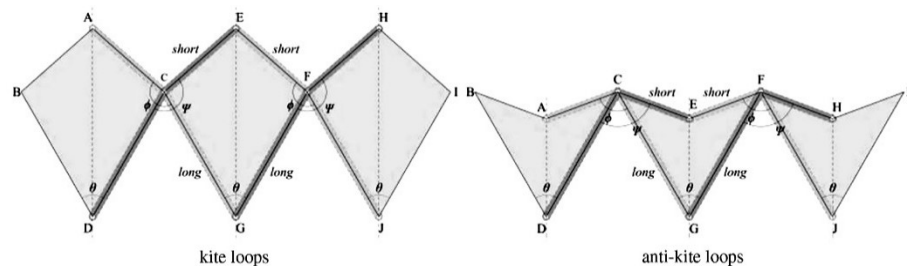


Figure 2.45.
 Yar *et al.*'s proposed
 Kite and Anti-Kite
 units
 Source: Yar *et al.*,
 2017

These units allow the structures to depart from a linear configuration (unit lines parallel) to convex or concave configurations. This means that the unit lines change their direction during deployment. The kite loops (**Figure 2.46**) maintain the kite form when bending downwards, but progressively turn into anti-kite loops when bending upwards. The anti-kite loops (**Figure 2.47**) maintain their form when bending upwards, but progressively turn into kite loops when bending downwards (Yar *et al.*, 2017)

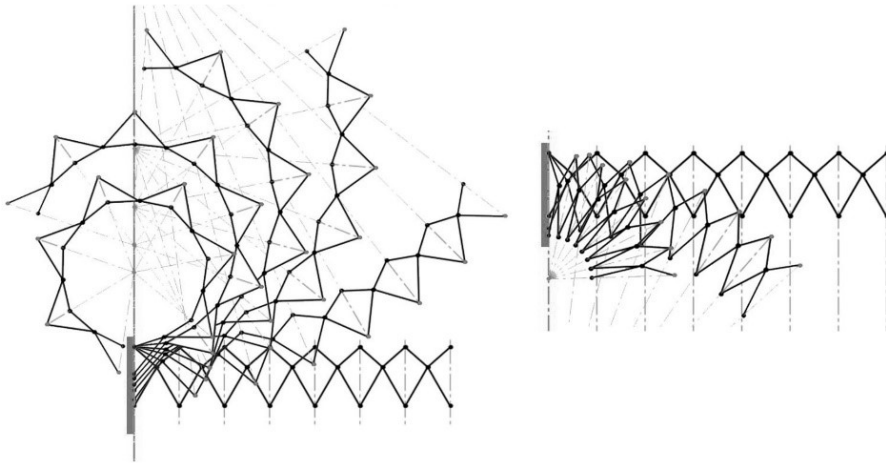


Figure 2. 46.
Deployment of kite
loop structures
Source: Yar *et al.*,
2017

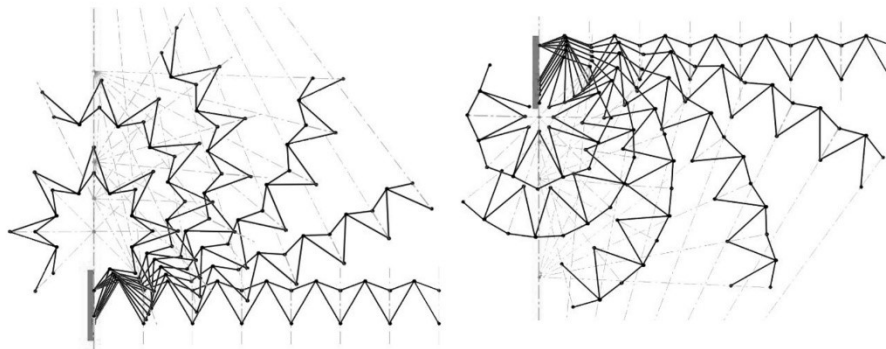


Figure 2. 47.
Deployment of anti-kite
loop structures
Source: Yar *et al.*,
2017

Other possibilities for Double Chain Linkages

Hoberman's Iris Dome

In 1991 Hoberman discovered a way to use angulated SLEs to create his Iris Dome (**Figure 2.48**), a dome that opens and closes in a similar way to the iris of an eye. This idea was first demonstrated in an indoor structure at The Museum of Modern Art (MoMa), NY, USA, 1994 and later used in outdoor structures, with variations in form. In 2000 it was used in a half ellipsoid form, in the Expo2000, Hanover, Germany (**Figure 2.49**), and in 2001 as the arch of the 2002 Winter Olympics in Salt Lake City, USA (**Figure 2.50**) (Hoberman, 2015).

Figure 2.48.
Iris Dome, MoMa,
1994
Source: Hoberman,
2012

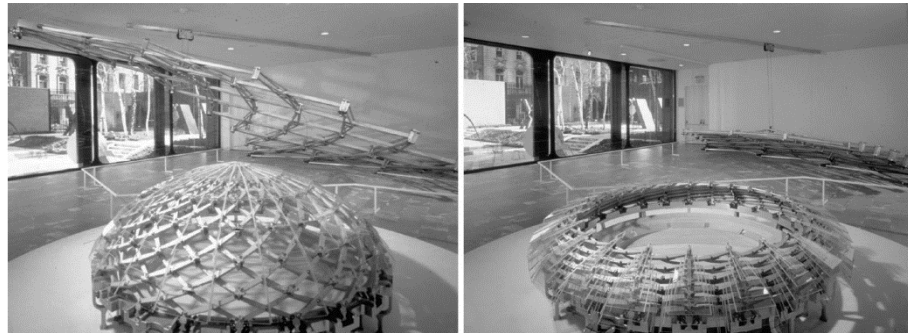
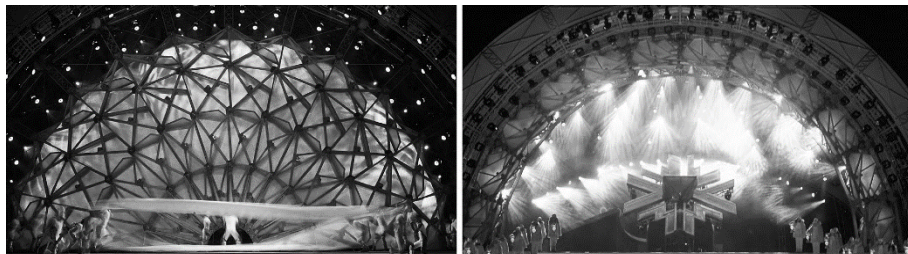


Figure 2.49.
Iris Dome, Hanover,
2000
Source: Hoberman,
2012



Figure 2.50.
Winter Olympics
Arch, Salt Lake City,
USA, 2002
Source: Hoberman,
2012



This technique originated by Hoberman shows that it is possible to use the angulated SLEs in a conical surface if all of the connectors are cylindrical

hinges perpendicular to the plane defined by the four extreme points of the angulated rods, “therefore, the pair of angulated rods is kinematically identical to a flat element (Pellegrino, 2001, pp. 33)”.⁶ Variants of plan shapes and domes following Hoberman’s work can be found in You and Pellegrino, 1997. In 2001, Pellegrino demonstrated the process for the design and assembly of angulated SLEs to be used in the construction of curved kinematic surfaces as shown in **Figure 2.51**.

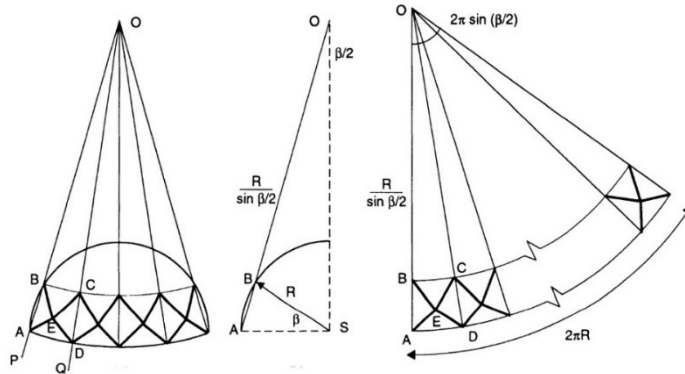


Figure 2. 51.
Relations for drawing
and assembly of
angulated SLEs for
curved surfaces
Source: Pellegrino,
2001

As a way of covering these pantographic retractable structures, Hoberman (1991) proposes the use of rigid panels that overlap in the retracted configuration, as shown in **Figure 2.52**.

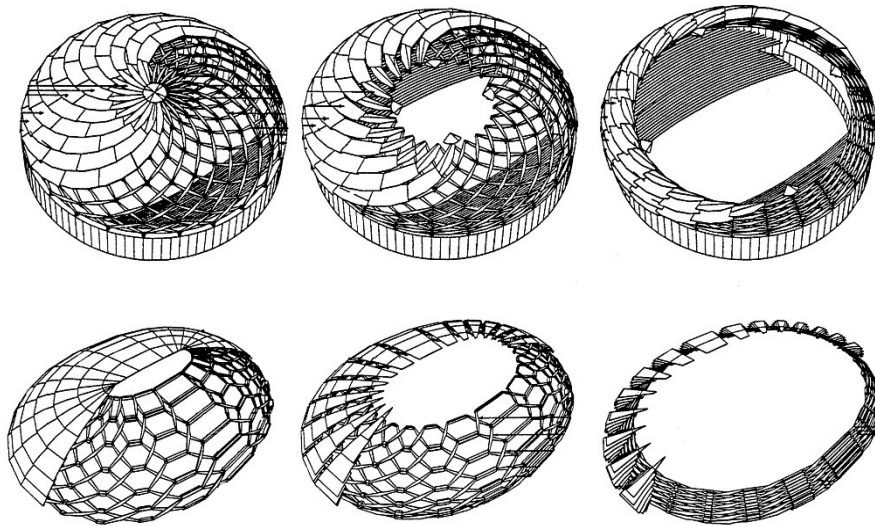


Figure 2. 52.
Hoberman’s proposal
for the cover of the
structures with rigid
panels
Source: Hoberman,
1991, adapted

⁶ For further explanations on how to design and connect SLEs to use in curved surfaces please refer to Pellegrino, 2001, pp. 31-34.

Pantographic Plates

Kassabian *et al.*, 1999, proposed a way of covering pantographic structures with rigid elements that could be attached to the structure and move with it during opening and closing without overlapping. They use a planar projection approach to guarantee the non-collision between elements, regardless of whether the structure is planar or three-dimensional. The elements can be triangles, or triangle-based forms, that can be reprojected onto the surface if the structure is not planar in order to determine their curvature. The authors propose covering solutions for circular (**Figure 2.53 (a) and (b)**) and elliptical planar projections (**Figure 2.53 (c)**) (Kassabian *et al.*, 1999).

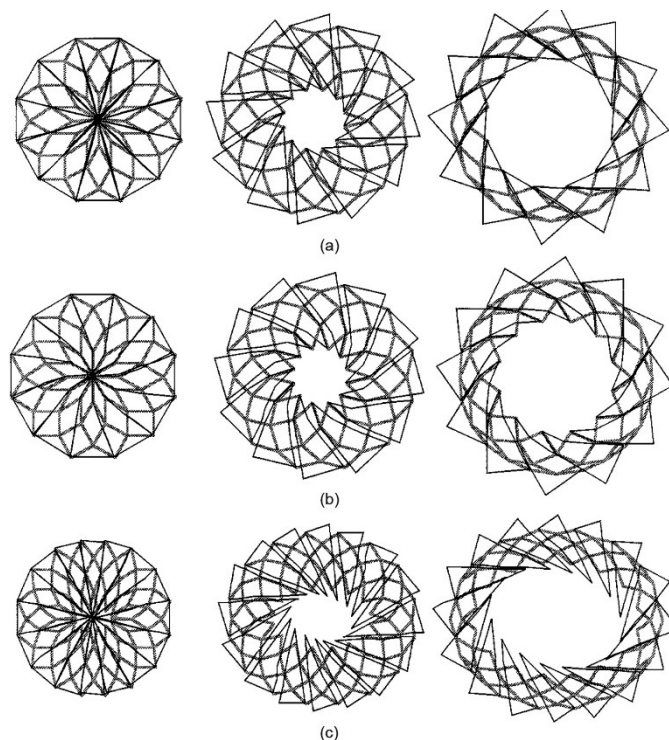


Figure 2.53.
Kassabian *et al.*'s
proposal for the
covering of
pantographic
structures, 1999
Source: Kassabian *et al.*, 1999

The work of Kassabian *et al.* (1999) was extended by Jensen and Pellegrino (2002), and Jensen (2004) for circular and non-circular planar structures with no overlapping. The authors use a different approach to Kassabian *et al.* (1999), instead of covering the pantographic structure they use pantographic plates. These plates have specific points of rotation between them that act as planar pantographic systems. At the same time, the rigid panels have a design that allow them to perfectly juxtapose in the closed position and ensures that there are no collisions, during deployment and retraction, between panels, as demonstrated by **Figures 2.54, 2.55 and 2.56** (Jensen and Pellegrino, 2002) (Jensen, 2004).

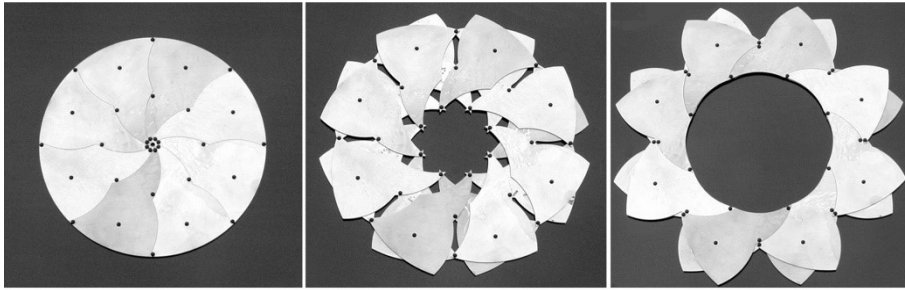


Figure 2. 54.
Model of planar expandable structure with rigid plates as pantographs
Source: Jensen and Pellegrino, 2002

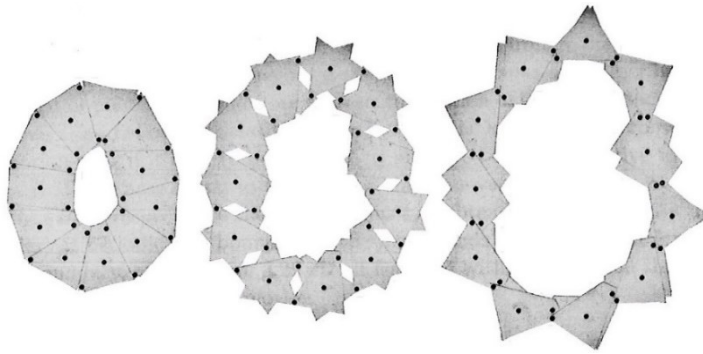


Figure 2. 55.
Cardboard model of non-circular plate structure
Source: Jensen, 2004

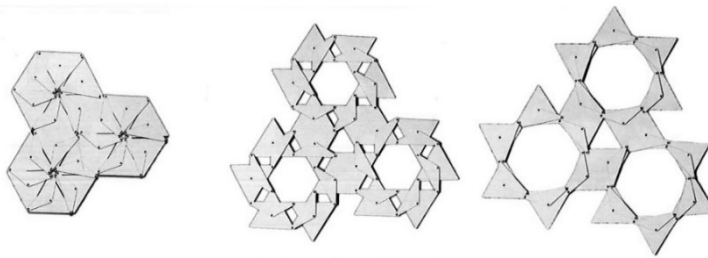


Figure 2. 56.
Cardboard model of the assembly of modular hexagonal structures
Source: Jensen, 2004

Origami as Spherical Mechanisms

You and Chen (2012), defined spherical mechanisms as “a mechanism where all of the links are constrained to rotate about the same fixed point in space” (You and Chen, 2012, pp. 9). This leads to concentric spherical trajectories of the points at the links around the centre point of the mechanism, to which all linkages converge, known as the concurrency point (You and Chen, 2012). A rigid origami vertex with n concurrent creases acts as a spherical mechanism where the vertex is a spherical joint and the creases are n revolute joints as demonstrated by You and Chen (2012) and shown in **Figure 2.57**.

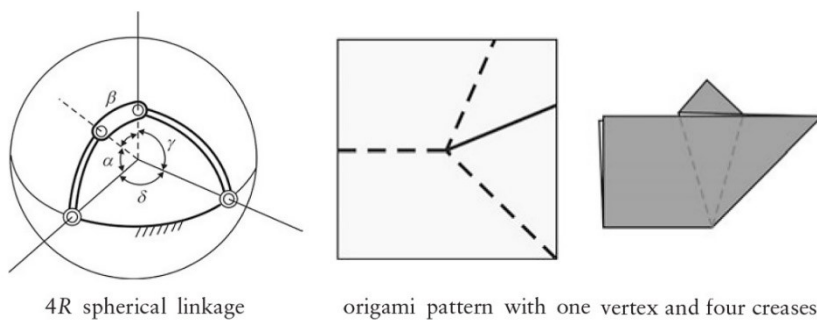


Figure 2. 57.
Comparison between 4R spherical linkage and an Origami vertex with four creases
Source: You and Chen, 2012

As defined by Edmondson *et al.*, 2015: “Kinematic origami may be modelled as a network of spherical mechanisms where panels are links and folds are joints and can be analysed using spherical kinematics theory. Each vertex within the structure is modelled as a spherical kinematic mechanism (Edmondson *et al.*, 2015, pp.150).”

Robert Lang (2018) determines that the DoF of a vertex of degree n is $n-3$, which means that a degree 4 vertex has only one DoF, and a degree-6 vertex has three Degrees of Freedom (Lang, 2018).

Bowen *et al.*, 2013, developed a classification for kinematic origami based on their actions as spherical mechanisms. The authors’ work intends to deeply understand the mechanisms that make origami⁷ models move but that are also relevant for general origami kinematics as well. The authors use graphs to establish the relationship between vertices that can be in an open chain or a network. In order to establish whether arrangement is an open chain or a network, it is necessary to define if it is possible to trace a closed path (loop) between at least three vertices; if not then the assembly is an open chain (Figure 2.58), if possible then it is a network (Figure 2.59) (Bowen *et al.*, 2013).

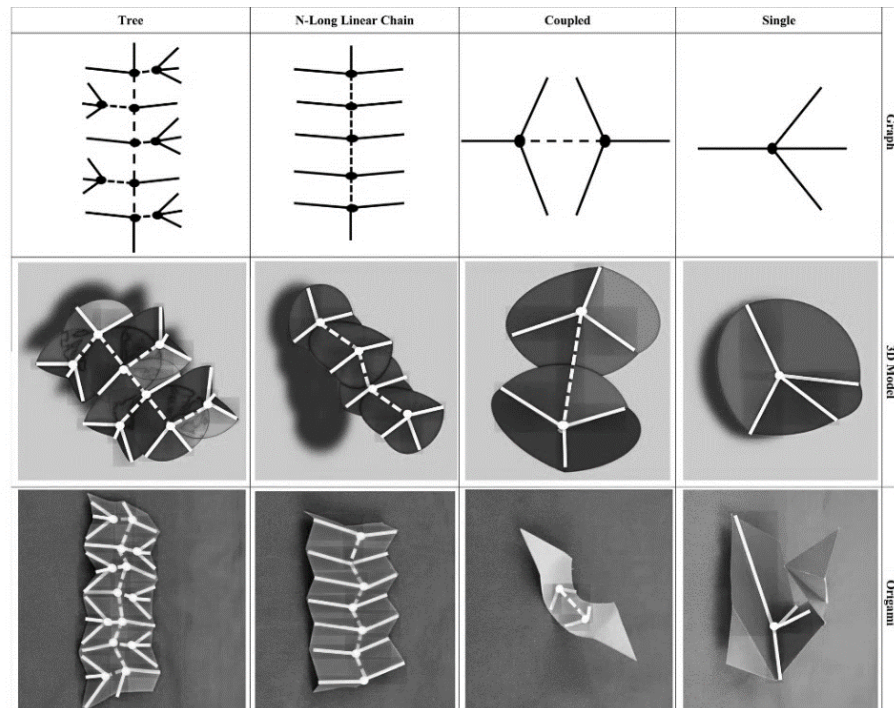


Figure 2. 58.
 Spherical
 Mechanisms in Open
 Chains
 Source: Bowen *et al.*,
 2013

⁷ Action Origami models are models that on the final folded state have mobility, like Shafer's "Chomper" or Robert Lang's "Indian Paddling a Canoe" and "Manatee" (Bowen *et al.*, 2013).

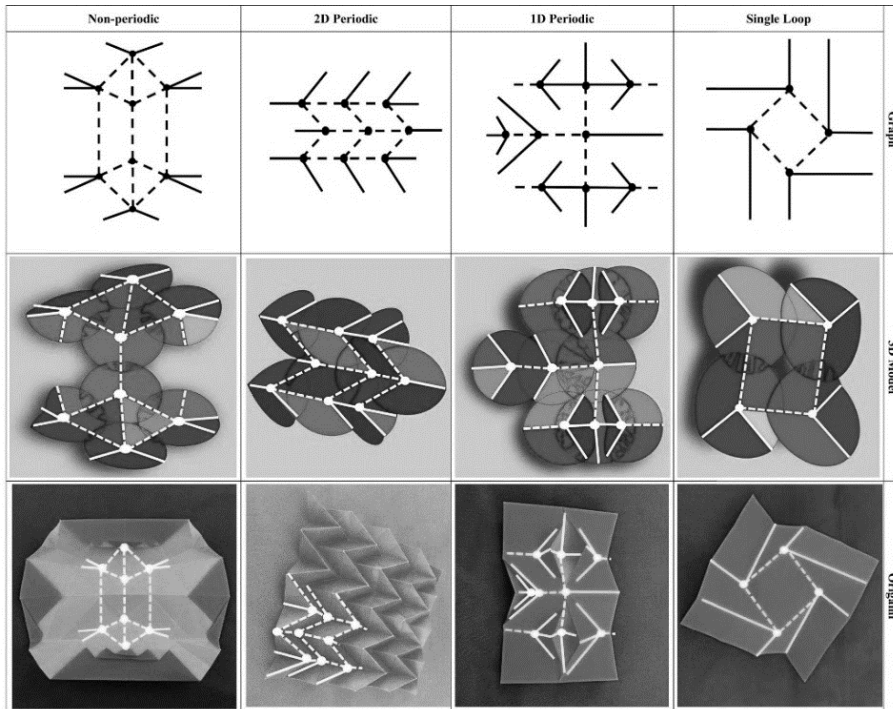


Figure 2. 59.
Spherical Mechanisms
in Networks
Source: Bowen *et al.*,
2013

Dureisseix (2012) and Zhang *et al.* (2015) also argue that Origami can be seen as a mechanism and prove it by analysing the kinematic properties of some crease patterns and constructing their equivalent kinematic model. Zhang *et al.* (2015) study the Huffman Base (a), Rectangular Tile (b) and the Waterbomb Base (c) through screw algebra and create the kinematic equivalent models for each one, as shown in **Figures 2.60** and **2.61**.

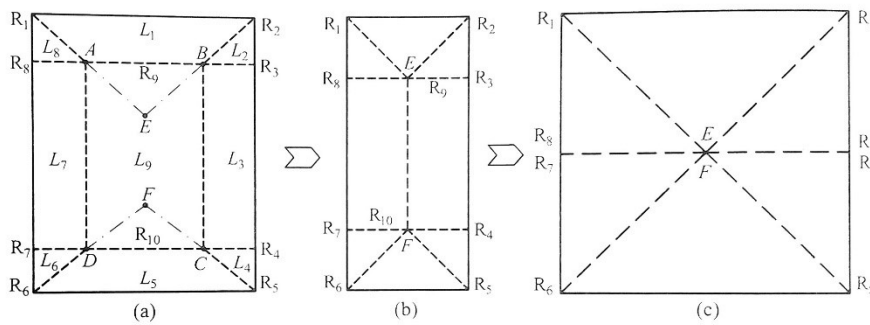


Figure 2. 60.
Crease Patterns of the
bases
Source: Zhang *et al.*,
2015

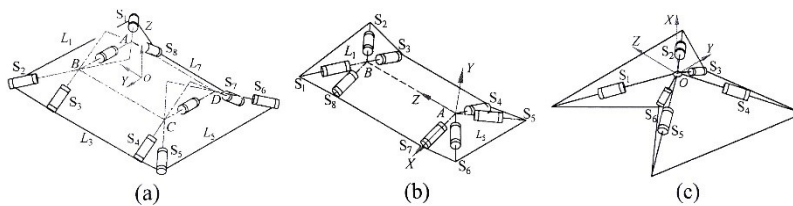


Figure 2. 61.
Kinematic equivalents for
each base
Source: Zhang *et al.*,
2015

The authors refer to origami bases as typical closed loop mechanisms with pure compliant rotary hinges and define origami tessellations as the sum of multiple bases which can be seen “as a *hyper-redundant mechanism with integrated closed-loop modules*” (Zhang *et al.*, 2015, pp. 140).

Smart Materials as Mechanisms

Since the 90s, architecture has witnessed a remarkable increase in the birth of a new type of materials, smart materials. These materials can change their properties at a micro or nano scale or can transform energy in response to stimuli from the environment or computer-controlled inputs (Addington and Schodek, 2005) (Schumacher *et al.*, 2010).

Schumacher *et al.* (2010) divided this new type of materials into semi-smart and smart materials. The semi-smart are materials that can change their properties once, or only a few times, and smart materials are those that are able to change their properties both reversibly and permanently (Schumacher *et al.*, 2010).

Addington and Schodek (2005) make a different division, as they split smart materials into two categories; materials that change one or more of their properties (Chemical, electrical, magnetic, mechanical or thermal) in response to direct stimuli from the surrounding environment, and materials that are capable of transforming received energy into other types of energy, like photovoltaic, thermoelectric, piezoelectric, photoluminescent and electrostrictive materials (Addington and Schodek, 2005) (Fox, 2015).

For the present dissertation the smart materials that are particularly important are those from the first group defined by Addington and Schodek, the ones that can lead to movement through a change in their properties, making these materials act as mechanisms, as defined by Fox (2015, pp. 165) “*the material structure itself is the machine.*”

A perfect example of the use of a smart material in this perspective is Achim Menges’s Hygroscope (**Figure 2.62**), created in collaboration with Steffen Reichert, and exhibited at the Centre Pompidou, in 2012. The smart material used is a very thin wood sheet that, due to the **intrinsic properties** of the material, bends when humidity levels change, without the need of any kind of technology, additional mechanisms or energy (Fox, 2015) (Parlac, 2015).



Figure 2.62.
Hygroscope, Achim
Menges in
collaboration with
Steffen Reichert,
Centre Pompidou,
Paris, 2012
Source:
achimmenges.net

Thermostatic bimetals have been used for many years in thermostats in order to switch devices on and off but are now being transferred to the scale of architecture (Parlac, 2015).

These materials are usually thin plates or bands that consist of two different metals with different thermal expansion coefficients, the one with the largest coefficient is called the active element. Typically, a combination of zinc and steel or bronze and steel is used and are fused together. Bimetals are capable of autonomously adapting to changes in temperature caused by solar radiation, such as Bloom by Doris Sung (2011) (**Figure 2.63**) a shading canopy that closes when heated and opens as temperature drops (Schumacher *et al.*, 2010) (Parlac, 2015).



Figure 2.63.
Bloom, Doris Sung,
M&A Gallery, Silver
Lake, CA, 2011
Source: dosu-arch.com

Furthermore, Shape Memory Alloys (SMA), made with plastics or metals, can deform in a predetermined manner. The most common metal SMAs include gold-cadmium alloys, copper-zinc alloys and nickel-titanium alloys (nitinol). These materials have shape memory properties, so they are able to deform and revert to their original form in response to changes in temperature or when an electrical current is applied (Schumacher *et al.*, 2010) (Parlac, 2015).

As examples of the research being done on these types of materials, there is the “Living Glass” prototype by David Benjamin and Soo-in Yang (the Living Office), which is a silicone membrane with slits lined with Flexinol (metallic SMA). When an electrical current is applied it opens allowing air to flow in and when it is off, it returns to a closed state. This same formal strategy was explored by Nick Puckett in “Dynamic Skin”. This is a shape memory polymer with open forms cut into the design, that bend when the polymer is exposed to light, creating air passages that close when it cools down.

The “Agile Spaces” prototypes, developed by Vera Parlac in the last few years, use SMA metallic wires that are strategically integrated into surfaces following their lattice structure, and that are activated through a network of sensors allowing the surface to sense its environment and respond by changing its shape. The “Flectofin Façade System”, by Simon Schleicher from ITKE – University of Stuttgart, is a hingeless system in which fins for solar shading can rotate 90° through changes in temperature but that can also be rotated by user’s decision if needed (Schumacher *et al.*, 2010) (Parlac, 2015). Other promising materials, that are still being developed and thus have not yet reached architectural use, are small computers that can work together to form shapes, such as the work being developed at Carnegie Mellon, and materials that are derived from synthetic biology. These materials are capable of decision making, and thus responsiveness, through chemical computation within their molecules, giving them the ability to change form, function, or appearance. Programmable Matter could also be a very promising material. Harvard Micro robotics Lab and MIT are developing a material that is pre-programmed sheet. This material is a thin resin-fiberglass composite sheet, divided into triangular faces that have heat sensitive connections that can fold into a particular shape, such as an origami boat or airplane, depending on the program used (Parlac, 2015).

Actuators

Any mechanical system needs a source of energy in order to move. The source can be direct actuation by a user (manual actuation) or it can have other energy sources. These can be natural sources such as gravity, solar or wind power, or other sources like thermal, electrical, pneumatic, hydraulic, biological, chemical or magnetic power (Kolovsky *et al.*, 2000) (Schumacher *et al.*, 2010) (Stevenson, 2011).

Energy sources make engines work which, in turn, provide mechanical power in the form of translational or rotational movements. These engines are the

actuators that put mechanical systems in action. The mechanical system may replicate the movement of the engine or turn it into another type of movement (translational, rotational, or combined) (Kolovsky *et al.*, 2000).

Electromechanical actuators, such as electric motors, might come in numerous configurations, scales and power capacity, but they always consist of at least one fixed element (stator) and one moving element (rotator or armature). Electric linear motors move the rotor in a linear way in respect to the stator. Electric rotary motors work by rotating the axis of the rotor (Schumacher *et al.*, 2010).

Working in a different way, but also with a need for electrical current, there are less complex elements that can be actuators such as electroactive polymers, plastic fibres, films and metal alloys that are used as actuators in wires, rods and springs. These materials deform when electricity is applied, and this deformation can be used as the movement actuator for a given mechanical system (Schumacher *et al.*, 2010).

Hydraulic and pneumatic actuators use the pressure of low-compression oils or gases to work. These actuators have great power capacity when compared to their size, but they are relatively inefficient and so require greater energy input. The basic element of these actuators is a motorised pump that builds up the necessary pressure using blades, gears, screws or pistons. It creates a volumetric flow that is conducted through pressure lines into a pressure cylinder or jack (translational movement) or a hydraulic or pneumatic motor (rotational movement). These actuators are usually very silent and very precise, since they use oil volume to generate movement and oil does not compress. These reasons make them very useful for architecture, but also, as discussed before, they need more regular maintenance compared to electrical ones (Schumacher *et al.*, 2010).

Pneumatic actuators in architecture have a particularly interesting case, as the pneumatic muscles (like tensairities) are usually tubular or cushion like chambers that expand and contract through the pressure of gases inside (Schumacher *et al.*, 2010).

A very important issue when deciding on actuators for architecture is the size of the element to move. Within the same building scale, it is possible to have structures with tonnes which require high capacity actuators such as those explained earlier, or light structures or skins that may be moved with micro actuators. When using micro actuators, the technology can be integrated directly into the moving element (Schumacher *et al.*, 2010).

Control

The control of the actuators for kinetic architectural structures can be done with a simple on/off switch or it can have a gradient of actions and velocities when controlling the structure. In the case of electrical motors, it is usually enough to apply different electrical voltages in order to control their speed (Schumacher *et al.*, 2010).

Computerized systems and **microcontrollers** are increasingly being used within the structure of the buildings. These devices can gather information, process it, and use it to regulate and control the behaviour of structures. Since 2005, with the appearance of the arduino microcontroller board in Italy, a whole new world of possibilities for controlling architectural structures has emerged. These boards can receive input from several types of sensors (light, motion, touch, sound, temperature, etc) and can output a range of responses for actuators. They started to be used in architecture Universities, and by architects, which brought them closer to understanding how these boards work and their immense potential to be used in the control of architecture systems and kinetics (Stevenson, 2011) (Parlac 2015).

Finally, and with the same type of reasoning as microcontroller boards but even smaller there are the **Micro-Electro-Mechanical Systems (MEMS)**. These are very small electro-mechanical devices made of miniaturized structures, sensors, actuators and microelectronics that, due to their scale, can be embedded in other materials and sense changes in temperature, light, etc, as well as trigger the appropriate action (Parlac 2015).

2.2 | *Origami Geometry and Foldability*

Origami is a Japanese word that combines two words, “oru” (fold) and “kami” (paper). It is a generalized idea that Origami is the Japanese art of paper folding because Japan was the country most responsible for the development and dissemination of this art. Japan is also home to the first known publication on Origami, *Hiden Senbazuru Orikata*, published in 1797. Nevertheless, the origins of Origami are not yet undoubtedly established. Some authors argue that it began with the invention of paper itself, being a natural response to such an invention and, in this way, after China, Korea, and Japan, Spain, Italy and England followed suit. Others argue that it was invented in China around two thousand years ago, where it was known as *Zhe Zhi*, only being embraced by Japan later who would have given it the prominence that it holds today (Demaine and O’Rourke, 2007) (Hatori, 2011).

The author Koshiro Hatori argues that origami may not have been born in either Japan or China, claiming that there is no conclusive data to confirm the location and time of the appearance of the first origami models. Hatori also argues that there is no certainty that it was Japan who transmitted this art form to Europe. Hatori studied the models of origami found in Europe and Japan from the eighteenth and nineteenth centuries and argues that there are very few coincident models. The figures and folding styles were also quite different, leading him to believe that this art was developed simultaneously and independently in both East and West (Hatori, 2011).

In the nineteenth century there was the beginning of an exchange of influences between Europe and Japan, during the Meiji Restoration (between 1860 and 1870), when the European education system was introduced there. In regard to origami, the introduction of the Kindergarten Movement was particularly important, idealized by Friedrich Froebel around 1835. This movement included paper folding in its educational activities as a way to learn geometry. From this moment begins an exchange of knowledge, through people traveling between East and West and giving rise to the origami we know today (Demaine and O’Rourke, 2007) (Hatori, 2011).

Geometric Exercises in Paper Folding, by T. Sundara Row, 1893, was of great importance in the understanding of the geometric potential of origami. In this publication several constructions, usually made with straight edge and compass, are replicated and explained with origami (Row, 1893) (Demaine and O’Rourke, 2007).

Although the origins of origami are not yet fully proved, there is no doubt that origami is present in all cultures around the globe and in several objects of our

everyday life. From a simple folded letter, paper boxes and bags to clothing, folded tents, art works, architecture, solar sails and panels for space satellites and even in medical devices like stents for blood vessels (Demaine and O'Rourke, 2007) (You and Kuribayashi, 2009) (Miura, 2009) (Evans *et al.*, 2015 (b)).

Despite this presence in our daily life and even though origami has been used for hundreds of years it was only in the 80s that its mathematical and geometrical properties have started to be studied on a deeper level, granting it the status of a scientific research subject.

2.2.1 | Origami Geometry

Before diving into the geometry of origami it is important to understand origami terminology, therefore a clarification of specific origami definitions, retrieved from the contributions of Hull (2002), Lang (2010), Evans *et al.* (2015 (b)), is presented followingly:

- **Fold:** the act of bringing one point or line of the paper onto the paper itself and crease/bend the paper.
- **Mountain crease (or Fold):** the crease comes upwards creating a convex form. Graphically signalled as a continuous line.
- **Valley Crease (or Fold):** the paper bends downwards creating a concave form. Graphically signalled as a dashed line.
- **Crease pattern (CP):** the set of all of the folds (or creases), with their identity (mountain or valley) represented, necessary to fold one model from the beginning to the end. The CP can also be described as a "*planar embedding of a graph which represents the creases that are used in the final folded object*" (Hull, 2002, pp. 29)
A CP can also be called a Mountain-Valley (MV) assignment, which is a function that maps the set of creases to the plane (Hull, 2002).
- **Model:** the final folded piece (or set of pieces).
- **Vertex degree:** the number of creases that meet at a determined vertex.
- **Twist-fold:** very common type of fold in origami models where a polygonal face has parallel pairs of creases extending from each vertex, making the polygon rotate around itself and creating the overlapping of the neighbouring faces under itself. This type of fold is usually non-rigidly foldable and leads to locked models from the perspective of movement.
- **Tessellation:** the covering of a plane with one or multiple shapes repeated infinitely without gaps or overlaps, it can be also called the tiling of the plane.

Subsequently will be made a revision on origami geometry topics believed to be important for architecture and most particularly for kinetic architecture.

Great part of the reviewed literature belongs to the **Origami, Science, Mathematics and Education (OSME) Meetings**. These meetings were instrumental in the cementation of the importance of origami as a scientific subject and allowed for the diffusion of origami research and connections between origami scholars, namely architects, designers, mathematicians and computer scientists.

During the first two meetings, seven axioms of origami geometry and mathematics were presented and proved, known as the Huzita-Justin Axioms, which are very similar to the Euclidean axioms for constructions with straightedge and compass.

The first six axioms were defined by Huzita and the seventh was defined by Hatori in 2002, although it had already been formulated by Justin in 1996. These axioms are usually known as Huzita-Hatori or Huzita-Justin; this thesis will follow the Huzita-Justin nomenclature as has been referenced during the 5th, 6th and 7th OSME meetings.

The axioms defined by Huzita, Justin and Hatori set the fundamental rules for any possible operation to divide paper and define crease patterns by only using hands and the paper itself and refer to one folding motion at a time (Scimemi, 2002) (Lang, 2010).

- **Axiom 1:** *Given two points P_1 and P_2 , we can fold a line connecting them.* (Figure 2.64, left)

- **Axiom 2:** *Given two points P_1 and P_2 , we can fold P_1 onto P_2 .* (Figure 2.64, right)

This crease will be a straight line perpendicular to the line P_1P_2 that passes at its medium point. This is the base of the Voronoi Systems construction with origami (Scimemi, 2002) (Lang, 2010).

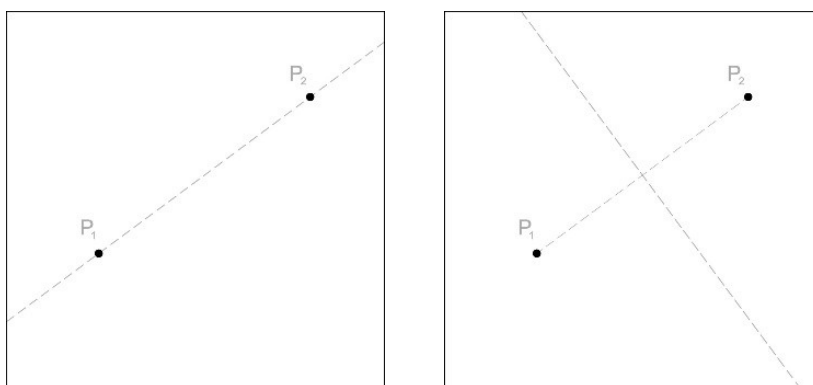


Figure 2. 64.
Axioms 1 and 2

-Axiom 3: Given two lines r_1 and r_2 , we can fold line r_1 onto r_2 . (Figure 2.65, left)

When r_1 and r_2 are not parallel this operation is the equivalent of finding the line that divides the angles formed by the two lines. If the lines are parallel, then this operation allows to find a third line that is parallel to the other two and equidistant to both (Scimemi, 2002) (Lang, 2010).

Axiom 4: Given a point P and a line r , we can make a fold perpendicular to r passing through the point P . (Figure 2.65, right)

To do this, it is necessary to make the line coincide with itself until the crease generated passes through P .

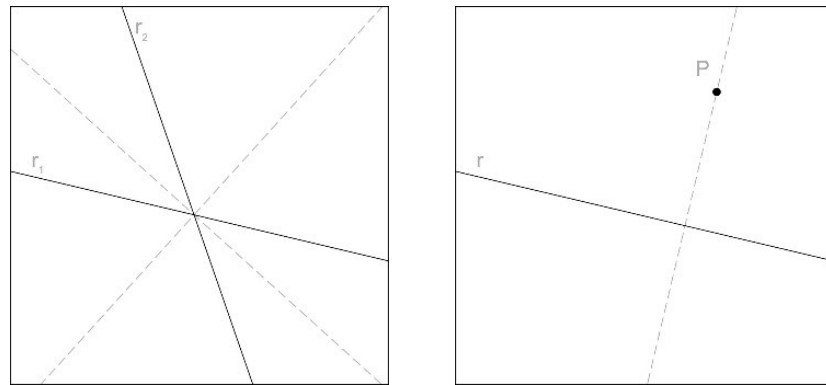


Figure 2. 65.
 Axioms 3 and 4

- Axiom 5: Given two points P_1 and P_2 and a line r , we can make a fold that places P_1 onto r and passes through the point P_2 . (Figure 2.66)

This axiom solves a quadratic equation; the obtained crease is the tangent to the parabola with focus on P_1 and directrix r (Lang, 2010).

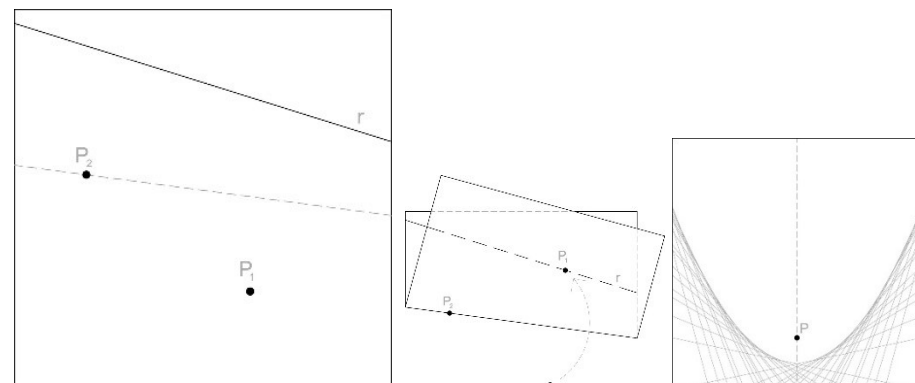


Figure 2. 66.
 Axiom 5

- **Axiom 6:** Given two points P_1 and P_2 and two lines r_1 and r_2 , we can make a fold that places P_1 onto line r_1 and places P_2 onto line r_2 . (**Figure 2.67, left**)

This axiom solves a cubic equation; the obtained crease is the tangent to two parabolas, one with focus on P_1 and directrix r_1 and the other with focus on P_2 and directrix r_2 (Lang, 2010).

- **Axiom 7:** Given a point P and two lines r_1 and r_2 , we can make a fold perpendicular to r_2 that places P onto line r_1 . (**Figure 2.67, right**)

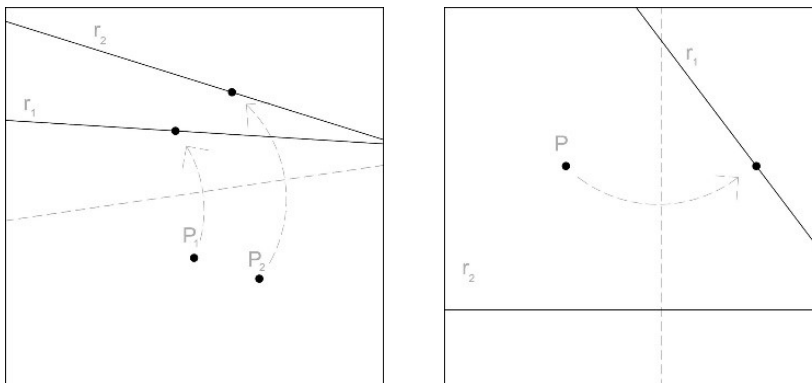


Figure 2. 67.
Axioms 6 and 7

Apart from the demonstration of the axioms, the OSME Meetings also enabled the presentation of uncountable two or three-dimensional **origami models**, from square or non-square paper, from one sheet only, several sheets or the combination of modules, where cutting was always forbidden. The presented origami models could range from the well-known, traditional figures of animals, flowers, boxes, etc, or the reproduction of mathematical models such as fractals and polyhedra with all the related geometric operations and relations described thoroughly (Kawamura, 2002) (Lang, 2002) (Ikegami, 2009).

Fractals and Polyhedra can often be achieved through the use of modular units. **Modular models** are made from the combination of identical units modelled from several sheets of paper that interlock to form the final model. The typically used units are the Sonobe units, created by Mitsunobu Sonobe in the 70s and the Phizz units (Pentagon - Hexagon - Zig - Zag) created by Thomas Hull in 1993.

Besides the traditional and modular origami models, there is another class of origami studied in depth by researchers at OSME, the origami tessellations. A tessellation, or tiling, from a mathematical point of view, is a subdivision of the plane with geometric forms with no overlapping or gaps. It may be achieved through the use of several axioms in a combined way. In the case

of an origami tessellation its CP is almost a pure mathematical model, if one disregards the small paper thickness. But when speaking about folded tessellated models (also called Crystallographic Flat origami by Kawasaki and Yoshida in 1988) the concept of tessellation must be less “mathematical” since there is often overlapping of the faces. In this type of model, the states that interest the folder are the unfolded and the final folded state, often locked due to the common use of twist-folds (De las Peñas *et al.*, 2015).

As far as kinetic architecture is concerned, and particularly with regard to this investigation, the most interesting tessellations are those that do not have locked states and thus can move continuously from the unfolded to the completely folded state and continuously make the reverse motion. Within this particular group it is possible to narrow down the tessellations under investigation even more by choosing the ones that can rigidly fold into a flat state. For rigid origami all the faces must remain rigid throughout the folding process, bending only happens at the crease lines which makes them act as revolute joints attached to stiff panels (Lang 2010) (Demaine *et al.*, 2011 (a)) (You and Chen, 2012).

2.2.2 | Origami Foldability

As has been stated before, the main focus of this research is Rigid origami tessellations, particularly the ones that can be folded flat.

Rigidly foldable origami means that there is a possible rigid motion that makes the pattern fold from the initial (planar) state to the final (folded) state where the faces remain rigid during the motion that is carried out by the creases that act as hinges (Demaine and O'Rourke, 2007).

Flat foldable origami means that the model will be collapsed into a planar shape at the end of the folding process. There are models that are rigid foldable but not flat foldable and vice-versa, as Watanabe and Kawaguchi (2009) demonstrate (**Figure 2.68**).

This particular group allows for the biggest possible compression from the unfolded state to a flat folded state, which can be extremely useful for architectural applications since the same surface can cover a determined area when unfolded and occupy the least space possible when completely folded.

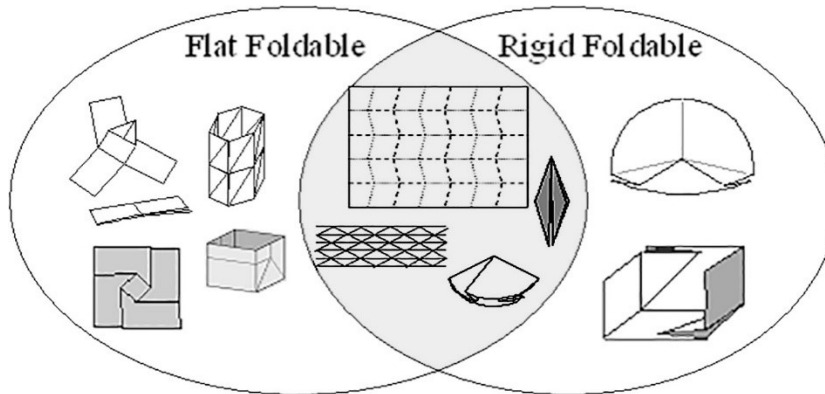


Figure 2.68.
Examples of Rigid and
Flat foldability
Source: Watanabe and
Kawaguchi, 2009,
adapted

Rigid-Foldability

The general rigid foldability of a non-regular crease pattern is very difficult to calculate, so most researchers test for it on each vertex of the CP, like Streinu and Whiteley (2001), Huffman (1976), McCarthy (1995), and Belcastro and Hull (2002) (Balkcom *et al.*, 2009).

Balkcom *et al.* (2009) solve the equations from these authors to compute three dependent crease angles as a function of the other crease angles. Their thesis is that if rigid folding is possible, the equations relating crease angles must always have a solution through the folding process (Balkcom *et al.*, 2009).

Watanabe and Kawaguchi (2009) propose another type of method to verify the rigid foldability of a vertex, the diagram method (**Figure 2.69**). The diagram method works with vectors on the creases, pointing to the vertex or away from the vertex depending on the assignment of the crease. Then one must put them together, head to tail, and in anti-clockwise order. The vectors must form a closed loop with intersecting areas, if the vectors cannot make a closed loop (c) or if the closed loop area is not zero (i) then the vertex cannot fold rigidly (Watanabe and Kawaguchi, 2009).

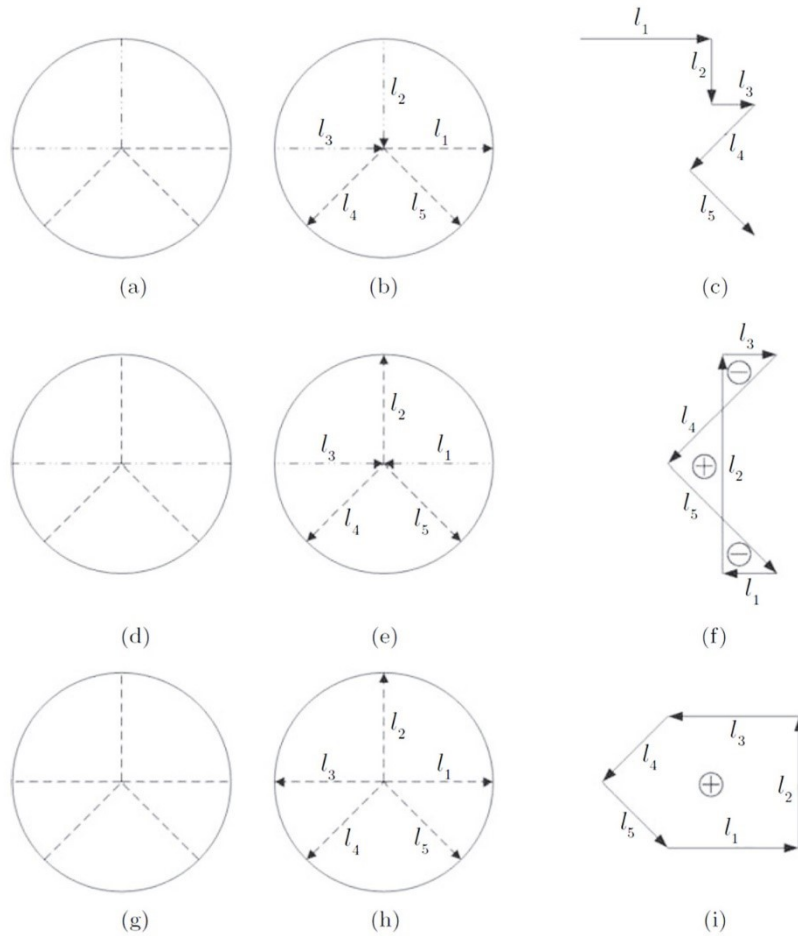


Figure 2.69.
 Three examples of
 the Diagram
 Method
 Source: *Watanabe
 and Kawaguchi,
 2009*

Evans *et al.* (2015 (b)), describe a method to evaluate the rigid foldability of origami tessellations with degree 4 vertices and apply it to Twist-Folds. The authors prove that there is no possible crease configuration to achieve a rigidly foldable triangle twist but there are many configurations that allow for the rigid folding of quadrilateral twists (Evans *et al.* 2015 (b)).

Strategies to Transform Non-Rigidly Folding Vertices

Usually the impossibility of rigidly folding each vertex is due to the lack of freedom caused by the angles between faces, so authors like Tomohiro Tachi suggest strategies to turn non-rigidly foldable vertices, or Closed Vertices as named by Tachi (2009 (a)) into rigidly foldable ones.

Tachi proposes two methods (**Figure 2.70**) to make vertices rigidly fold. One way is to add crease lines and split the angle so that it allows the vertex to rigidly fold. The other way is to reduce the inside angle, so his proposal is to change the CPs by adding crease lines and triangulating polygons (Tachi, 2009 (a)).

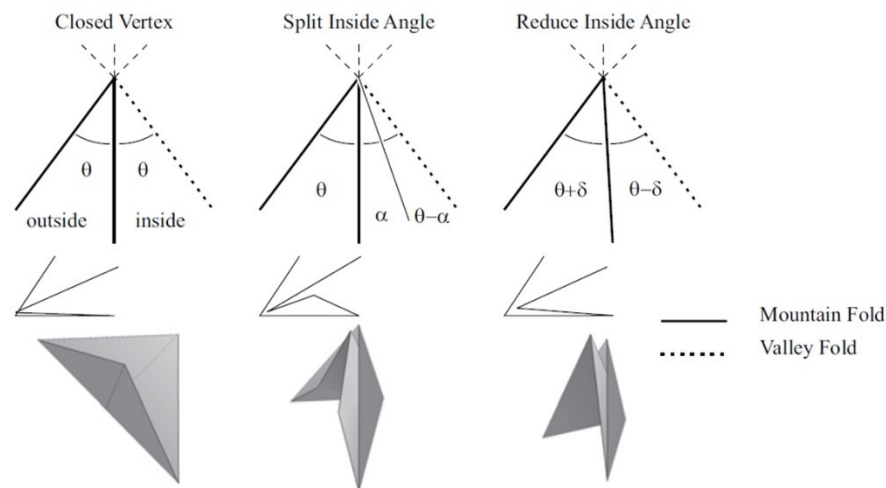


Figure 2. 70.
Two strategies
proposed by Tachi to
transform a Closed
Vertex
Source: Tachi, 2009(a)

Similarly, Demaine *et al.*, 2011 (a), demonstrate that by adding neutral creases to origami CPs, this may allow these to be mathematically folded, Abel *et al.*, 2016, prove the condition that allows a single vertex to be rigidly folded depending only on its intrinsic geometry (Demaine *et al.*, 2011 (a)) (Abel *et al.*, 2016).

Evans *et al.* (2015 (a)) developed tools for the modification of existing tessellations in order to make them rigidly fold, which they called origami gadgets. Lang (2011) defines an origami gadget as “a localized section of crease pattern that can replace an existing patch to add functionality or otherwise modify the pattern (Evans *et al.*, 2015 (a), p.9)”.

The authors determine two ways of using their proposed gadgets. One is to use them to replace portions of an existing CP that already rigidly folds but has collision problems. The other way is to use the gadgets to create new rigidly foldable patterns. The proposed gadgets are the corner gadget, the triple parallel gadget and the level shifters (**Figures 2.71, 2.72 and 2.73**).

The corner gadget can be used on degree 4 vertices; it maintains the original crease direction and creates four new degree 4 vertices on each one, generating a second rigidly foldable form.

The triple parallel gadget can be used on any flat-foldable degree-4 origami vertex that does not have two collinear crease lines and does not contain any 90° sector angles. The triple parallel gadget modifies the vertex and turns it into a network of four degree-4 vertices around two isosceles triangles. The network is composed of six creases where three are parallel to one of the original creases and the other three are coincident with the remaining three original creases.

The level shifters are commonly used in origami design in order to bring together two sections of a CP that are on different levels. These gadgets allow for the widening of determined parts of a CP and can be symmetric or asymmetric (Evans *et al.*, 2015 (a)).

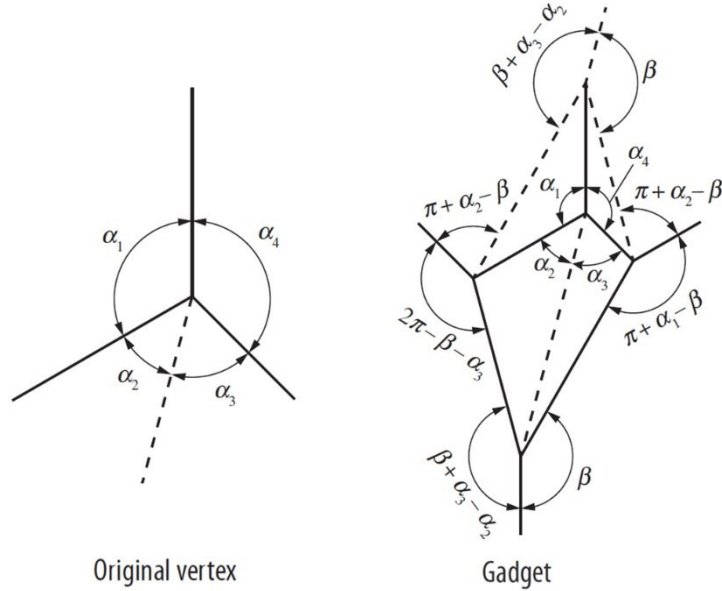


Figure 2.71.
 Corner gadget
 Source: Evans *et al.*, 2015 (a),
 adapted

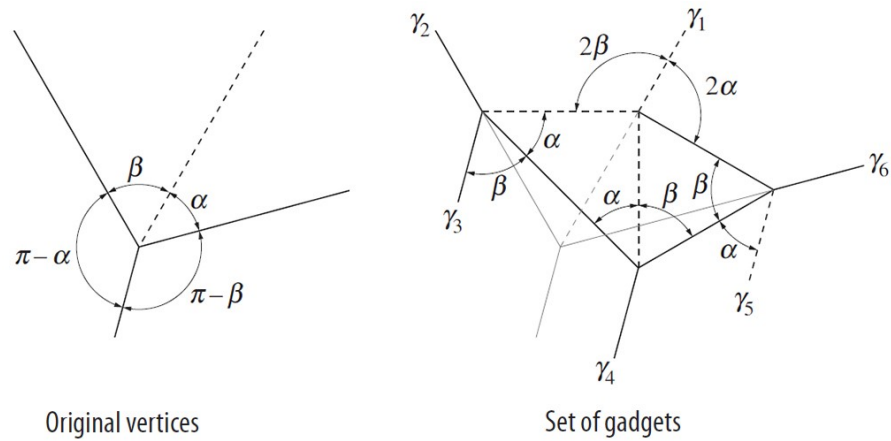


Figure 2.72.
 Triple parallel
 gadget
 Source: Evans *et al.*, 2015a, adapted

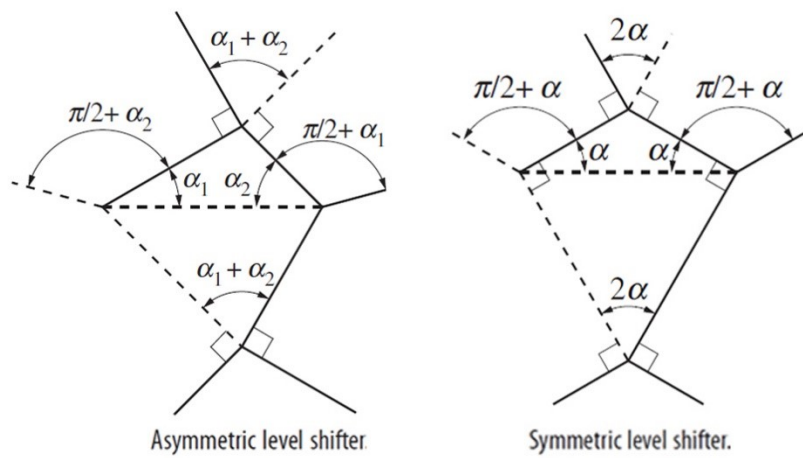


Figure 2.73.
 Level shifters
 Source: Evans *et al.*, 2015a, adapted

Flat-Foldability

“A flat-foldable vertex begins in an initial flat position and can be folded to achieve a secondary flat position (Evans *et al.*, 2015 (a), p. 2)”.

The flat foldability of a CP is still an open research subject being studied by authors like Erik Demaine, Robert Lang, Bern and Hayes, Thomas Hull, Tomohiro Tachi, Jun Mitani among others. The authors reached several conclusions, mainly regarding one vertex and not the entire CP, that are necessary but not sufficient as will be detailed subsequently.

As Demaine and O'Rourke (2007) put it, “*local flat foldability is easy*” but “*global flat foldability is hard*” (Demaine and O'Rourke, 2007, pp. 214, pp. 217).

The global flat-foldability of a given crease pattern is NP-hard, as proven by Bern and Hayes in 1996. Nevertheless, some conditions have been discovered in recent years that are necessary though not sufficient, to verify if a CP will generate a flat-foldable model.

There is only one rule that might be applied to the entire CP, the Two-colourability Rule (**Figure 2.74**). That states that for a crease pattern to be flat foldable it must be possible to colour each face of the crease pattern in a way that two faces with the same colour never share a crease, which implies that the number of faces around any vertex must be even (Demaine and O'Rourke, 2007) (Hull, 2002).

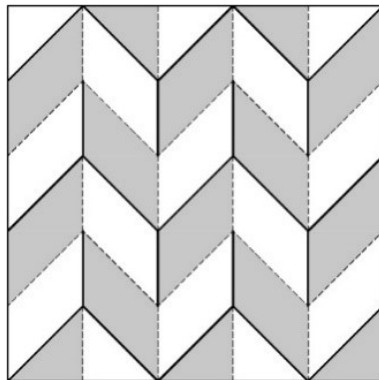


Figure 2. 74.
Graphic representation
of the two-colourability
rule

The Kawasaki-Justin and the Maekawa-Justin Theorems are also necessary conditions to verify for flat-foldability. These theorems are not applicable to an entire CP at once but must rather be used to test each vertex individually. That is, when inspecting a CP, it is necessary to verify all of the interior vertices (the ones on the border are disregarded, since they are open, that is, there is not 360° of paper around them, which makes them open vertices) to check if they verify these theorems.

The **Maekawa-Justin Theorem** states that a crease pattern is flat foldable if at every interior vertex the number of valley (V) and mountain (M) folds differs by two (**Equation 2.2**).

Equation 2.2.
 Maekawa-Justin
 Theorem

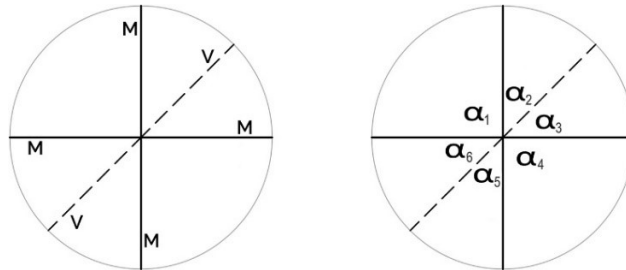
$$\sum V - \sum M = \pm 2$$

The **Kawasaki-Justin Theorem** states that a crease pattern is flat foldable if at every interior vertex the sum of the even and odd angles defined by the creases are equal to 180° (**Equation 2.3**).

Equation 2.3.
 Kawasaki-Justin
 Theorem

$$\alpha_1 + \alpha_3 \dots + \alpha_{2n-1} = \alpha_2 + \alpha_4 \dots + \alpha_{2n} = 180^\circ$$

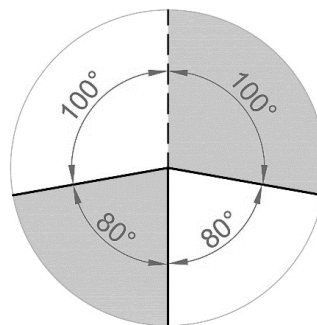
Figure 2. 75.
 Graphic
 representation of
 Maekawa-Justin
 and Kawasaki-
 Justin Theorems



Just as in the two-colourability rule, these two theorems also imply that the number of faces around a flat-foldable vertex must be even.

A vertex may obey both theorems and still be unable to flat fold (**Figure 2.76**), due to the intersection between the faces, which brings another rule, the **Big-Little-Big Lemma** (Hull, 2002) (Demaine and O'Rourke, 2007) (Hull, 2015).

Figure 2. 76.
 Example of a vertex
 that obeys the three
 rules but is not flat
 foldable



This lemma states that if an angle θ_i is a strict local minimum, that is to say that it is smaller than the two neighbouring angles ($\theta_{i-1} > \theta_i < \theta_{i+1}$), then the two creases that define angle θ_i must have an opposite mountain-valley assignment so that the vertex may fold flat (Demaine and O'Rourke, 2007). In the image example, the only way that the vertex would fold flat would be if the valley fold was between the 80° angles.

Strategies to Transform Non-Flat-Foldable Vertices

When a vertex does not obey the theorems and lemma, as in rigid foldability, it may be possible to transform it into a flat foldable one through certain strategies proposed by various authors.

Bern *et al.* (2002) and (Demaine *et al.* 2011 (a)) propose the addition of creases in order to fulfil the theorems and make vertices flat-fold, thus changing the degree of the vertex.

Bern *et al.* (2002), further propose that the use of disk packing algorithms (based on the disk packing technique first introduced by Lang in 1996) in order to generate flat-foldable crease patterns made up of triangular and quadrilateral faces. These CPs depart from a limit form (in the case of the next example image, a rectangle (R)) and a polygon (P) contained on R. The objective of the authors is to generate a flat foldable CP that, with one single cut, detaches the polygon from the rectangle. This is not the scope of this research but the reasoning behind disk packing algorithms can be extremely useful when analysing CPs to test for collisions and flat foldability.

The authors propose the placing of circles along the edges of the polygon and the rectangle, and start by placing the centre of the circles on each vertex of the figures. The circles must be tangent every time possible and must cover the totality of the edges. Whenever the gaps between the created circles are not limited by 3 or 4 arcs new circles must be added until the space is completely tessellated with circles and 3-gaps or 4-gaps, which the authors do by computing a Voronoi diagram of the placed circles. Finally, triangles and quadrilaterals are induced from the disk-packing and a CP is created (**Figure 2.77 (a) and (b)**) (Bern *et al.*, 2002).

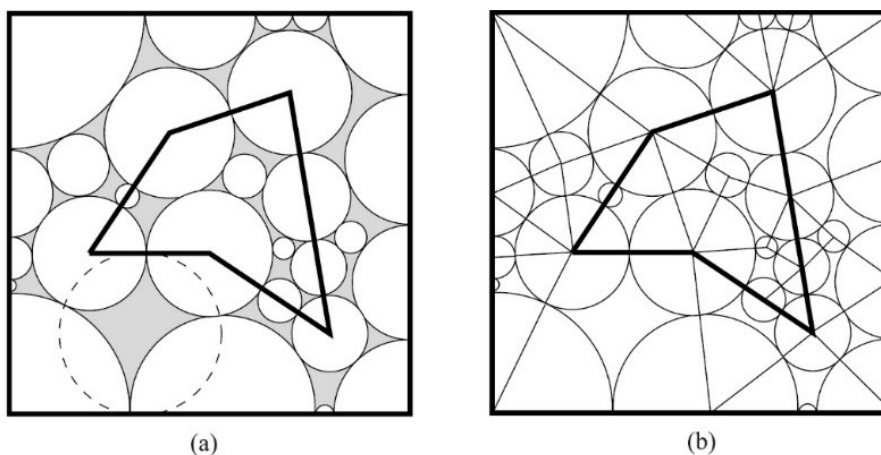
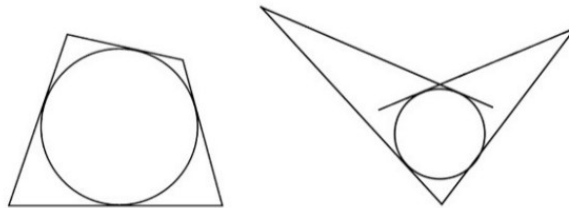


Figure 2. 77.
 (a) Disk-Packing example
 (b) Induced triangles and quadrilaterals
 Source: Bern *et al.*, 2002

Kawasaki (2002) demonstrates how to achieve flat-foldable quadrilaterals, which the author calls the “good flat quads”. Kawasaki proves that for any convex quadrilateral inside which it is possible to create an inscribed circle (a unique circle tangent to all edges), or to any quadrilateral with a re-entrant angle inside which can be inscribed a circle tangent to the extensions of the edges of the re-entrant angle and the other two edges (**Figure 2.78**), it is possible to fold them by bisecting the angles between all edges. The bisection crease lines converge on a vertex that coincides with the centre of the inscribed circle (Kawasaki, 2002).

Figure 2. 78.
Example of quadrilaterals that are good flat quads, a convex one and another with a re-entrant angle
Source: Kawasaki 2002, adapted



Azuma (2009) proposes the use of projective geometry and isogonal conjugates to determine flat foldable crease patterns on symmetric quadrilaterals (Azuma, 2009).

Even if every vertex on a CP is flat-foldable this is not enough to ensure that the whole pattern is flat-foldable. It is also fundamental to verify that there is no crossing between faces on the flat folded state or during the folding process (Bern *et al.*, 2002) (Demaine and O’Rourke, 2007) (Tachi, 2009 (a)) (Lang and Demaine, 2009) (Lang, 2018).

Non-crossing Conditions

In order to guarantee that a given CP can fold rigidly and flat, it is also necessary to ensure that there will be no intersecting between faces during the folding process (Bern *et al.*, 2002) (Demaine and O'Rourke, 2007) (Tachi, 2009 (a)) (Lang and Demaine, 2009) (Lang, 2018).

Therefore, in order to verify that a pattern can fold without having faces collide or cross each other, three non-crossing axioms were proposed by Jacques Justin in 1997. These axioms (**Figure 2.79**) concern the layer ordering that define the stacking order of faces of an origami model. These are therefore directly related to the creases MV assignment, since this will define the direction of folding, that is the relation between any two faces that overlap in the folded state (Lang and Demaine, 2009) (Lang, 2018).

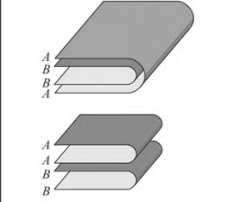
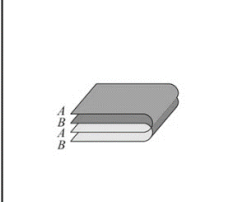
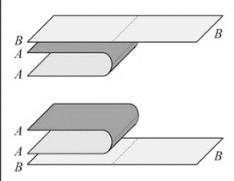
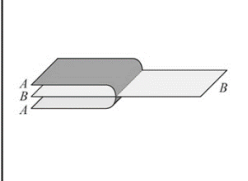
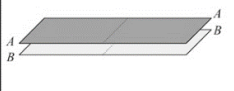
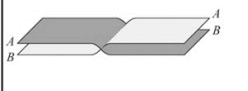
Conditions	Allowed Stacking Order	Forbidden Stacking Order
If two creases overlap each other so that their facets overlap, then the facet pairs incident to the two creases cannot be interleaved.		
If a layer of paper overlaps a crease, it cannot lie between the facets incident to the crease.		
If one facet lies above another on one side of an unfolded crease, it cannot lie below the other facet on the other side of the same line.		

Figure 2. 79.
Justin's Non-Crossing
Conditions
Source: Lang 2018,
adapted

As in the cases of rigid and flat foldability, it is very difficult to test an entire CP for self-intersecting situations. In this way, authors like Robert Lang, Marshall Bern, Erik Demaine and Tomohiro Tachi also use the “disk packing” technique described in the previous section to test for self-intersection on each vertex and those surrounding it (Bern *et al.*, 2002) (Lang and Demaine, 2009) (Tachi, 2009 (a)).

For the purpose of this investigation this problem becomes simplified since the scope of our study relates to regular crease patterns, so the mathematical complexity of testing several different vertices can be reduced to the testing of a small portion of the plane that contains at least one vertex of each type on the CP.⁸

⁸ For more information on Origami mathematics, proven concepts and generalizations please refer to Hull (2002), Demaine and O'Rourke (2007), Alperin and Lang (2009), Lang (2010), Hull (2013) and/or Lang (2018).

Furthermore, the scope of this research is not to develop new CPs or generate an algorithm to test for any given regular or irregular CP, but rather to study the *Corpus* of already developed models with regular CPs and to extend their utilization to architecture.

Origami Tessellations

For the selection of CPs, several books and other media have been studied which contain the most relevant contributions for regular origami tessellations to be used in kinetic architecture: Fujimoto and Nishiwaki's "*Invitation to Creative Playing with Origami*" (1982), "The Ron Resch Paper and Stick Film" (1992), Eric Gjerde's "*Origami Tessellations*" (2008), Paul Jackson's "*Folding Techniques for Designers*" (2011), Fuse (2012), the valuable contribution of Evans *et al.*, (2015 (a)), and the proceedings of the 3rd, 4th, 5th, 6th and 7th OSME meetings.

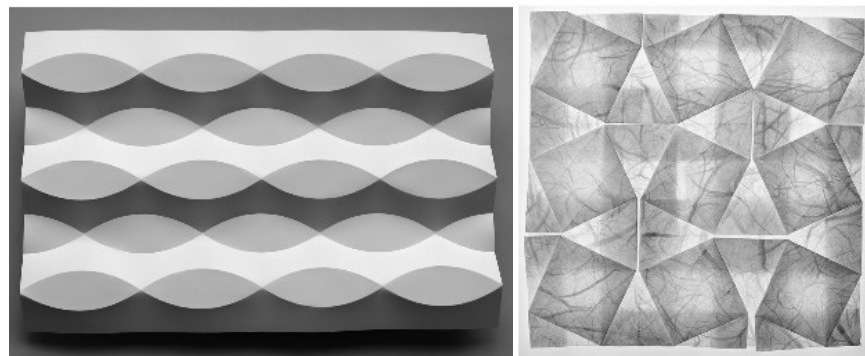
Since the aim of this selection is to determine patterns with multiple faces that can be used in architecture and engineering for kinetic purposes, several CPs were disregarded because they lack kinetic potential or are believed to be unsuitable for rigidly folding origami surfaces with non-zero-thickness.

This is the case for all curved tessellations, as curved creases from planar materials are restricted, they have only one stable state and cannot move easily between several states (Demaine *et al.*, 2015) (Demaine *et al.*, 2018) (**Figure 2.80**), hence these were disregarded.

This is also the case for "crystallographic flat origamis" as named by Kawasaki and Yoshida, 1988 (Demaine and Demaine, 2002), intensively studied by Alex Bateman and Robert Lang, in the development of the Tess software. Most of these tessellations have a flat folded state that is locked through twist folds and the overlapping of faces. The way to fold these models is not rigid and the locked state is contrary to the intention of using them in kinetic structures (**Figure 2.81**) (Demaine and Demaine, 2002) (Bateman, 2002) (Lang, 2018)

Figure 2.80.
Huffman's design with
circles
Source: Demaine *et al.*, 2011 (b)

Figure 2.81.
Square Twisted
Tessellation
Source: Gjerde, 2008



After the first criteria to dismiss inappropriate designs has been applied, several patterns with small number of faces were also disregarded as these are used as modules and not as regular, periodic surfaces or tessellations due to their simplicity and restricted paths of movement.

Finally, patterns that do not fold rigidly as well as patterns with vertices of degree higher than 6 were also disregarded.

The reason for this dismissal is that vertices with more than 6 creases meeting at a point have too much stresses concentrated at that point, which is particularly important in the case of patterns to be used in architectural kinetic structures that will have thickness. These stresses would probably be a major problem in larger scale structures and therefore in order to narrow down the scope of this research in a reasonable way for architectural structures, these were overlooked.

All of the patterns that will be followingly demonstrated are rigid and flat foldable except for three that are believed to be interesting for kinetic architecture surfaces and that are rigidly foldable but not flat-foldable. These are the squared waterbomb and hexagonal waterbomb that have a CP that combines vertices of degree-5 and degree-6, as well as the Ron Resch pattern that only has degree-6 vertices but cannot flat fold, since neither vertex complies with the Maekawa-Justin Theorem (**Figure 2.82**).

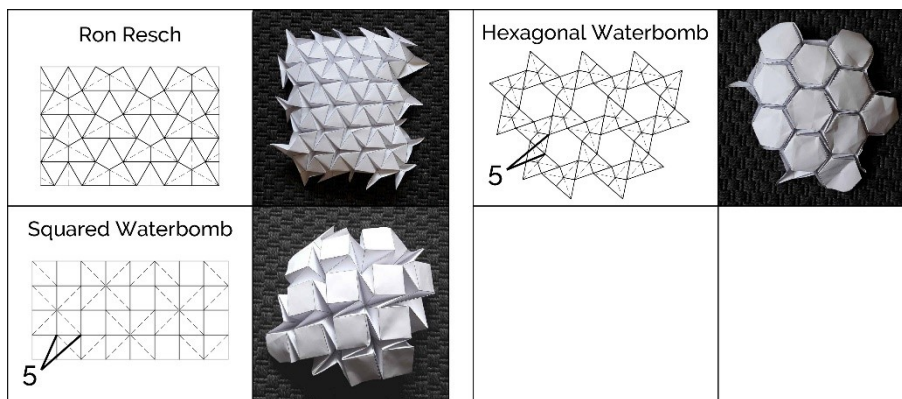


Figure 2. 82.
The Resch Family
Patterns

These patterns were called the “Resch Family Patterns” by Gardiner (2018). All depart from the plane and all assume double curvature configurations, spherical if the folding angles are constant during the folding process. Ultimately all of these end up in a completely folded configuration, but this configuration is not flat (Gardiner, 2018).

Since the remaining patterns have only one type of degree for all interior vertices, they have been grouped by vertex degree. Every pattern presented at the following sections correspond to the previously explained criteria, namely being regular tessellations, rigid and flat foldable and applicable for kinetic structures with thickness.

Degree-2 Crease Patterns

The degree-2 CPs are probably the most common patterns inside and outside of origami community. They contain the “accordion-like” patterns, folded almost unconsciously by everyone in a multiplicity of occasions.

The interior degree-2 vertices are not perceivable at first glance, but as Hull (2002) established, within any crease one may imagine a vertex that has two creases of the same identity emanating from it. Only the interior vertices are considered as the border vertices are “open-vertices” *i.e.* they do not have 360° of paper around them (Hull, 2002) (Jackson, 2011).

In **Figure 2.83** are presented the patterns with degree-2 vertices retrieved from literature with one column for the CP and another with an example of one folding state.

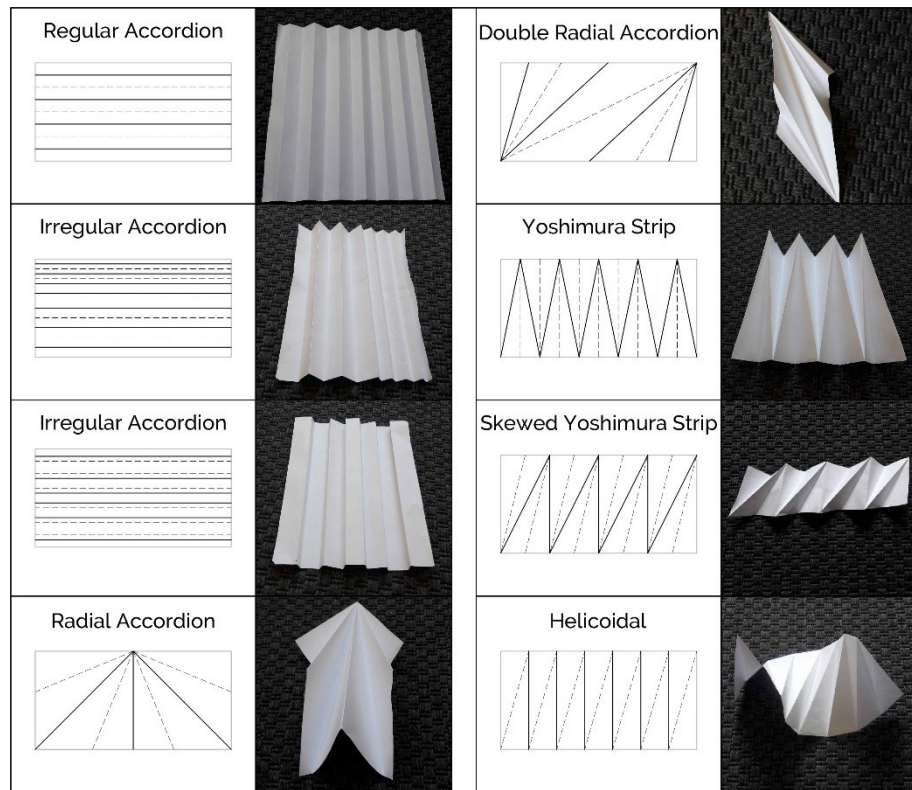


Figure 2. 83.
Degree-2 crease
patterns

Degree-4 Crease Patterns

In order to fulfil the Maekawa-Justin Theorem, degree-4 vertices must have three Mountain folds and one Valley fold (or vice-versa). These creases have only one option of arrangement around the vertex. Three creases of the same

identity always surround the only crease of the opposite identity (Hull, 2002) (Demaine and O'Rourke, 2007) (Hull, 2015).

Due to the Big-Little-Big Lemma the “lonely” crease must define the smaller angles that surround the vertex, otherwise it will not flat-fold.

These are the type of vertices used in the **Miura-Ori** pattern (first named developable double corrugation (DDC) surface in 1970 by Miura), established by the Japanese astrophysicist Koryo Miura. The Miura-Ori comes from geometries found in nature that fulfil the principle of minimum potential energy (Miura,2009). This pattern deploys simultaneously and homogeneously in orthogonal directions, has only one DoF and both deployment and retraction follow the same path (Miura, 2009).

The **MARS** pattern, developed by Taborda Barreto in 1982, has a CP that departs from the Miura but introduces an intended irregularity as the faces are composed of squares and rhombuses, instead of parallelograms (Barreto, 1994). This particular feature leads the pattern to achieve a non-conventional flat state.

The **Chicken-Wire** pattern (named by Evans *et al.*, 2015 (a)), is a CP that uses trapeziums; this causes inflexions at the ends of the quadrilaterals leading to cylindrical folding surfaces. The **Huffman Grid** (developed by David Huffman and named by Evans *et al.* (2015 (a))), is also a pattern that tends to fold into a cylinder. All of the vertices are of the same kind ($3M+1V$) and the CP seems perfect for folding a rigid and flat-foldable model, but the kite configuration of the faces leads to collisions between adjacent faces, so this model can never fold completely into a flat state (Evans *et al.*, 2015(a)).

Finally, the seventh CP in study is the **quadrilateral meshed pattern**, also named by Evans *et al.* (2015(a)) and that also folds into a cylindrical form.

In **Figure 2.84** are presented the described patterns with degree-4 vertices, retrieved from literature and shown with the CP and an example of one folding state.

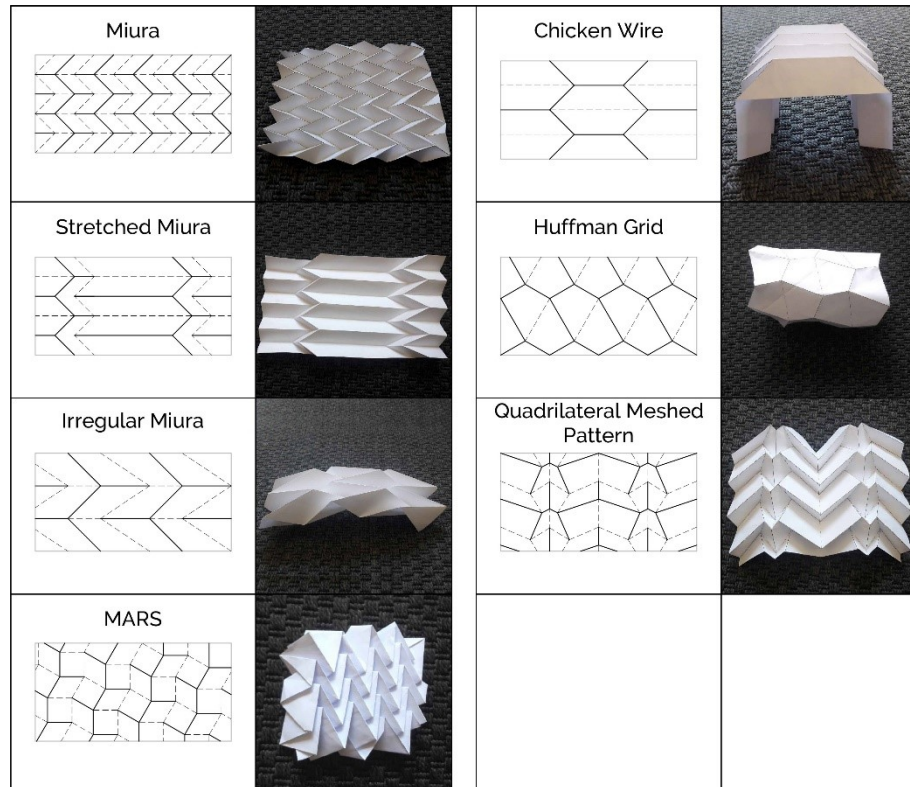


Figure 2.84.
 Degree-4 crease patterns

Degree-6 Crease Patterns

In order to fulfil the Maekawa-Justin Theorem, degree-6 vertices must have four Mountain folds and two Valley folds (or vice-versa).

The well-known **Yoshimura Pattern** belongs to this group, discovered by Yoshimaru Yoshimura in 1955 through the study of the buckling of cylinders subjected to forces in the direction of their axis. Similar to the Miura pattern, the Yoshimura can also be found in nature and satisfies the principle for minimum potential energy.

Biruta Kresling also studies patterns that can be found in Nature, and tests for what she calls “failure patterns”, or patterns that emerge in specific plants and from crushing, using minimum energy. Through this method the author presented the **Kresling Pattern** in 1997, which is obtained when bidirectional forces are applied to cylinders, a linear force in the axis direction followed by a rotational force (Kresling, 1997).

Taking the helicoidal pattern presented for patterns with degree-2 vertices, this research also proposes the study of the **double helicoidal** and **symmetric helicoidals**, extensively studied by Ron Resch and Tomoko Fuse (2012) (Jackson, 2011).

Tomoko Fuse also developed progressions for the **Whirlpool Spirals**. Fuse (2012) determines three parameters that should be used in order to achieve rigid and flat foldable models without self-intersection, as will be detailed in **Section 3.3.1** for the crease pattern analysis.

Finally, the study of the **Fujimoto and Nishiwaki Pattern** is proposed. This name was chosen as the first known reference to this pattern is in the book “Invitation to Creative Playing with Origami” by Fujimoto and Nishiwaki (1982), although some authors refer to it as the “Ananas Pattern” as called by N. Maillard (Kresling, 1997).

This was the pattern used by You and Kuribayashi (2009) in their proposed stent graft to be used in blood vessels. These authors also propose a variation of this pattern to be used in a conical configuration, which this thesis calls the **radial Fujimoto and Nishiwaki**.

Some of the patterns studied in the literature seem to be variations of the Yoshimura pattern, for example the whirlpool spiral, the skewed Yoshimura and the double helicoidal.

In **Figure 2.85** the chosen patterns retrieved from literature are represented showing the CP and one example of one folding state.

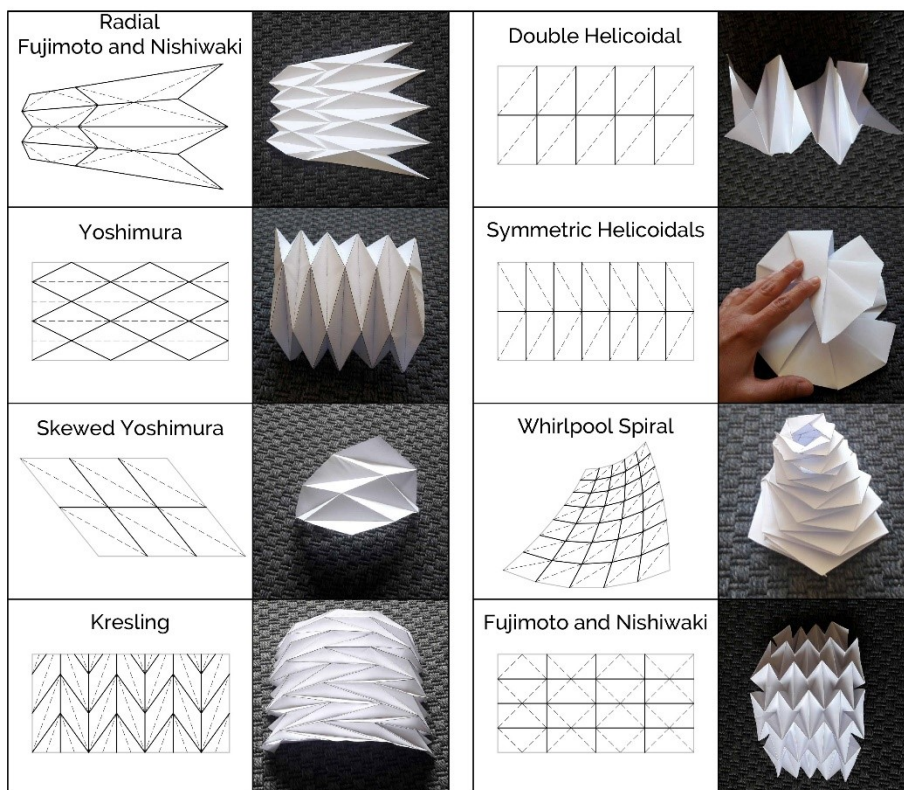


Figure 2. 85.
Degree-6 Crease
Patterns

Thick Origami

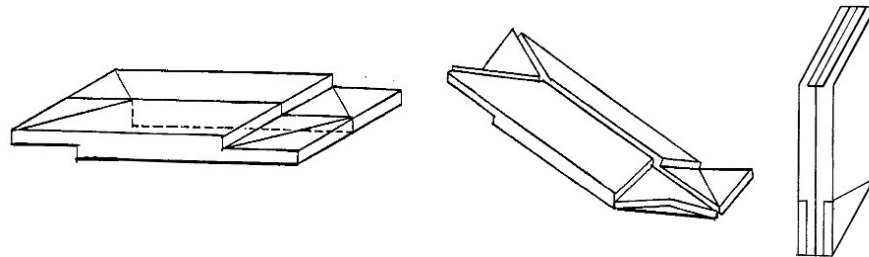
Up until this point, origami has been discussed in a pure mathematical sense, as if the surface is the summation of perfect, planar faces, without thickness. The same assumption is made when speaking about origami kinematic models, with hinges translated into straight creases, without volume, that correspond perfectly to the boundaries of the faces.

When the rules and properties of origami are brought from mathematics into the architectural scale, the matter of thickness can be a limitation. Structures need to have a thickness that allow them to bear gravity and other loads, which becomes even more complex when the structure is required to move and to behave like kinematic models (Tachi, 2011) (Lebée, 2015) (Edmondson *et al.*, 2015).

Several authors have developed strategies to deal with origami thickness while maintaining the mobility of the structure and kinematic behaviour.

Hoberman (1988) developed a method, to collapse degree 4 vertices by moving the axis of rotation and giving two levels of thickness to the surfaces around the vertex. Hoberman's method, the **axis shift method (ASM)** (due to the shifting of the hinges to the valley side of the panel) can only be used on patterns with symmetric and flat-foldable vertices (**Figure 2.86**). Additionally, Tachi points out that this method is limited because it does not allow for multiple overlapping of faces (Hoberman, 1988) (Tachi, 2011).

Figure 2. 86.
Hoberman's
method for
symmetric degree-4
vertices. Three
states of folding
*Source: Hoberman,
1988, adapted*



Trautz and Kunstler, 2009, propose a method that allows for hinges to slide along the fold lines, the **slidable hinges method** shown in **Figure 2.87**. The authors demonstrate their method on four symmetric degree-4 vertices arranged in a squared loop. This way the amount of sliding is compensated for by each vertex and the model can be collapsed completely (Trautz and Kunstler, 2009) (Tachi, 2011).

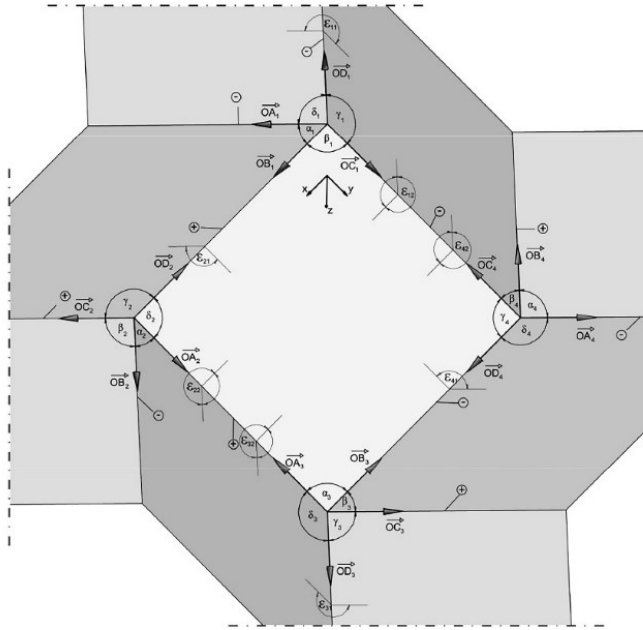


Figure 2.87.
Trautz and Kunstler
Example
Source: Trautz and
Kunstler, 2009

Tachi (2011) argues that this method is not suitable as a general approach since there are patterns where compensation is not possible and demonstrates this with a simple example where the sliding gets accumulated at one extreme of the pattern. On the example presented in **Figure 2.88** the sliding amount ultimately leads to the disconnection or intersection of volumes (Tachi, 2011).

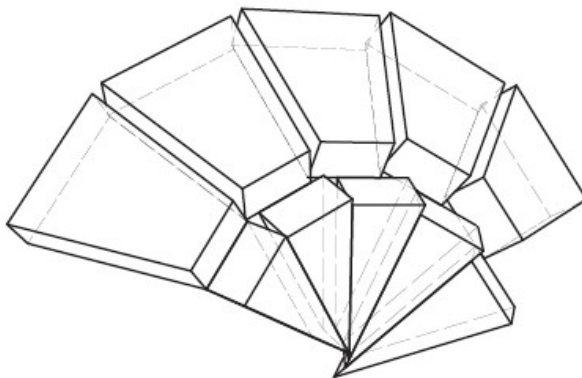


Figure 2.88.
One example of the
non-generality of the
slidable hinges method
Source: Tachi, 2011

In 2011, Tachi proposed a general geometric method to use on thick origami that preserves the kinematic behaviour of rigid origami. Tachi's method is called the **tapered panels method** and is achieved by thickening the origami surface on both sides and then trimming the thickening in the direction of the valley side of the folds, demonstrated in **Figure 2.89**. This method folds from the 0 angle to a predetermined angle smaller than 90° (depending on the thickness of the panel and trimming angle), this method maintains the kinematic behaviour of rigid origami and can be applicable to human scale structures (Tachi, 2011).

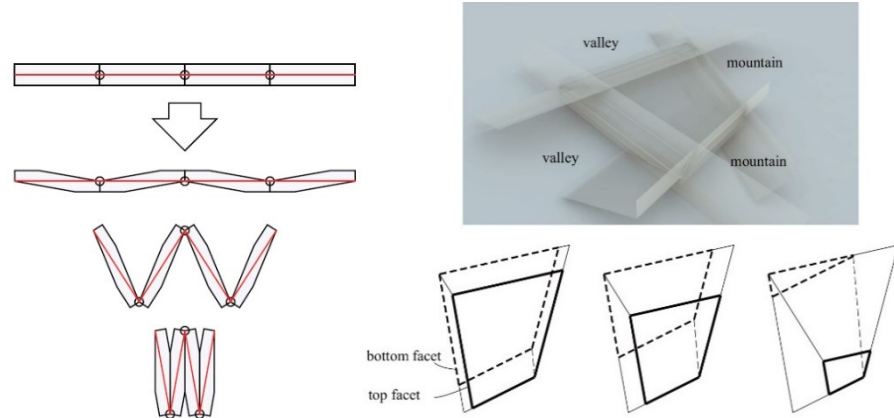


Figure 2.89.
 Tapered Panels
 Method
 Source: Tachi, 2011

Edmondson *et al.* (2015) review the most relevant methods to accommodate origami thickness in the context of the architectural scale, they disregard the slidable hinges method, and propose a new one, the offset panel technique.

Figure 2.90 shows the summary made by Edmondson *et al.* (2015) between the considered methods using a simple parallel accordion with four faces.

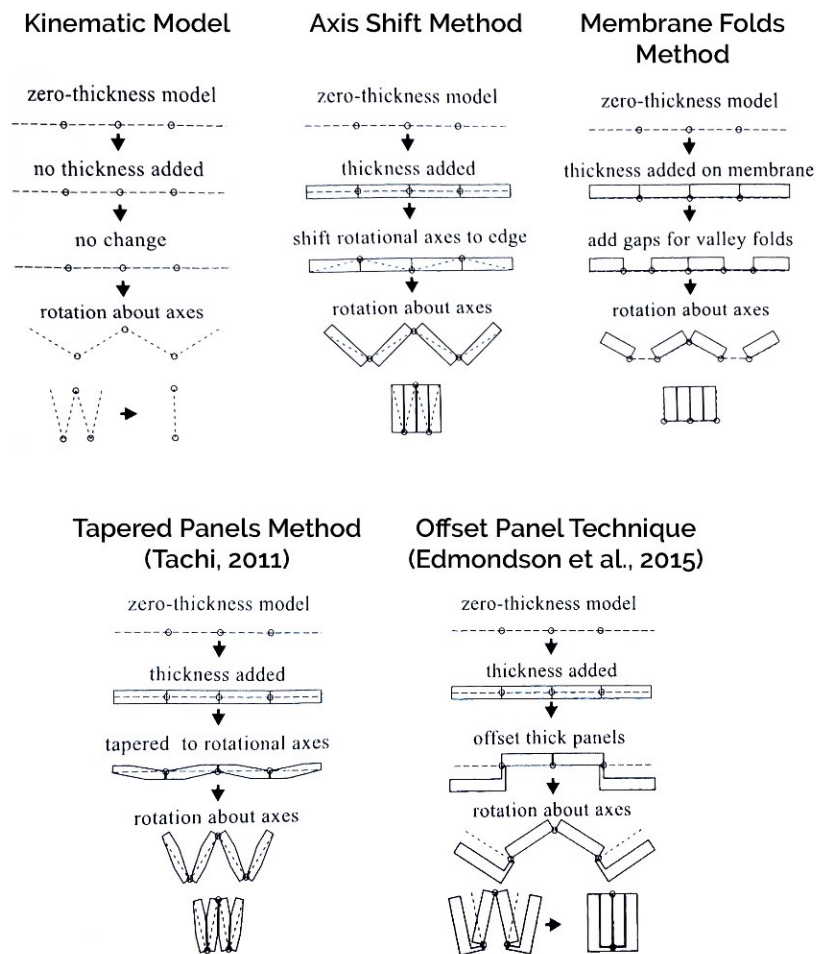


Figure 2.90.
 Existing methods
 for thick origami
 and proposed offset
 panel technique by
 Edmondson *et al.*
 Source:
 Edmondson *et al.*,
 2015, adapted

The authors developed the **offset panel technique** to maintain the kinematics of a zero-thickness model through all its motion. It accommodates the thickness of the panels, whether it varies or not, as well as offset panels or gaps between panels (Edmondson *et al.*, 2015).

This method departs from the “joint plane”, this plane is the equivalent to the zero-thickness planar CP and all joints lie on it. The facets are offset from the original plane, with a dimension that corresponds to the number of other facets that will be accommodated and connected to the joints through extensions (Edmondson *et al.*, 2015).

De Ruysser (2015) proposes the thickening of fabrics, to be used on clothes and accessories, thus on a scale much smaller than architectural structures, but that can also be used as a process to achieve thick origami. The proposed material, the Metalized Folding Textile (MFT), departs from a thin textile that is subjected to electroforming to place copper (or other materials) on both sides of the textile. The fabric has the CP imprinted in a way that does not allow for the metallic particles to be placed on the creases, which must be wide enough to accommodate the thickness of the faces (De Ruysser, 2015). De Ruysser’s approach (**Figure 2.91**) could be included in the membrane folds method, if it is accepted to thicken the plates on both sides of the membrane. If so, naturally it should be necessary to create gaps on both sides since the valley folds will exist either on one or the other.

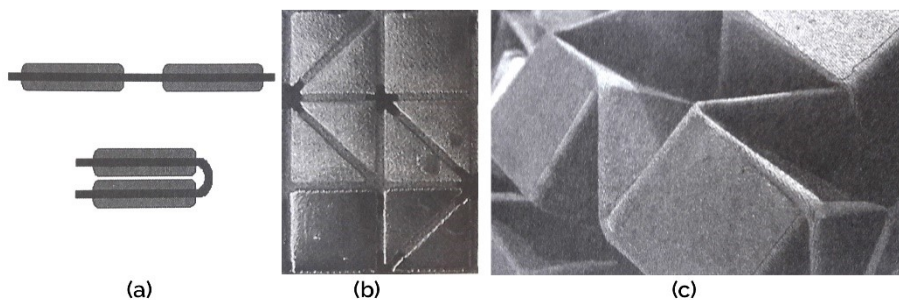


Figure 2.91. Thickening on both sides of the origami surface.
a) Section diagram
b) Plane CP
c) Folded CP
Source: De Ruysser, 2015, adapted

Seymour *et al.* (2018) use a similar approach in their development for a deployable ballistic barrier (**Figure 2.92**), but they use a stiff material in the centre and the textiles on the outside. The core of faces is made of 3mm Omega Bond panels, that are surrounded by six layers of Kevlar and a final layer of Ballistic Nylon. The excess of the textile layers gets squashed in the creases area (Seymour *et al.* (2018).

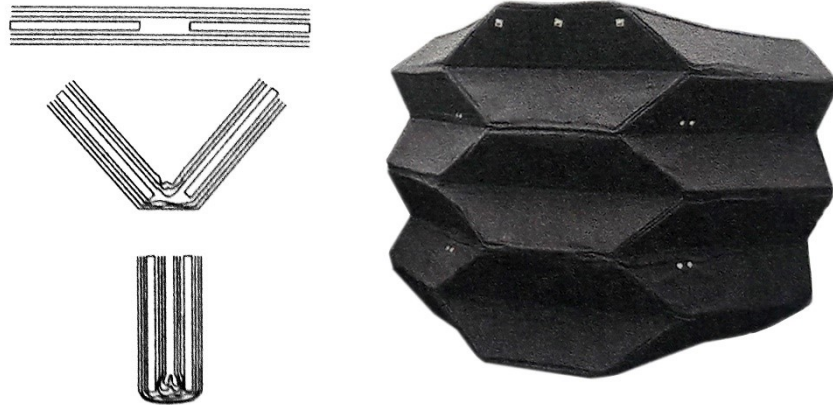


Figure 2.92.
 Deployable
 Ballistic Barrier
 by Seymour *et al.*,
 2018
 Source: Seymour *et al.*, 2018, adapted

Wang *et al.*, 2018, use the ASM in conjunction with kirigami. The proposed strategy is to shift the axis of rotation to the valley side and cut the creases that prevent the model from folding, additionally the authors use different thicknesses on the faces in order to facilitate the accommodation of faces in the completely folded state. Although the kinematic of the plan model is not preserved, there is no need to offset the panels, several constraints to movement are avoided by slitting the crease and the final folded model becomes perfectly flat folded, as demonstrated in **Figures 2.93** and **2.94** (Wang *et al.*, 2018)

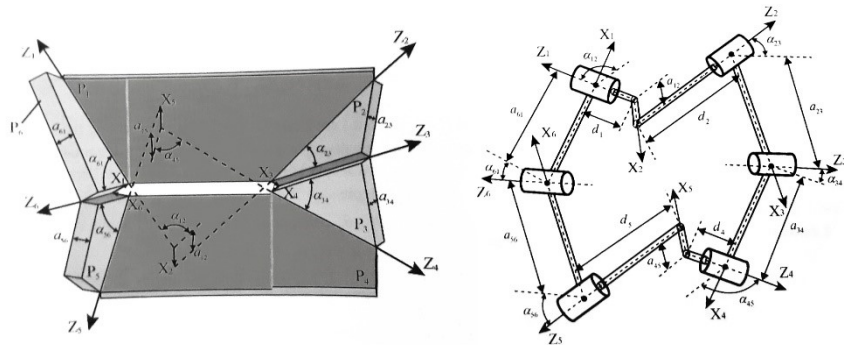


Figure 2.93.
 Kinematic diagram
 for patterns with two
 degree-4 vertices by
 Wang *et al.*, 2018
 Source: Wang *et al.*,
 2018, adapted



Figure 2.94.
 Physical prototype
 folding sequence by
 Wang *et al.*, 2018
 Source: Wang *et al.*,
 2018

The last sections have presented the state-of-the-art for origami surfaces to be used on kinetic architectural structures. The laid-out topics for origami geometry allowed to understand that origami tessellations have several issues that must be accounted for when developing rigidly folding surfaces. Namely, if the design of the CP respects the rules for rigid and flat foldability, if there will be self-intersection between faces during folding, even though there are strategies that allow for CP alteration to prevent those issues.

The thickening of the tessellation seems to be one of the most delicate subjects to be attentive to when using rigidly folding origami surfaces in the architectural scale. The next section presents the known examples of origami used in architecture to allow to draw conclusions regarding origami thickening.

2.2.2 | *Origami in Architecture*

The first known example of experimentation with Origami to be used in architecture was Joseph Albers' course at Bauhaus in the 1920s, where the students developed deployable origami models (**Figures 2.95** and **2.96**) and curved creased models (**Figure 2.97**) in paper (Demaine *et al.* 2015) (Lebée, 2015).

Figure 2. 95.
Joseph Albers playing
with Miura-Ori
Source: Lebée, 2015

Figure 2. 96.
Origami model from
Joseph Albers' course,
1927-28
Source:
[erikdemaine.org/
curved/history/](http://erikdemaine.org/curved/history/)

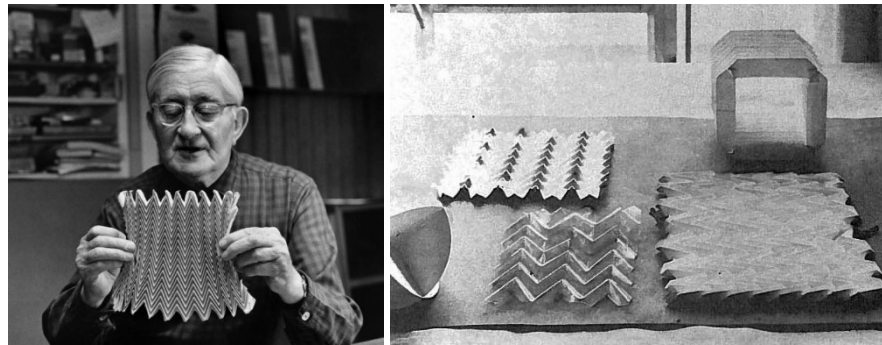


Figure 2. 97.
Origami model from
Joseph Albers' course,
1927-28
Source: Demaine *et al.*
2015



Nowadays it is possible to find examples of the utilization of origami in buildings or parts of buildings. The existing examples of origami utilization in architecture can be organized into three main groups: a) Static; b) Deployable; c) Kinetic. (**Figure 2.98**)

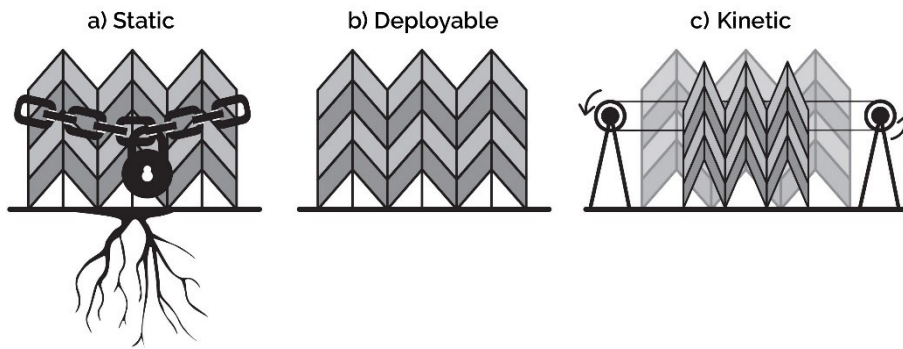


Figure 2.98.
Groups of origami in
architecture
Source: Osório *et al.*
2017

Static origami in architecture happens when a building is constructed with an origami form, but this form remains with the same configuration through time. From the range of states that an origami surface can assume, only one state is chosen to reproduce in a permanent way. This state is chosen due to aesthetical and/or structural reasons, since a pleated form has structural qualities that a plane form does not, such as the division of the forces that the structure might be subjected to. Examples of this kind of utilization of origami in architecture are Hut by Ryuichi Ashizawa (2009) or the Bloomberg Pavilion by Akihisa Hirata (2012) (Osório *et al.*, 2017).

Deployable origami structures are structures that take advantage of the self-supporting capabilities of origami surfaces and of their possible flat-foldability. These surfaces can be easily assembled and disassembled without the need for additional supporting substructures, are usually rigidly foldable and their flat-foldability allows for easy transportation and storage (Osório *et al.*, 2017). Examples of Deployable origami structures are “Packaged”, designed by Miwa Takabayashi in 2007, which was a small pavilion to use in a Shopping Centre made of corrugated cardboard. “Xile”, 2008, by Mats Karlsson, was a 35-meter-long translucent tunnel created to connect two buildings during the design fair *Interieur*. Matthew Malone developed the Recover Shelter in 2008, a temporary shelter to be used in emergency situations made with polypropylene. In 2009 the students in their third year of architecture in the University of Cambridge designed, fabricated and assembled a temporary cardboard pavilion for a banquet at the University gardens. David Penner created the “Corogami Folding Hut” in 2010, a collapsible ice-skating change hut, made with doubled wall polypropylene. More recently, in 2014, students at the University of Southern California made a pavilion in polycarbonate that occupies an area of 15m x 3m and is 3m high. All these examples are rigidly foldable, able to support themselves without the addition of alternative structural systems and are also flat foldable. They are used in a static way, which means that they are used only used in a specific folding state but are

able to be deployed in order to reach that state and also folded into a flat folded position (Osório *et al.*, 2017).

The use of **kinetic** origami allows for a more versatile utilization. The same model can undertake several folding states during its use.

This type can be found in a wide variety of applications, from folded solar sails launched into space, medical devices, reconfigurable walls, shading systems, acoustic enhancement or artistic responsive installations (Osório *et al.*, 2017). The existing examples of the utilization of origami in a kinetic way, that will now be presented, can be divided in two main groups: a) Modules; b) Surfaces.

These groups were chosen by analysing the CP of the structures in regard to their geometry; if they have a small amount of faces, arranged around a centre and the movement is very simple, and often centralized, then they are considered as **modules**. If the CPs have a large number of faces and work through complex movement, then they can be considered **surfaces**.

Auxetic Origami as outlined by Christopher Connock and Amir Shahrokhi from Yale University, 2011, was a structure with sixteen flower-like modules that responded to the amount of light in the surrounding environment by opening or closing themselves (**Figure 2.99**). In 2011 David Lettellier exhibited Versus, two modules of origami “talking” flowers placed on opposite walls that reacted to sound and communicated constantly with each other (**Figure 2.100**).

Figure 2. 99.
Auxetic Origami
Source:
amirshahrokhi.christopherconnock.com

Figure 2. 100.
Versus
Source:
davidletellier.net



In 2012 AHR Architects finished the construction of the Al Bahr Towers where they used a façade protection system composed of several triangular modules with six faces. These modules protect the building from sandstorms and excessive sunlight (**Figure 2.101**).

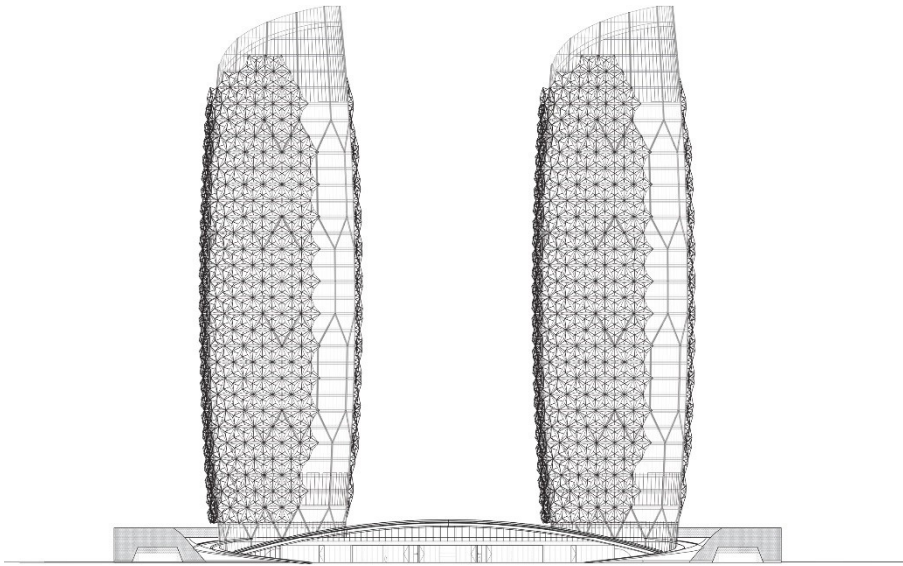


Figure 2. 101.
Al Bahr Towers
Source: Courtesy of
AHR Architects

In 2015 mechanical engineering students of the Compliant Mechanisms Research Group of the Brigham Young University (BYU) designed the Origami Kinetic Sculpture based on the square twist pattern to be presented at the exhibition "*Folding Paper: The Infinite Possibilities of Origami*" at the BYU Museum of Art, where they used the Offset Panel Technique, described in the previous section (**Figure 2.102**).



Figure 2. 102.
Origami Kinetic
Sculpture
Source: *Compliant-
mechanisms.byu.edu*

Regarding the utilization of kinetic origami as **surfaces** instead of modules, there is an interesting example of Tachi (2011) who developed a structure based on the Miura pattern with a thick material that is able to fold rigidly and to a flat state, as shown in **Figure 2.103** (Tachi, 2011). Furthermore, Wallbot, made in 2010 by Otto Ng at the John H. Daniels Faculty, University of Toronto used the Miura Pattern, able to stretch from 1m to 1,5m, in mobile pieces of wall that worked together while responding to behavioural patterns and thermic conditions (**Figure 2.104**).



Figure 2. 103.
Tachi's Rigid Thick
origami Prototype
Source: Tachi 2011

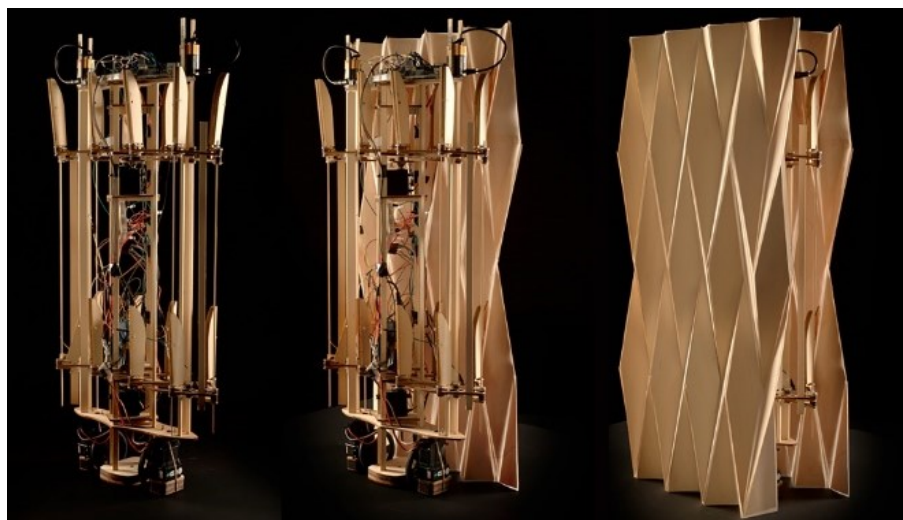


Figure 2. 104.
Wallbot
Source: ottocad.net

In 2010, Fishtnk created the first version of the Tunable Sound Cloud (**Figure 2.105**), a surface able to modify itself to enhance the acoustic performance of spaces. With the same goal, David Lettellier created Tessel (**Figure 2.106**), also in 2010, and the Resonant Chamber (**Figure 2.107**), was developed in 2012 by RVTR in partnership with ARUP acoustics.



Figure 2. 105.
Tuneable Sound Cloud
Source: *fishtnk.com*

Figure 2. 106.
Tessel
Source:
davidletellier.net

Figure 2. 107.
Resonant Chamber
Source: *rvtr.com*

Cerebral Hut was designed in 2012 by Guvenc Ozel and Alexandr Karaivanov. It was an installation made with 11 hexagonal modules of surfaces folded in the line with the Ron Resch Pattern that reacted to the user's brain frequencies with the objective of allowing the users to control it with their minds as demonstrated by **Figure 2.108**. In 2014 Foldhaus created Blumen Lumen, an interactive art installation that uses the Miura pattern to create 10 animatronic flowers that open and close in response to the people around them (**Figure 2.109**).

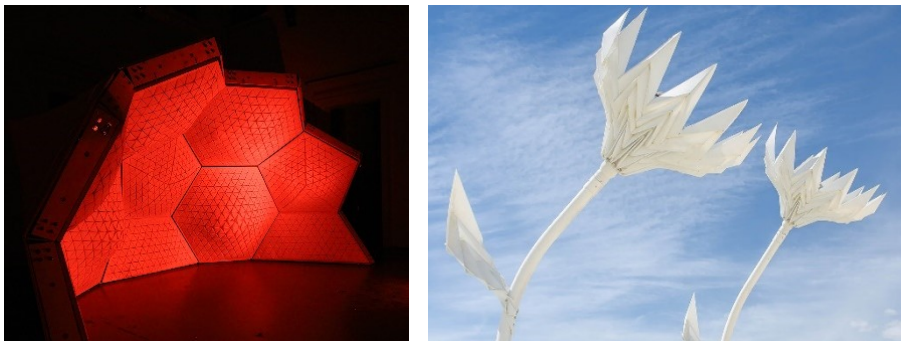


Figure 2. 108.
Cerebral Hut
Source: *ozeloffice.com*

Figure 2. 109.
Blumen Lumen
Source:
blumenlumen.com

Matthew Gardiner must be mentioned due to his continuous work in joining origami and robotic technology. Through the past years Gardiner has created a series of Oribotics, folding robots. His first experiments were flower modules with a small number of faces, like Atom Flower, exhibited at the Next Wave Festival in Melbourne in 2004 (**Figure 2.110**) and 2005 (**Figure 2.111**). Atom flower is a pentagonal flower with an actuator that works as a hand and makes it open and close (Gardiner, 2009).

After the initial experiments, Gardiner developed two new versions of Oribotics, one in 2007 and another in 2010. These new versions also work with a robotic hand but use surfaces with several faces instead of the modules of the earlier versions, as seen in **Figures 2.112** and **2.113** (Gardiner, 2011).

Figure 2. 110.
Atom Flower 2004
Source: Gardiner,
2009

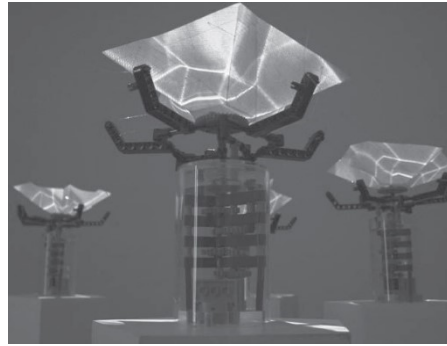


Figure 2. 111.
Atom Flower 2005
Source: Gardiner,
2009

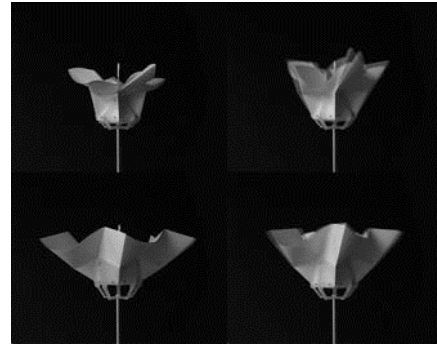


Figure 2. 112.
Oribotics evolution
Source:
Gardiner, 2011

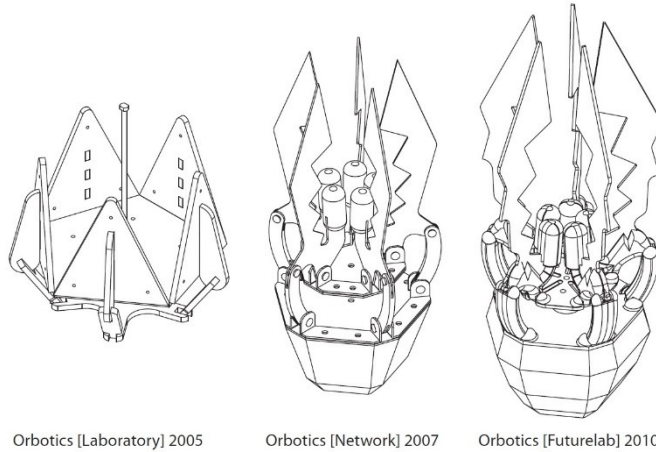
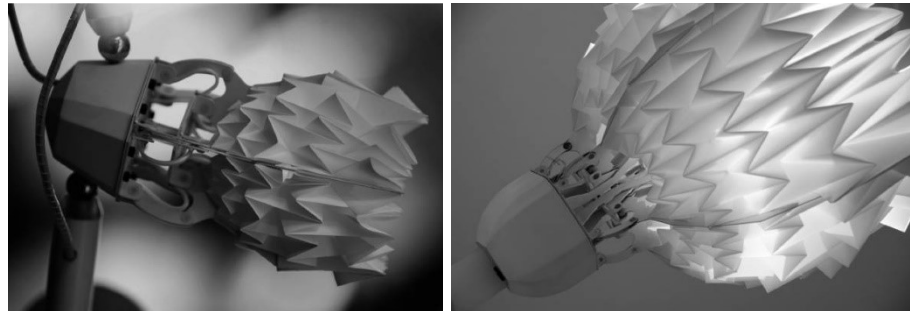


Figure 2. 113.
2007 and 2010
versions
Source:
Gardiner, 2011



From the examples shown, it is possible to understand that the potential of utilizing origami in architecture has deserved attention from architects for at least the last hundred years. Origami's ability to turn a thin, flat element into a self-supporting one through folds allows for its utilization in static buildings but also in deployable, lightweight structures, able to support themselves and to reach a flat state that allows for easy transportation and storage. Nevertheless it seems that the utilization that can take the best advantage of the properties of origami, such as rigid folding motion and flat-foldability, is kinetic utilization, where an origami model can be used either as a module or a surface, able to assume a range of configurations from the unfolded to the completely folded state, at any time during its life. Kinetic origami can be used as a versatile motion structure able to reconfigure itself in response to varied stimuli.

2.3 | Computational Design

Computational design tools are being increasingly used by architects and designers in order to help in the form finding process, performance-based design, structural analysis, environmental behaviour, etc. These tools enable architects to save time and resources in the design process and allow multicriteria to influence the design of buildings in a way that the human mind would probably not be able to.

As Terzidis (2006) and Ahlquist and Menges (2011) have noted, the use of computers in architecture today is mostly as a computerized way; entities or processes that exist in the designer's mind are entered, manipulated and stored in a computer system. On the other hand, the use of computation as a design tool seems to be generally limited and designers appear not to take advantage of the computational power of the current tools. For Menges and Ahlquist (2011) the computational design approach is the one which focuses on the execution of variational methods to resolve operating methods in architectural complexities due to the interdependences of material structures and dynamic environments. Therefore, the designer is posited as the author of the rules as implicit descriptions for the development of form (Ahlquist and Menges, 2011).

In the particular case of origami for kinetic structures, these tools can be extremely powerful for the design and adjustments of origami CPs and also to simulate their folding. The utilization of origami in large scale kinetic structures demands a profound knowledge of its structural behaviour and motion paths. The digital simulation tools may be a way to quickly simulate and test the kinematics of the moving/folding surface in order to predict the movement of faces and incorporate it into the global design.

Several authors dedicate their research to the establishment of the mathematical and geometrical properties of origami and to the development of simulators that integrate those properties. The next section is about the existing computational tools for origami simulation in their varied contexts.

2.3.1 | Folding Algorithms and Simulators

Lebée (2015) argues that computational design for folded structures can be a very useful tool for the form-finding process, however the author warns that there is a need for special care when these tools are used on the architectural scale, since they can lead to very complex patterns while their target is purely geometric, with no consideration for thickness, load bearing and stability. Lebée considers that a folded shape, if free to move, "*is not a structure. It is a*

mechanism (Lebée, 2015, p.63).” this means that if the structure’s movement is not locked in some way then the structure will behave as a mechanism and not as a structurally efficient pleated structure (Lebée, 2015).

Nevertheless, and even if a bit far from reality, zero-thickness folding simulations are very important tools for understanding the movement made by the structures, the possibility of collisions and the mechanical behaviour, even if the structures need to be evaluated further by other simulators that allow for the thickening of the faces and placing of hinges.

In the zero-thickness folding simulations area there are various authors that have been developing tools for computational origami.

Demaine and Demaine (2002) state that computational origami can be distinguished in two groups: a) Origami Design; b) Origami Foldability

In the group of **origami design** the authors state that the algorithms start with the target for the final folded state and generate a valid CP to fold that model.

In the group of **origami foldability**, the starting point is the CP and the target is unknown, the goal of these simulators is to fold a specific CP, with its MV assignment, regardless of expected results (Demaine and Demaine, 2002).

With regard to the utilization of simulators for architecture, and more specifically for kinetic architecture, it seems important to further subdivide the origami foldability group into the simulators that just give the final folded state and those that allow for the visualization of the folding process (**Figure 2.114**). For the specific case of kinetic architecture, the possibility of visualizing the folding motion of the surface may help in the understanding of the behaviour of the structure when in motion.

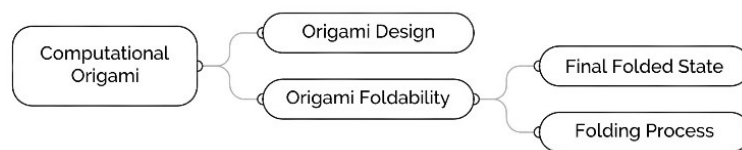


Figure 2. 114.
Origami Simulators
Diagram

If a designer needs to choose a particular folding state to be used in a static building, then it seems to be of great importance to use simulators that allow the architect to test individual folding states. If the aim is to develop kinetic buildings then this importance is emphasised further as the kinematic process is also part of the design and should be subjected to evaluation regarding collisions, loads and general movement paths.

The known simulators in the reviewed literature will now be presented regarding the subdivision of Computational Origami proposed by Demaine

and Demaine (2002) and the further division of Origami Foldability into Final Folded State and Folding Process.

Origami Design

Tree Maker is based on a method that has been developed by Robert Lang since 1993. The method allows for the generation of CPs for complex figures, usually animals or insects, with many limbs. It starts from an uniaxial base with the limbs attached, like a 2D graph, and generates the CP from there. The software started to be developed in 2004⁹ (Demaine and O'Rourke, 2007) (Lang and Demaine, 2009).

Tess is a program created by Alex Bateman 2002, used to design origami tessellations. These tessellation models are flat but are not usually rigidly foldable due to the common use of twist folds. The program was further developed by Bateman and Robert Lang, 2011. Tess transforms a tiling of the plane into a flat foldable CP, by scaling and rotating the base polygons and creating an orthogonal dual for the flat folding (Bateman, 2002) (Lang and Bateman, 2011).

Tachi developed two software programs¹⁰ for origami design. **Freeform Origami**, that enables the direct manipulation of the folded model and generates the CP and **Origamizer** that generates the CP of a three-dimensional model (Tachi, 2009 (b)).

With a similar approach to Origamizer, Heng Yi Cheng developed an algorithm that uses vector and angle calculations to define the folding of convex biplanar polyhedra gadgets between consecutive walls. The user starts by defining the desired volumetric form and the program generates the CP to fold that form (Cheng, 2011).

Origami Foldability - Final Folded State

Oripa¹¹, was developed by Jun Mitani in 2005 and calculates the folded shape of a pattern that can be drawn and altered by the user, providing a very quick response. Unfortunately, this software does not give the intermediary steps or folding motion, just the final step (Mitani, 2005).

⁹ Available at www.langorigami.com/article/treemaker

¹⁰ Available at origami.c.u-tokyo.ac.jp/~tachi/software/

¹¹ Available at mitani.cs.tsukuba.ac.jp/oripa/

Foldinator by John Szinger allows the user to record each step of the folding sequence and create diagrams for folding. It only shows the initial step and the folded step and not the motion in between (Szinger, 2002).

eGami is similar to Foldinator and is also used for diagramming. It was developed by Jack Fastag, 2009, and allows for direct manipulation of the model with real-time simulation. The diagrams are fully customizable and printable, and it is possible to create step-by-step animated folding tutorials (Fastag, 2009).

Finally, there is Tsuruta *et al.*'s (2011) algorithm for folding simulation and diagramming of flat folding models. This algorithm allows the user to introduce mountain or valley folds and takes the last folding step and the Huzita-Justin axioms to predict the most probable options for the next step, allowing users to choose the intended one. The simulator also has the capacity to record the history of steps for easy diagramming and folding simulation (Tsuruta *et al.*, 2011).

Origami Foldability - Folding Process

Tachi also developed a simulator based on rigid origami, the **Rigid Origami Simulator**¹². His simulator uses the fold angles of all crease lines as variables and the method is based on projection into the constraint space allowing for the folding motion of all crease lines to be the driver of folding. This simulator allows for the visualization of the folding process and for adjustments of the CP, such as the triangulation of faces if the outcome is not as expected (Tachi, 2009 (a)).

This simulator accepts CPs in DXF or Oripa formats. In order to avoid self-intersection between adjacent faces the fold angles of mountain or valley folds are limited to $[-\pi, \pi]$, and to avoid intersection among faces around the same vertex the added crease lines have the fold angle limited by the fold angles of adjacent crease lines. Although these limitations cannot avoid global self-intersection, they are enough for most cases. Additionally, this simulator can be used to draw diagrams since it allows for the transition from one-fold state to another (Tachi, 2009 (a)).

Gray *et al.* (2011), developed the Foldable Programmable Matter Editor; a simulator for Foldable Programmable Matter (FPM), *i.e.* smart self-folding sheets, which interprets crease patterns as rigid sheets, connected by revolute joints. It simulates rigid origami folding for programmable matter

¹² Available at origami.c.u-tokyo.ac.jp/~tachi/software/

structures where actuators, and their properties, may be involved in the folding motion. However, this simulator is restricted to the positions of the actuators throughout the sheet and the experiments made by the authors refer to small scale prototypes (Gray *et al.*, 2011).

Casale and Valenti (2012) provide several rigid simulations based on pure geometry that are “custom made” for each CP, similar to the work developed by Kong *et al.* (2015). Both contributions use Grasshopper for Rhino and have accurate geometric processes to determine the folding of patterns (Casale and Valenti, 2012) (Kong *et al.*, 2015).

Later, Casale *et al.* (2016) provide a more versatile simulator based on Grasshopper and Kangaroo for Rhinoceros. This more recent simulator is close to reality but the rigidity in folding is not rigorous, since Kangaroo allows for elasticity in the creases in order to make the surfaces fold (Casale *et al.* 2016).

Finally, there is a component developed by Daniel Piker for Grasshopper, called origami. This component was created to fold CPs with many faces via the definition of the mesh created by the faces and the assignment of the mountain and valley folds, nevertheless it works in the same way as Casale *et al.* (2016) simulations, *i.e.* it uses springs and elasticity, thus making it not strictly rigid.

03 | REACHING KOS

03 | Reaching Kinetic Origami Surfaces

From the presented state-of-art of the main areas under investigation in this thesis, Chapter 03 will make a critical analysis of kinetic architecture, origami geometry, mechanisms and control and materials and digital fabrication.

Regarding kinetic architecture, a detailed classification will be proposed first of all with a view to a specific area within the group of demountable/transportable structures, which is the group of deployable structures. As described in **Section 2.1.1**, the mechanisms used for kinetic structures and the ones used for the seployable structures are often similar and many authors speak about both as if there was no distinction. This thesis argues that there is a notable difference between the two groups, in particular the time when the action of movement takes place, as stated by Korkmaz (2004) and further debated on **Section 3.1.1**.

Due to the similarity between mechanisms, the taxonomy of kinetic structures will be made after that of the deployables. The proposal of this thesis on the taxonomy of kinetic structures intends to be comprehensive and strictly built on the contributions from the authors described in the previous chapter, constructed particularly through the criterion of structural aspects, as will be justified further ahead. This taxonomy is believed to be important in placing the current investigation within the existing kinetic structures for architecture, justifying the individuality of rigid foldable origami surfaces category and offering a full spectrum for comparison.

In Chapter 03 an attempt to establish the relation between the kinematic joints and mechanisms for architecture will be made, including the type of links of the described mechanisms and their structural ability, subsequently relating it to every branch of kinetic architecture typologies proposed in the taxonomy.

The analysis of origami geometry for rigid and flat foldable surfaces will be made through the analysis of the *Corpus* of Crease Patterns (CP) presented in **Section 2.2.2**. These patterns will be analysed first in regard to the degree of the vertices, their rigid and flat-foldability, and the type of geometric form each one tends to fold into. Moreover, the similarities between the patterns will be pointed out, in order to create more general families

The section on origami analysis will provide the inputs for this thesis' proposed folding simulations for degree-4 and degree-6 CPs, developed on Grasshopper (GH) for Rhinoceros. Besides allowing for folding simulation, these algorithms will allow also to make adjustments to the CP at any moment during the folding process.

Section 3.4 will provide an analysis of the materials suited for thick origami surfaces and in **Section 3.5** the experiments conducted during this investigation will be described. These experiments will allow conclusions to be drawn on origami geometry (CP and folding simulation), the behaviour of materials, digital fabrication, “thick origami” strategies and the behaviour of constructed surfaces. Furthermore, the methodology used in the development of each experiment will be described and analysed to serve as justified input for the development of the proposed workflow to generate kinetic origami surfaces (KOS) with controlled motion, from concept to construction.

3.1 | Proposed Classifications

The proposed classifications depart from a first, more generic examination of the definitions described in **Section 2.1.1**. From the authors’ contributions, it is possible to extract seven used criteria:

- a) Structural Aspects
- b) Application
- c) Type of Material
- d) Type of Movement
- e) Morphological Aspects
- f) Kinematic Properties
- g) Inspirational Source

In **Figure 3.1** it is possible to understand the relationship between the criteria used by the authors in their contributions, the number of authors that used each criterion and which criteria were used only once or twice.

Structural aspects is clearly the most recurrent, as it is used by all of the authors and the remaining criteria are shared only by two, three or four authors.

This was the first guideline for taxonomies proposed by this thesis, they are primarily organized regarding the structural aspects of each category and include all the categories mentioned by the analysed authors, unless explicitly justified.

Authors Criteria	Zuk and Clark	Frei Otto	Merchan	Hanaor and Levy	Gantes	Pellegrino	Korkmaz	Schumacher et al.	Stevenson	Del Grosso and Basso	Rivas Adrover
Structural Aspects											
Application											
Type of Material											
Type of Movement											
Morphological Aspects											
Kinematic Properties											
Inspirational Sources											

Figure 3. 1.
Relation between the criteria used by each author for the kinetic structures definitions

In the following paragraphs, the two proposed taxonomies for demountable/transportable structures and kinetic structures will be explained. This research believes that by providing both it may help to understand the differences between the two categories since, by comparison, the scope of each may become clearer as well as the different utilization of similar mechanisms.

3.1.1 | Demountable and Transportable Structures

Concerning transportable and demountable structures, Korkmaz (2004) proposes some categories that do not incorporate movement in the structures in the physical sense.

The author considers that buildings with variable location or mobility can be subdivided into portable buildings, relocatable buildings and demountable buildings. The relocatable structures will not be considered as an independent group since they seem redundant, transportable and demountable buildings have relocation implied in their meaning.

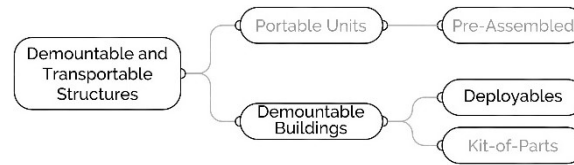
The category of portable buildings will be named **portable units**, so that it can contain units that are buildings as well as buildings constituted by several transportable units. These would be the prefabricated and **pre-assembled** modules that can be transported and settled in any location, described by Zuk and Clark, 1970, as mobile architecture.

In the development of these kinds of structures the dimensions are usually the main concern since they must be assembled and then transported to the place of use (Zuk and Clark, 1970) (Kronenburg, 2003).

Regarding the **demountable buildings**, two main categories, defined by De Temmerman *et al.* (2012), are being considered, **deployables** and **kit-of-parts** (Figure 3.2). The deployables group includes the structures that use mechanisms, which enable the structure to have a compact configuration (for transportation or storage) and an expanded state that fulfils its architectural

function. The kit-of-parts group includes structures that are composed of elements with reversible connections, allowing the structure to be assembled and disassembled, and where the components can be reconfigured, replaced and re-used (de Temmerman *et al.*, 2012).

Figure 3. 2.
General proposed
classification for
demountable/transportable
structures



Deployables category is referred to across the reviewed literature by almost every author, only Zuk and Clark (1970) call them dynamically self-erecting structures and reversible architecture. This is the category that will be further subdivided here since these are the structures that have mechanisms associated for deployment and retraction, and thus is the one that relates the most to kinetic structures and from which several types of structures can be brought into the context of kinetic structures.

Throughout the revised classifications there is a common division between rigid and deformable (often described as “flexible”) components that are responsible for movement, which is natural since the kinematics associated with each type are quite different and correspond to completely distinct structural aspects, this division will also be the starting point for the proposed classification.

Inside the **rigid components** group two major subdivisions are proposed; **bar structures**, as nominated by Korkmaz, 2004 (strut structures by Merchan, 1987; lattice and skeletal by Hanaor and Levy, 2001; structural mechanism by Pellegrino, 2001; lattice work by Rivas Adrover, 2015) and **surface structures**, as described by Merchan, 1987 and Korkmaz, 2004 (continuous or stressed skin by Hanaor and Levy, 2001; solid surface by Rivas Adrover, 2015).

In relation to bar structures, this classification will not consider Hanaor and Levy’s subdivision into DLG, SLG and spine, the aim is to make a more general classification where all bar structures can be incorporated and later subdivided into more specific groups. Bar structures is subdivided into **umbrella mechanisms** (Merchan, 1987), **pantographs** (scissor-hinged mechanism, Merchan, 1987; scissor like mechanism, Del Grosso and Basso, 2013), **articulated joints**, as nominated by Hanaor and Levy (Hinged collapsible Strut mechanism, Merchan 1987; morphing truss structure, Del Grosso and Basso, 2013; folding articulated trusses, Pellegrino, 2001), **ruled**

surfaces (Hanaor and Levy, 2001), and **mutually supported elements** (Del Grosso and Basso, 2013).

In relation to surface structures, only one category defined by Hanaor and Levy will be used, **rigid foldable origami** as defined by Del Grosso and Basso, 2013 (folded rigid panels, Merchan 1987; folded plates, Hanaor and Levy, 2001; rigid panel structure, Pellegrino, 2001; origami paper pleat, Rivas Adrover, 2015). As Hanaor and Levy's subgroup curved surface is not really a deployable, it is the Laminar Geodesic Dome by Buckminster Fuller, 1960, that is a mountable and demountable building, thus it would be more accurately categorized under the kit-of-parts category. Regarding the folded plates category this classification will not use Hanaor and Levy's further categorization into linear deployment and radial deployment, because the direction of movement is not considered in any other category and rigid foldable origami can also undertake combinations of directions depending on the geometry of the CP.

For the **deformable components**, a first subdivision is proposed that differs slightly from the one proposed by Hanaor and Levy, 2001. Instead of lattice and skeletal, **linear elements** is proposed, referring to the deformable components such as cables and rods, instead of referring to the rigid ones as Hanaor and Levy did. Regarding the continuous or stressed skin, **continuous surfaces** is simply proposed since the aim is to include also structures that would not fit into the "skin" nomenclature.

The linear elements are further subdivided into **strut-cable systems** (tensegrities) as referred to by several authors, and a new category is added, **coiled rods**, as introduced by Pellegrino, 2001.

The continuous surfaces are subdivided into the **bi-stable structures** (Flexible Shells, Pellegrino, 2001), **foldable membranes** as described by Stevenson, 2011 (continuous flexible material, Merchan 1987; deformable fabrics and nets, Rivas Adrover, 2015) and **tensioned membranes**. This latter group is subdivided into tensioned fabrics or nets, that need the aid of anchors, cables, masts or other support elements in order to be tensioned, and pneumatics, which need the aid of air or other gaseous pressure to be tensioned. Pneumatics are further subdivided into air-inflated and air supported as described by Gantes, 2001 and referred to often by Fenci and Currie, 2017, in substitution of Hanaor and Levy's high and low pressure, respectively.

Compliant mechanisms were not introduced into the table since there is not yet any example of their effective utilization in architectural structures (Del Grosso and Basso, 2013).

Figure 3.3. shows the complete tree classification of the category of deployable structures inside the **demountable/transportable structures**.

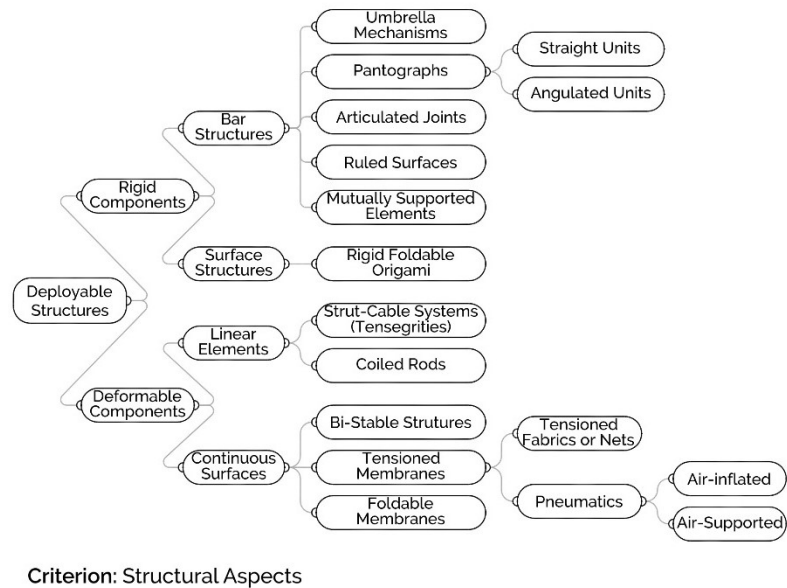


Figure 3.3.
 Deployable structures' proposed classification for demountable/transportable structures

3.1.2 | Kinetic Architecture

When discussing **kinetic structures**, that is to say structures that must move often in their lifetime, several deployables can be useful, especially the ones whose structure also acts as a mechanism. From the previous table all the structures that belong to the rigid components will also be used for the classification of kinetic structures, except two groups, the ruled surfaces group and the mutually supported elements.

Ruled surfaces will not be considered because, as stated by Hanaor (2009), theoretically these structures seem to be able to open and close into a bundle, but in practice the elements must be very long and massive and the bundles are not very compact, and so the author argues that this concept is more suitable for dismountable structures (Hanaor, 2009). Structures built with the system of mutually supported elements have great potential but are usually static and/or dismountable, and it seems that there is not yet any significant progress in the field of kinetic architecture (Del Grosso and Basso, 2013).

Structures that belong to the deformable components > linear elements are not suited for kinetic utilization since they have only two states that can be easily controlled, the fully erected and the compacted one; the in-between states are not controllable or demand additional mechanisms. (Del Grosso and Basso, 2013). In a kinetic context the possibility to control and predict the

behaviour of the structure is of significant importance, even more so due to the scale of the structures, their weight and safety requirements, consequently this group will not be part of kinetic structures.

Regarding continuous surfaces, bi-stable structures will also be disregarded since their behaviour is somehow like the previous ones, they have only two stable states (as the name implies) and their geometry may change too fast and too unpredictably from one state to the other, making them difficult to be used in kinetic structures on a large scale. In respect to tensioned membranes only the air-inflated ones can be considered since the other categories have only two states, in tension or without tension, so there is no potential to use them in a kinetic way from one state to the other (Schumacher *et al.*, 2010). Foldable membranes are perfectly applicable to kinetic structures, as countless examples demonstrate in our everyday life, such as canopies with textile coverings or awnings, and will certainly be considered.

Figure 3.4 shows the proposed deployable structures classification with highlighted categories, which will be considered for the classification of kinetic structures.

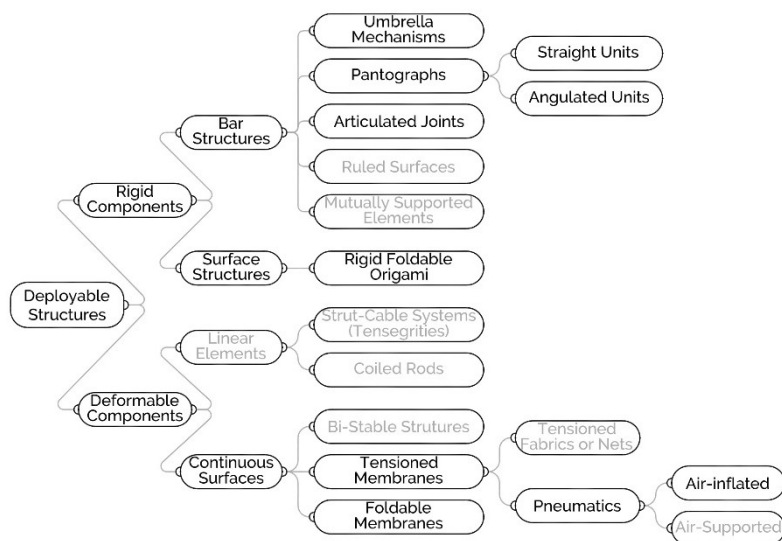


Figure 3.4. Deployable structures, categories for kinetic structures

Finally, some other kinds of structures will be added to kinetic architecture classification. One important aspect to consider in kinetic structures is that the structures are not constrained to be the whole building, as often happens with deployables. The classification tries to be general enough in order to be able to include elements such as walls, floors, inner and outside elements, façades, roofs, etc, and structures that are both wall and roof, that is, that act as an entire building, the diagram for the classification of kinetic structures is in **Figure 3.5**.

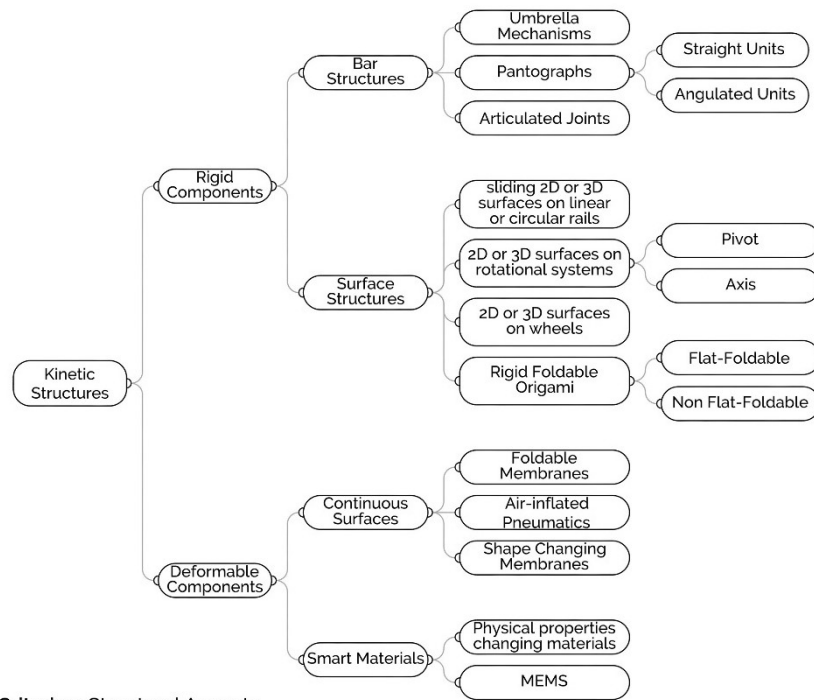


Figure 3.5.
 Kinetic Structures
 proposed classification

Criterion: Structural Aspects

Just as in the classification of deployables, the **classification of kinetic structures** is divided according to the main structural aspects of the categories. It is first divided into rigid and deformable components relating to the mechanism and the morphology of the structure that changes through movement.

Rigid components are subdivided into **bar structures** and **surface structures**. This division is made according to the geometry of the structural components, since the distribution of forces is different on each one. In the bar structures the forces are linearly conducted while in the surface structures the forces get distributed through the entire surface.

The Bar Structures group includes umbrella mechanisms, pantographs and articulated joints. This division relates to the kinematics and directions allowed for movement in each system (**Figure 3.6**).

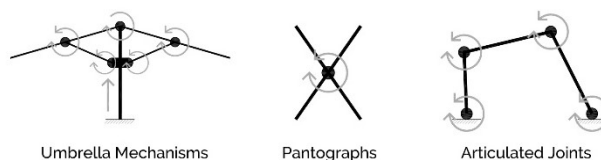


Figure 3.6.
 Schematic description
 of Bar Structures

An example of the **umbrella mechanisms** could be the 250 umbrellas designed by Mahmoud Bodo Rasch for the Medina Haram Piazza in Saudi Arabia in 2010.

The bar structures category also includes the **pantographs** group, that are subdivided into **straight units** (translational or polar) and **angulated units**. Examples of the utilization of the pantograph system with straight units include Emilio Pinero's Mobile Theatre, 1961, or Félix Escrig's Cover for a swimming pool in Seville. The Iris Dome designed by Hoberman for MOMA, in 1994, is made with angulated scissor elements.

The **articulated joints** category includes structures whose mechanisms are based on linkages, such as the ones described by You and Chen (2012), the NASA deployable truss structures, such as NASA PACTRUSS, developed by Alan Britt and Haresh Lalvani in 1997, or the Rolling Bridge by Heatherwick Studio, 2004.

The **surface structure** group considers solid surfaces, planar or three-dimensional, which are divided in respect to the mechanism that makes them move. Whether these are **rails**, which can be linear or circular (this category includes telescopic structures), **rotational systems**, the rotation can either be made around a **pivot**, which can lead to diaphragm-like systems, or around an **axis**, like a simple hinge, or free systems like units on **wheels**.

Examples of surfaces that slide on rails in a telescopic way include the Sliding House, in Suffolk, UK, designed by dRMM Architects and completed in 2009, or the roof of the Mellon Arena in Pittsburgh, constructed in 1961 and demolished in 2012, designed by Mitchell & Ritchey Architects.

The Qizhong Forest Sports City Tennis Centre, by Mitsuru Senda, built in 2005, is an example of eight surfaces, placed on a circular perimeter, that rotate around pivots in a diaphragm-like movement. The Star Light Theatre by Studio Gang O'Donnell finished in 2005 is composed of planar, solid surfaces that rotate around an axis, in the same way as TetraScript, by Gonçalo Castro Henriques, that designed and constructed a light responsive pavillion finished in 2009. Also, Calatrava's Brise Soleil for the Milwaukee Art Museum (2001), may be an example where several thin and long elements rotate in turn of an axis and define organic surfaces.

An example of relatively free systems, such as surfaces on wheels, is the Naked House, by Shigeru Ban, where each room is a unit that can be "parked" anywhere inside the house.

Finally, surface structures have a last group called the **rigid foldable origami**, which is subdivided into **flat-foldable** and **non-flat-foldable**. In this context these two groups are of particular importance since they define if the kinetic surfaces will be able to be completely compacted or not. The Origami Kinetic Sculpture by the Compliant Mechanisms Research Group of the BYU and Tomohiro Tachi's Prototype (2011), are two examples of rigid foldable origami

structures that fold flat. The Resonant Chamber by RVTR and ARUP and the Cerebral Hut, designed by Guvenc Ozel and Alexandr Karaivanov are two examples of rigid origami surfaces that are not flat-foldable, both use Ron Resch's pattern.

For the **deformable components** the division is made into continuous surfaces and a new proposed category, the smart materials.

Regarding the **continuous surfaces** group some categories are maintained from the deployables classification, such as foldable membranes and air-inflated pneumatics, like tensairities and pneumatic muscles and a new one is proposed, **shape changing membranes**.

Several examples of **foldable membranes** can be found in canopies or retractable roofs for sports facilities, such as the retractable roof for BC Place Stadium, designed by Stantec Architecture in a partnership with Hightex, finished in 2012.

Currently **air-inflated pneumatics** are being intensively investigated for use in soft robotics, such as Furl, developed by Francois Mangion and Becky Zhang at the Interactive Architecture Lab at the Bartlett School of Architecture, in 2014. As far as **shape changing membranes** are concerned, an example is Hyposurface, developed by Mark Goulthorpe from MIT.

The **smart materials** category includes **physical properties changing materials**, or materials that modify the shape of their inner structure when subjected to environmental changes, which reflects in their overall geometry, such as Achim Menge's Hygroscope and Shape Memory Alloys (SMA) as used by Doris Sung in her shading canopy Bloom, built in 2011.

Smart Materials are further subdivided into **micro-electro-mechanical systems** (MEMS) that allow for shape alteration in response to predetermined stimuli, such as the Programmable Foldable Sheets developed by Hawkes *et al.* in 2010.

Table 3.1 summarizes the proposed classification and related examples for each distinct group of kinetic structures for architecture.

Kinetic Structures in Architecture			Examples	
Rigid Components	Bar Structures	Umbrella Mechanisms	Medina Haram Piazza, Mahmoud Bodo Rasch	
		Pantographs	Straight Units	Mobile Theater, Emilio P. Pinero Swimming Pool Cover, Félix Escrig
			Angulated Units	MOMA Iris Dome, Hoberman
		Articulated Joints	NASA PACTRUSS, Britt and Lalvani Rolling Bridge, Heatherwick Studio	
	Surface Structures	Sliding 2D or 3D surfaces on linear or circular rails		Sliding House, dRMM Architects Mellon Arena, Mitchell & Ritchey
		2D or 3D surfaces on rotational systems	Pivot	Qizhong Tennis Center, Mitsuru Senda
			Axis	Starlight Theater, Studio Gang O'Donnell Milwaukee Art Museum, Santiago Calatrava
		2D or 3D surfaces on wheels		Naked House, Shigeru Ban
		Rigid Foldable Origami	Flat-Foldable	Origami Kinetic Sculpture, BYU Tomohiro Tachi's Prototype, 2011
			Non Flat-Foldable	Ressonant Chamber, RVTR Architects Cerebrat Hut, Guvenc Ozel and Alexandr Karaivanov
Deformable Components	Continuous Surfaces	Foldable Membranes	Retractable Roof of BC Place Stadium, Vancouver	
		Air-inflated Pneumatics	Furt, Francois Mangion and Becky Zhang	
		Shape Changing Membranes	Hyposurface, Mark Goulthorpe	
	Smart Materials	Physical properties changing materials		Hygroscope, Achim Menges Bloom, Doris Sung
		MEMS		Programmable Foldable Sheets, Hawkes et al.

Table 3.1.
Summary table for kinetic architecture structures with examples

From Table 3.1 it is intended to make clear that the structural behaviour and global form of each example is distinct and belongs to the group that each specifies. No example would be correctly placed under any other category. Within the rigid components group the bar structures are formally different from the surface structures. The first ones are lighter and behave as a skeletal, hence being less opaque. These structures have the inherent capability of collapsing (or shrinking) into a small volume and expanding from it, thus needing an extra element, like a skin, that is able to follow the movement of the structure movement and cover it. In the case of umbrella mechanisms the deployed forms are usually conical around a mast, next to which it becomes compacted, so the compacted form points to a bidimensional form, while on the pantographs the compacted form is three-dimensional and is a scaled version of the deployed object. The articulated joints offer more options between the compacted and deployed form depending on the design of the skeletal and placing of the joints.

With regard to surface structures, compared to the bar structures, the overall form tends to be more opaque, massive, solid, and is usually subdivided into similar forms that collapse next to each other (Sliding House, Mellon Arena), at the periphery (Qizhong Tennis Centre, Starlight Theatre, Milwaukee Art Museum), or freely (Naked House).

Rigid foldable origami combines the qualities of both types described above, these surfaces can shrink and expand and are both skin and structure at once. In the deformable components the continuous surfaces are moved by external mechanical systems that apply tension to push and pull the surfaces, while in the smart materials it is the intrinsic nature of the material, on a micro or nano-scale, that react to stimuli and produce movement.

3.2 | Mechanisms

As explained in **Section 2.1.2** a mechanism is a connected system of bodies that transforms energy into mechanical motion. The bodies that constitute a mechanism are called links, these links may be rigid or flexible (Kolovsky *et al.* 2000).

When the mechanism is also the load bearing structure, that is, when its links guarantee motion and also the erection and stability of the object, it can be called a Motion Structure (You and Chen, 2012).

In this section, the mechanisms for Kinetic architecture will be analysed in respect to their types of movement, degrees of freedom, types of joints and types of links.

Following this analysis, a new comparison relating the kinetic architecture classification and the kinds of mechanisms associated with each category will be made in order to prove that the type of mechanism is directly related to the structural aspects that led to the kinetic architecture taxonomy, since they all behave as motion structures according to You and Chen's (2012) definition.

In the previous chapter the main kinematic joints used in mechanisms were described. These kinematic pairs are summarized in **Table 3.2** regarding the type of pair, movement and degrees of freedom, adapted from You and Chen, 2012.

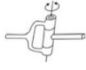

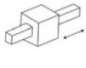
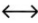
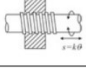

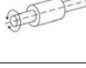



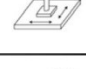


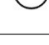

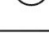
Kinematic Joints	Name	Symbol	Type(s) of Movement	Degrees of Freedom
Lower Pair	Revolute			1
	Prismatic			1
	Screw			1
	Cylindrical			2
	Spherical			3
	Planar			3
Higher Pair	Cylindrical Roller			1
	Spatial Point Contact			5

Table 3. 2.
Kinematic joints
Source: adapted from
You and Chen, 2012

In **Section 2.1.2** simple mechanisms, linkages, smart materials and pressure were described as the main mechanisms that may be used for kinetic architectural structures. **Table 3.3** tries to give an overview of the described mechanisms and the existing subcategories for each main group. The table later provides the types of movement, degrees of freedom, type of joints present and the type of links for each mechanism's subcategory.

Through Table 3.3 it is easier to reach several conclusions regarding mechanisms for kinetic architecture, their similarities and differences. It is also possible to understand that the mechanisms used for large scale architectural structures, are not as complex as in other types of machines. The mechanisms do not usually have many degrees of freedom and often just one type of mechanism is used for an entire structure.

The real complexity in architecture is the scale of the elements, their weight and the frequent need for repetition of the mechanical system. It is the case of linkages or pantographic mechanisms where, besides scale, it is the repetition of the same element that introduces complexity into the system.

Another reason that may justify the use of simple or repetitive mechanisms with low degrees of freedom is that architectural structures are meant to be used by people, and too many possibilities for movement in such a structure could be dramatic if it could result in unpredictable behaviour putting the users at risk. Low degrees of freedom in these types of mechanisms allow for

certainty on the trajectories undertaken by the kinetic elements and the geometric behaviour of the structure as a whole.

Category	Subcategory	Symbol	Type(s) of Movement	Degrees of Freedom	Type of Joints	Type of Links	
Simple Mechanisms	Hinges			1	Revolute or Cylindrical	Rigid	
	Rotary Bearings			1	Revolute	Rigid	
	Translational Bearings			1	Prismatic	Rigid	
	Open or closed circuits of: Ropes, Belts or Cables on Pulleys or Toothed Wheels (includes winches)			1	Revolute and Prismatic	Rigid and Flexible	
Linkages	Non-Pantographic Linkages			depends on the geometry of the linkage	Revolute, Cylindrical and/or Spherical	Rigid	
	Pantographic	Straight Translational			1	Revolute	Rigid
		Straight Polar			1 depends on fixed point(s)	Revolute	Rigid
		Angulated			1 depends on fixed point(s)	Revolute	Rigid
Smart Materials as Mechanisms	Hygroscopic		depends on material's intrinsic properties	depends on material's intrinsic properties	-	-	
	Shape Memory Alloys (Plastic or Metals)		depends on material's intrinsic properties	depends on material's intrinsic properties	-	-	
	Programmable Matter		depends on material's properties and code	depends on material's properties and code	-	-	
Pressure as Mechanism	Flexible Materials (includes Pneumatics)		depends on material's intrinsic properties and geometry of the inflatable element	depends on material's intrinsic properties and geometry of the inflatable element	-	Flexible	

Table 3.3.
 Mechanisms Comparison table for architectural application

The types of joints used in architectural mechanic systems are usually the revolute, prismatic, cylindrical or spherical joints. Revolute joints are the most common and are present in seven of the eight subcategories that have joints. No higher pair joint was found in these mechanisms.

The links are in most cases rigid, which was expected, since these are motion structures, thus the mechanism is both responsible for motion and load-bearing. When the links are flexible, the way of using them is in tension, otherwise they have no structural contribution to lend to the mechanism.

From the observation of the table it is also possible to conclude that the use of smart materials or pressure as mechanism do not have clear and obvious connections to the types of movement and degrees of freedom of the

structures. The behaviour of these mechanisms depends greatly on the properties and/or geometry of the elements that compose the “machine”.

Table 3.3 refers to all of the mechanisms mentioned in Section 2.1.2 but is very generic. The next table tries to be more tangible by relating every category proposed for the kinetic structures classification to the mechanism associated with them, and also with the mechanism’s structural ability, if they are the main load-bearing structure and if they accomplish this with the help of other elements, external to the mechanism.

The association between categories and mechanisms was made by observation of the examples presented in Section 3.1.2, Table 3.1, of this Chapter.

From **Table 3.4** it is possible to comprehend that the type of kinetic structure is almost always directly related to the mechanism that makes it move. It is the type of mechanism that defines the type of structure and the mechanism is partially or completely responsible for the stability of the structure.





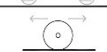









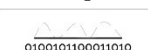
Proposed Kinetic Architecture Classification			Mechanism	Mechanism is main load-bearing structure?	
Rigid Components	Bar Structures	Umbrella Mechanisms		Yes	
		Pantographs	Straight Units		Yes
			Angulated Units		Yes
		Articulated Joints			Yes
	Surface Structures	Sliding 2D or 3D surfaces on linear or circular rails			Yes + surface's structure
		2D or 3D surfaces on rotational systems	Pivot		Yes + surface's structure
			Axis		Yes + surface's structure
		2D or 3D surfaces on wheels			Yes + surface's structure
		Rigid Foldable Origami	Flat-Foldable		Yes
			Non Flat-Foldable		Yes
Deformable Components	Continuous Surfaces	Foldable Membranes		Yes	
		Air-inflated Pneumatics		Yes (membrane tension)	
		Shape Changing Membranes		Yes (membrane tension)	
	Smart Materials	Physical properties changing materials			Yes
		MEMS			May be

Table 3.4. Mechanisms for kinetic architecture

One clarification should be made in respect to rigid foldable origami. In the case of these structures the chosen mechanism was Hinges (with revolute joints) but, as explained in **Section 2.2.4**, each vertex of an origami surface can be seen as a spherical joint with several bars (that correspond to the concurrent creases at that vertex) attached. When speaking about origami surfaces it is implied that these surfaces will have multiple faces and multiple vertices, and consequently the movement around each vertex will not be as a pure spherical joint anymore but will rather be constrained by the geometry of the face and the connection to the consequent faces and vertices. For this reason, the spherical joint possible behaviour of one single vertex was overlooked, at the limit the vertices could even be cut off the surface and it would retain its kinematic mobility, as happens in the Kinetic Sculpture by BYU. This proves that the hinges, and their constrained motion in relation to nearby hinges through the connection by rigid links (faces), are the main mechanism when referring to surfaces with multiple vertices.

3.3 | *Origami Geometry*

In this section an analysis of origami CPs to be used for the purpose of kinetic structures will be made, through the origami properties described in **Section 2.2**. The analysis will include the rigid and flat foldability theorems and lemmas and the rules for non-crossing faces applied to the selected patterns described in **Section 2.2.2**.

The analysis of the patterns will start from the zero-thickness perspective, understanding the forms into which they fold and compliance with the explained rules and theorems. Afterwards the existing thick origami strategies and their pertinence for specific CPs will be critically analysed, in order to transform the zero-thickness surfaces into kinetic surfaces able to be used in an architectural context.

Finally, after consideration of the simulators described in **Section 2.3**, the proposed simulators for kinematic motion of CPs with vertices of degree-4 and degree-6 will be presented.

3.3.1 | *Crease Patterns*

In **Section 2.2.2** the patterns selected for the analysis were described. the group of chosen patterns does not include curved creased patterns, crystallographic flat origamis, patterns with a small amount of faces and centralized folding motion (modules) nor does it include patterns with vertices of degree higher than six, since these were found to lack kinetic potential and/or would generate surfaces too complex to be used in architecture due to the excess of thickness around the vertices.

The group of patterns that will now be analysed have vertices from degree-2 to degree-6, are all rigidly foldable and, except for the Resch Family's patterns, are also flat foldable.

The selected patterns were first grouped by vertices degree in order to create clusters of patterns that may relate to each other and to try to understand if there are similarities among them that can make them a family.

The patterns will be analysed with respect to the rules for rigid and flat-foldability, such as the Maekawa-Justin and Kawasaki-Justin theorems, the Big-Little-Big Lemma, the ability to rigidly fold and the verification of non-intersection.

Most patterns were proven to be rigid and flat-foldable by other authors and ourselves through the verification of the described rules and also through geometric and physical experimentations on the patterns (Tachi, 2009 (a))

(Wang and Chen, 2011) (Tachi, 2015) (Evans *et al.*, 2015(a)) (Evans *et al.*, 2015(b)).

The patterns will also be examined in regard to their compression capacity, in the “Comp.” column (100% for pure flat-foldable patterns, lower values for special cases of flat foldability or non-flat-foldable CPs), and the type of geometry they tend to achieve when folding with regular folding angles.

There are three patterns that cannot be grouped inside a single type of vertex family, but that still may be very interesting to be used in architecture. These are the Resch Family Patterns (Gardiner, 2018), used in several of the examples presented for origami in architecture.

The Resch Family patterns group includes the squared waterbomb and the hexagonal waterbomb, which have a combination of vertices of degree-5 and degree-6, as well as the best-known Resch Pattern, which only has degree-6 vertices. All of them are rigidly foldable and have a folding motion that allows for no intersection amongst faces, but neither are flat foldable, since none verifies the Maekawa-Theorem and only the Resch Pattern verifies the Kawasaki Theorem.

All of the Resch Family Patterns assume double curvature configurations during the folding motion, spherical if the folding angles are constant, and ultimately all of these end up as a planar configuration, even if not flat. When the patterns reach the maximum point of folding it is possible to analyse their compression capacity, which corresponds to the “tucking faces” around the faces that remain visible at the end of the folding process.

Table 3.5 summarizes the described analysis.

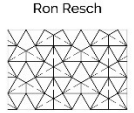


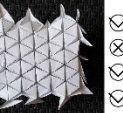
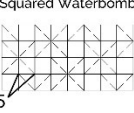


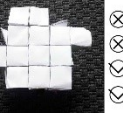




Crease Pattern	Folding State 1	Folding State 2	Folding State 3	Rigid and Flat-Foldable	Comp.	Folds Along
Ron Resch 				<input checked="" type="checkbox"/> Kawasaki <input checked="" type="checkbox"/> Maekawa <input checked="" type="checkbox"/> No Self-Intersection <input checked="" type="checkbox"/> Rigidly Foldable	66,66%	Double Curvature
Squared Waterbomb 				<input checked="" type="checkbox"/> Kawasaki <input checked="" type="checkbox"/> Maekawa <input checked="" type="checkbox"/> No Self-Intersection <input checked="" type="checkbox"/> Rigidly Foldable	80,00%	Double Curvature
Hexagonal Waterbomb 				<input checked="" type="checkbox"/> Kawasaki <input checked="" type="checkbox"/> Maekawa <input checked="" type="checkbox"/> No Self-Intersection <input checked="" type="checkbox"/> Rigidly Foldable	57,14%	Double Curvature

Table 3.5.
 Resch Family CPs
 with Degree-6 and
 Degree-5 vertices

As the patterns in study in this section are generally regular tessellations with the same faces repeated continuously throughout the plane, the approach

used in this thesis was, whenever possible, the study of the “base faces”, that is a small set of faces that are repeated throughout the tessellation and that can define the behaviour of the entire surface. This approach was undertaken by other authors that used different names for the base faces, such as “fundamental region” (Miura, 2002), “origami molecule” (Halloran, 2009), “unit cells” (Klett, 2011), or “fold-molecule” (Gardiner, 2018).

The “base faces” is the set of faces that if copied and attached to one another, in the symmetry directions, make the entire surface. With this set of faces selected it is possible to study the behaviour of the folding on the present faces and vertices and assume that they represent everything that will happen on the surface. So, if the fundamental region is rigid and flat foldable then all of the surface will be. The most important thing to pay attention to when using this methodology are the non-crossing conditions that sometimes cannot be perceived through manipulation and geometric analysis of the base faces alone, so it is necessary to construct a big enough array of base faces and check for self-intersection.

Figure 3.7 exemplifies the selection of base faces and the corresponding tessellations using the Resch Family patterns.

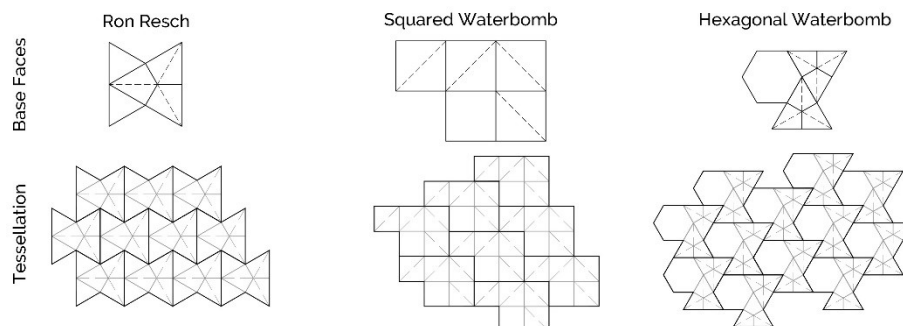
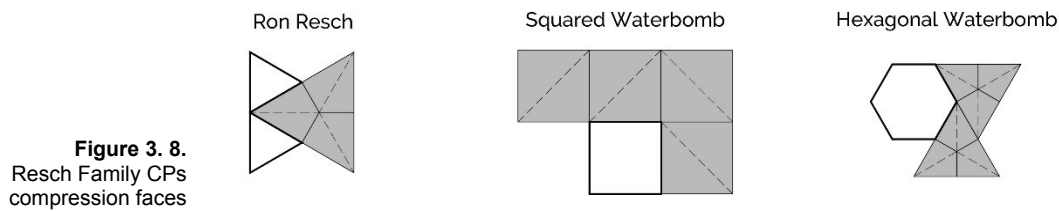


Figure 3.7.
Resch Family CPs
base faces and
respective tessellations

In the particular case of the Resch Family the base faces were also used to define the capacity of compression of each pattern presented in Table 3.5. The faces that remain visible in the completely folded state were considered to be without compression (white in **Figure 3.8**), and the faces that are responsible for the double curvature configurations and that “disappear” in the final state are those that really generate the compression from the first to the final state (grey in **Figure 3.8**). In this way, a direct relation between these two types of faces is what defines the capacity of compression for each pattern. In the case of the Resch Pattern the compression is $2/3$ (66,66%), the Squared Waterbomb compresses $4/5$ (80%), and the Hexagonal Waterbomb has the worst compression capacity, $4/7$ (57,14%).



Another line of this study is related to the main grid of the patterns. The grid of a pattern is set by the group of crease lines that cross the entire plane without changing direction in spite of whether they are always mountain, valley or if they have both identities. The grids are usually found to be parallel, orthogonal, parallelogram like, triangular or hexagonal, each grid as different implications of the geometries that the CPs can assume in the configuration of the individual faces. It will also be studied how the sequences of vertices along the directions of the grids influence the geometries assumed by the models and the implications of changing the angles between creases around the vertices.

Finally, it is necessary to establish some common ground for every pattern so that the results may be simplified and comparable. It is assumed that the CPs depart from the XY plane, with the valley folds attached to that plane (whenever possible) and that all faces fold with equivalent angles throughout the folding process. This assumption intends to establish the same referential for all geometries and to help to understand which patterns are caused to leave the “ground plane” due to the geometry of the faces, the MV assignment and the relation between consecutive faces. In this way it is also possible to understand the “natural” movement of a CP, regardless of whether it can achieve other, more complex, forms if it was supported by other geometries than the plane.

Some conclusions were reached from a very direct analysis. The faces on the Degree-2 flat-foldable CPs are always triangles or quadrilaterals, on Degree-4 CPs are always quadrilaterals and on Degree-6 the faces are always triangles for flat-foldable CPs, as will be demonstrated in the following sections.

It was also verified that the vertices of any degree can only be two types, that is, the degree-2 vertices can be 2M or 2V, the degree-4 can be 3M+1V or 3V+1M and the degree-6 can only be 4M+2V or 4V+2M.

The type of vertices defines whether the folding is progressively done in the same direction, if all vertices are of the same type, or if the folding is done in one direction and then the opposite, if the vertices alternate between the two types.

Degree-2 Crease Patterns

The degree-2 CPs are the “accordion-like” patterns, in order to be flat foldable these usually have a progression of alternate creases, causing them to inflect and deflect progressively, like an accordion.

These patterns are often the base for more complex patterns since they set the parallelism existent on the grid of a great number of models.

The chosen patterns for analysis are depicted in **Figure 3.9** and their names were assigned by this thesis in order to facilitate their identification.

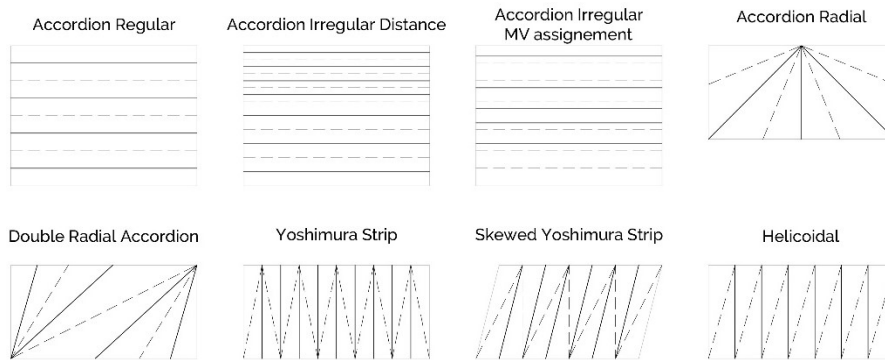


Figure 3. 9.
Degree-2 CPs

The family of **degree-2** CPs has creases that run from one border to the other and are usually parallel or radial. This makes it difficult to understand where the vertices are, but as Hull (2002) established, for degree-2 CPs one must imagine a vertex in the middle of a line, this would mean that there are in fact two creases, of the same identity, originating from it. Only the interior vertices are considered since the border vertices are “open-vertices” as they do not have 360° of paper around them. From this perspective it is possible to directly verify that the Kawasaki-Justin and Maekawa-Justin theorems are fulfilled as demonstrated in **Figure 3.10** and **Table 3.6**.

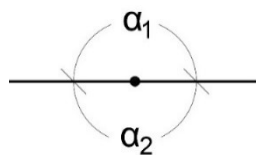


Figure 3. 10.
Degree-2 Vertex

Maekawa-Justin Theorem	or	Kawasaki-Justin Theorem
$2M - 0V = 2$		$\alpha_1 = \alpha_2 = 180^\circ$

Table 3. 6.
Maekawa and
Kawasaki Theorems
for degree-2 vertices

The Big-Little-Big Lemma does not apply in this case since there is not any minimum angle, there are only two angles, and both are 180°.

Almost all “accordion-like” patterns fold on the plane if the folding angles between faces are constant. These patterns can achieve ruled surface

configurations, cylindrical and/or conical, if they have such support and/or if it is allowed that the folding angles between faces are not constant.

One of the immediate conclusions that stands out is that the valley folds will be the ones that support the model on the ground and that the maximum height each pattern may achieve is measurable through a perpendicular distance from the valley fold and the furthest point on the closest mountain fold **Figures 3.11** and **3.12**. In **Figures 3.13** and **3.14** are shown folding simulations of the radial accordion and Yoshimura strip patterns folding on the plane.

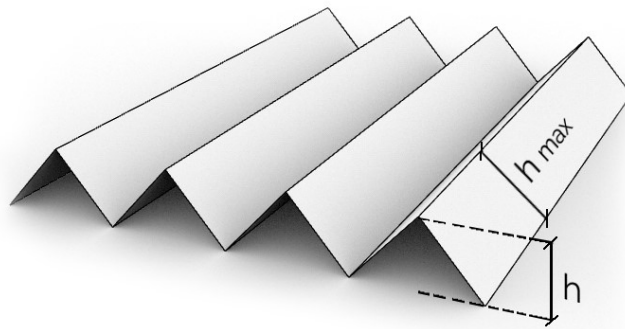


Figure 3.11.
 Regular accordion
 transitional folding
 state and heights

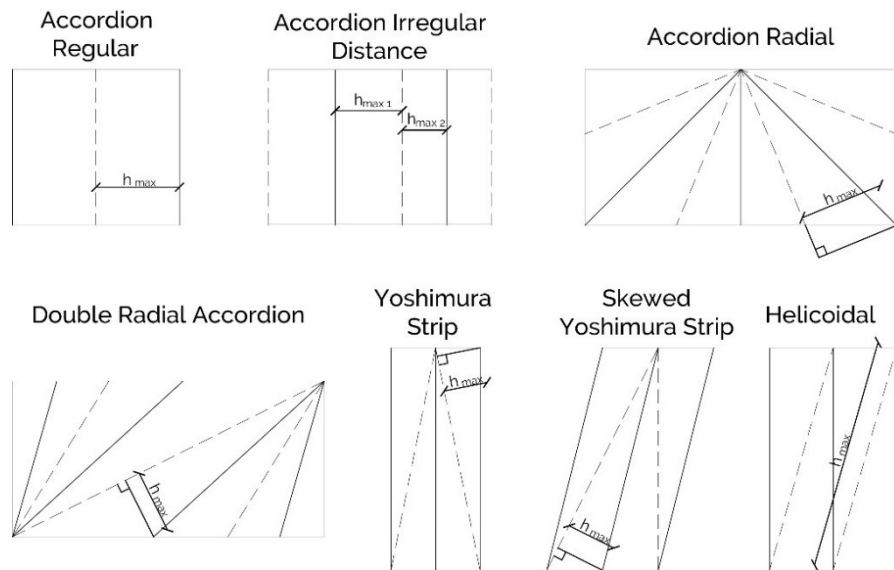


Figure 3.12.
 Maximum height for
 each degree-2 CP

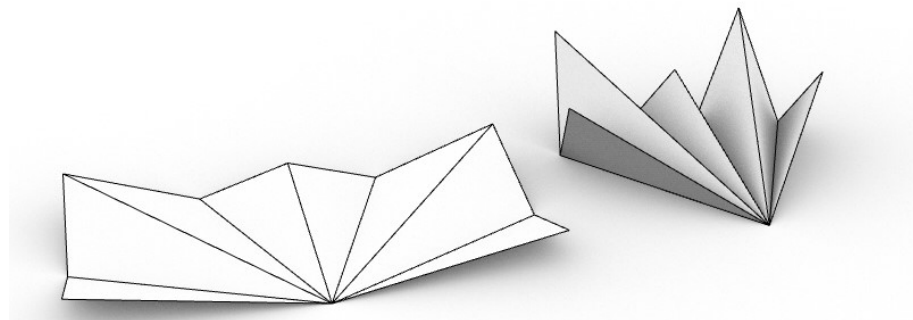


Figure 3.13.
 Simulation of radial
 accordion pattern,
 two folding states

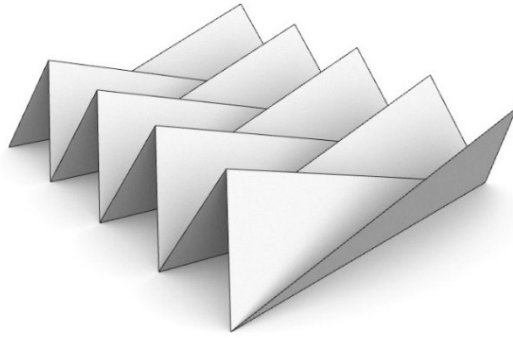


Figure 3. 14.
Simulation of
Yoshimura strip
pattern, one folding
state

There are two patterns that do not fit these conclusions completely, the accordion with irregular MV assignment and the helicoidal. The Accordion with Irregular MV Assignment has creases that do not succeed in a MVMVMV (...) progression, which leads to the transport of valley folds outside the XY plane. Additionally, the flat-foldable behaviour of this pattern is not typical, the other patterns depart from the XY plane and arrive to a flat folded state on a vertical plane, the accordion with irregular MV assignment has both states on the same XY plane, so its capacity for compression is not 100% as with the other patterns, and the percentage of compression depends on the distance between creases (**Figure 3.15**).

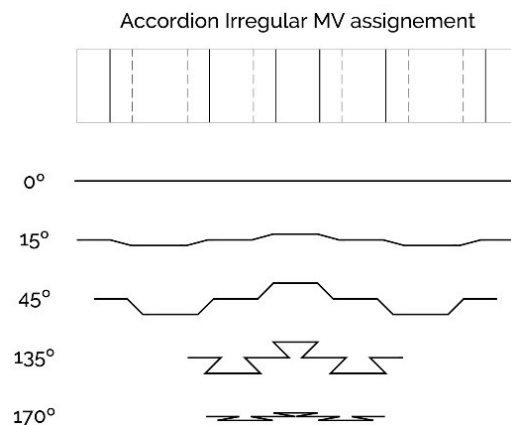


Figure 3. 15.
Plan and sections of
the folding states of the
accordion pattern with
irregular MV
assignment

The helicoidal pattern leaves the XY plane due to the consecutive parallel diagonals, that cause a progressive torsion on the model (**Figure 3.16**).

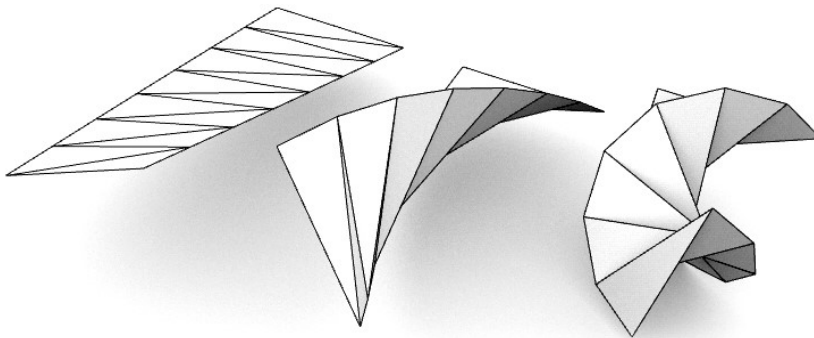


Figure 3. 16.
Simulation of the
helicoidal pattern,
three folding states

In **Table 3.7** it is possible to see the summary of the analysis for each pattern, three folding states, from unfolded to completely folded, the verification of the rules for flat-foldability, self-intersection and rigid foldability, their capacity for compression and finally, the form into which each pattern folds if they are supported by the plane XY and have constant folding angles.

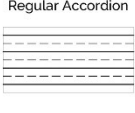


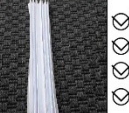
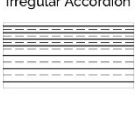


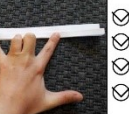
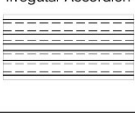


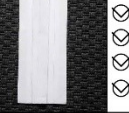
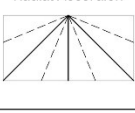


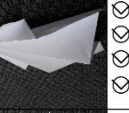



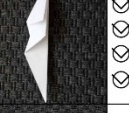
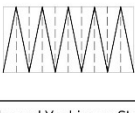



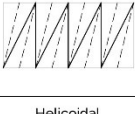


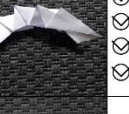



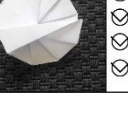
Crease Pattern	Folding State 1	Folding State 2	Folding State 3	Rigid and Flat-Foldable	Comp.	Folds Along
Regular Accordion 				<input checked="" type="checkbox"/> Kawasaki <input checked="" type="checkbox"/> Maekawa <input checked="" type="checkbox"/> No Self-Intersection <input checked="" type="checkbox"/> Rigidly Foldable	100%	Plane
Irregular Accordion 				<input checked="" type="checkbox"/> Kawasaki <input checked="" type="checkbox"/> Maekawa <input checked="" type="checkbox"/> No Self-Intersection <input checked="" type="checkbox"/> Rigidly Foldable	100%	Plane
Irregular Accordion 				<input checked="" type="checkbox"/> Kawasaki <input checked="" type="checkbox"/> Maekawa <input checked="" type="checkbox"/> No Self-Intersection <input checked="" type="checkbox"/> Rigidly Foldable	< 100%	Plane
Radial Accordion 				<input checked="" type="checkbox"/> Kawasaki <input checked="" type="checkbox"/> Maekawa <input checked="" type="checkbox"/> No Self-Intersection <input checked="" type="checkbox"/> Rigidly Foldable	100%	Plane
Double Radial Accordion 				<input checked="" type="checkbox"/> Kawasaki <input checked="" type="checkbox"/> Maekawa <input checked="" type="checkbox"/> No Self-Intersection <input checked="" type="checkbox"/> Rigidly Foldable	100%	Plane
Yoshimura Strip 				<input checked="" type="checkbox"/> Kawasaki <input checked="" type="checkbox"/> Maekawa <input checked="" type="checkbox"/> No Self-Intersection <input checked="" type="checkbox"/> Rigidly Foldable	100%	Plane
Skewed Yoshimura Strip 				<input checked="" type="checkbox"/> Kawasaki <input checked="" type="checkbox"/> Maekawa <input checked="" type="checkbox"/> No Self-Intersection <input checked="" type="checkbox"/> Rigidly Foldable	100%	Plane
Helicoidal 				<input checked="" type="checkbox"/> Kawasaki <input checked="" type="checkbox"/> Maekawa <input checked="" type="checkbox"/> No Self-Intersection <input checked="" type="checkbox"/> Rigidly Foldable	100%	Double curvature

Table 3.7.
 Patterns with degree-2 vertices analysis

Degree-4 Crease Patterns

The vertices of degree-4 CPs must have three Mountain folds and one Valley fold (or vice-versa), in order to verify the Maekawa-Justin Theorem (Table 3.8), and these creases have only one option of arrangement around the vertex, three creases of the same identity must surround the only crease of the opposite identity.

Maekawa-Justin Theorem		Kawasaki-Justin Theorem
$3M - 1V = 2$	or	$3V - 1M = 2$
		$\alpha_1 + \alpha_3 = \alpha_2 + \alpha_4 = 180^\circ$

Table 3. 8.
Maekawa- Justin and
Kawasaki-Justin
Theorems for degree-
4 vertices

Due to the Big-Little-Big Lemma the individual crease of opposite identity must define the smaller angles that surround the vertex, otherwise it will not flat-fold (Figure 3.17).

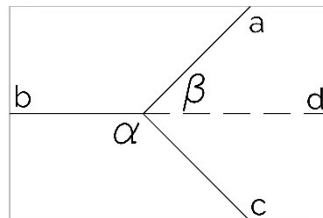


Figure 3. 17.
Typical Degree-4
Vertex

If the valley fold **d** and mountain **b** are in the same direction and the mountains **a** and **c** are arranged symmetrically then this kind of fold causes an inflexion in the model and the faces collapse coincidentally. As the angle **α** decreases and angle **β** increases, the inflexion gets more accentuated as seen in Figure 3.18.

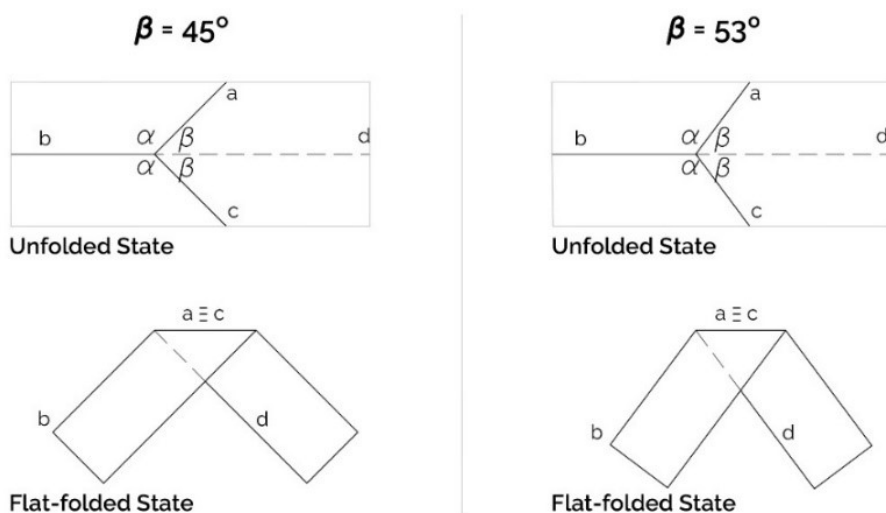


Figure 3. 18.
Degree-4 vertex
inflexion examples for
 $\beta=45^\circ$ and 53°

These are the types of vertices present in the **Miura-Ori**. In this pattern there are two main orthogonal directions that define the grid of the model. On the vertical direction all vertices are the same on the same line, so they cause a line of inflexion on the surface (all vertices $3M+V$) or deflection (all vertices $3V+M$) across the model. In the horizontal, straight direction, the vertices change from inflexion to deflection. The regularity of this pattern and the sequence of vertical lines that inflect and deflect cause it to fold on the plane with compression in both directions.

For the analysis of patterns this thesis proposes also the study of two variations of the Miura-Ori, the **stretched Miura**, where some faces are stretched, which introduces interesting variations on the surface, although it still folds in the plane, and the **irregular Miura**, where the faces are not parallelograms, which leads to cylinder folding surfaces.

The **MARS** pattern seems very similar to the Miura, but it has an irregularity, consciously introduced by Taborda Barreto (1992). In its general grid it does not have straight parallel directions for the creases since the faces are squares and rhombuses, instead of parallelograms.

The **Chicken-Wire** pattern faces seem similar to the Miura pattern but symmetry is applied inside the faces turning them into trapeziums, which causes inflexions at the ends of the quadrilaterals leading to cylindrical folding surfaces.

The **Huffman Grid** is also a pattern that tends to fold into a cylinder, all of the vertices are of the same kind ($3M+1V$). When verifying if it complies with the Kawasaki-Justin and Maekawa-Justin Theorems it seems perfect to be a flat-foldable model pattern, but in reality, the kite configuration of the faces leads to collisions between adjacent faces, so this model can never fold completely into a flat state, as proven by Evans *et al.* (2015 (a)).

The final pattern in study for the degree4 CPs Family is the **quadrilateral meshed pattern**, which also tends to fold into a cylindrical form. This pattern could also be called “Super-Irregular Miura” or “Irregular Miura in Two Directions”, since one could depart from the Miura-Ori base faces and “simply” move the central vertex.

The motion of the central vertex of the base faces for the Quadrilateral Meshed Pattern would have direct consequences on the “V” shaped creases in order to fulfil the Maekawa and Kawasaki Theorems and the Big-Little-Big Lemma. Therefore, it would define a Miura Pattern as irregular in two directions, on the zig-zag lines and also on alternate lines of the straight direction.

The patterns for degree-4 CPs are presented in **Figure 3.19**, and the proposed sets of base faces in **Figure 3.20**.

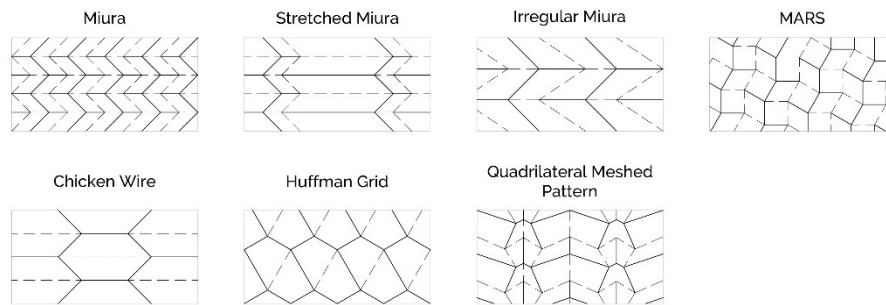


Figure 3.19.
Degree-4 CPs

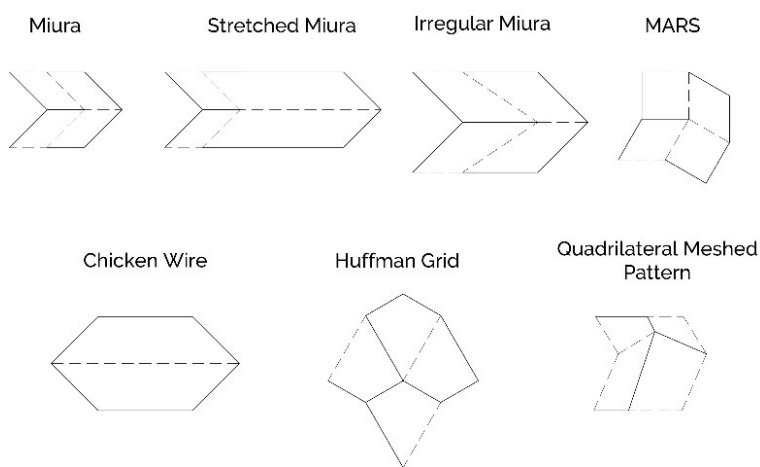


Figure 3.20.
Base faces of degree-4 CPs

One conclusion that can be drawn already is that the CPs fold into the plane if the faces are parallelograms and into cylinders if the faces are not parallelograms, as proven by Wang and Chen (2011) and Evans *et al.* (2015(a)).

Another conclusion that seems possible to draw from this analysis is that if the patterns are composed only by one type of vertices, like $3M+1V$, the models can only fold into cylinders, and if the vertices are of the two types than the models can fold either into the plane or cylinders, as grouped in **Table 3.9**.

DEGREE-4 One Type of Vertices		
Fold in the plane	Fold into single curvature (Cylinder)	Fold into double curvature
Two Types of Vertices		
Fold in the plane	Fold into single curvature (Cylinder)	Fold into double curvature

Table 3.9.
 Patterns with degree-4 vertices analysis on type of vertices and folding forms

In **Table 3.10** is possible to see the summary of the analysis for each pattern, three folding states, from unfolded to completely folded, the verification of the rules for flat-foldability, self-intersection and rigid foldability, their capacity for compression and finally, the form into which each pattern folds.

It is possible to verify that the analysed regular tessellations with degree-4 vertices only fold on the plane or into cylindrical forms, no patterns were found that fold into double curvature or conical configurations with degree-4 vertices in a regular CP with constant folding angles.

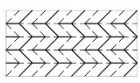







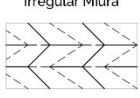



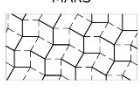



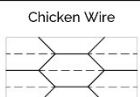

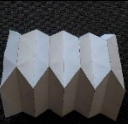





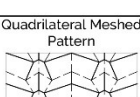



Crease Pattern	Folding State 1	Folding State 2	Folding State 3	Rigid and Flat-Foldable	Comp.	Folds Along
<p>Miura</p> 				<input checked="" type="checkbox"/> Kawasaki <input checked="" type="checkbox"/> Maekawa <input checked="" type="checkbox"/> No Self-Intersection <input checked="" type="checkbox"/> Rigidly Foldable	100%	Plane
<p>Stretched Miura</p> 				<input checked="" type="checkbox"/> Kawasaki <input checked="" type="checkbox"/> Maekawa <input checked="" type="checkbox"/> No Self-Intersection <input checked="" type="checkbox"/> Rigidly Foldable	100%	Plane
<p>Irregular Miura</p> 				<input checked="" type="checkbox"/> Kawasaki <input checked="" type="checkbox"/> Maekawa <input checked="" type="checkbox"/> No Self-Intersection <input checked="" type="checkbox"/> Rigidly Foldable	100%	Single Curvature
<p>MARS</p> 				<input checked="" type="checkbox"/> Kawasaki <input checked="" type="checkbox"/> Maekawa <input checked="" type="checkbox"/> No Self-Intersection <input checked="" type="checkbox"/> Rigidly Foldable	100%	Plane
<p>Chicken Wire</p> 				<input checked="" type="checkbox"/> Kawasaki <input checked="" type="checkbox"/> Maekawa <input checked="" type="checkbox"/> No Self-Intersection <input checked="" type="checkbox"/> Rigidly Foldable	100%	Single Curvature
<p>Huffman Grid</p> 				<input checked="" type="checkbox"/> Kawasaki <input checked="" type="checkbox"/> Maekawa <input checked="" type="checkbox"/> No Self-Intersection <input checked="" type="checkbox"/> Rigidly Foldable	< 100%	Single Curvature
<p>Quadrilateral Meshed Pattern</p> 				<input checked="" type="checkbox"/> Kawasaki <input checked="" type="checkbox"/> Maekawa <input checked="" type="checkbox"/> No Self-Intersection <input checked="" type="checkbox"/> Rigidly Foldable	100%	Single Curvature

Table 3. 10.
Patterns with degree-4
vertices analysis

Degree-6 Crease Patterns

The degree-6 CPs must have vertices composed of four Mountain folds and two Valley folds (or vice-versa) in order to fulfil the Maekawa Justin Theorem (Table 3.11).

Table 3. 11.
 Maekawa- Justin and
 Kawasaki-Justin
 Theorems for degree-
 6 vertices

Maekawa-Justin Theorem	Kawasaki-Justin Theorem
$4M - 2V = 2$ <i>or</i> $4V - 2M = 2$	$\alpha_1 + \alpha_3 + \alpha_5 = \alpha_2 + \alpha_4 + \alpha_6 = 180^\circ$

The creases can only have three options of arrangement around the vertex. From the reviewed literature, the most common is MMVMMV, it was also found MVMMM and, theoretically an arrangement like VVMMMM could also exist and, if complying with the Kawasaki-Justin theorem and Big-Little-Big Lemma, could determine a vertex that folds flat, as shown in **Figure 3.21**.

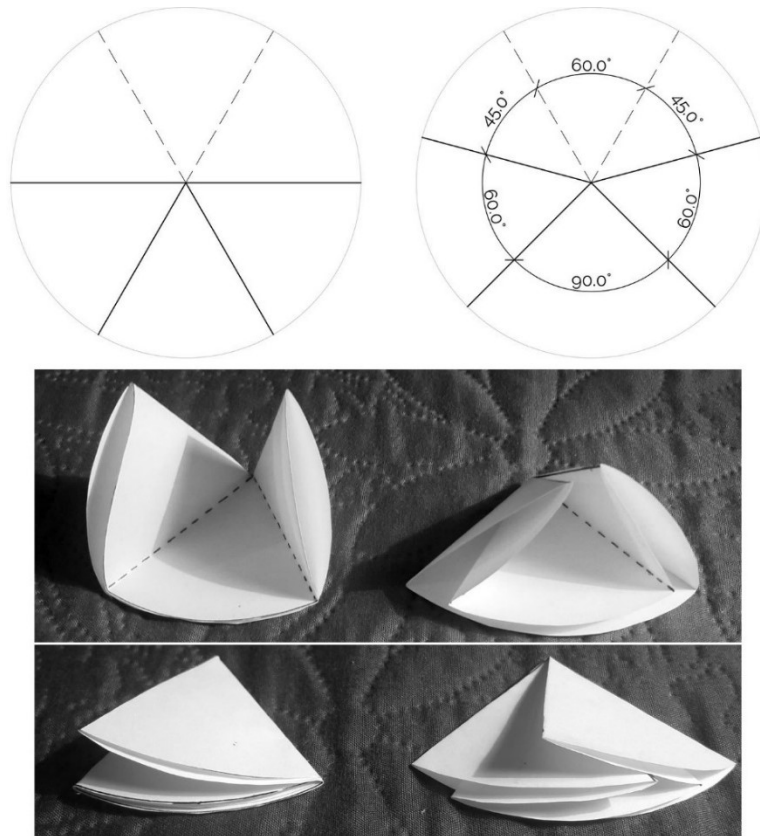


Figure 3. 21.
 Two flat foldable
 vertices with a
 VVMMMM
 arrangement

However, among the reviewed patterns no arrangement of VVMMMM was found, probably because they would lead to collisions between the faces on a CP with numerous vertices. This type of arrangement leads to several

overlapping of faces on the same side, due to the four consecutive Mountain creases, as seen in the previous figure.

The most commonly found arrangement of creases around the vertices, in the chosen degree-6 CPs, is the MMVMMV and the great majority of patterns are composed by only one type of vertex.

This group includes the renowned **Yoshimura pattern**, **Kresling pattern** and the **whirlpool spiral**. The whirlpool spiral CP design must follow three parameters in order to achieve rigid and flat foldable models without self-intersection as determined by Tomoko Fuse (2012). The example shown in **Figure 3.22** uses the parameters 5/10/31. This progression means that there must be 5 columns for a pattern with 31° , in the inferior inside angles, and each set of two faces rotates 10° in relation to the last one. Each line of the pattern is subjected to a scaling and rotation operation in order to fit the preceding line.

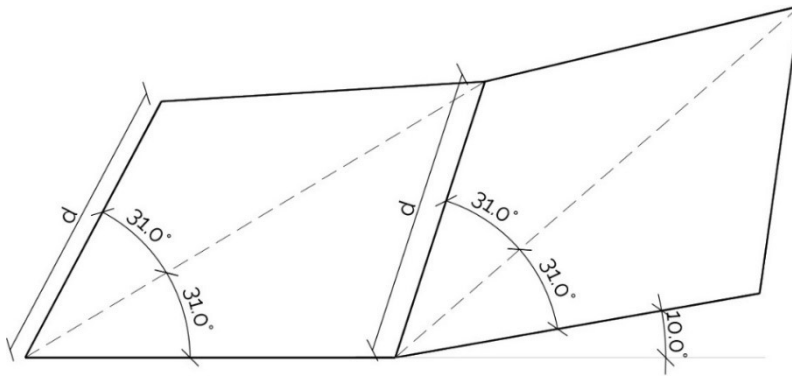


Figure 3. 22.
Fuse's Whirlpool Spiral
geometric relations

This research also proposes the study of the **double helicoidal** and **symmetric helicoidals** by altering the helicoidal pattern described for patterns with degree-2 vertices. During the folding motion these patterns determine helicoidals that can be inscribed in cylindrical forms.

Finally, the analysis of the **Fujimoto and Nishiwaki pattern** or "Ananas Pattern" (Kresling, 1997) is proposed. This pattern was redesigned by You and Kuribayashi (2009) to be able to achieve a conical configuration, which this thesis calls the **radial Fujimoto and Nishiwaki**.

The Fujimoto and Nishiwaki patterns are the only ones, out of all the degree-6 CPs in study, that have two types of vertices, the radial folds only on the plane (without additional support or closure into a cone) because the distortion of the orthogonal grid into a radial one blocks the movement of the faces, but the regular Fujimoto and Nishiwaki Pattern can fold into doubly curved forms. **Figure 3.23** summarizes the CPs for the chosen degree-6 patterns in analysis.

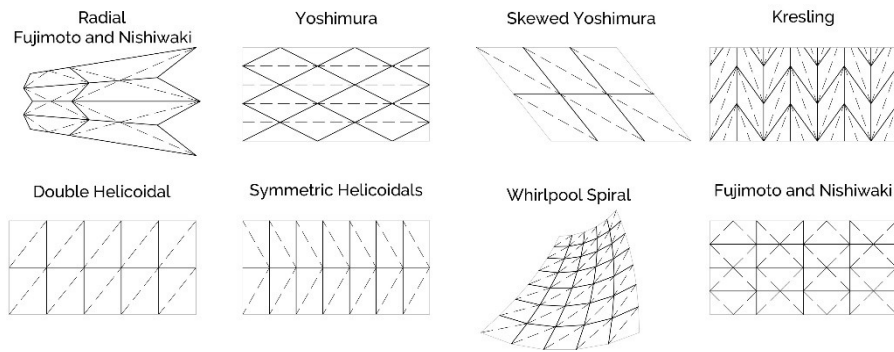


Figure 3.23.
 CPs with Degree-6
 Vertices

Some of these patterns can be seen as variations of the Yoshimura pattern, like the skewed Yoshimura, the double helicoidal or the whirlpool spiral. The grid of these patterns usually has two main directions with the same identity (Mountain or Valley) and another direction that passes through the intersections of the first ones with the opposite identity. Often, in the degree-6 CPs, the folding leads to cylinders, cones or spirals and usually the main direction of the grid corresponds to the section of the volume into which they fold (**Figure 3.24**).

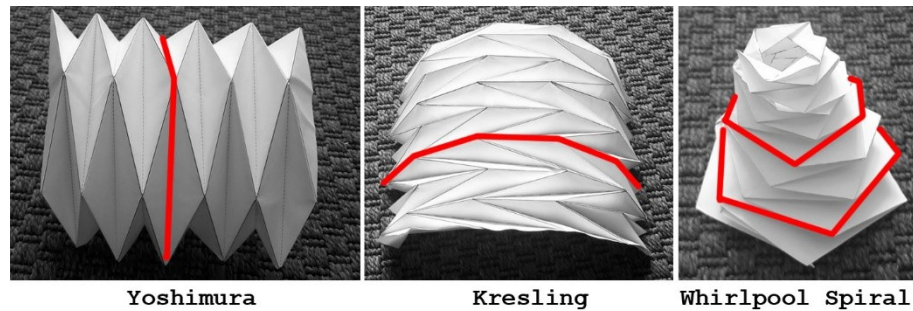


Figure 3.24.
 Examples of folded
 models and volume's
 section

The chosen base faces for the presented patterns are not always the strict minimum because, although they would be enough to create the tessellation of the entire surface, they would not suffice to understand the implications of the folding by using only the smallest set of base faces. It is the attachment between consecutive base faces to the following ones that determines the curvature of the forms into which they fold, hence the need to include more faces than the minimum.

Figure 3.25 illustrates the chosen base faces for the degree-6 CPs.

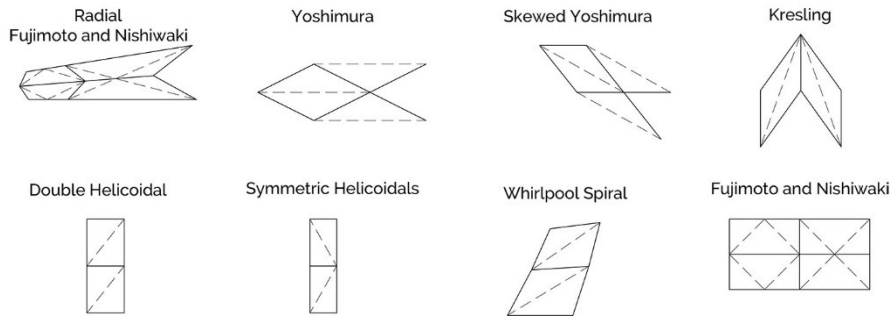


Figure 3.25. Base faces for Degree-6 CPs

The Yoshimura base faces can be determined to create cylinders with specific dimensions by using their interior angles. As the angle β increases, the inflexion created by the set of base faces becomes more accentuated. When the base faces are completely folded, they determine a new angle, Ω , as demonstrated in **Figure 3.26**.

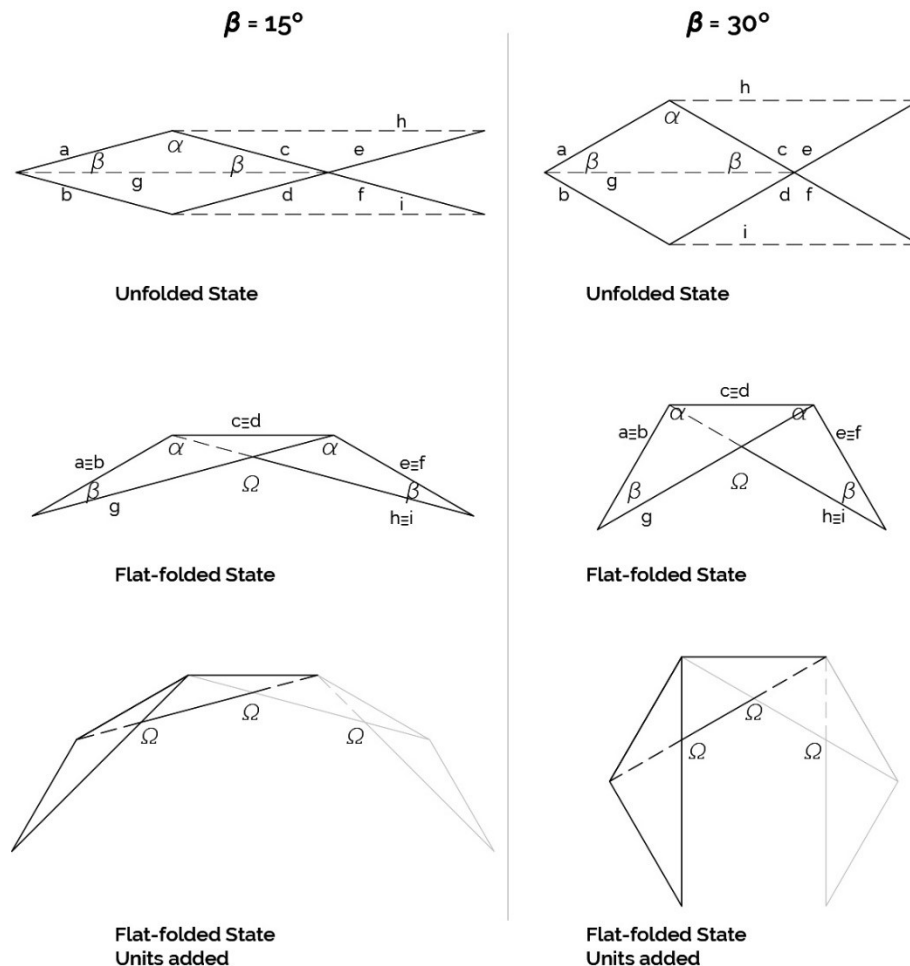


Figure 3.26. Yoshimura Vertex Inflexion examples for $\beta=15^\circ$ and 30°

From this demonstration it is possible to understand that there is a direct relation between the angles α , β and the angle Ω . The angle Ω is always equal to 180° minus 2β , which is equal to α (**Equation 3.1**).

Equation 3.1.
 Proposed equation for
 the relation between
 angles for regular
 Yoshimura

$$\Omega = \alpha = 180^\circ - 2\beta$$

As a result, a very direct observation can be made, a cylinder obtained through the folding of a regular Yoshimura pattern will have an inside polygon that is directly related to the β angle. As the angle β increases, less modules are needed to make a cylinder through a regular Yoshimura pattern, also the bigger the angle β is, then the bigger shell of the cylinder will be, until a maximum of $\beta = 45^\circ$, as can be seen in the **Table 3.12**.

Table 3.12 considers the completely folded state of the patterns. In order to fold these patterns rigidly they must depart from a planar state, which means that, in the end, they will reach the state shown in the table, but before that final state the cylinders must be open.





POLYGON	Angle $\alpha = \Omega$	Angle β	Number of Yoshimura modules
 square	90°	45°	2
 pentagon	108°	31°	2.5
 hexagon	120°	30°	3
 heptagon	128.57°	25.715°	3.5
 octagon	135°	22.5°	4
 nonagon	140°	20°	4.5
 decagon	144°	18°	5
 hendecagon	147.27°	16.365°	5.5
 dodecagon	150°	15°	6

Table 3.12.
 Relation between α , β
 and Ω angles for
 Regular Yoshimura
 CPs and generated
 cylinders

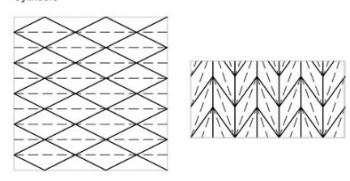
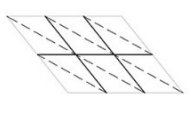
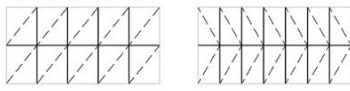
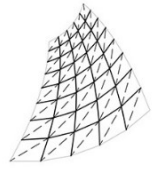
Tachi (2015) demonstrates that a generic periodic triangulated origami tessellation rigidly folds into a cylindrical form (Tachi, 2015). All of the proposed patterns designated in **Figure 3.23**, have triangular faces and the ones that fit Tachi's (2015) definition of generic triangulated tessellation fold into cylinders.

Additionally, the studied patterns prove that if a degree-6 CP has only vertices of one type ($4M+2V$ or $4V+2M$) it will fold into single curvature forms, and if the vertices are of two types then it can fold in the plane or into double curvature forms.

Table 3.13 places the eight proposed patterns in relation to their type of vertices and the forms they fold into.

DEGREE-6

One Type of Vertices

Fold in the plane	Fold into single curvature (Cylinder or Cone)	Fold into double curvature
	<div style="display: flex; justify-content: space-around;"> <div style="text-align: center;"> <p>Cylinders</p>  </div> <div style="text-align: center;"> <p>Helicoidal Cylinders</p>  </div> </div>	
	<div style="display: flex; justify-content: space-around;"> <div style="text-align: center;"> <p>Spirals</p>  </div> <div style="text-align: center;"> <p>Conical spiral</p>  </div> </div>	

Two Types of Vertices

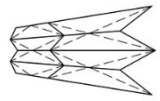
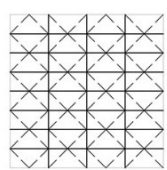
Fold in the plane	Fold into single curvature	Fold into double curvature
		

Table 3. 13.
Patterns with degree-6
vertices analysis

In **Table 3.14** it is possible to see the summary of the analysis for each pattern, three folding states, from unfolded to completely folded, the verification of the rules for flat-foldability, self-intersection and rigid foldability, their capacity for compression and finally, the form into which each pattern folds if the folding angles remain constant during folding.

Crease Pattern	Folding State 1	Folding State 2	Folding State 3	Rigid and Flat-Foldable	Comp.	Folds Along
Radial Fujimoto and Nishiwaki 				<input checked="" type="checkbox"/> Kawasaki <input checked="" type="checkbox"/> Maekawa <input checked="" type="checkbox"/> No Self-Intersection <input checked="" type="checkbox"/> Rigidly Foldable	100%	Plane
Yoshimura 				<input checked="" type="checkbox"/> Kawasaki <input checked="" type="checkbox"/> Maekawa <input checked="" type="checkbox"/> No Self-Intersection <input checked="" type="checkbox"/> Rigidly Foldable	100%	Single Curvature
Skewed Yoshimura 				<input checked="" type="checkbox"/> Kawasaki <input checked="" type="checkbox"/> Maekawa <input checked="" type="checkbox"/> No Self-Intersection <input checked="" type="checkbox"/> Rigidly Foldable	100%	Single Curvature
Kresling 				<input checked="" type="checkbox"/> Kawasaki <input checked="" type="checkbox"/> Maekawa <input checked="" type="checkbox"/> No Self-Intersection <input checked="" type="checkbox"/> Rigidly Foldable	100%	Single Curvature
Double Helicoidal 				<input checked="" type="checkbox"/> Kawasaki <input checked="" type="checkbox"/> Maekawa <input type="checkbox"/> No Self-Intersection <input checked="" type="checkbox"/> Rigidly Foldable	100% if there is no intersection depending on creases length	Single Curvature
Symmetric Helicoidals 				<input checked="" type="checkbox"/> Kawasaki <input checked="" type="checkbox"/> Maekawa <input type="checkbox"/> No Self-Intersection <input checked="" type="checkbox"/> Rigidly Foldable	100% if there is no intersection depending on creases length	Single Curvature
Whirlpool Spiral 				<input checked="" type="checkbox"/> Kawasaki <input checked="" type="checkbox"/> Maekawa <input checked="" type="checkbox"/> No Self-Intersection <input checked="" type="checkbox"/> Rigidly Foldable	100%	Single Curvature
Fujimoto and Nishiwaki 				<input checked="" type="checkbox"/> Kawasaki <input checked="" type="checkbox"/> Maekawa <input checked="" type="checkbox"/> No Self-Intersection <input checked="" type="checkbox"/> Rigidly Foldable	100%	Double Curvature

Table 3.14.
 Patterns with degree
 6 vertices analysis

3.3.2 | Proposed Origami Folding Simulations

As discussed in **Section 2.3**, parametric simulations can be extremely useful in the architectural form-finding process. The parameterization of geometries lets designers test, in a very direct and graphic way, several solutions in order to choose the most appropriate for a particular building, site or function and to optimize the chosen solution before its construction. These types of tools can be even more useful when referring to kinetic buildings, structures that move, and whose motion might interfere with existing objects or with their utilization by people. With these tools it is possible to test for collisions and paths of the moving parts in a three-dimensional simulation, which allows for the visualization of the complete picture without having to spend time and money on the construction of prototypes or models at the same time that they help to prevent unanticipated issues.

From the described simulators in the previous chapter, the most useful for the scope of this research are those within the origami foldability category that give access to the entire folding motion, and most particularly the ones that permit a true rigid kinematic simulation, like Tomohiro Tachi's Rigid Origami Simulator (Tachi, 2009 (a)), Casale and Valenti's (2012) and Kong *et al.* (2015) Grasshopper definitions.

The other simulators are very interesting and useful in order to visualise the forms into which the patterns fold but do not provide a reliable kinematic simulation since they allow for elasticity (even if small) on faces and hinges.

Despite usefulness of these simulators all have the same limitation, it is not possible to considerably change the geometry of the faces in the middle of the folding process, so it is not possible to optimize the geometry without restarting the process from the beginning.

This thesis proposes the use of general algorithms that allow for rigid kinematic simulation, that is, pure rigid folding of planar surfaces around straight hinges, at the same time that it provides the option of changing the geometry of the base faces, at any step of the folding process.

The proposed algorithms take the defined families of degree-4 and degree-6 CPs and try to represent the folding of clusters of patterns within the tessellations illustrated in **Tables 3.10** and **3.14**, by using a geometric approach to create definitions in Grasshopper for Rhinoceros. For the degree-2 CPs no algorithm was developed since these are very simple and tangible models, even though it could be done as future work.

The algorithms within this thesis have an approach similar to Casale and Valenti's (2012) and to Kong *et al.* (2015), but are intended to be more generic,

and therefore applicable to the families of regular tessellations instead of being created from scratch for a specific CP.

In order to do this, **local** rules are defined for the folding of the base faces that are then replicated throughout the tessellation, thus generating the **global** behaviour of the surface.

The methodology (**Figure 3.27**) used to develop these definitions encompasses six steps:

- 1 – Analysis of regular tessellations to define their base faces
- 2- Definition of the geometric rules for the drawing and folding of the base faces
- 3 – Clustering of the base faces with similar drawing rules
- 4 – Creation of a geometric definition that allows for the creation of every type of base face in the cluster by manipulating vertices and creases, at the same time that the compliance with the rules for rigid and flat foldability and attachment of base faces is guaranteed
- 5 – Implementation of the folding of the base faces from the unfolded state to the completely folded state (local behaviour)
- 6 – Generation of the complete tessellation through vectorial copies of the base faces (global behaviour), where the vectors for copy are continuously redefined during the folding process.

Through this methodology two simulators were developed (available for download at https://cutt.ly/FilipaOsorio_KOS) that are believed to be of great help for designers as a tool to control the tessellation's geometry and its alteration at any step of the folding. The algorithms allow, not only to change the geometry of the base faces, but also the dimension of the tessellation by letting users decide the number of copies of the base faces.

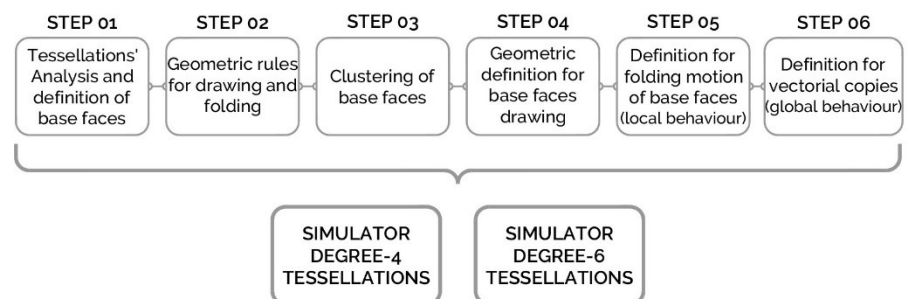


Figure 3.27.
 Methodology for the development of the simulators

In the established definitions the base faces are always on the first quadrant and there is always one point, or crease, that maintains its position during the

folding. This element behaves as the attachment to the XYZ referential, it is the centre of all the transformations, in relation to which all other elements move.

In order to simplify the user analysis on the generated CP were added the name and coordinates of the manipulable points. These annotations, attached to the base faces design, are intended to help on the understanding of the dimensions of the faces and to simplify the decision-making process for the designer.

Additionally, and since Grasshopper is a tool within Rhinoceros, it is possible to export the surfaces to any desired position (or folding step) and use it on three dimensional models of buildings or spaces. Rhinoceros can be used as the CAD system for drawing or to export the model to any mainstream CAD software.

Folding Simulator for Degree-4 Tessellations

The algorithm that is going to be presented is able to fold a cluster composed by the Miura, Stretched Miura, Irregular Miura and Quadrilateral Meshed patterns (**Figure 3.28**). Through these patterns it is possible to achieve tessellations that fold on the plane or into cylindrical forms. The base faces of these tessellations can be described the same way, they are all composed of four quadrilaterals, all have one interior vertex, all have two straight and parallel limits, all fold rigidly and flat.

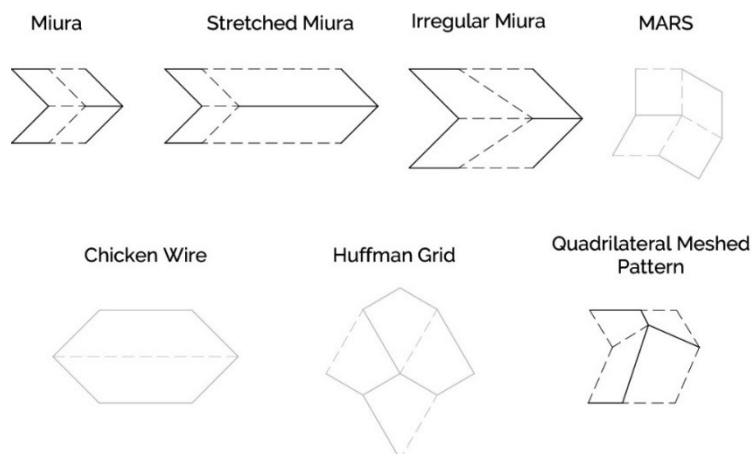


Figure 3. 28.
Cluster of Degree-4
base faces

The base faces for every tessellation can be defined through equivalent points and lines, with the same nomenclature, as **Figure 3.29** illustrates.

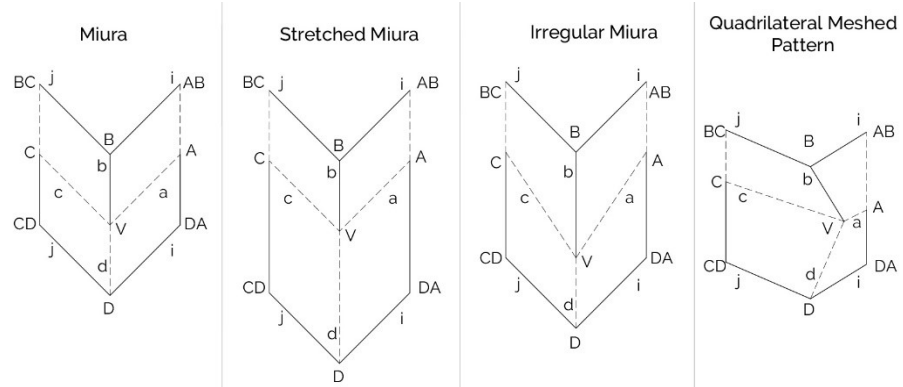


Figure 3.29.
 Base faces geometry
 and nomenclature

The Grasshopper (GH) definition starts by letting the user define if point **V** will have the same X coordinate as points **B** and **D**, by using a simple True/False Boolean Toggle, this way a first distinction is made between the first three tessellations and the Quadrilateral Meshed Pattern.

Then the user must decide the XY coordinates for point **V**, the Y coordinates for points **B** and **D**, which are dependent on V_y 's, since **B** must never have an Y coordinate smaller than **V**, and **D** should never have the same coordinate higher than **V**. This rule is accomplished through operations of addition and subtraction between V_y and the sliders for B_y and D_y . Then the user decides the XY coordinates for point **A**.

At this point it is possible to define the creases **a**, **b** and **d**, through vectors with origin in **V** and tip on **A**, **B** and **D**, respectively.

The **c** crease is defined by the Kawasaki-Justin Theorem and point **C** is found when the crease meets the Y axis, that is when $x=0$.

Now the user can define point **AB** by deciding its Y coordinate, which must be higher than B_y in order to maintain the general directions of the creases, the X coordinate for point **AB** cannot be decided by the user, since it is constricted to be always equal to A_x (**Figures 3.30 and 3.31**).

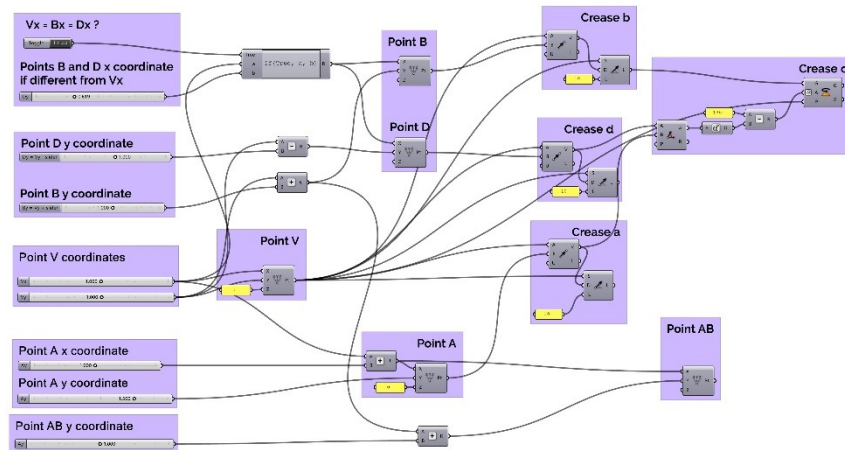


Figure 3.30.
 First Step for the
 definition of the base
 faces' geometry –
 GH Definition

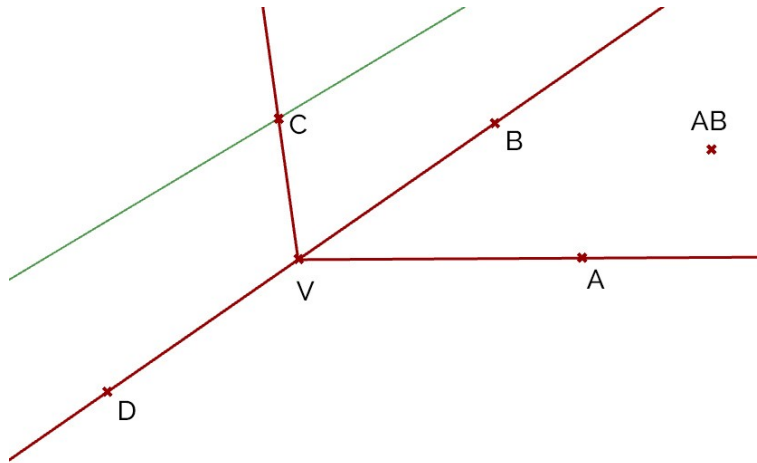


Figure 3. 31.
First Step for the definition of the base faces' geometry – Graphical Representation

With point **AB** defined, crease **i** is also defined (from **B** to **AB**). From the crease **i**, it is possible to draw crease **j**, that is the rotation of vector **B→AB** with an angle of 180° minus the angle between vectors **B→V** and **B→AB** and plus the angle between **B→AB** and **D→V**, so it verifies the Kawasaki-Justin Theorem for flat-foldability.

After the definition of creases **j** and **i**, these are then translated from point **B** to point **D**, which will guarantee that the attachment between sets of base faces will fit perfectly.

Through the two sets of creases **j** and **i** it is then possible to find the points **DA**, **CD** and **BC** in the intersection points with lines $x=0$ and $x=A_x$.

With all points created, **faces a**, **b**, **c** and **d** also become defined (**Figures 3.32** and **3.33**).

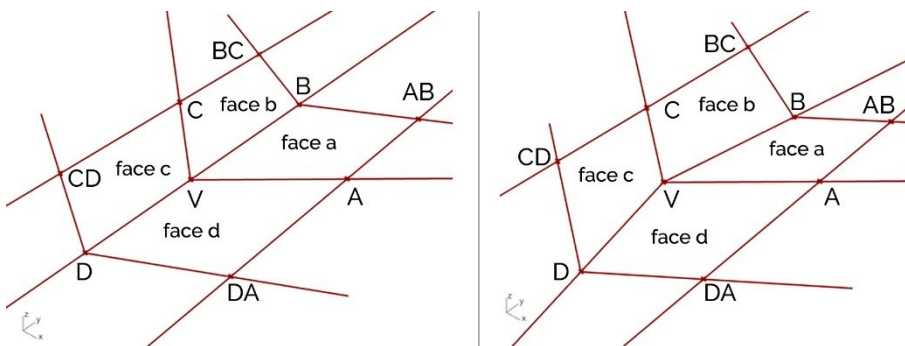
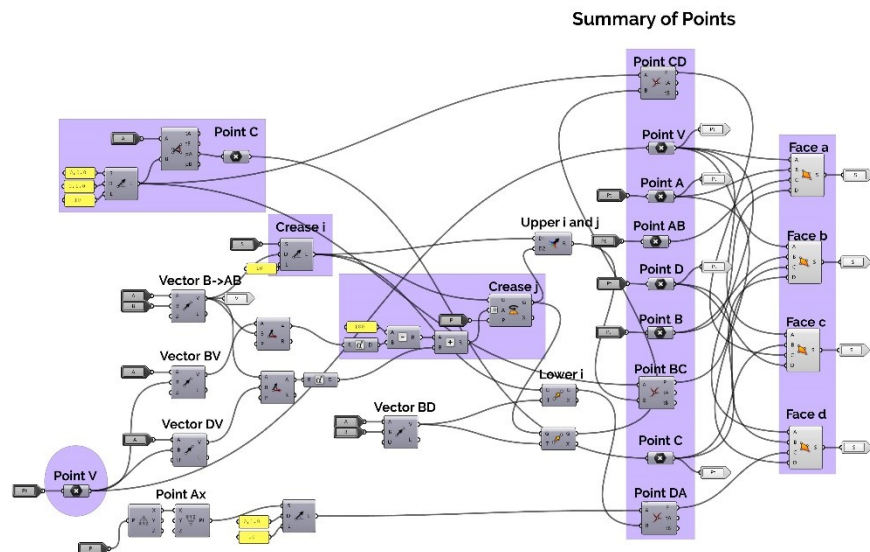


Figure 3. 32.
Second Step for the definition of the base faces' geometry – Graphical Representation of two options

Figure 3.33.
 Second Step for the
 definition of the base
 faces' geometry –
 GH Definition



At this point it is possible to start the folding of the set of base faces. First the algorithm makes face **a** and face **b** rotate 90° around crease **b**. This was the chosen crease since it is the only mountain fold, all the others are valley folds. As a way of making the four surfaces fold in any type of pattern, the found strategy was to find point **D** continuously throughout the folding motion. At this point the algorithm gets a bit more complex, but this guarantees its generality for the four types of CPs.

Point **D** is found at the intersection of two circles. These circles have their centres on creases **a** and **c**, are perpendicular to these creases and have a radius equal to the shortest distance between point **D** and the creases. The circles always have two points of intersection when the folding starts, so **D** is chosen to be the one with the highest Z coordinate.

Since the circles move along with the rotation of faces **a** and **b**, point **D** is continuously updated. The faces **c** and **d** are then simply oriented with the “new” point **D** and with the rotated points **C** and **V** (that define crease **c**), and **A** and **V** (that define crease **a**).

In such a manner it is possible to guarantee that the geometry of the initial faces and their planarity is not altered along the folding process, since their dimensions and inside angles are restricted to the initial ones, at the same time that the angle for the folding of each face is defined naturally and in relation to the folding of the first two faces, **a** and **b** (Figures 3.34 and 3.35).

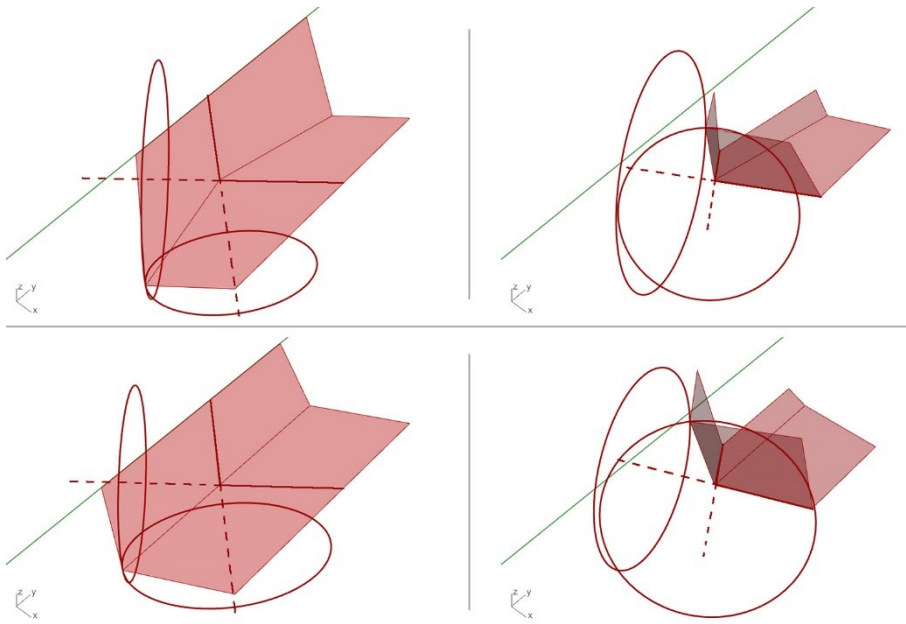


Figure 3.34.
Third Step, folding of
the base faces –
Graphical
Representation of two
options with
correspondent circles
to define point D

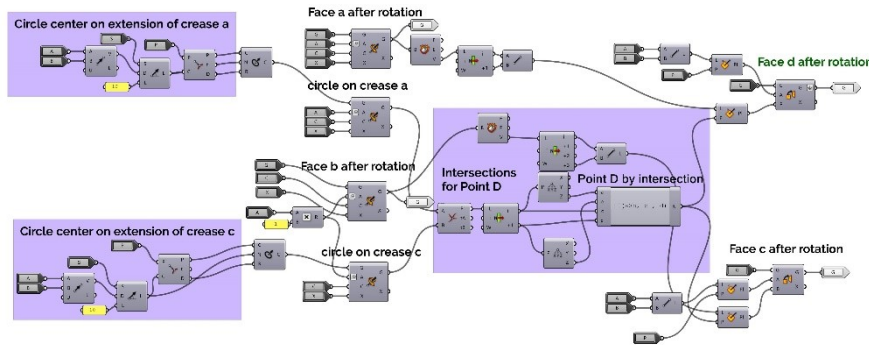


Figure 3.35.
Third Step, folding of
the base faces – GH
Definition

After this a mirror operation was created of the base faces with a vertical mirror plane that passes through point **A** and point **DA** when the folding angle is 0, and that passes through points **DA**, **A** and **AB** when the folding angle is different from 0. The mirror operation is only necessary due to the Quadrilateral Meshed pattern, since in the other three cases the mirrored version could easily be made through a translation operation, nevertheless this ensures the usability of the algorithm for each one of the four cases in the cluster.

Several copies of the two sets of base faces are then created through a vector that goes from Point **C** to the mirrored point **C'**. In the algorithm these copies can be determined by the user through the slider "**Number of Columns**".

The vector that allows the definition of the number of columns is the same in the case of the tessellations that fold into cylinders as the ones that fold on the plane. In the other direction this definition is not so simple because, for tessellations that fold on the plane it would only be necessary to define the

vector $D \rightarrow B$ and the copies would be linear and very straightforward, but in the case of tessellations that fold into cylinders the angle between the first line and the second is always changing during folding. The strategy found to be able to determine the radius of the cylinder and the angle between lines of base faces was to make a first copy of the base faces through an orientation operation. The orientation operation takes the first set of base faces and creates a new one where the first line is oriented from the plane defined by the points CD , DA and mirrored D (D') to the plane defined by the points BC , AB and mirrored B (B') (Figures 3.36 and 3.37).

Figure 3.36.
 Mirrored faces and points for orientation operation. Exemplification with the Miura and Quadrilateral Meshed Patterns

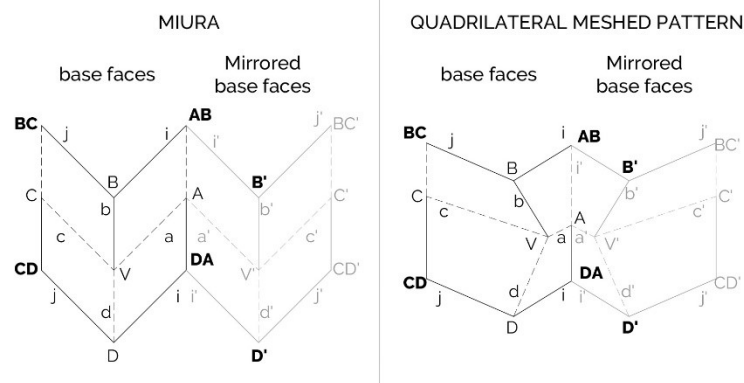
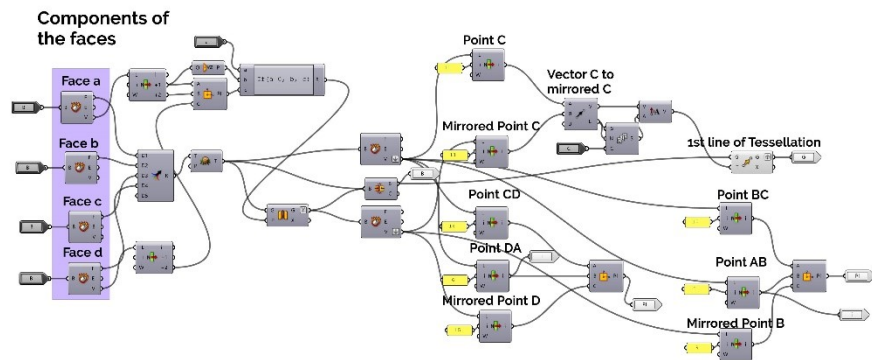


Figure 3.37.
 Fourth Step, mirrored base faces and columns on the first line of the tessellation – GH Definition



Now a circle can be defined that passes through points DA , AB and *moved* AB (circle p). The circle is redefined at every step of the folding and, with it, also the **two vectors** that start at the centre of the cylinder and that have tips at points AB and *moved* AB (Figure 3.38).

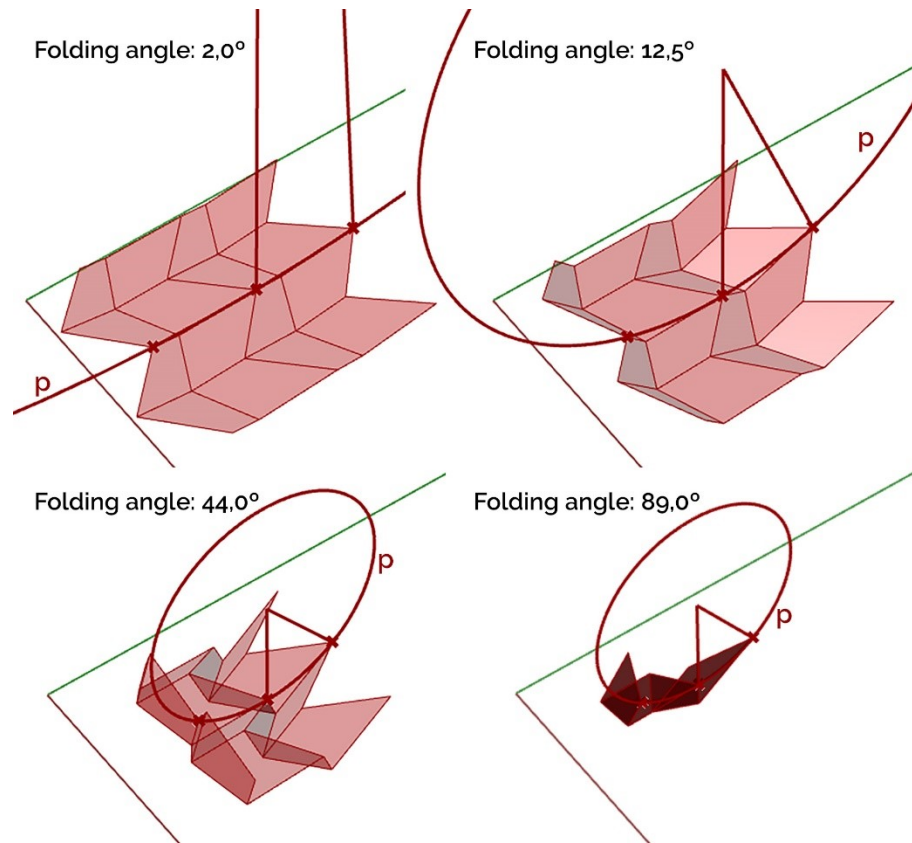


Figure 3.38. Four steps of folding and correspondent circles defined by points DA, AB and moved AB, vectors from centre of the circle

With these two vectors it is possible to find, at any moment of the folding, the angle between the various lines of the tessellation. This angle will be used to determine polar copies around the centre of circle p .

At this point there is a need to make a branching on the algorithm, since the way to make lines on the tessellation is different whether it is a CP that folds on the plane or that folds into cylinders. Therefore, there is a first “If-then” condition where the algorithm tests if creases a and i are parallel and gives a True/False response. If the answer is “True” then this means that it is a pattern that folds on the plane so linear copies are made in the direction of the $DA \rightarrow AB$ vector, if the answer is “False” then polar copies are made with centre on the centre of p and controlled by the angle between the vectors that start at its centre and have tips at points AB and **moved AB**.

Nevertheless, this branching still has one unresolved problem, that is when crease a is not parallel to crease i but the angle for folding is still 0. Although it will be a CP that folds into a cylinder when there is not a folding angle it is not possible to define circle p . Consequently, the definition allows to define the CPs of cylindrical tessellations through linear copies when the folding angle is 0 (**Figure 3.39**).

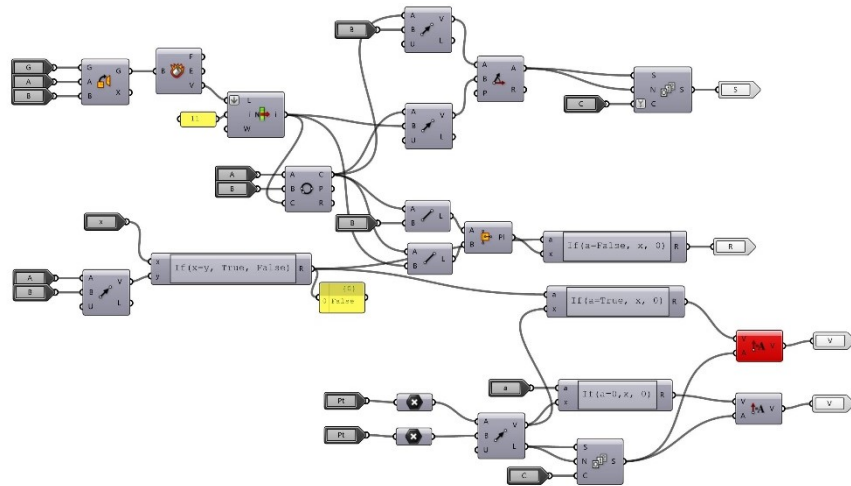


Figure 3. 39.
 Fifth Step, copy of first
 line of the tessellation
 through linear or polar
 copies – GH Definition

Subsequently will be demonstrated the versatility of the Folding Simulator for Degree-4 CPs through examples of tessellations and their states of folding.

Figure 3.40 presents the coordinates for the main points for every Degree-4 CP that compose the cluster folded by the presented algorithm.

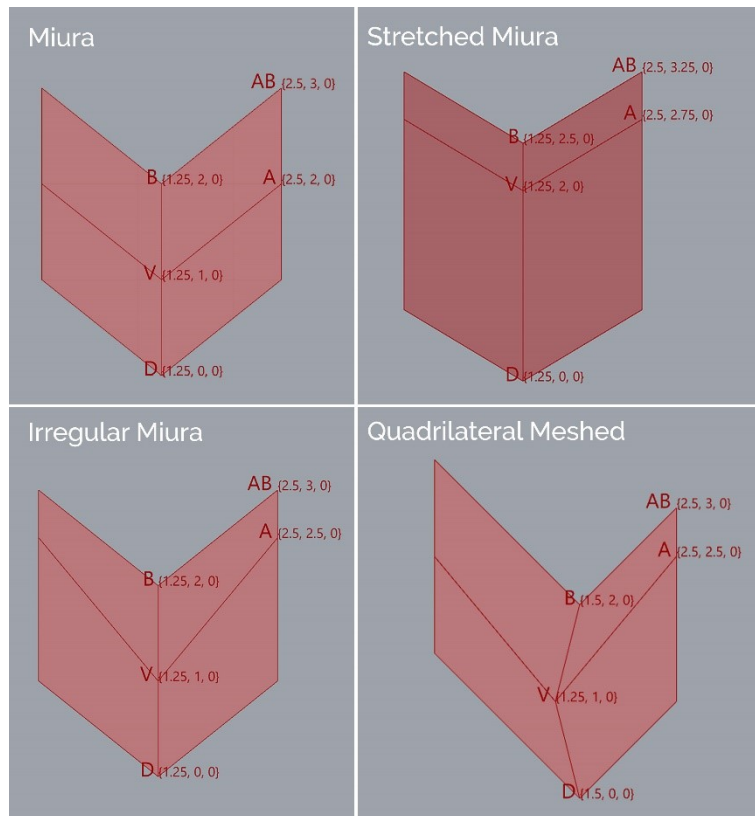


Figure 3. 40.
 Examples of Base
 faces for simulations
 on the four patterns

In **Figures 3.41, 42, 43** and **44** are shown four folding states, at 0°, 15°, 45° and 89° for each of the folded patterns.

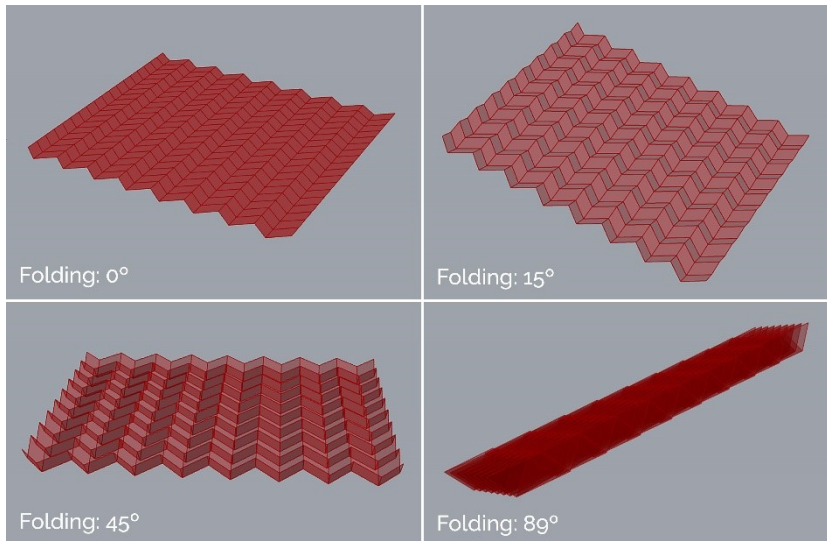


Figure 3. 41.
Four Folding States
of Miura Pattern
through D4 Simulator

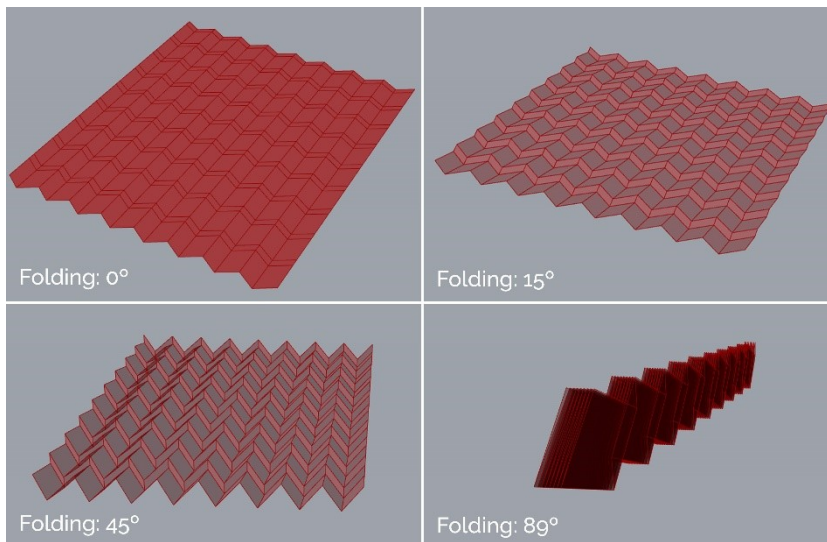


Figure 3. 42.
Four Folding States
of Stretched Miura
Pattern through D4
Simulator

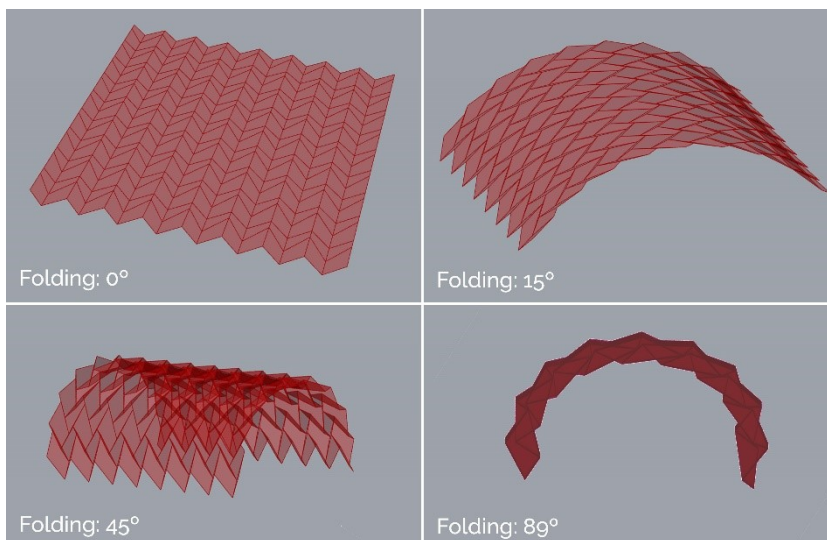


Figure 3. 43.
Four Folding States
of Irregular Miura
Pattern through D4
Simulator

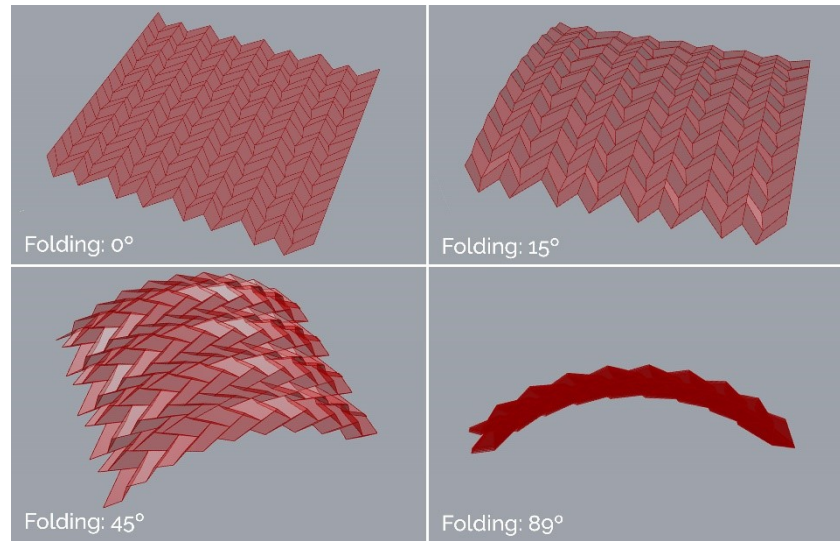


Figure 3.44.
Four Folding States of
Quadrilateral Meshed
Pattern through D4
Simulator

Finally, and so that the algorithm can be more easily manipulated by any user, only the geometry of the base faces are left visible and points A, B, D, V and AB coordinates, previously to the folding, and the complete tessellation (Figure 3.45). Every step is clustered and password protected, to prevent any accidental alteration to the algorithm.

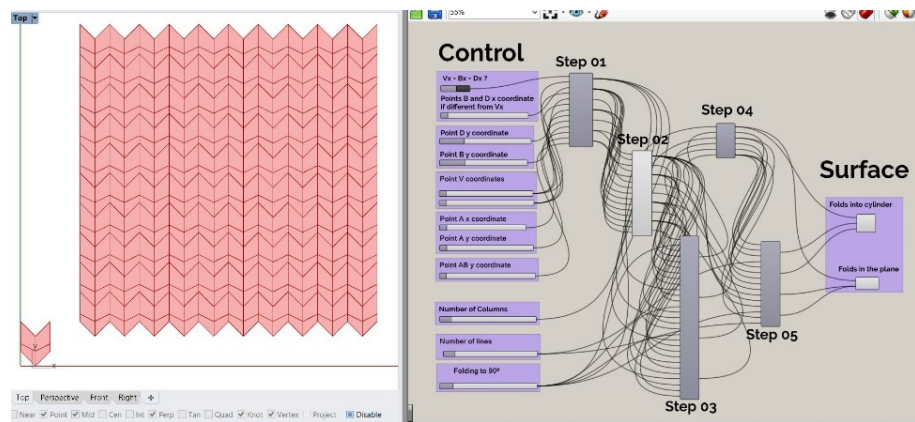


Figure 3.45.
Interface appearance
to the user

Folding Simulator for Degree-6 Tessellations

The algorithm that will now be presented is able to fold a cluster composed by the Yoshimura, Skewed Yoshimura and Double Helicoidal Patterns. These patterns are able to fold into single curvature forms, cylinders or helicoidals.

The base faces of these tessellations can be described the same way, they are all composed by four triangles and when attached to other base faces all the interior vertices are of the same type, $4M+2V$. Additionally the tessellations composed by these base faces have a grid of parallel valley folds that cross the entire tessellation from one extreme to the other, and the mountain folds follow continuous directions.

The similarities between these patterns allow to understand the dismissal of the other Degree6 studied patterns. The Fujimoto and Nishiwaki patterns, regular and radial, have two types of interior vertices and do not have a straight, parallel direction for the valley folds when attached to other base faces. The Kresling Pattern, Symmetric Helicoidals and Whirlpool Spiral have only one type of vertices and the base faces are composed by four triangles, but the tessellations of these patterns do not have a grid of parallel valley folds, and the remaining folds do not follow continuous lines.

Figure 3.46 demonstrates the base faces presented on the last section and the ones chosen for the simulation algorithm.

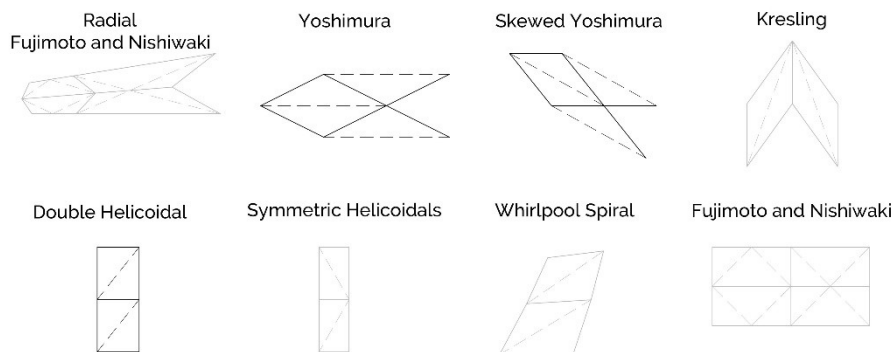


Figure 3. 46.
Cluster of Degree-6
base faces

In order to simplify the simulation, the base faces of the Double Helicoidal were changed to relate more closely to the geometry of the other two patterns folded by the algorithm nevertheless, the first set and the second are equivalent.

Figure 3.47 depicts the base faces for the Degree-6 Cluster where for every set of base faces are defined equivalent points and lines, with the same nomenclature, as done for the degree-4 simulator.

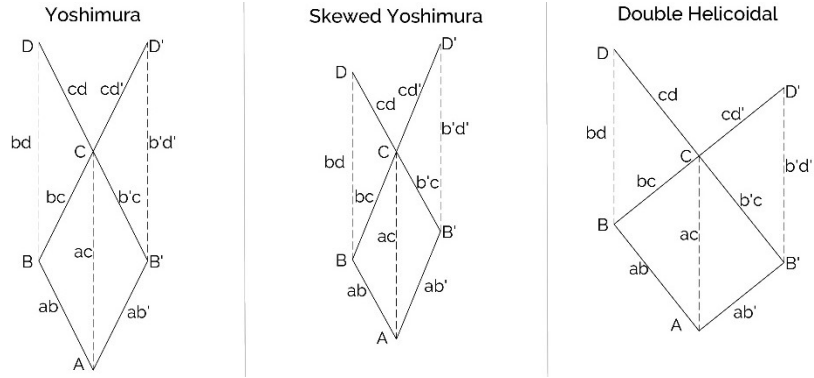


Figure 3. 47.
 Cluster of Degree-6
 base faces

From the analysis of the base faces is possible to understand that the Y coordinate for points **B** and **B'** is not the same on the case of the Skewed Yoshimura and the Double Helicoidal, as well as the Y coordinate for points **D** and **D'**. For the Yoshimura pattern these coordinates are the same.

Hence, during the algorithm development, was decided to make it follow two main branches, one for the Skewed Yoshimura and Double Helicoidal, and another one for the Yoshimura Pattern. This decision relates directly with the different geometric needs for the vectorial copies, since the different directions for vectors **B**→**B'** and **D**→**D'** influence greatly the options when creating the tessellation, as will be described later at this section.

While developing the branch for the Yoshimura pattern was tried to make it more versatile and give it the feature of folding irregular Yoshimura patterns. The folding logic is the same and this option is believed to make the simulator more robust and helpful for architectural simulations since it gains the ability of folding more than just regular Yoshimura patterns.

So, the branch developed to fold the Yoshimura Patterns can be subdivided into Regular and Irregular Yoshimura. The irregular Yoshimura allows for the definition of much more vertices and has fourteen faces.

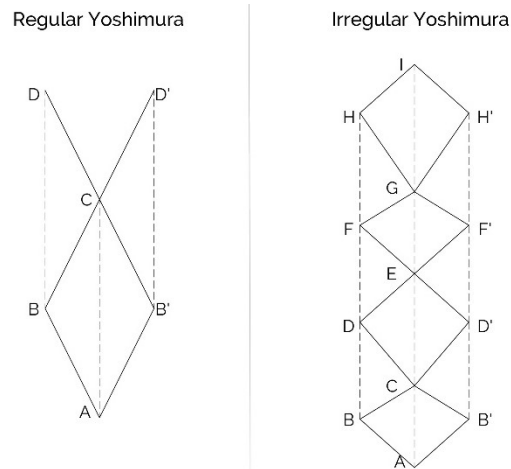


Figure 3. 48.
 Additional Base faces
 for Irregular
 Yoshimura

For the **Regular Yoshimura** the user has only to determine the X coordinate for point A ($A_y=0$) and the Y coordinate for point B ($B_x=0$). From these two

values the entire pattern gets defined, since B' has the same Y as B and its X coordinate is twice A_x . Point C has the same X coordinate as A and its Y coordinate is twice B_y . Point D has the same X coordinate as B and its Y coordinate is three times B_y . The points B' and D' are mirrored in respect to the axis defined by A and C , as **Figure 3.49** demonstrates.

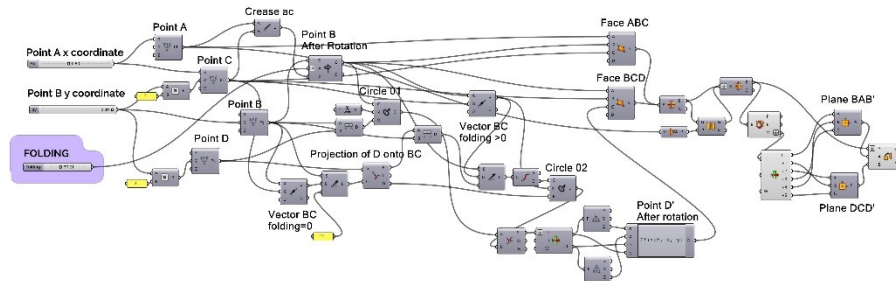


Figure 3.49. Definition of Points A, B, C and D, faces and mirrored faces.

The folding of point B is very straightforward, it is a simple rotation around crease AC from 0 to 90° . The folding of Point D is not so straightforward. It is found during the entire motion through the intersection of two circles, 01 and 02.

Circle 01 is defined by having its center on point B , radius equal to the distance between B and D (at the unfolded state) and it is always on a perpendicular plane parallel to the plane ZY since, as described before, the valley folds of the Yoshimura pattern move on a perpendicular sense to its axis.

Circle 02 has its center (point P) on the extension line with direction $B \rightarrow C$, is always perpendicular to that line (which is the circle normal) and P maintains its distance to point B through motion. The location of point P at line BC is defined by the shortest distance between D and the line when the surface is unfolded. This way is determined the path of rotation of point D around BC line, since any point belonging to face BCD must maintain the same distancing to BC line when rotating around it, so the radius of Circle 02 is the distance between P and D , at the unfolded state.

Naturally that the intersection operation between the two circles only gives one point as output on the unfolded state, while folding it gives always two points, from these points is chosen the one with lowest Z coordinate since it is a mountain fold. On **Figure 3.50** is represented the described geometric operation to find point D .

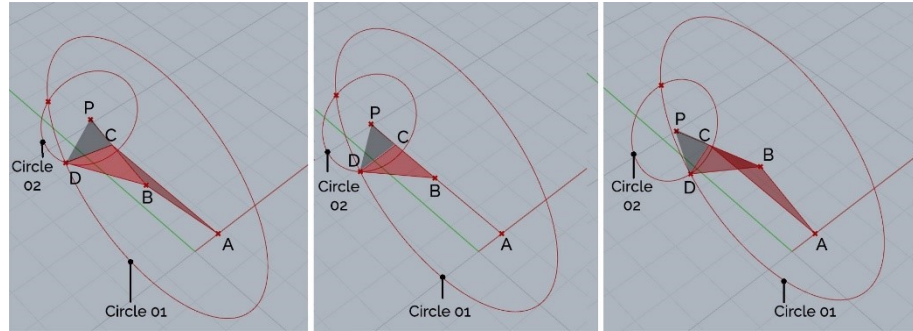


Figure 3. 50.
 Intersection between
 circles 01 and 02 to
 find Point D

The set of folding faces **ABC** and **BCD** is subjected to a mirror operation through a vertical plane that passes through line **AC**, in order to create the folding faces **AB'C** and **B'CD'**.

After the mirror operation is created a copy of the base faces through an orientation operation that departs from plane **BAB'** and arrives to plane **DCD'**. Just as in the Degree4 algorithm these two sets of base faces allow to define the circle that rules the folding of this cylindrical folding tessellation.

The circle defined by points **A**, **C** and the **new point C** (from the orienting operation) allows to define a circle through three points. From the vectors that start at the center of the circle and have tip at points **A** and **C** gets defined the needed angle to create polar copies of the base faces.

This method allows to create the simulation of the folding surface, but causes an impossibility of determining the CP when the folding angle is 0, since it is not possible to generate the circle with three collinear points. For that matter the algorithm has a possibility of making linear copies on both directions when the surface is at the unfolded state so the user can visualize the entire tessellation and decide on its size, just as was done for the Degree4 Simulator.

Figure 3.51 depicts this part of the algorithm and in **Figure 3.52** are shown four states of the folding of a regular Yoshimura pattern with three Lines and five columns of base faces and where the defined coordinates were $A_x=0,8$ and $B_y=2$.

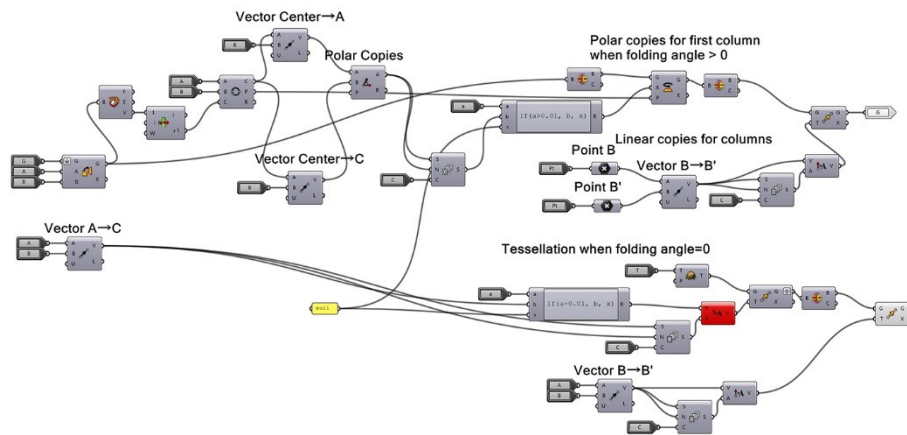


Figure 3. 51.
Surface for Regular
Yoshimura

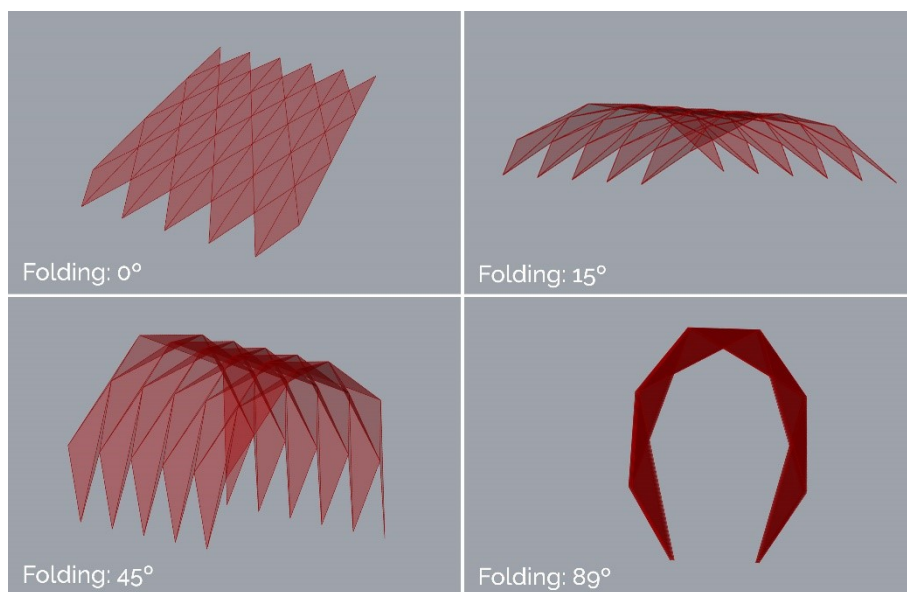


Figure 3. 52.
Four folding states of
Regular Yoshimura

For the **Irregular Yoshimura** the user can define points A and B as in the regular case but then is also possible to determine the Y coordinate for points C, D, E, F, G, H and I. These points X coordinate is always related to A_x or B_x , depending on their position on the tessellation and their Y coordinate is always dependable from the previous one. The dependency between Y coordinates guarantees that the vertices along the valley line can not be lower in Y than the previous ones, **Figure 3.53**. This way is possible to guarantee that the created pattern is always Yoshimura and does not turn into a “tucking faces” type of pattern, such as the Kresling pattern.

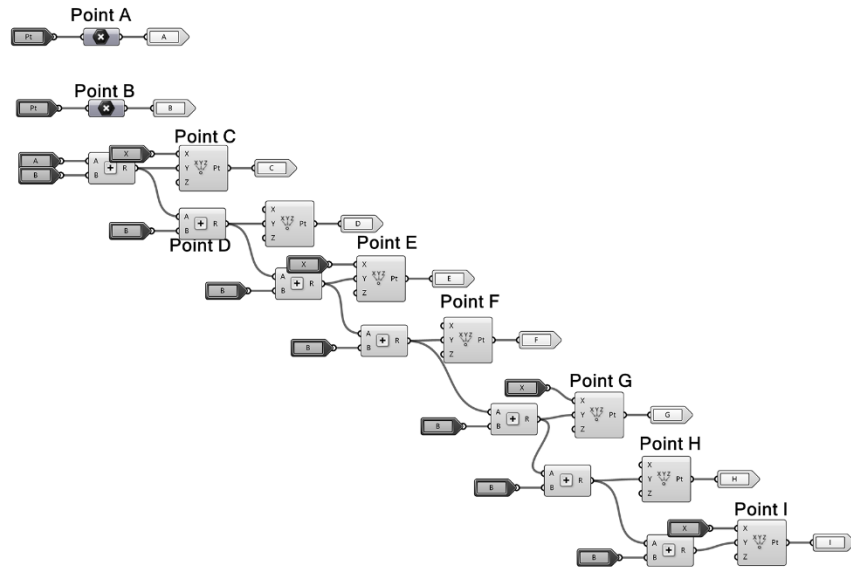


Figure 3.53.
 Points definition for
 Irregular Yoshimura

The folding of the tessellation follows the same strategy as the one described on the previous case. Point **B** is rotated around crease **AC** and then is found point **D**, continuously through folding from the intersection of circles 01 and 02, as seen on **Figure 3.50**. After this operation are defined the faces on the left and then is used a mirror operation to determine the ones on the right. Since the Irregular Yoshimura does not have a unique set of four base faces that are repeatedly reproduced to compose the tessellation it was tried to subdivide the column of faces into four separate sets that are folded and then reoriented in respect to the previous one. This way is possible to have congruent folding angles, since every set is ruled by the folding of one vertex from 0° to 90° . The four sets are represented on **Figure 3.54**.

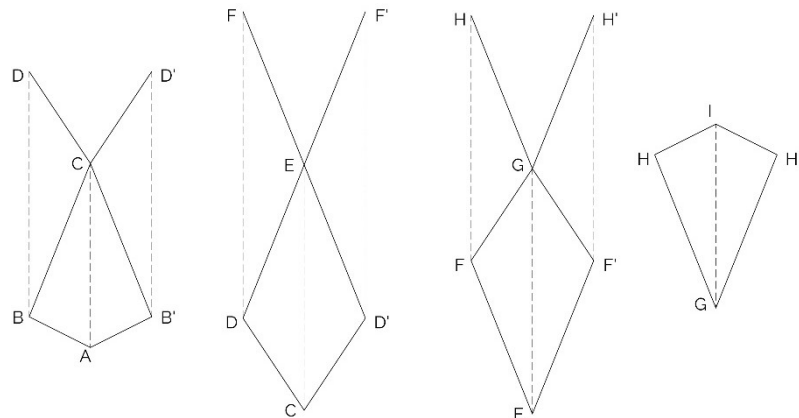


Figure 3.54.
 Four sets of base
 faces for Irregular
 Yoshimura

Every set of base faces is folded by the algorithm in the same way. First the lowest point on the left is rotated around the valley crease and the point at the upper part on the left is found through the intersection between the two circles. After the definition of the two faces, that are created from the rotating points, is found the symmetric pair by a mirror operation through a vertical plane that

passes on the valley crease. Only the last set of base faces has a simpler procedure where point *H* is simply rotated around crease *GI* and then the face is mirrored as seen on **Figure 3.55**.

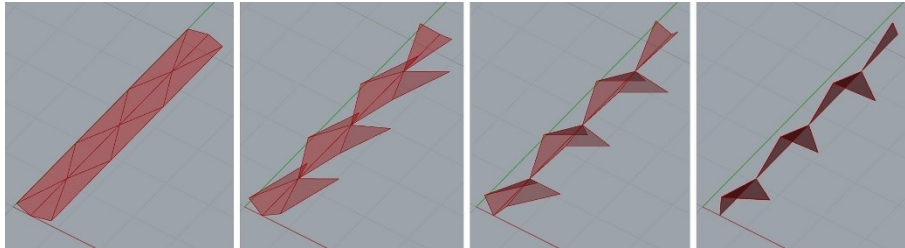


Figure 3.55. States of folding for each of the four sets of base faces

The detailed Grasshopper definition of the folding of each set of base faces can be seen in **Figures 3.56, 3.57, 3.58** and **3.59**.

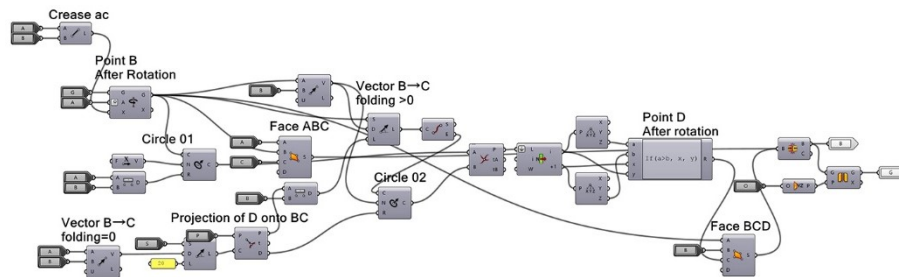


Figure 3.56. Folding of first set of base faces

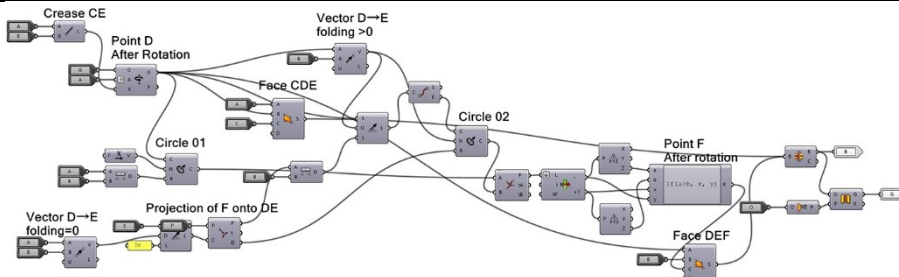


Figure 3.57. Folding of second set of base faces

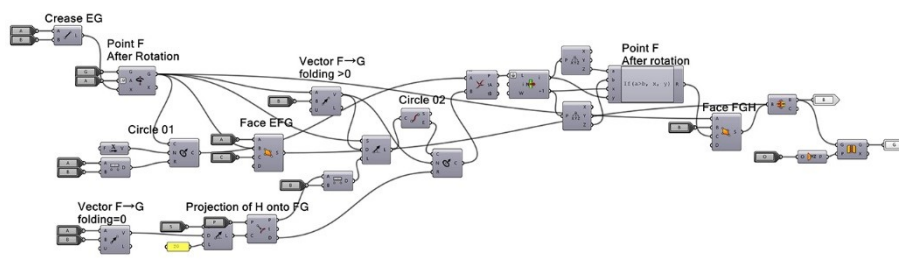


Figure 3.58. Folding of third set of base faces

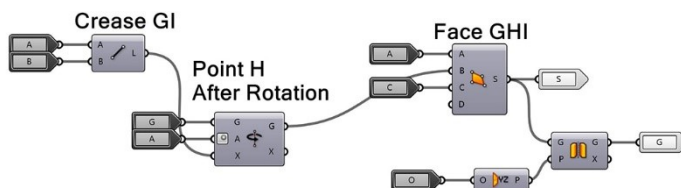


Figure 3.59. Folding of fourth set of base faces

After the determination of the folding of each base faces set each one is oriented in respect to the previous one. When the column is complete it is possible to make multiple copies through $B \rightarrow B'$ vector and the slider for "Number of Columns". **Figure 3.60** demonstrates the Grasshopper definition for the alignment of base faces and the vectorial copies.

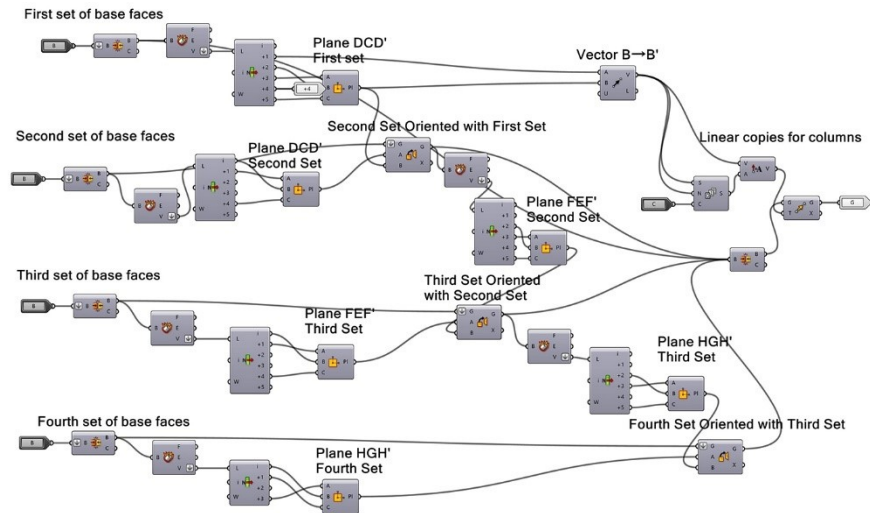


Figure 3. 60.
 Alignment of base faces and copies for Irregular Yoshimura Surface

Four states of the folding of an Irregular Yoshimura Surface are shown on **Figure 3.61**.

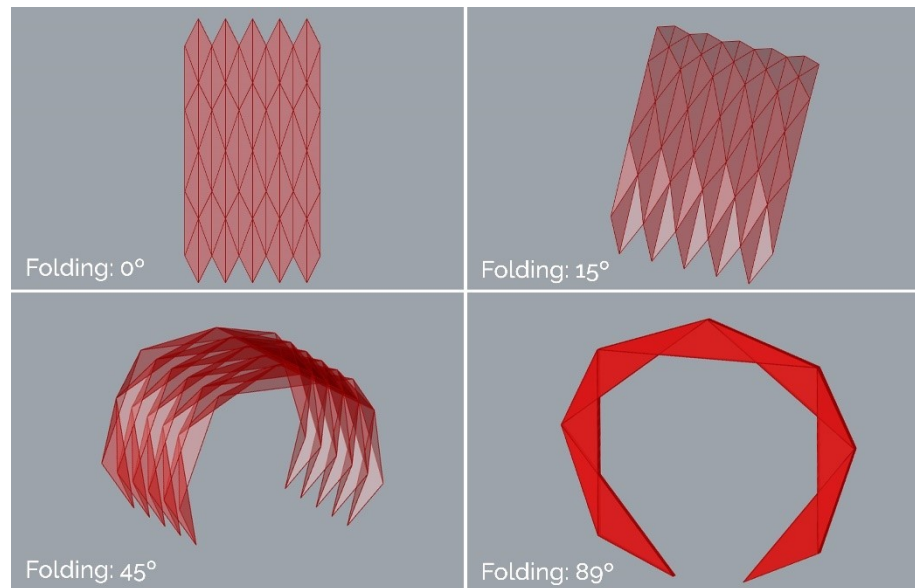


Figure 3. 61.
 Folding of Irregular Yoshimura Surface

During the development of the algorithm another path was created for the folding of the **Double Helicoidal** and **Skewed Yoshimura**, since the two patterns have different Y coordinates for points B, B' and D, D'. The Double

Helicoidal is a special case of the Skewed Yoshimura, that is when the **angles ABC, BCD, AB'C and B'CD'** are straight.

For these patterns the user may first set A_x and B_y , just as for the other patterns. If the intention is to fold the Double Helicoidal, then it is not possible to define anything else, since the algorithm can create the base faces by the definition of points **A** and **B** alone. The **crease AB** is rotated 90° to find point **C**, and **crease BC** is moved through vector $B \rightarrow A$ to find point **B'**. If the user wishes to fold the Skewed Yoshimura then is possible to define C_y , which is directly related to B_y , as can be seen on **Figure 3.62**.

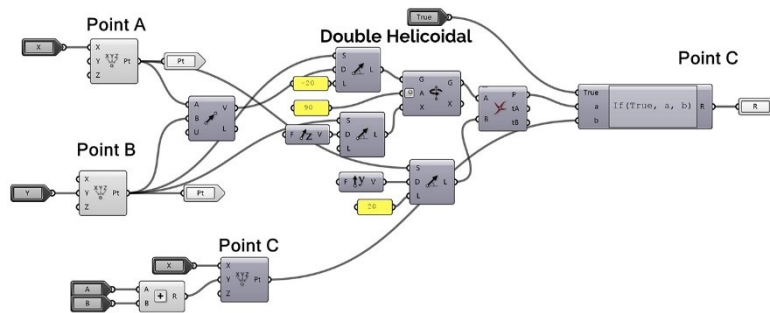


Figure 3. 62. Definition of points A, B and C for Skewed Yoshimura or Double Helicoidal

Subsequently are defined the points **D** and **D'** through the previously explained method of the intersection between Circle 01 and 02. When every point is created is then possible to create the base faces of the tessellation, demonstrated on **Figure 3.63**.

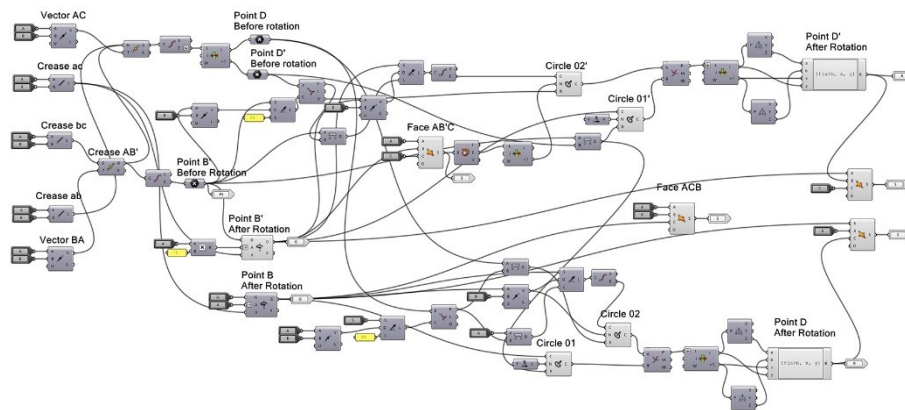


Figure 3. 63. Definition of base faces for Skewed Yoshimura or Double Helicoidal

The set of base faces gets copied and oriented from plane **BAB'** to plane **DCD'**. From the angle defined by the two sets of base faces is possible to calculate the angle for the next base faces. That way the user may define the number of base faces that compose a column, through the slider "Number of Lines"

To copy the columns and form a surface is taken the first column and copied through vector $B \rightarrow B'$. Since points **B** and **B'** do not define a line parallel to **XX** axis there is the need to rotate each new column in respect to the last one.

the rotation angle is found through the difference between vectors $B \rightarrow D$ and $B' \rightarrow D'$. Each copy of the columns demands for movement and subsequent rotation. It was not found yet an option among GH components able to do this operation in an iterative way. For that reason was created a pseudo-iteration that takes both the translation and rotation operations and applies it to the geometry in a consecutive way. **Figure 3.64** demonstrates the detailed definition for the construction of the unfolded tessellation and the folding one through iteration.

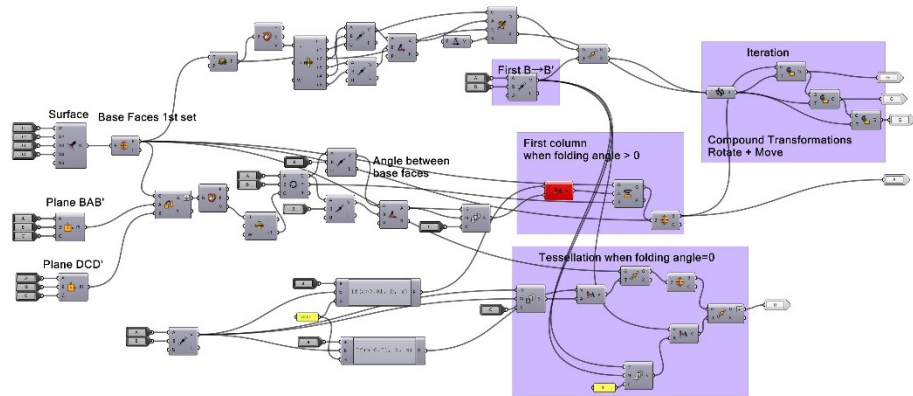


Figure 3. 64.
 Surface for Skewed
 Yoshimura or Double
 Helicoidal

Figures 3.65 and 3.66 reveal four folding states of the Double Helicoidal and Skewed Yoshimura.

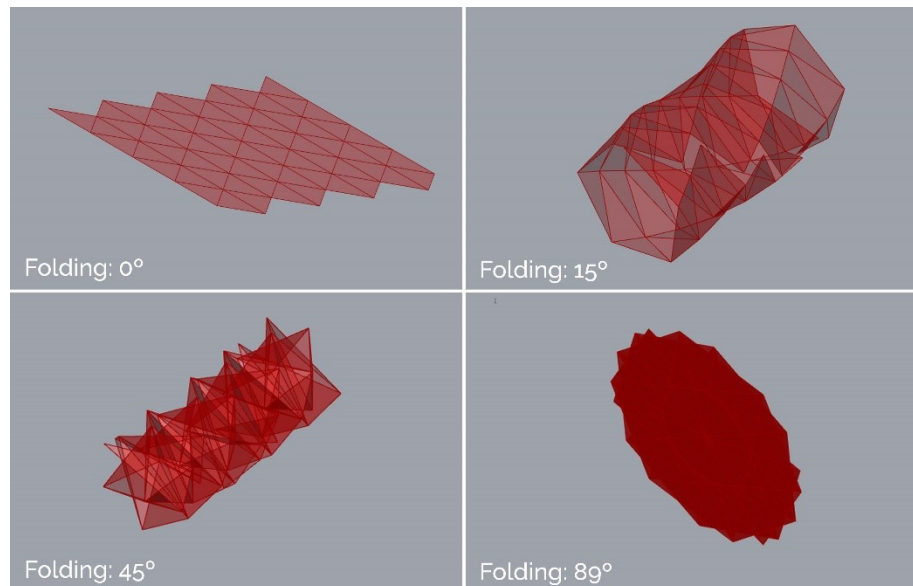


Figure 3. 65.
 Folding of Double
 Helicoidal

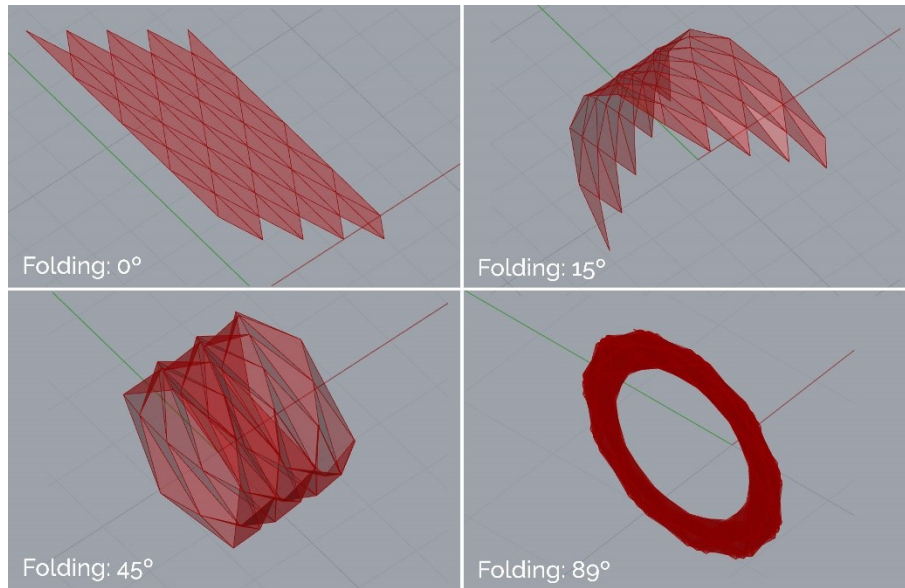


Figure 3.66. Folding of Skewed Yoshimura

For the choice between the Double Helicoidal and the Skewed Yoshimura the user has the possibility of using a boolean toggle. **Figure 3.67** demonstrates the positions of the control parts, the folding surfaces for geometry visualization and export, as well as the relation between every cluster of the simulator for degree-6 Cps.

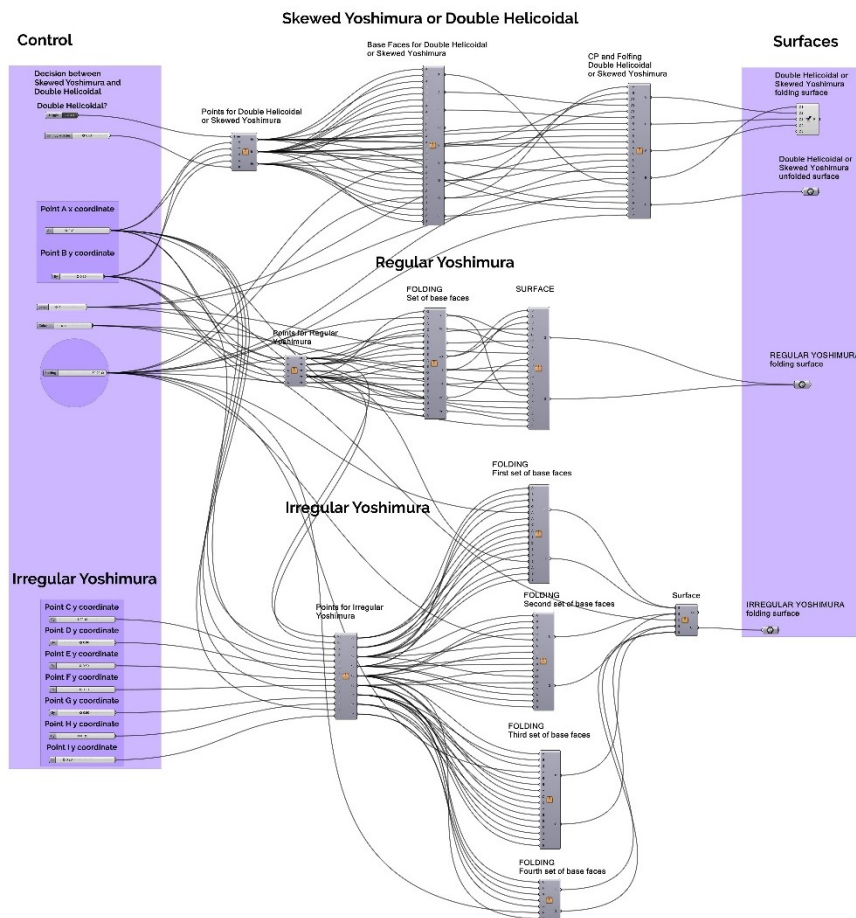


Figure 3.67. Relationship between every step of the folding simulator for degree-6 CPs

3.3.3 | Origami Thickness

As described In **Section 2.2.1**, strategies already exist to turn non-thick origami into thick surfaces which maintain the kinematic behaviour of the pure, zero-thickness origami surface.

The existing, scientifically defended methods are the Axis Shift Method (ASM), Membrane Folds Method (MFM), Tapered Panels Method (TPM) and the Offset Panel Technique (OPT) which are represented at **Figure 2.90**, of the previous Chapter.

The ASM is probably the easiest to use. It allows panels with thickness to be used by simply moving the hinges to the side of the panel where they correspond to the valley creases. In reality this method alters the initial dimensions of the CP, but it is not a problem since the whole pattern is augmented consistently. In the next image is possible to see that the original dimension of any face would be **a**, which gets altered through the ASM to **b** (**Figure 3.68**).

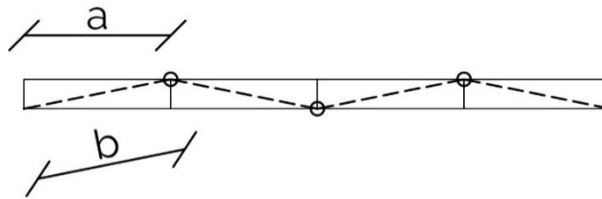


Figure 3. 68.
Dimension alteration
through Axis Shift
Method

Another good characteristic of this method is that it naturally constrains the faces to rotate only on the valley sense and does not allow them to make a mountain fold. This can be extremely useful for architectural structures for safety reasons and to maintain the integrity of the structure and the intended direction of folding (**Figure 3.69**).

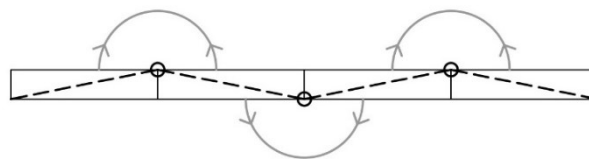


Figure 3. 69.
Valley folding restriction
through Axis Shift
Method

Although there are very good reasons to use this method it does not work for every CP. It works on CPs that have parallel stacking and no faces tucking inside other faces. For example, it works perfectly for the shown degree2 CPs, but does not work for the Miura tessellations or the Kresling Pattern. It is however perfect for the Yoshimura pattern.

In **Figure 3.70** stretching at the hinges is clearly shown, caused by the thickness of plywood in the tucking areas.



Figure 3.70.
Miura tessellation with
plywood rigid faces using
the Axis Shift Method

Contrarily it works very well in the Yoshimura Pattern since the faces simply sit next to each other on the flat folded state (**Figure 3.71**)

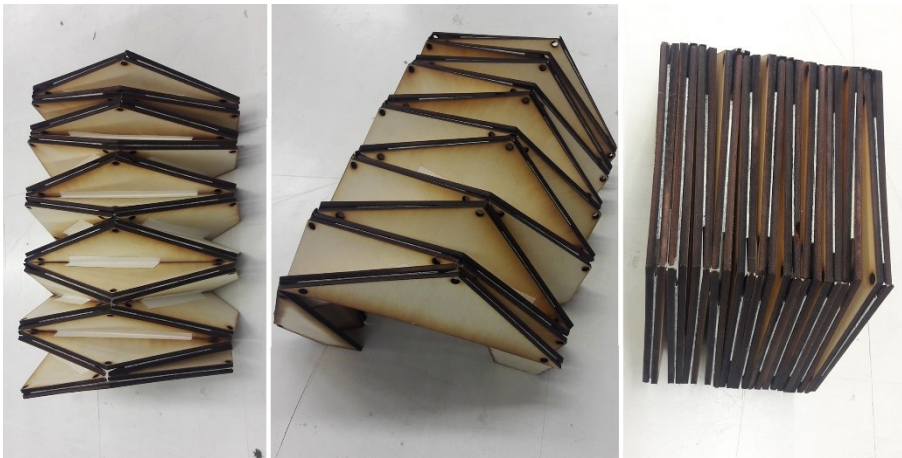


Figure 3.71.
Yoshimura tessellation
with plywood rigid faces
using the Axis Shift
Method

The MFM may not be the best method to use in a structure that needs to be stable and controllable. The gaps opening in the valley folds are really creating additional complexity in the model. Instead of having one hinge it starts to have two and these hinges are free to rotate 360° , since the method, by itself, does not constrain their motion (**Figure 3.72**). This method alters completely the kinematics of the original CO (Edmondson *et al.*, 2015) in fact, it generates an entirely new CP.

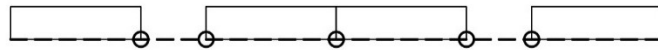
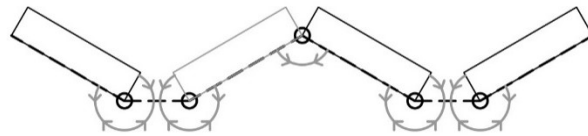


Figure 3. 72.
Gaps for valley folds and
rotation movement on
hinges on the
Membrane Folds
Method



This method seems more suitable to use on surfaces that are intended to behave fluidly, like fabric, than on surfaces where structural rigidity is desirable.

The TPM (Tachi, 2011), works more closely to the ASM and the tapering of the faces makes usable on CPs that have tucking faces. This method allows faces to accommodate next to each other in the completely folded position without producing additional forces on the neighbouring faces and causing hinges to open.

As described in Chapter 02 (**Figure 2.89**) the TPM was Tachi's method to produce a folding surface based on the Miura pattern.

This technique applies the tapering on the valley side of the thick material and thus facilitates a larger compression of the tessellation than the ASM, that is it permits a state closer to the completely flat folded position of the kinematic surface.

Similar to the ASM, it also prevents faces from rotating in the opposite direction than the intended one, but for materials with the same thickness, the TPM produces more fragile areas next to the hinges since the material loses half his thickness.

The Offset Panel Technique (OPT) (Edmondson *et al.*, 2015) has advantages as referred to by the authors. It preserves the kinematics of the full range of motion of the corresponding zero-thickness origami surface (the "joint plane"), unlike the methods seen before. Unfortunately, it may need clearance holes to avoid self-intersection and in large CPs with many faces accumulating on specific parts the offset can be too big and compromise the integrity of the structure (Edmondson *et al.*, 2015).

3.4 | Materials

For the material choice it is necessary to understand the needs for a kinetic surface based on rigid and flat-foldable origami tessellations, as well as its scale and structural behaviour. It seems to be impossible to use a material with the same characteristics as paper to build a structure of this scale.

While paper behaves perfectly on a small scale with its rigid faces and straight creases that allow for the material to bend along specific lines, when passing to the architectural scale the behaviour of the material is not the same, the size and weight of the structure causes faces to deform, thus losing their rigidity, and the creases do not act as straight hinges anymore, they also become deformed.

Some materials could possibly be used as gigantic sheets that can be bent along specific lines and maintain rigidity on faces, the materials that seem to be the best candidates for this type of approach would be corrugated cardboard, metal or polymers sheets. Nevertheless, such a material, with big enough dimensions to build a large-scale prototype, was not found and the practical difficulties of creasing and bending such a big sheet seemed too inaccessible for this research. Furthermore, there are not any known examples of pure folded metal used for origami surfaces in a kinetic context. The known examples that used pure metal sheets without hinges or additional mechanisms bend the sheet along the crease lines, until a desired point and then are left with that form, permanently.

Other materials that could be used as gigantic sheets could be PVC, PP or cardboard sheets, but in the developed experiments (**Section 3.5**) they were not found to be good enough candidates for large scale structures.

Another approach was decided, in line with experiments from other authors, that was to make each face independently and attach it to the other faces of the structure in a way that the kinematics of rigidly folding origami is preserved. The faces will behave, at the same time, as structure and mechanism, they must be able to support themselves and the rest of the structure without bending or collapsing, thus maintaining the rigidity and undeformability characteristic of rigid origami surfaces.

In this way the material must be rigid (high Young's Modulus) and resistant to bending, tension and compression, since it will be subjected to all directions of forces when moving and when static.

For a more profound analysis of materials, Ashby's method of comparing families of materials through two mechanical properties was used (Ashby, 2005, 3rd Edition).

The author states that there are six main families for materials: Metals, Ceramics, Glasses, Polymers, Elastomers and Hybrids (where Wood is included) (**Figure 3.73**).

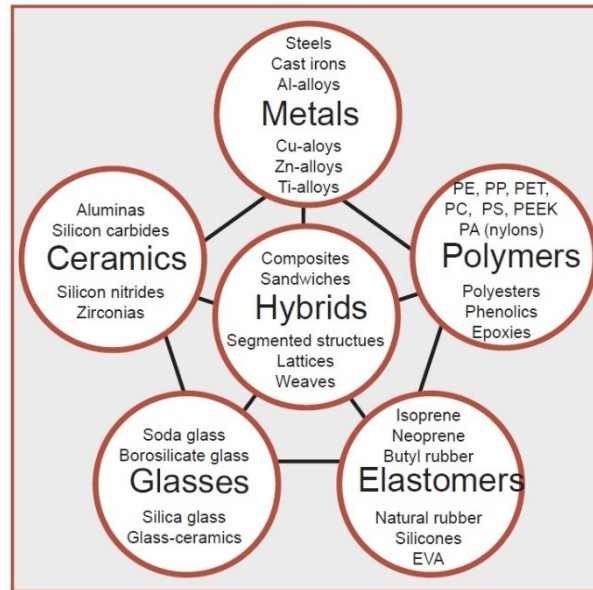


Figure 3.73.
Materials' Families
Source: Ashby, 2005
3rd Edition

Some materials can be empirically disregarded, like Glasses, Elastomers and Ceramics. Although Ceramics have good mechanical properties, they are brittle materials, that is, very weak to stress concentrations, which make them unsuitable for load-bearing (Ashby, 2005, 3rd Edition).

Ashby's Properties Charts are very useful because they condense a lot of information related to all families of materials in charts where two properties are plotted against each other. The main properties that this research needs to address are the Young's Modulus, that translates the rigidity of a solid material (bigger values mean stiffer materials), Density (smaller values mean lighter materials), Resistance to Compression and Tension (strength) and Resistance to Fracture.

Since the aim is to create structures as light as possible with the best possible performance in terms of rigidity the first comparison chart is the one that compares these two properties (**Figure 3.74**). From the chart it is possible to see that the materials that have a better compromise between the two properties would be Metals, Composites, Wood and some Polymers.

On the chart that compares the Young's Modulus and Strength (**Figure 3.75**) the result is similar, Composites, Wood and Polymers have good results, but Metals are the clear winners.

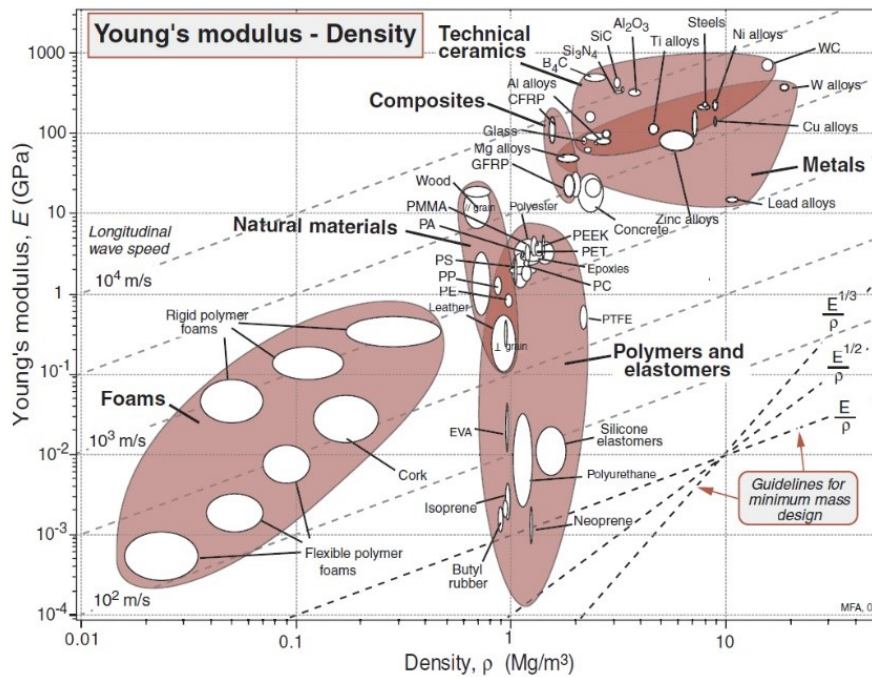


Figure 3. 74.
Young's Modulus and Density
Source: Ashby, 2005 3rd Edition

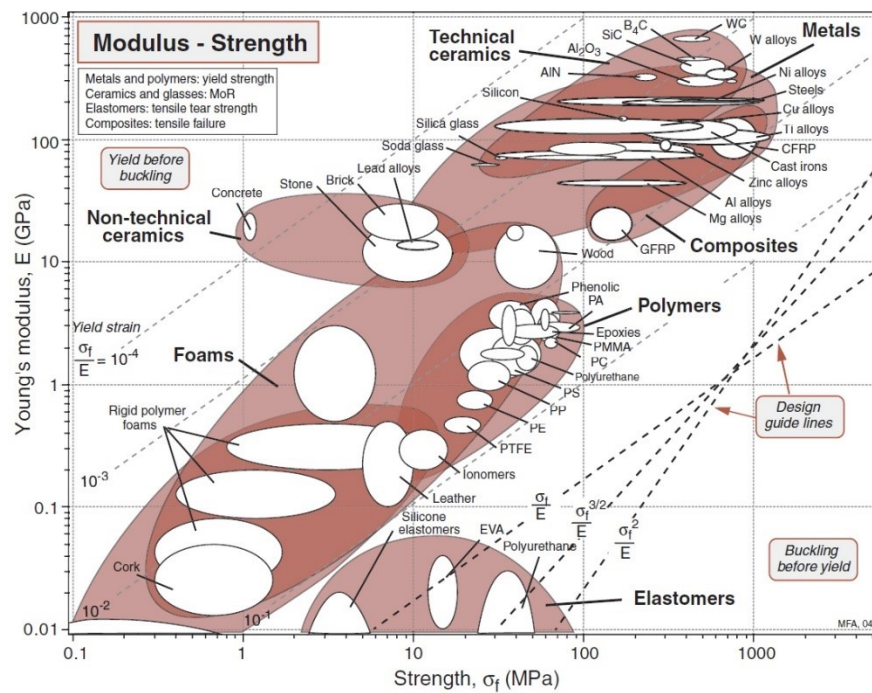


Figure 3. 75.
Young's Modulus and Strength
Source: Ashby, 2005 3rd Edition

On the next chart the Fracture Toughness is compared to the strength of materials (**Figure 3.76**). From this chart Polymers get overlooked, their resistance to fracture is too low when compared to the other groups. Besides that, Polymers do not behave very well when temperatures are low or high (Ashby, 2005, 3rd Edition), and for that reason are excluded from the material choosing process for these kinetic structures.

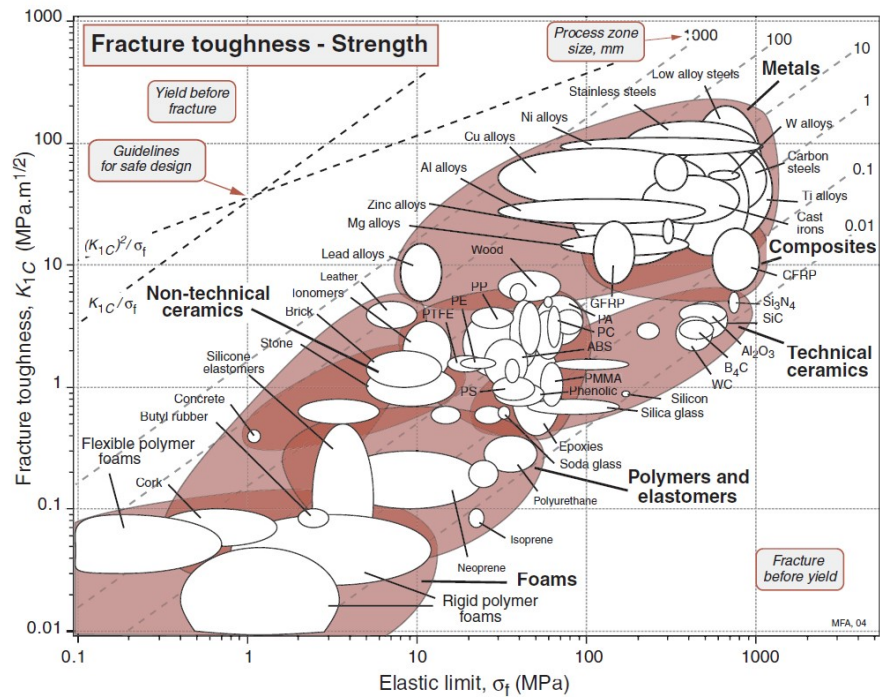


Figure 3.76.
 Fracture Toughness
 and Strength
 Source: Ashby, 2005
 3rd Edition

Another important factor for the decision on materials is the cost of the material to be used in Architectural scale structures, and particularly on the Proof-of-Concept prototype, from Ashby's next chart Wood seems to be the best choice, thus excluding Metals and Composites (**Figure 3.77**).

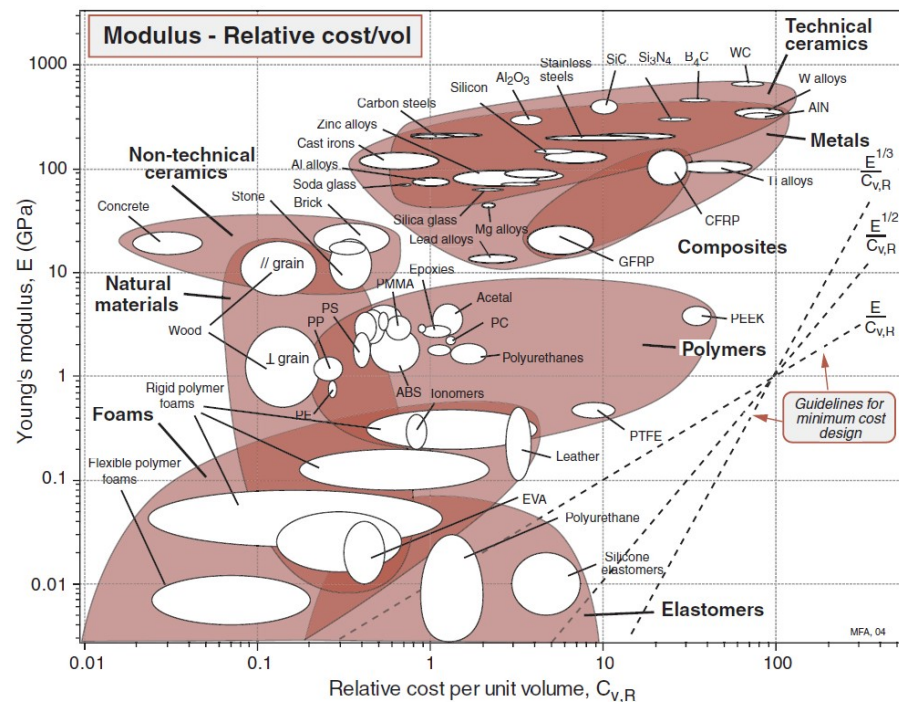


Figure 3.77.
 Fracture Toughness
 and Strength
 Source: Ashby, 2005
 3rd Edition

Additionally, wood-based products are easier to find and to transform in the available CNC milling machine for this research, at the same time that they have mechanic properties in accordance with the needs of the prototype.

When deciding on which type of wood-based product should be used, materials such as OSB or wood particle boards were dismissed, because these products might have good mechanical properties to be used as boards with several support points, that is, they have good resistance if forces are applied perpendicularly to the main face, but if we use them as strips they lose that resistance capacity and fracture. These materials are not suitable to be used as structural materials.

With all these needs and demands in mind the type of materials that seem to be the best candidates to be used for the final prototype for this thesis would be wood based products, such as plywood or MDF.

Plywood and MDF have generally, good mechanical properties to be used on structures that need to be rigid and act as a mechanism. Additionally, these are controlled production materials and have an homogeneous behaviour through the panels since their intrinsic properties allow an even distribution of forces (Cachim, 2007) (Stevenson, 2011).

Since these materials are not suitable for direct creasing and bending, they will be used in conjunction with metallic hinges in order to reproduce the kinematic properties of rigid folding origami.

3.5 | Analysis of Experiments

Throughout the progress of this research over the years, several prototypes were developed that enabled to shape the research. The prototypes helped to better understand origami geometry, the methods for thickening origami surfaces, mechanical movements and control. Ultimately, these experiments were the drivers for the establishment of a workflow and for the aims and conditionings of the Proof-of-Concept (PoC) prototype.

In this way, the approach followed by this thesis is based on a “thinking-through-making” philosophy, as argued by Burry and Burry (2016). Prototyping has always been a way to test and evaluate architectural ideas by overcoming two-dimensional representation limitations through three-dimensional models. In the age of digital architecture, prototypes seem to be even more useful due to the available digital fabrication tools, which allow to quickly fabricate models, and the possibility of linking them with parametric design. As advocated by Burry and Burry (2016) “*Prototyping for architects looks at every aspect of the realization of ideas, experiments and investigations as physical or digital artifacts during the design process. Prototyping (...) is an element of novelty and testing*” Burry and Burry (2016, pp. 12).”

The process used for the development of each prototype is analysed, along with the shown limitations, to propose a workflow that is believed to allow for a complete and rigorous approach for the design of kinetic origami surfaces, with an integrated vision from concept, to implementation, passing through digital simulation, computational control and fabrication.

As will be demonstrated through the executed experiments, the workflow is not straightforward, since it was often found to be necessary to revisit previous steps when problems were found later on, especially when the designer is new to the specific theme. The final proposed workflow comprehends several stages but works as an algorithm where critical judgment is essential.

In the subsequent section, ten constructed experiments will be analysed through the same criteria, to allow a comparison of all of these, which will shape the designing aims and boundaries for the final prototype.

The criteria can be grouped into three main topics, origami geometry, materials and digital fabrication, mechanism and control. Each topic is further subdivided into four specific subjects for evaluation, defined in **Table 3.15**.

Criteria for Analysis of Experiments				
Origami Geometry	Rigid Foldability	Flat Foldable	Rigidity of Simulation	Reality vs. Simulation
Materials and Digital Fabrication	Fabrication Method	Thickness Method	Faces Behaviour	Hinges Behaviour
Mechanisms Control	Mechanism Behaviour	Control of Folding Angles	Stability of Structure	Computational Control

Table 3. 15.
Criteria for
Experiments' Analysis

To each criterion will be assigned an evaluation, where 1 is the lowest possible, and means that a specific experiment was very poor on the matter, and 5 means the experiment behaved very well on that specific subject.

On the topic of **Origami Geometry**, the criteria for analysis will be:

- a) Rigid Foldability: where the geometry of the CP and its behaviour in the folding process will be graded in respect to its rigid foldability, independently of the constructed result.
- b) Flat-Foldable: if the CP is flat-foldable regardless of the ability of the experiment to reach a flat-folded position
- c) Simulation's Rigidity: If the used digital simulation relied on rigid kinematics or on approximate methods.
- d) Reality vs. Simulation: where the real, physical behaviour of the experiment is graded in respect to simulated behaviour of the geometry.

On the topic of **Materials and Digital Fabrication**, the criteria for analysis will be:

- a) Fabrication Method: if the chosen fabrication method, along with the properties of the material, behaved well in accordance with the geometry of the surface, intended movements and kinematics.
- b) Thickness Method: if the chosen method for thick materials helped the rigid foldability behaviour, that is, if it enabled the folding of the surface or if otherwise prevented it.
- c) Faces behaviour: If the faces maintained their planarity when unfolded, during folding and when completely folded.
- d) Hinges behaviour: if the hinges allowed faces to easily rotate, as expected with rigid kinematics, and if they maintained their straightness during the folding process, as demanded by rigid foldability.

On the topic of **Mechanisms and Control**, the criteria for analysis will be:

- a) Mechanism Behaviour: if the mechanism worked as expected. If it made the structure move in the anticipated paths, hence reaching the desired folded states and geometry.
- b) Control of Folding Angles: if the mechanism allowed for the individual control of angles between faces or if it swept the faces, in a “Curtain” type of action.
- c) Stability of the Structure: if the structure was found to be reliably stable when static and also during motion.
- d) Computational Control: if the programmed control allowed to make a satisfactory connection between the inputs for movement and the response of the mechanism and surface.

The graphical representation of the analysis of each experiment will be depicted in a spider scheme, exemplified in **Figure 3.78**. In the scheme the space is subdivided into the three main areas for origami geometry, materials and digital fabrication and mechanism control. Within each area there is a scale for each of the correspondent criteria. The grades on each scale will be connected, resulting in a polygon. The polygons help to quickly understand the relation between the graded criteria of each experiment and the comparison between several experiments. The best possible prototype would be one that led to a regular dodecagon with radius five.

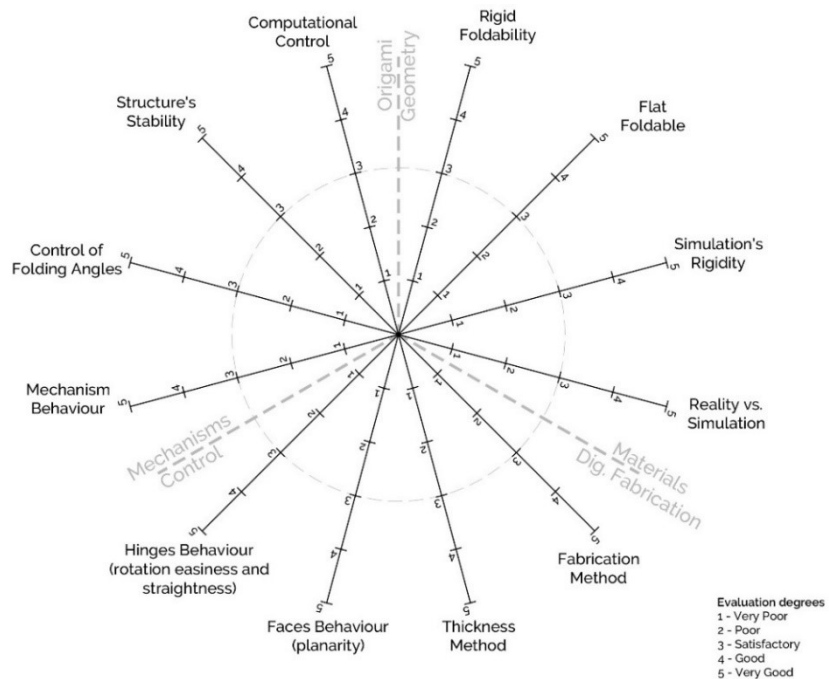


Figure 3.78.
 Spider scheme

At the end of the section a comparison will be made between the ten experiments, as well as the conclusions reached, which guided the

construction of the final prototype. The used workflow will also be detailed and analysed along with each experiment, which will generate the definition for the PoC workflow.

3.5.1 | Experiment 01

The first experiment was developed as the final work for the *Curso em Estudos Avançados em Arquitetura Digital* (CEAAD), that is, the Advanced Studies Course in Digital architecture, that was attended during the academic year of 2012/2013.

For this prototype the Fujimoto and Nishiwaki Pattern as well as the Miura pattern were tested, both with regular tessellations. The patterns were first tested on paper and directly manipulated, as can be seen in **Figures 3.79, 3.80 and 3.81**.

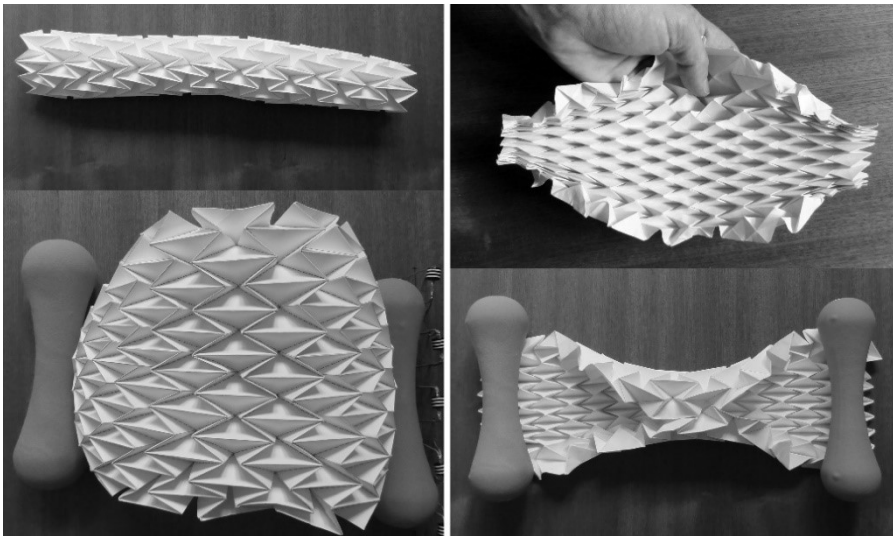


Figure 3. 79.
Fujimoto and Nishiwaki
paper model

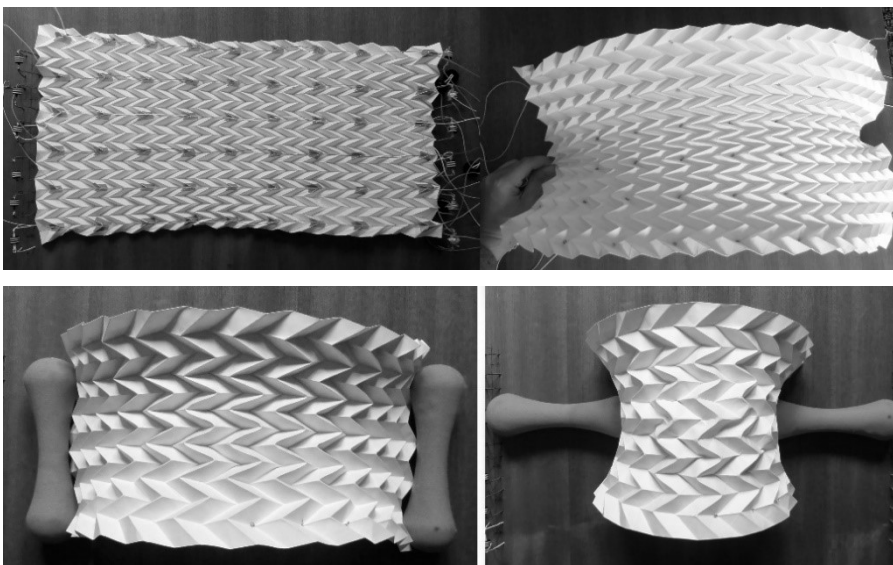
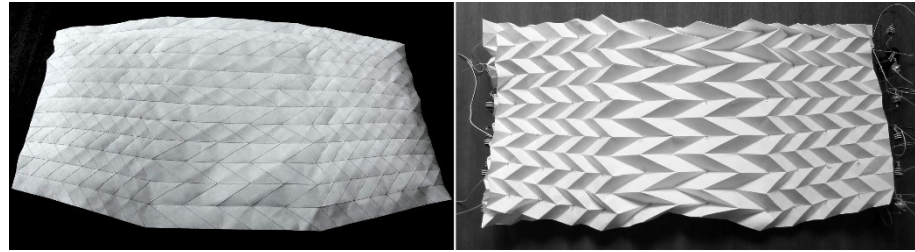


Figure 3. 80.
Miura with regular
Tessellation paper
models

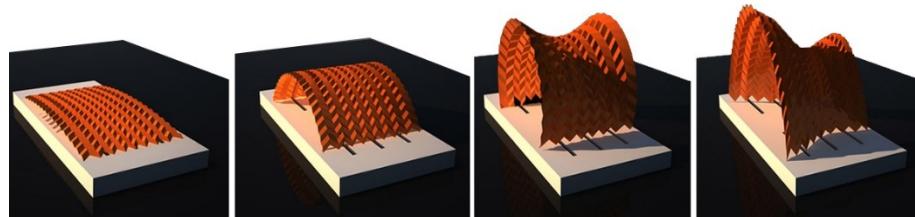
Figure 3. 81.
Miura with Irregular
Tessellation paper
model



For the final prototype the regular Miura Pattern was chosen as it seemed to have the best compromise between the demands of self-supporting abilities, the predictability of the geometry and ease of control.

The simulation was done in a very early stage of the investigation, with non-parametric tools. The result of the kinematic simulation was wrong and completely inaccurate for the chosen pattern. The objective was to have a surface that could assume double curvature geometries, as done on the paper models, but it was impossible to simulate without changing the dimensions of the faces. For the simulation, that was really just a static 3D model, the faces were distorted in order to achieve the configurations shown in **Figure 3.82**.

Figure 3. 82.
Intended Geometry
with non-parametric
simulation



In fact, the paper models and the final prototype were able to assume double curvature geometries, but it was because the material did not behave rigidly, and it let the faces bend, turning its vertices from degree-4 to degree-6 through the addition of invisible neutral folds, that is, that can behave as mountain or valley, depending on the forces they are subjected to.

The chosen material for the surface was 0,8mm thick Polypropylene (PP) since, as with paper, it is isotropic with a very low density, it is rigid and at the same time flexible so it can bear multiple folds and unfolds.

The global surface was subdivided into eight sheets that were cut and engraved on the CNC milling machine, folded by hand and finally attached to each other with metallic fasteners (**Figure 3.83**). A regular tessellation was constructed with total dimensions of 1,5m x 2m when unfolded.

No specific method for thickening the surface was used for this prototype, so the material was used as if it was paper, was bent and left under compression for several hours in order to minimize the bending in the creases area.

The surface was attached to a substructure of PVC tubes with 1,5cm diameter, but did not have fixed points.

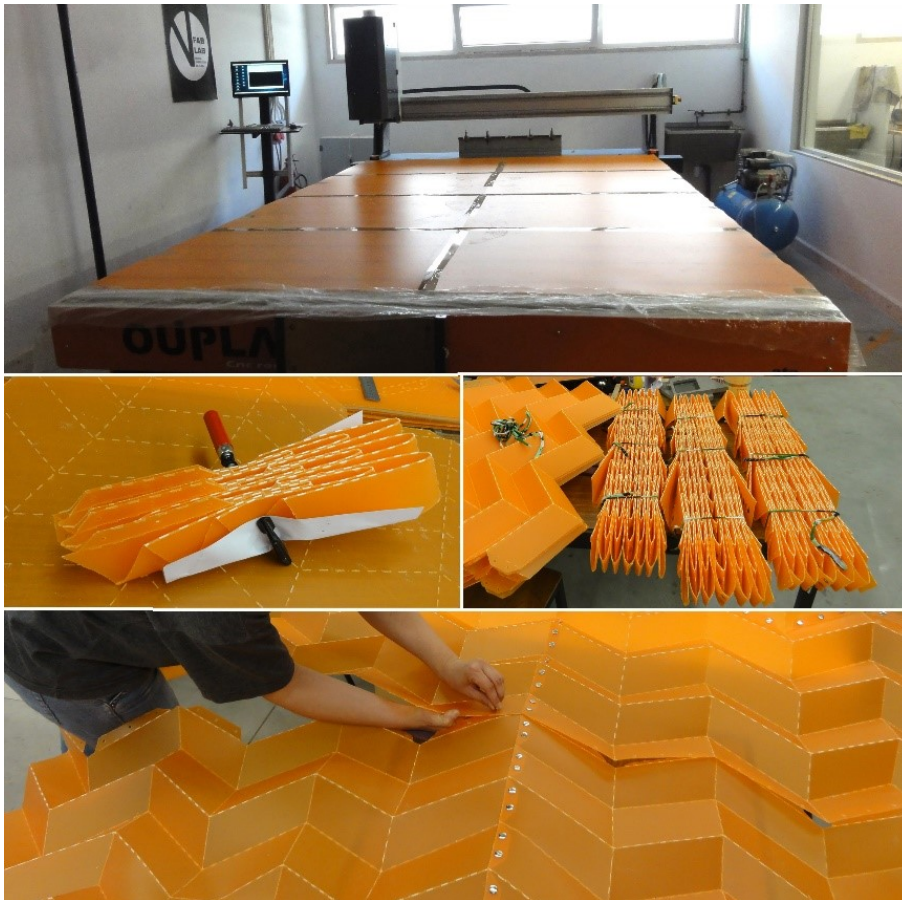


Figure 3. 83.
Digital Fabrication,
faces under
Compression and
fastening of the sheets

The mechanical system was composed of three lines of tensioned cables that slid on pulleys, the extreme points of the PVC tubes (labelled as “guide” in **Figure 3.84**) were connected to each of the movement lines which, through a reversing course pulley, were pulled at the same time in opposite directions. The motors used were shutter engines that could rotate both ways and with enough strength to make the structure move, stop, and to maintain it steadily so the tensions between faces and the force of its own weight would not make it move or collapse.

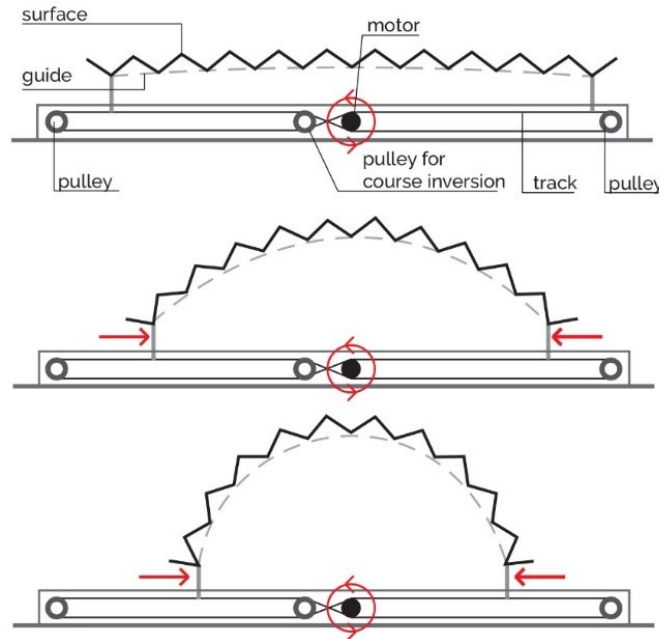


Figure 3. 84.
Mechanical system
movement scheme

For the movement of the structure, and to allow for a multiplicity of folding geometries, three parallel independent lines of action were created in the horizontal plane that would make the surface rise in Z direction.

The control of movement was made through a small-scale model of the surface, which could be manipulated and would allow for control and direct evaluation of the user in respect to the goal geometry.

A microcontroller board (Arduino compatible) was used to control the structure. The shape of the miniature was read by three potentiometers, one for each line of action. Using this information, the microcontroller would adjust the turns of the engines in the structure in order to replicate the shape of the miniature.

When the control points reached the desired positions, the microcontroller would stop the shutter engines until a new order was received. The controller's main cycle consisted of reading the potentiometers values, that corresponded to the position of the control points, reading the distance sensor values and, for each line of action, setting the motor speed so that the two values converge. In **Figure 3.85** is demonstrated the storyboard of the movement of the surface.

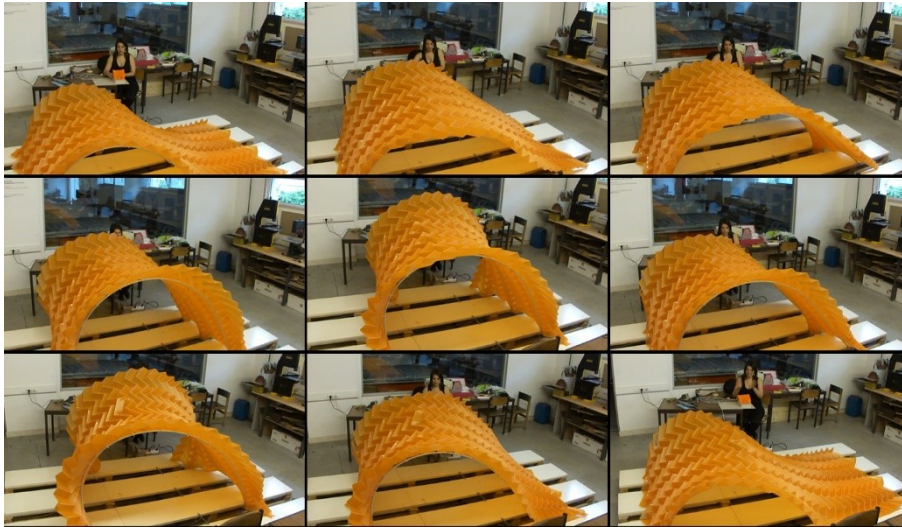


Figure 3.85.
Steps of Motion

The evaluation for this experiment is as follows:

Origami Geometry:

a) Rigid Foldability: Evaluation - 1

The CP, since it was the Miura-Ori, is rigidly foldable, but the intended way to use it would never rigidly fold.

b) Flat-Foldable: Evaluation – 1

The CP was flat-foldable, since it was the Miura-Ori, but the intended way to use it would never flat fold.

c) Rigidity of the Simulation: Evaluation – 1

The simulation consisted only of different three-dimensional models, made “by hand” for four folding states, as depicted in Figure 3.82. The purpose of these images was to make clear the intentions for the structure and do not rely on precise simulation based on rigid kinematics, thus the lowest grade.

d) Reality vs. Simulation: Evaluation – 1

At first glance, it seems that the final prototype was able to reach the intended geometries, but in fact it did not behave in the same way as the simulation. In reality the faces did not stretch but did bend, which was not, at all, the base of the three-dimensional modelling. The faces were not planar at all time, they bent during the folding process due to the surface weight, the forces applied by the PVC tubes and the loss of consistency where four sheets of PP met.

Materials and Digital Fabrication:

a) Fabrication Method: Evaluation – 3

The chosen fabrication method proved to be a satisfactory way of plotting the CP on the material. Nevertheless, it did not allow for the

definition of the identity of the creases on Polypropylene, hence there were too much stresses around the creases. Even after several hours of compression (Figure 3.83, middle) the stresses on the PP next to the crease lines were still visible to the naked eye.

b) Thickness Method: Evaluation – 1

For this prototype, no particular thickness method was used but should have been, because 0,8mm PP is a thick enough material to interfere with the behaviour of a structure at that scale.

c) Faces behaviour: Evaluation – 1

As said before, the faces did not behave at all as expected for a Rigid origami Tessellation, if they did the Miura surface would have folded only on the plane and could never achieve the double curvature configurations.

d) Hinges behaviour: Evaluation – 2

The hinges did not allow a free enough rotation of the faces due to the bending of the material in the area right next to them. Additionally, they did not remain perfectly straight during folding. That way it was decided to rate them with a two, they had several problems but still allowed for a close enough behaviour to the origami surface.

Mechanisms and Control:

a) Mechanism Behaviour: Evaluation – 5

The mechanical system behaved perfectly as expected. The motors were strong enough to push, pull and stop the structure, the cables were well tensioned and had good friction around the motors and course inversion pulley. This criterion was the best graded in this experiment.

b) Control of Folding Angles: Evaluation – 2

This structure moved by a dragging type of movement with no direct control of the folding angles between faces. Nevertheless, it did not impede the structure from moving and reaching satisfactory folding angles since the attachment points around the PVC tubes were loose enough to allow the structure to evenly distribute the folding angles and accommodate the configuration of the tubes.

c) Stability of the Structure: Evaluation – 3

The structure was found to be especially stable in static positions. During motion it trembled a bit but never lost integrity or collapsed.

d) Computational Control: Evaluation – 4

The computational control behaved very well in respect to reading the control points position with the potentiometers and ordering the

motors to move to the specific positions. However, it was a bit difficult to get millimetre accuracy due to the course size of the potentiometers, which was only 7cm. This is the reason why this criterion did not reach the best grade possible.

In **Figure 3.86** is the global evaluation of the structure on the spider scheme. The configuration of the polygon, with a low area, irregular and with peaks permits to understand that this experiment had a great disparity in the evaluation of the criteria and several low grades.

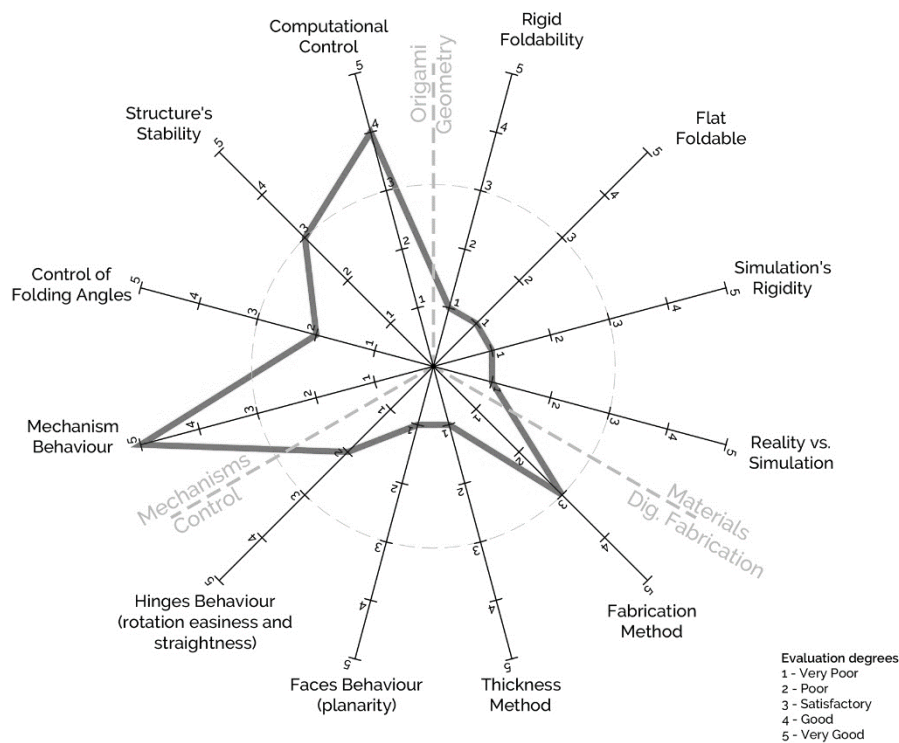


Figure 3. 86. Summary of grades for the evaluation of Experiment 01

In the development of this experiment, during the first stages, some mistakes were made as well as some naive assumptions. The workflow started by defining intentions for the surface geometric configurations with the knowledge at the time. It was the aim of the experiment to achieve double curvature configurations with the tessellations best known by then, the Nishiwaki and the Miura patterns.

The paper folded models demonstrated that it was possible with the Miura pattern, but a less naïve approach and a closer look at the models depicted in **Figure 3.80** (bottom) would have helped. In this figure the distortion in the creases can be seen getting bigger as the surface is forced to achieve more complex configurations. When making the three-dimensional models it was

very difficult to find the correct angles between faces to achieve the desired configurations, so the model had to be distorted.

To determine and test the mechanical system small scale models with pulleys and strings were created that were later replicated in the real scale prototype. The workflow used in this experiment can be schematically described as shown in **Figure 3.87**.

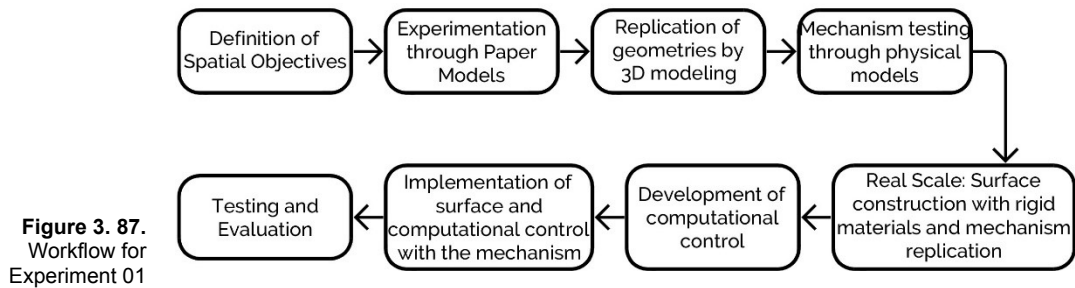


Figure 3.87.
Workflow for
Experiment 01

When testing the surface's movement in the real scale prototype, the mechanical system and the use of computation to control the movement and different geometries proved to be well achieved goals.

Overall the workflow allowed the construction of a functioning prototype but was very permissibile at particular steps such as the Replication by 3D modelling and the surface construction with rigid materials.

From this workflow and the resulting prototype it was possible to conclude that these steps should be different and able to guarantee a close and truthful relationship between simulation and construction, accurately fulfilling the kinematics and rigid folding of origami surfaces.

3.5.2 | *Experiment 02*

The second experiment includes four prototypes (A, B, C and D) and was developed at the Responsive Surfaces Summer School held in September 2015 at La Sapienza, University of Rome.

At this Summer School the objective was for each group of students to develop a kinetic surface to be replicated in a 4x4 matrix on a 1x1m wooden frame that would stand, vertically, as a self-sustained wall.

As a workflow the students had to first test different geometries, by hand, with paper or cardboard, decide a module and then replicate it into a four-module arrangement.

After the geometry definition all groups tested their CPs folding through a Grasshopper (GH) with Kangaroo Physics simulation. The plugin Kangaroo is a physical simulator that allows to create interactive simulations through forces applied to the objects (Piker, 2013). It is a quick way of understanding the tendential folding of a particular surface subdivided into faces, by determining anchor points, assigning mountain and valley folds and forces to start the folding motion. Even though it is a very interesting approach it does not rely on rigid kinematics, it allows faces and creases to tolerate dimensions and makes them act as springs instead of rigid elements. Nevertheless, it was through the simulations that the students were able to evaluate if their CP behaved as expected or if it had to be adjusted.

The available materials for the construction of the modules were 3mm thick Poly Vinyl Chloride (PVC) and 0,5mm thick Polypropylene (PP). The PVC behaved very well in the rigidity criteria; in fact, it was so rigid that it broke every time one tried to fold it. Due to that reason the faces on PVC were used as individual faces and the Axis Shift Method was used for the thick surface, with duct tape on the valley side of the surface to act as a hinge. The fabrication method used for all experiments was by a Cutting Machine (Valiani Mat Pro Ultra), this machine has great precision and is able to cut and engrave materials, until 10mm thick, in a variety of angles. The cutting and engraving for every experiment was done at 90 degrees in relation to the material's surface.

Behind the surfaces was the mechanical system composed by one or two step motors that were connected to two or four lines of movement materialised by tense cables that were attached to specific points of the surfaces. Every surface had a fixed edge or point towards or around which the movement was created. This approach is very often found in experiments with kinetic origami and is called, by this thesis, the **Curtain Method**, since it works as the

dragging of curtains, where a part of the surface remains fixed and the rest gets pushed or pulled in relation to the fixed part.

The mechanical system used for these experiments was controlled by Arduino boards that read the approach of a user through distance sensors and put the step motors in action which, in turn, pulled or pushed the tensioned cables. Although the step motors were a bit slow, they behaved well and had enough strength to push and pull the surfaces. The workflow used during the Summer School may be described as in **Figure 3.88**.

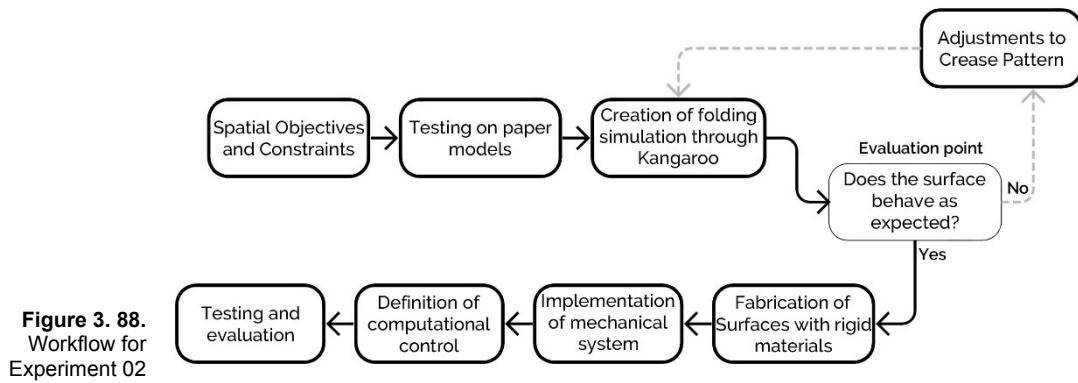


Figure 3.88.
 Workflow for Experiment 02

In respect to the movement and achieved geometries, almost every group used “folding on the plane” patterns, only group B tried to use a pattern that had to leave the plane, rotate around itself and then flat fold, which did not happen.

On **Figure 3.89** can be seen the CPs developed by each group, the fixed points or hinges, and the directions of movement of the surfaces from the unfolded to the folded state.

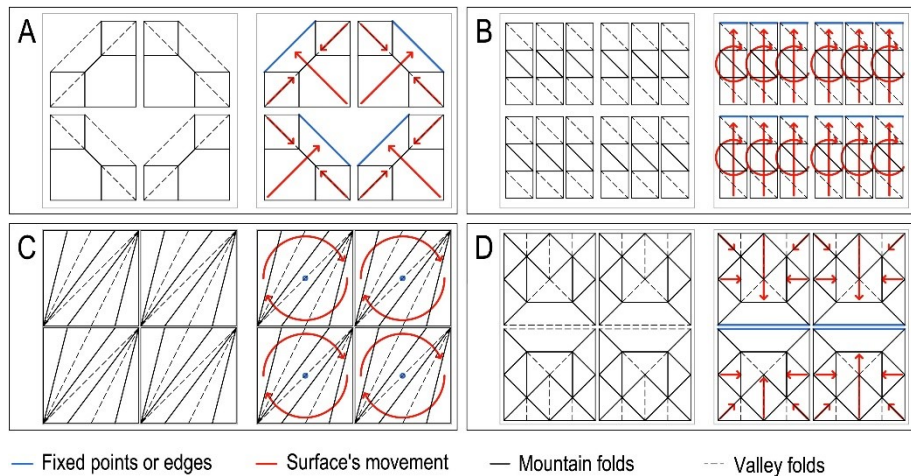


Figure 3.89.
 CPs Geometry and movement schemes

Every group used different movements, linear vertical, horizontal or diagonal and also rotational. The method to make the surfaces move was similar for all, they used tensioned cables behind the surfaces that moved points of the surface on a determined plane.

Groups A and C chose patterns that fold rigidly and flat. Group D chose a pattern that folded rigidly but could not achieve a flat-folded state since the faces collided with each other before reaching that state.

The prototype that used PP (group B) never worked, although on a small scale, the bending of the material did not allow for the modules to behave as in the kinematic simulation and the mechanical system was not carefully designed for the intended movement. **Figure 3.90** shows the constructed prototypes.

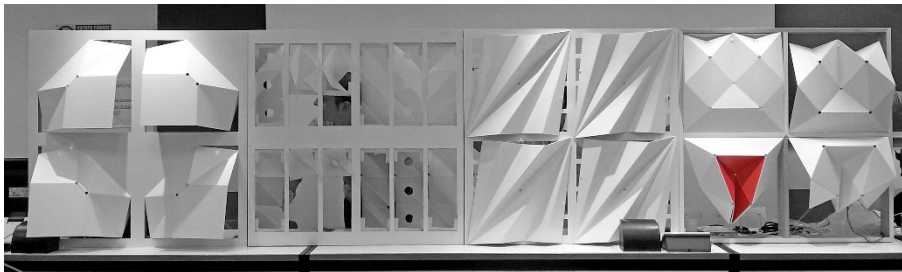


Figure 3.90.
Final Prototypes

The prototypes demonstrated another important matter to be attentive to, they were developed and tested always in the horizontal position, so when they were put up to behave as a wall, gravity started to have an impact, and the prototypes performed worse than when tested on the table and the motors had to make increased force.

The workflow was successfully followed with three of the prototypes in Experiment 02. Groups A, C and D followed every step of the workflow and were able to produce a functioning prototype that behaved in the same way demonstrated by the simulation and as the intended geometric objectives. The prototype from group B was not able to replicate the kinematic simulation for two main reasons; a poor choice for the surface material and the creation of a mechanical system that could not recreate the forces experimented on in the digital simulation. Hence the system was unable to make the surface depart from the unfolded position, rotate around itself, and then achieve a flat folded state.

The individual evaluation for the prototypes is detailed followingly.

Experiment 02 – Group A

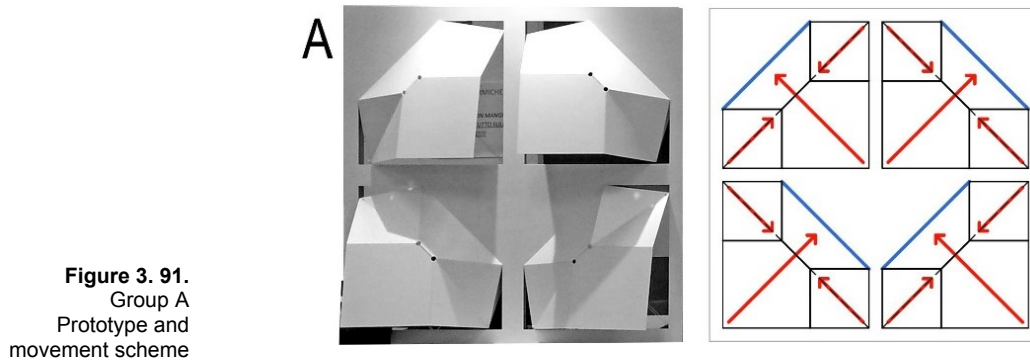


Figure 3. 91.
Group A
Prototype and
movement scheme

Origami Geometry:

a) Rigid Foldability: Evaluation – 5

The designed CP was able to rigidly fold from the unfolded to the completely folded position, without collisions or intersections.

b) Flat-Foldable: Evaluation – 5

The CP had only degree-4 vertices that respected all theorems for flat foldability, and it was able to reach a perfectly flat folded state.

c) Simulation Rigidity: Evaluation – 4

The simulation was not based on rigid kinematics. The springs had a very low elasticity, but still had it.

d) Reality vs. Simulation: Evaluation – 4

The simulated behaviour for the surfaces and their performance in reality were very close, but the constructed prototype was not able to reach a completely flat folded state.

Materials and Digital Fabrication:

a) Fabrication Method: Evaluation – 5

The used fabrication method was a simple straight cut to generate the individual faces on 3mm PVC, which worked very well for the specific experiment.

b) Thickness Method: Evaluation – 5

The used thickness method was the “Axis Shift” that worked very well for the surface geometry and folding process, some vertices had to be cut out in order to not interfere with the folding.

c) Faces behaviour: Evaluation – 5

The faces maintained their planarity and stiffness throughout the complete folding process.

d) Hinges behaviour: Evaluation – 5

The hinges maintained their straightness and allowed the attached faces to rotate according to their Mountain or Valley identity.

Mechanisms and Control:**a) Mechanism Behaviour: Evaluation – 3**

The mechanism behaviour was the criterion with the lowest grade for this experiment because, although the objective was to reach a flat-folded state, the mechanism was unable to do so. Nevertheless, it was able to make the surface move for almost the whole intended course.

b) Control of Folding Angles: Evaluation – 4

Since the surface CP was so simple, with only six faces per module, it was relatively easy to have the mechanical system attached to two points of each module and thus, control the angles between faces on the entire module.

c) Stability of the Structure: Evaluation – 5

The structure remained stable throughout the folding process and when static.

d) Computational Control: Evaluation – 5

The computational control was revealed to be very accurate in the reading of the proximity of users and in the subsequent ordering of the step motors.

In **Figure 3.92** is the global evaluation of the structure on the spider scheme. The configuration of the polygon, with generous area, almost regular and with no significant peaks allows to demonstrate that this experiment, performed very well, globally.

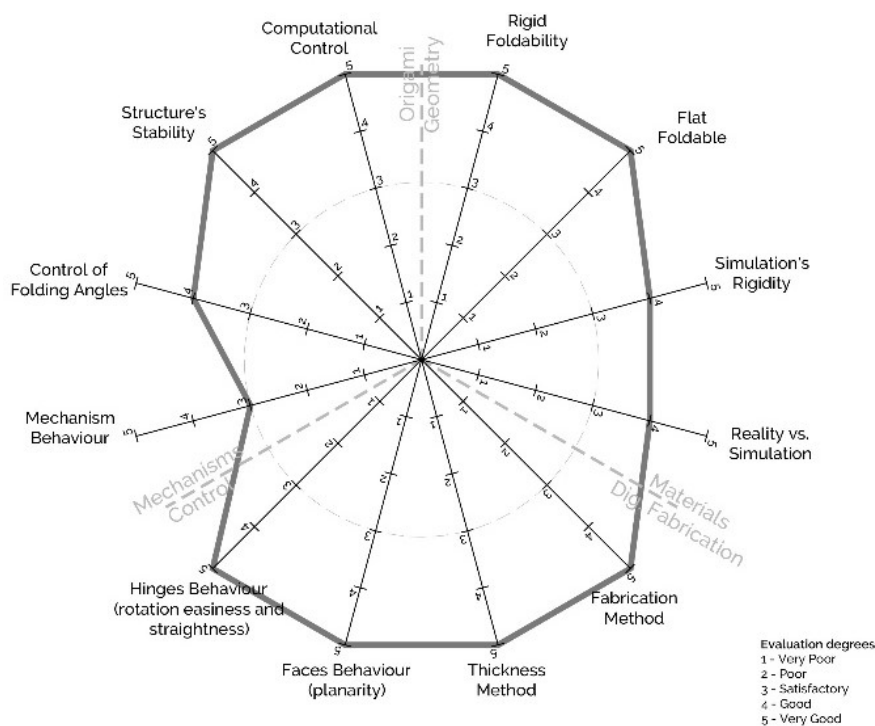


Figure 3. 92. Summary of grades for the evaluation of Experiment 02 - A

Experiment 02 – Group B

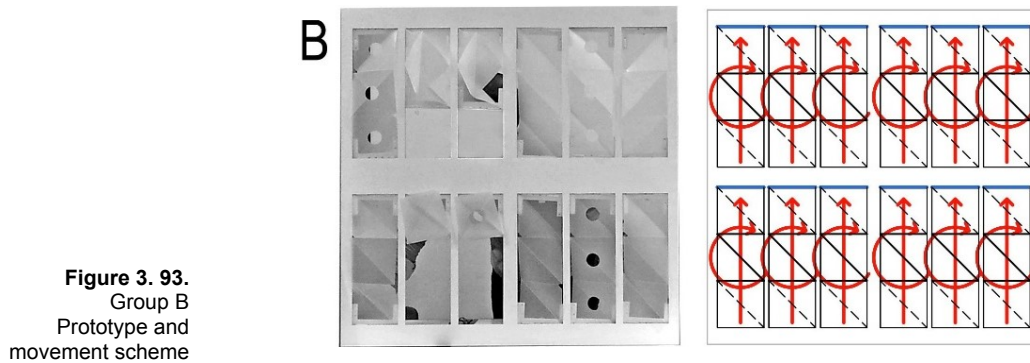


Figure 3.93.
Group B
Prototype and
movement scheme

Origami Geometry:

a) Rigid Foldability: Evaluation – 1

The designed pattern was not possible to rigidly fold with the intended path. The only way to replicate the intended folding process was by bending specific faces.

b) Flat-Foldable: Evaluation – 5

The designed pattern could be perfectly flat folded.

c) Simulation Rigidity: Evaluation – 2

The simulation was not based on rigid kinematics and the CP was impossible to rigidly fold, thus it was necessary to increase greatly the elasticity of the springs which made the simulation not rigid at all.

d) Reality vs. Simulation: Evaluation – 1

The prototype did not function as in the created simulation, it did not work at all.

Materials and Digital Fabrication:

a) Fabrication Method: Evaluation – 2

The chosen fabrication method was the engraving of the PP (0,5mm thick) on both sides. It did not work very well, just as in Experiment 01 there were too much stresses around the hinges, which made the faces bend.

b) Thickness Method: Evaluation – 2

No thickness method was used and the material was not able to work as expected for an origami surface.

c) Faces behaviour: Evaluation – 1

The faces bent completely and were never planar, not even in the unfolded state.

d) Hinges behaviour: Evaluation – 1

The hinges did not remain straight during folding and could not work properly due to the chosen fabrication method and inefficient mechanism.

Mechanisms and Control:

a) Mechanism Behaviour: Evaluation – 1

The mechanism behaved very poorly and could not make the surface move as was the initial objective.

b) Control of Folding Angles: Evaluation – 1

There was no control of the folding angles.

c) Stability of the Structure: Evaluation – 1

The structure was completely unstable and unable to reproduce the intended folding.

d) Computational Control: Evaluation – 1

The computational control could not function with a deficient mechanism.

In **Figure 3.94** is the global evaluation of the structure on the spider scheme. The configuration of the polygon, with a very small area, irregular and with a peak allows to demonstrate that this experiment overall, performed very poorly having had only one positive grade, for flat-foldability.

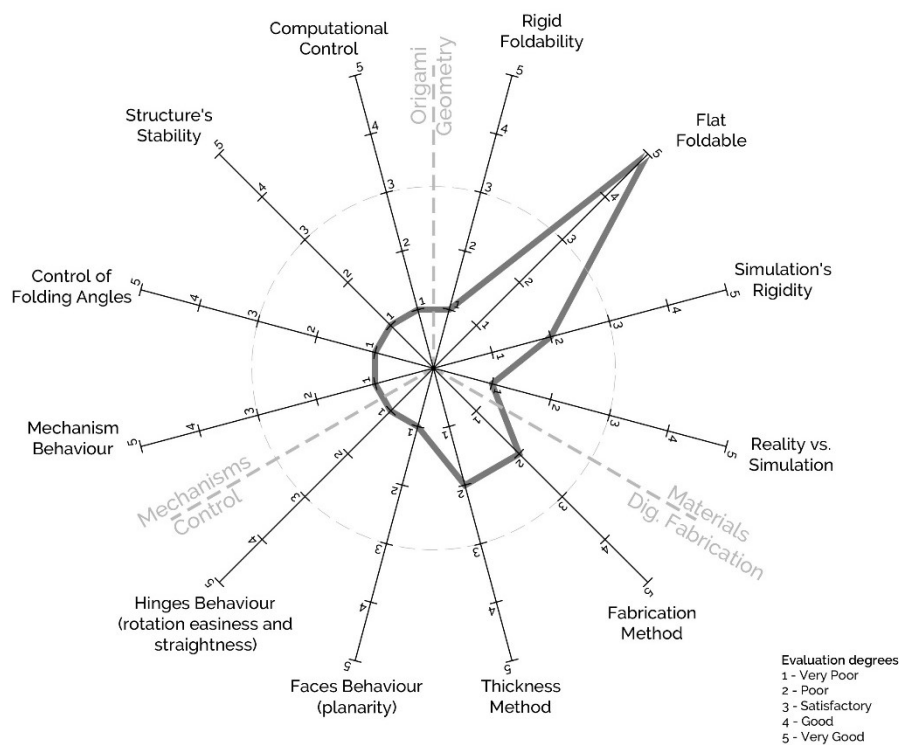


Figure 3. 94.
Summary of grades for
the evaluation of
Experiment 02 - B

Experiment 02 – Group C

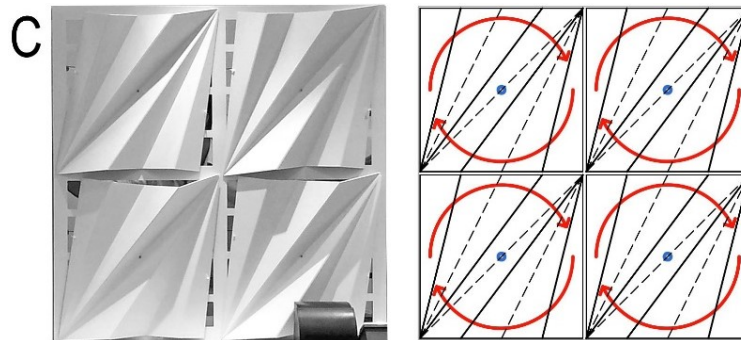


Figure 3.95.
Group C
Prototype and
movement scheme

Origami Geometry:

a) Rigid Foldability: Evaluation – 5

The designed CP was able to rigidly fold from the unfolded to the completely folded position, without collisions or self-intersections.

b) Flat-Foldable: Evaluation – 5

The CP only had degree-2 vertices that respected all theorems for flat foldability, and it was able to reach a perfectly flat folded state.

c) Simulation Rigidity: Evaluation – 4

The simulation was not based on rigid kinematics. The springs had a very low elasticity, but still had it.

d) Reality vs. Simulation: Evaluation – 4

The simulated behaviour for the surfaces and their performance in reality were very close, but the constructed prototype was not able to reach a completely flat folded state and did not depart from an unfolded configuration, it departed from a semi-folded state.

Materials and Digital Fabrication:

a) Fabrication Method: Evaluation – 5

The fabrication method used was a simple straight cut to generate the individual faces, which worked perfectly for the intentions of the prototype.

b) Thickness Method: Evaluation – 5

The thickness method used was the “Axis Shift” that worked very well for the surface geometry and folding process.

c) Faces behaviour: Evaluation – 5

The faces maintained their planarity and stiffness throughout the complete folding process.

d) Hinges behaviour: Evaluation – 5

The hinges maintained their straightness and allowed the attached faces to rotate according to their identity.

Mechanisms and Control:

a) Mechanism Behaviour: Evaluation – 4

The mechanism worked well in this experiment, it was able to make the surface move as intended. It was not graded 5 just because there were occasional collisions between faces from different modules.

b) Control of Folding Angles: Evaluation – 3

The folding angles were not controlled individually, the faces adjusted their folding angles according to the movement of the guiding faces. Nevertheless, it worked satisfactorily.

c) Structure's Stability: Evaluation – 4

The structure remained stable throughout the folding process and when static, with occasional trembling when there were collisions between modules.

d) Computational Control: Evaluation – 4

The computational control was revealed to be accurate in the reading of the proximity of users and in the subsequent ordering of the step motors, nevertheless the mechanism was not perfectly designed, hence the collisions between modules.

In Figure 3.96 is the global evaluation of the structure on the spider scheme. The configuration of the polygon, with generous area, almost regular and with no significant peaks allows to understand that this experiment, performed very well, globally.

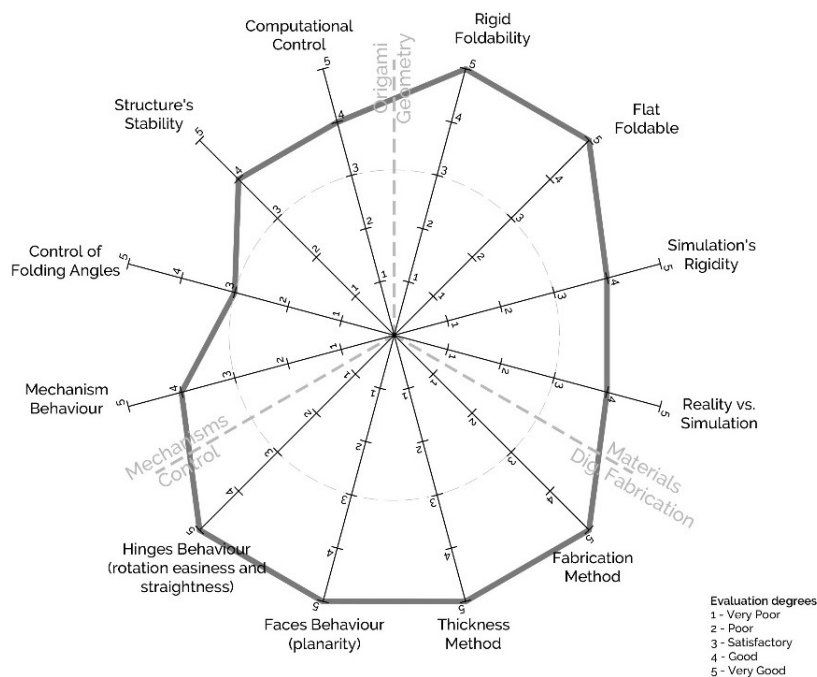


Figure 3.96. Summary of grades for the evaluation of Experiment 02 - C

Experiment 02 – Group D

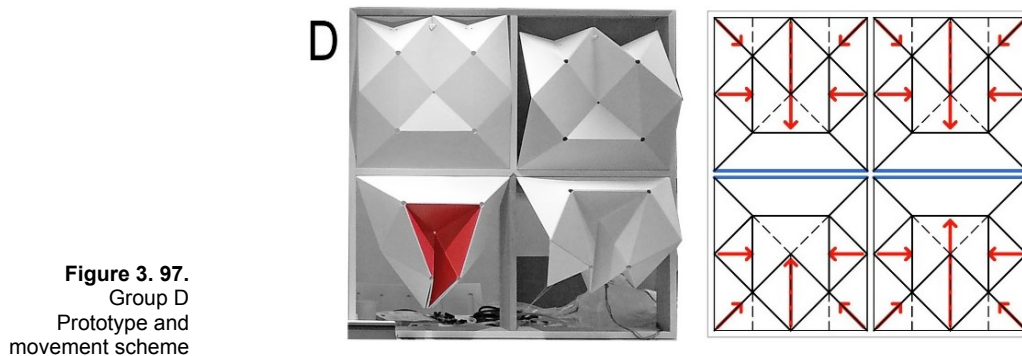


Figure 3. 97.
Group D
Prototype and
movement scheme

Origami Geometry:

a) Rigid Foldability: Evaluation – 5

The designed CP was able to rigidly fold without bending of faces or hinges.

b) Flat-Foldable: Evaluation – 1

The CP had degree-5 and degree-6 vertices, hence could never flat fold.

c) Rigidity of the Simulation: Evaluation – 4

The simulation was not based on rigid kinematics. The springs had a very low elasticity, but still had it.

d) Reality vs. Simulation: Evaluation – 4

The built prototype could reproduce very closely the simulated folding but was not able to fold as much as in the simulation.

Materials and Digital Fabrication:

a) Fabrication Method: Evaluation – 5

The used fabrication method was a simple straight cut to generate the individual faces, which worked perfectly for the intention of the prototype

b) Thickness Method: Evaluation – 5

The used thickness method was the “Axis Shift” that worked very well for the surface geometry and folding process, some vertices had to be cut out in order not to interfere with the folding.

c) Faces behaviour: Evaluation – 5

The faces maintained their planarity and stiffness through the complete folding process.

d) Hinges behaviour: Evaluation – 4

The hinges maintained their straightness and allowed the attached faces to rotate according to their identity (Mountain or valley), however slightly constrained their movement as the folding process developed.

Mechanisms and Control:**a) Mechanism Behaviour: Evaluation – 4**

The mechanism worked well but was not strong enough to make the modules fold until the maximum position simulated.

b) Control of Folding Angles: Evaluation – 4

The folding angles were not controlled individually, the faces adjusted their folding angles according to the movement of the guiding faces. Nevertheless, it worked very well.

c) Stability of the Structure: Evaluation – 4

The structure remained stable throughout the folding process and when static but had strong internal forces that opposed the mechanical system.

d) Computational Control: Evaluation – 4

The computational control revealed to be accurate in the reading of the proximity of users and in the subsequent ordering to the step motors, nevertheless the mechanism was not strong enough to make the surface respond quickly and completely.

In **Figure 3.98** is the global evaluation of the structure on the spider scheme. The configuration of the polygon, generally with vertices on grades 4 and 5, allows to understand that it performed generally well except for the inward peak for flat foldability.

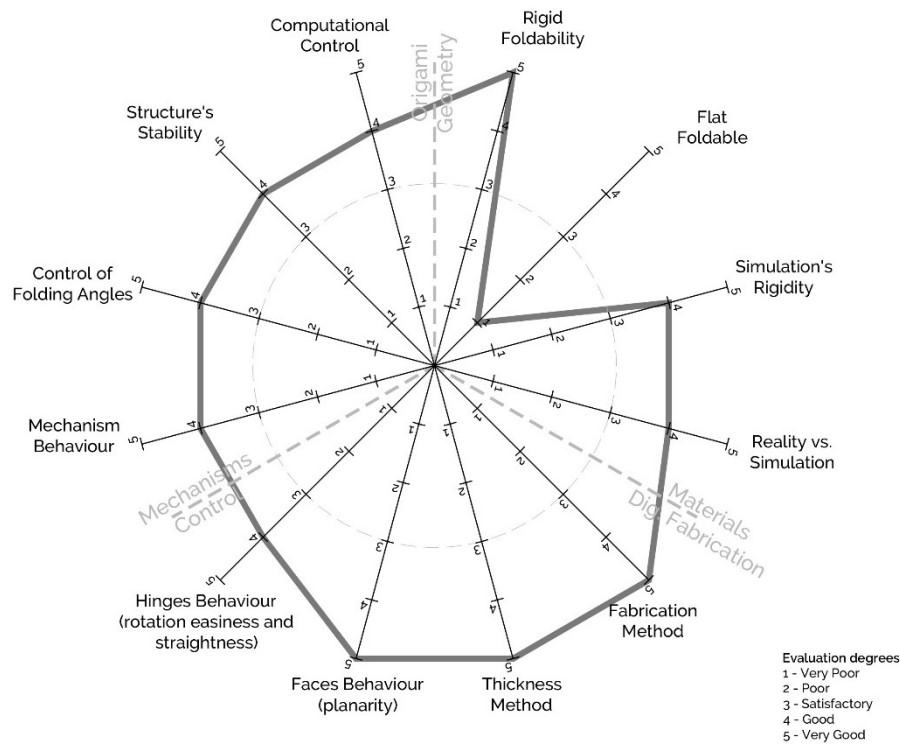


Figure 3.98. Summary of grades for the evaluation of Experiment 02 - D

3.5.3 | Experiment 03

In 2016 another Summer School, **Surfaces INPLAY**, was organized by ISCTE-IUL in a partnership with La Sapienza.

The Summer School was part of a broader event that had a Call for Papers, peer reviewed, and two days of lectures with keynote speakers on the subjects of kinetic and interactive architecture (Michael Fox and Ruairi Glynn), origami (Paul Jackson) and parametric design (Arturo Tedeschi) (Guimarães *et al.*, 2016).

The Summer School followed the conference days and had masterclasses for mechanics, electricity, arduino programming, origami and parametric design (Grasshopper, Weaverbird and Kangaroo).

This way was intended to give some basic knowledge to the students of the several areas involved so they could follow the workflow (**Figure 3.99**) more or less independently.

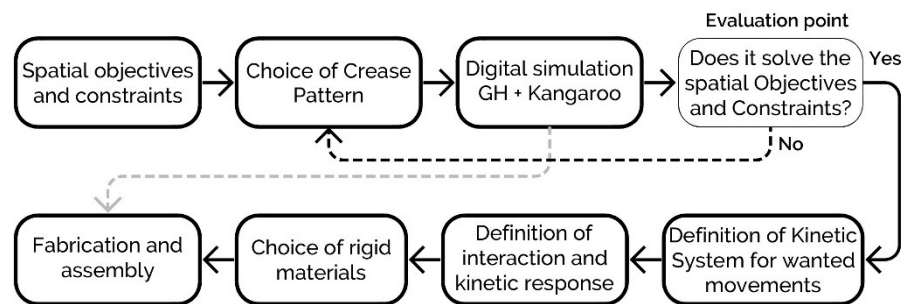


Figure 3. 99.
Workflow for
Experiment 03

The practical objective of the Summer School was the development of prototypes that would use only Rigid and Flat-foldable patterns that could be materialized in PP, paper or plywood. These materials should replicate the rules of rigid origami, guaranteeing that all faces were planar at all times in order to maintain the integrity of the simulation and the surface behaviour in a real context.

Just as in the preceding Summer School, the prototypes had a limited dimension of 1x1m, but this time a squared plywood board with 1x1 meter was used as a base for suspended origami surfaces and also to hold and hide the actuator and all of the mechanical system.

The only mandatory constraints were the limits of the board and the four points that would be used to attach the prototypes to the ceiling. The remaining configuration of the boards could be freely decided for each prototype, so it was possible to make the rails, holes and attachment points needed for each specific movement directly on the base.

After the masterclass on origami geometry the students started conducting their first geometric experiments with paper, paperboard and cardboard. When a CP was achieved its folding was simulated as in the Rome Summer School, with Rhinoceros, Grasshopper and Kangaroo, from which the necessary adjustments were made to the geometry of the pattern in order to achieve the intended effect.

Prototype A constituted four symmetrical modules that were intended to be four birds that opened and closed their wings in a diagonal movement set with vertical and horizontal moving points of the surfaces.

Prototype B used a parallel pattern with an inflexion in order to create four surfaces that were like a hybrid between a hand fan and a shell. These four surfaces open and close in a radial movement.

The geometry defined for prototype C had some similarities with the previous one, it was also a shell-like surface, but instead of having parallel creases the creases were radial and the faces used to achieve the inflexion on the surface were fewer.

Prototype D used the Yoshimura Pattern in sixteen helicoidal cylinders. This was the only prototype that used the movement in a vertical direction while all the other structures moved on the horizontal plane.

Prototype E used the Ron Resch pattern to create a surface that would act as a fluid when subjected to forces at different points. This was the only Non-Flat Foldable surface since the Ron Resch pattern does not verify Maekawa's theorem, but it was the students' group choice to use it anyway. The objective of this prototype was to make one unique surface that would have different things happening at the same time, pulling and pushing at different points, which did not really happen.

The simulation images of the developed prototypes and movement schemes are shown in **Figures 3.100** and **3.101**.

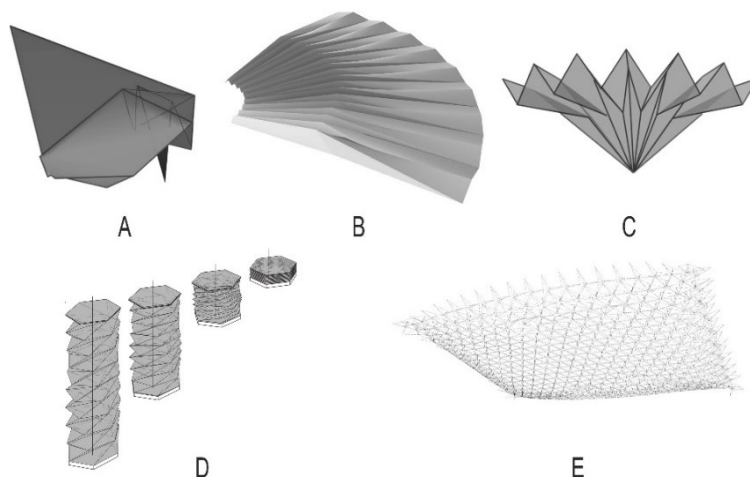


Figure 3. 100.
INPLAY's Digital
Simulations

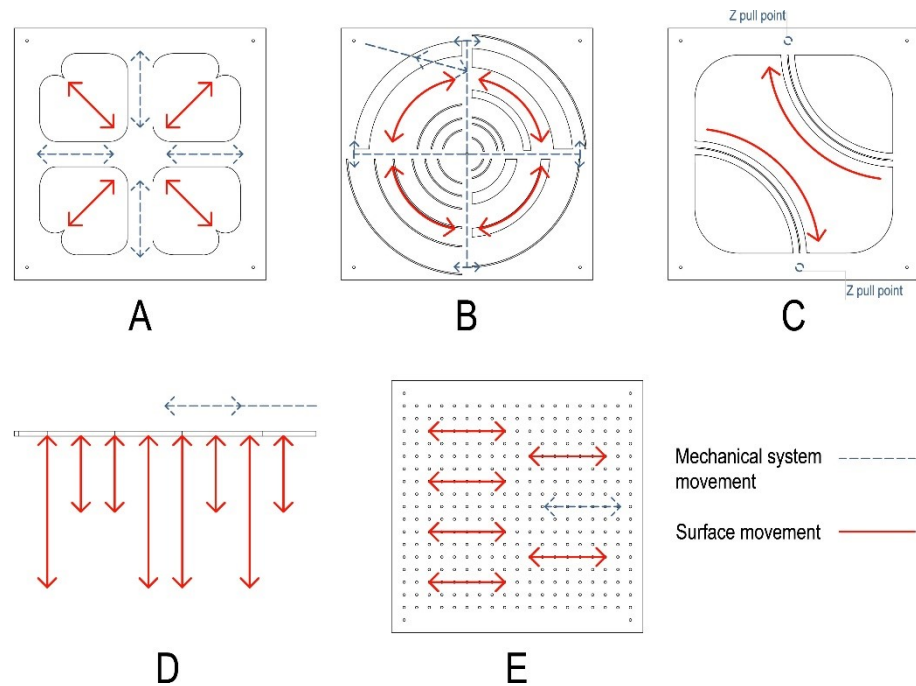


Figure 3. 101.
 Movement schemes

Next the students had to determine the mechanism that would make the surface move and the type of interaction it would be subjected to.

For the kinetic system all groups, except C, used one motor actuator SuperJack of 12" (around 30,5cm), since one of the objectives was to use only linear movement with only one actuator, that would work the whole system.

Prototype A used rails on the plywood base for the moving pieces, like a cross, and had four voids behind the birds where the beak of each bird would always be in touch with the base. For this prototype a mechanism was used with pulleys and cables that, with the force of the linear motor, made all the lines of movement work in a perfectly synchronised way, with this system all the birds moved at the same time in symmetric ways. This prototype did not have fixed points in the geometry, only moving points.

Prototype B was divided into four spaces with circular rails cut into the plywood. Each origami surface was attached to the plywood base at one extreme as the other one was attached to the rotating cross, put into motion by the linear actuator. The movement was rotational and worked like four curtains that open or close at the same time when the motor made a rigid wood cross rotate 90 degrees.

Group C did not use the motor, the movement was achieved when a user pulled cords to open or close the two-module surface. This prototype used the

upper and lower parts of the plywood base to place the surfaces, i. e. one was suspended while the other was supported by the base.

Prototype D had the plywood base completely redrawn, the limit shape was completely changed, although respecting the attaching points, in order to place and create an attaching base for each cylinder. To make the cylinders compress and expand, the linear motor was used in an horizontal position that would rotate 8 horizontal wheels with different diameters. These wheels made the cylinders move in a vertical direction at different speeds.

Prototype E had a grid of holes on the plywood base so that it would be possible to choose freely where to attach the cables to the structure's moving points. The linear actuator, placed on the XY plan, made the points of the surface move in Z creating an effect of compression of the surface at some points while at others the effect was of decompression.

For the interaction system the available sensors were light and distance sensors, but it was also possible to use potentiometers to mimic other kinds of interactions. Prototypes A, B, D and E used the distance sensors, so their structures moved every time a person, or an object, got in the range of the sensor. The values of the sensors would be read by the arduino that would then make the motor work inside a pre-programed range that fitted the purpose of the surface.

Group C explored more the interaction between the object and the user and worked the arduino possibilities the most. Every time a user opened the C prototype surfaces there was a little "being" inside that would react badly to the intrusion making an awful sound and flashing a light so that the user would feel obliged to close it again so the "creature" could be comfortable in its cocoon, and silent.

Regarding the choice of material and type of fabrication, the students that used polypropylene made the creases directly on the material with the laser cutter either with dashed lines where the dashes were cut all the way through (A and E) or by engraving the creases on both sides of the polypropylene (B). All these three prototypes had to have the vertices cut away where there would be more forces in action so that they would not inhibit the structure's movement.

Prototype C used the 3mm plywood and encountered a problem that did not exist with the other prototypes since it was the only one that used a material with considerable thickness. This group used the Axis Shift Method by laser cutting each face individually and then stitching them in a way that would only allow the faces to fold in one way, defining like this the mountain and valley folds (**Figure 3.102**).



Figure 3. 102.
Experiment 03
Group C - Plywood
Stitching

For prototype D it was initially tried to perforate the paper at the laser cutter to make a sort of pre-crease, but it did not work, the paper would tear apart after having only been used a few times. As a result, the pattern was simply printed on paper and the folds were made by hand.

The finished prototypes are shown in **Figure 3.103.**

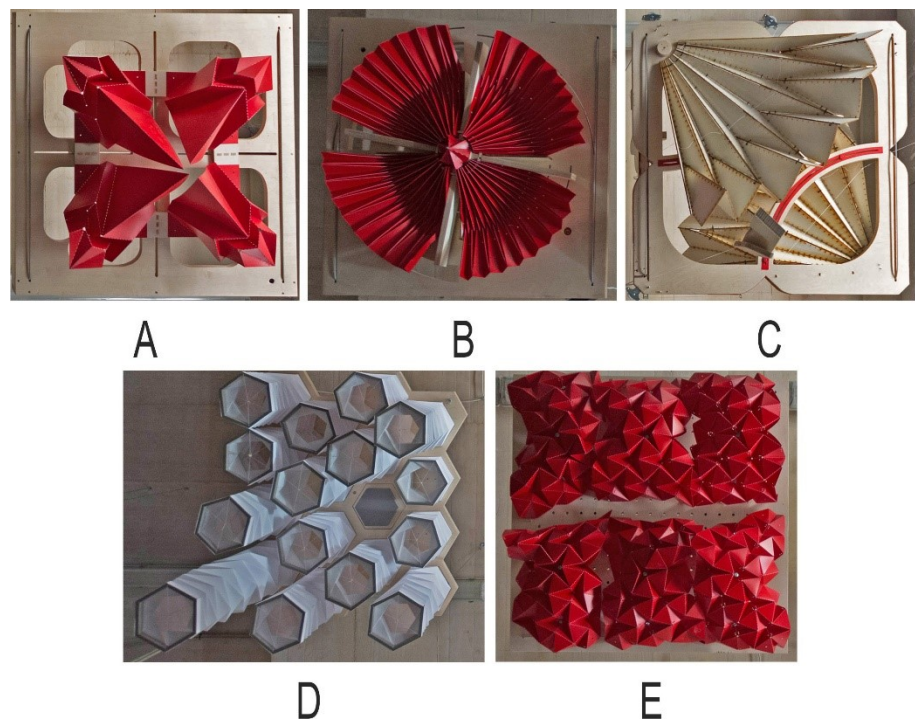


Figure 3. 103.
Final Prototypes

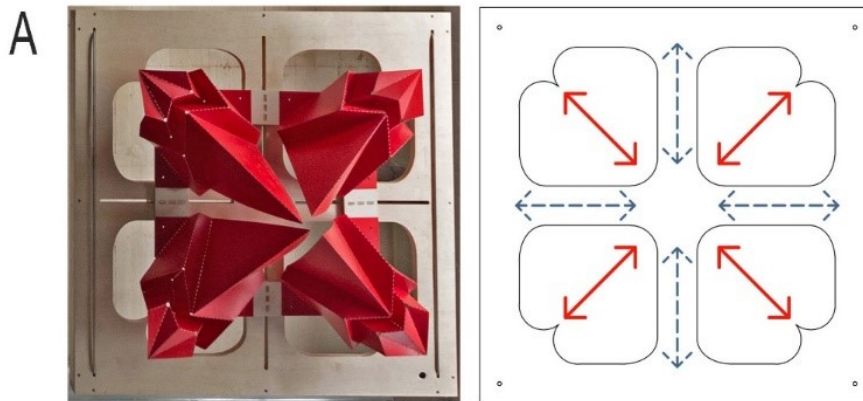
Experiment 03 – Group A

Figure 3. 104.
Group A
Prototype and
movement scheme

Origami Geometry:**a) Rigid Foldability: Evaluation – 5**

The achieved CP was able to rigidly fold from the unfolded to the completely folded positions.

b) Flat-Foldable: Evaluation – 5

The CP has degree4 and degree6 vertices that obeyed the flat foldability rules and the pattern was able to fold flat without intersections.

c) Rigidity of the Simulation: Evaluation – 4

The simulation was not based on rigid kinematics. The springs had very low elasticity, but still had it.

d) Reality vs. Simulation: Evaluation – 4

The constructed prototype behaved similarly to the simulation, however, in the simulation, the course of the pulling points was not considered, which made the surface achieve an almost flat state that was not possible in reality.

Materials and Digital Fabrication:**a) Fabrication Method: Evaluation – 4**

The chosen fabrication method was laser dashing the crease lines, cutting off the vertices, and then folding the PP as paper, several times in both directions in order to break the stresses around the crease lines, it did not work perfectly but worked well for the specific CP and material, that is for the relation between the size of the faces and the thickness of the material.

b) Thickness Method: Evaluation – 4

There was no choice for a specific thickness method, regular folding was used as if it was paper, it worked well but not as well as if it was a no-thickness material.

c) Faces behaviour: Evaluation – 4

The faces behaved well and were very close to plan through the folding. The fact that the faces had relatively big dimensions helped to soften the tendency to bend.

d) Hinges behaviour: Evaluation – 5

The hinges behaved very well and the successive folding to break the stresses around them worked well on 0,5mm thick PP.

Mechanisms and Control:

a) Mechanism Behaviour: Evaluation – 5

The mechanism was very well designed and materialized, the four modules folded in a perfectly synchronised way and the behaviour was as intended.

b) Control of Folding Angles: Evaluation – 5

Due to the symmetry of the CP, non-existence of fixed points, strength of the motor and attuned mechanism the folding angles between faces were very well controlled, even if there was no control for the individual angles.

c) Stability of the Structure: Evaluation – 5

The surfaces presented very good stability during the folding and unfolding motions.

d) Computational Control: Evaluation – 5

The computational control consisted in the use of distance sensors to detect proximity of objects and to make the actuator move accordingly, it worked very well.

In **Figure 3.105** is the global evaluation of the structure on the spider scheme. The configuration of the polygon, with generous area, almost regular and with no significant peaks allows to demonstrate that this experiment, performed very well, globally, with seven criteria graded as 5 and five criteria graded as 4.

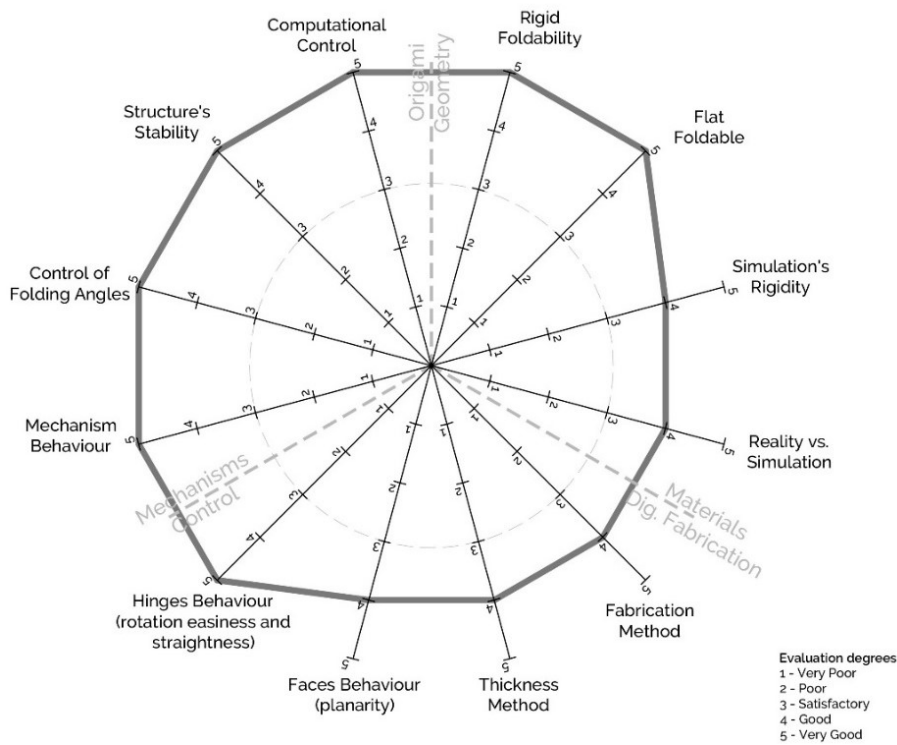


Figure 3. 105.
Summary of grades for the evaluation of Experiment 03 - A

Experiment 03 – Group B

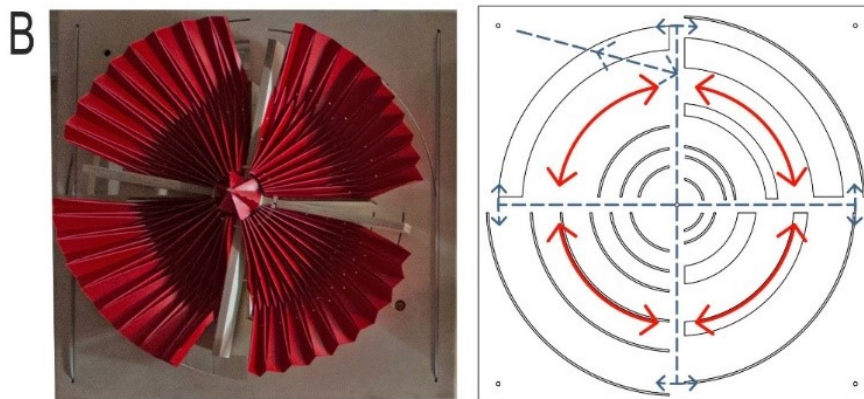


Figure 3. 106.
Group B
Prototype and movement scheme

Origami Geometry:

a) Rigid Foldability: Evaluation – 5

The designed pattern was able to rigidly fold from the unfolded to the folded position.

b) Flat-Foldable: Evaluation – 5

The CP has only degree4 vertices that obeyed the flat foldability rules and the pattern was able to fold flat without intersections.

c) Rigidity of the Simulation: Evaluation – 4

The simulation was not based on rigid kinematics. The springs had very low elasticity, but still had it.

d) Reality vs. Simulation: Evaluation – 4

The constructed prototype behaved similarly to the simulation, however, in the simulation, the surface folded with even angles and in reality, due to the Curtain type of movement, the angles between faces were not constant.

Materials and Digital Fabrication:

a) Fabrication Method: Evaluation – 4

The chosen fabrication method was laser engraving the valley crease lines on both sides of the PP sheet and cutting off the vertices. Then the PP was folded as if it was paper, several times in both directions, it did not work perfectly but worked well for the specific CP and material.

b) Thickness Method: Evaluation – 4

There was no choice for a specific thickness method, regular folding was used as if it was paper, it worked well but not as well as if it were a no-thickness material.

c) Faces behaviour: Evaluation – 3

The faces behaved reasonably, due to their reduced dimension in one of the directions, the tendency to bend was clear.

d) Hinges behaviour: Evaluation – 4

The hinges behaved well but the bending tendency of the faces affected their efficiency.

Mechanisms and Control:

a) Mechanism Behaviour: Evaluation – 5

The mechanism was very well designed, and well materialized on passing from linear to rotational motion. It had enough strength to push and pull the four modules at the same time.

b) Control of Folding Angles: Evaluation – 3

Since the folding method was by having a fixed face and dragging the others as a Curtain, there was no real control of the folding angles.

c) Stability of the Structure: Evaluation – 5

The surfaces presented very good stability during the folding and unfolding motions.

d) Computational Control: Evaluation – 5

The computational control consisted of the use of distance sensors to detect proximity of objects and to make the actuator move accordingly, it worked very well.

In **Figure 3.107** is the global evaluation of the structure on the spider scheme. The configuration of the polygon, with substantial area, almost regular and with not very significant peaks allows to demonstrate that this experiment, performed well, globally, and there were no great discrepancies between the grades for the criteria.

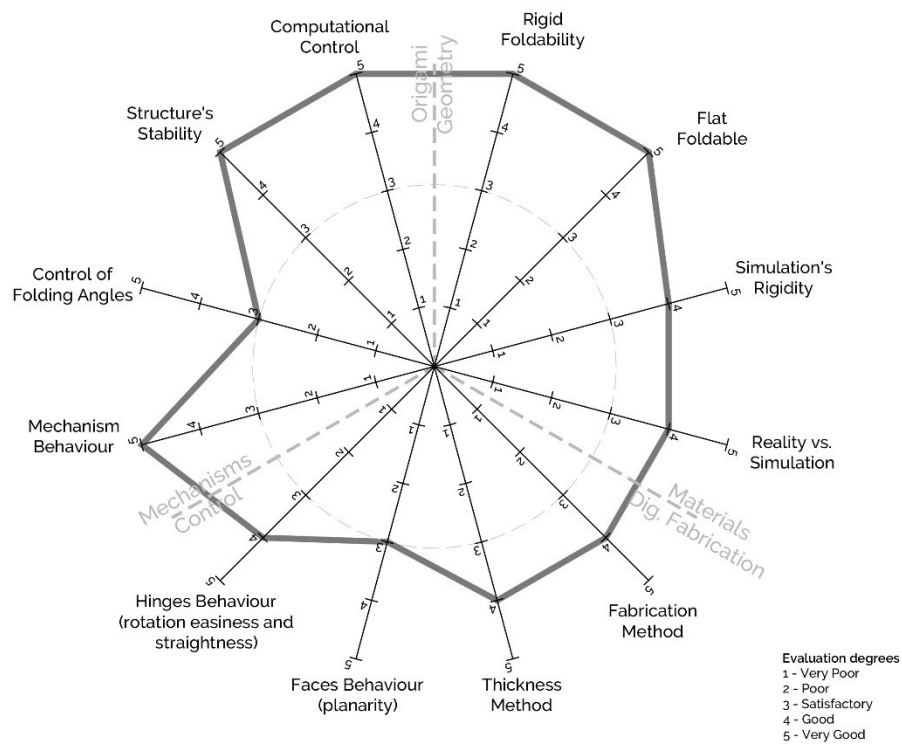


Figure 3. 107.
Summary of grades for
the evaluation of
Experiment 03 - B

Experiment 03 – Group C

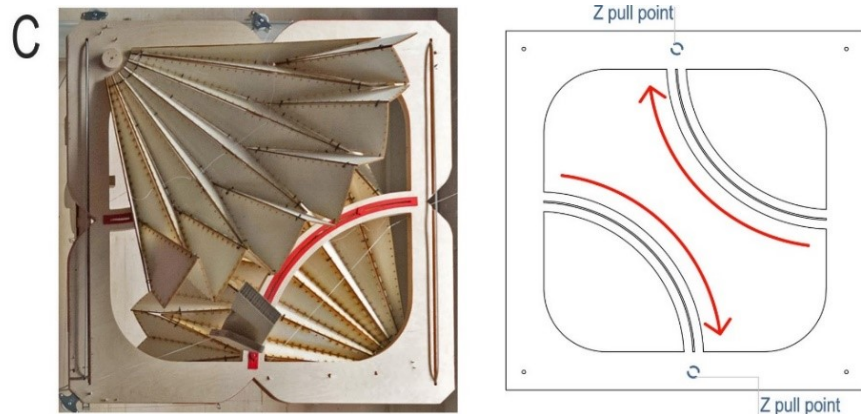


Figure 3. 108.
Group C
Prototype and
movement scheme

Origami Geometry:

a) Rigid Foldability: Evaluation – 5

The designed pattern was able to rigidly fold from the unfolded to the folded position.

b) Flat-Foldable: Evaluation – 5

The CP only has degree4 vertices that obeyed the flat foldability rules and the pattern was able to fold flat without intersections.

c) Rigidity of the Simulation: Evaluation – 4

The simulation was not based on rigid kinematics. The springs had very low elasticity, but still had it.

d) Reality vs. Simulation: Evaluation – 4

The constructed prototype behaved similarly to the simulation, however, in the simulation, the surface folded with even angles and in reality, due to the Curtain type of movement, the angles between faces were not equal and constant throughout the folding process.

Materials and Digital Fabrication:

a) Fabrication Method: Evaluation – 5

The fabrication method was laser cutting the faces individually and also cutting holes for the stitching, which allowed for great accuracy in the assembling of the different faces.

b) Thickness Method: Evaluation – 5

The thickness method used was the axis shift method that worked perfectly for the particular surface geometry.

c) Faces behaviour: Evaluation – 5

The material for the faces was 3mm plywood, which allowed them to be perfectly stiff and planar at all times.

d) Hinges behaviour: Evaluation – 5

The hinges created through the stitching with nylon thread allowed for perfect free motion of the faces according to their identity of mountain or valley.

Mechanisms and Control:**a) Mechanism Behaviour: Evaluation – 3**

The mechanism behaved reasonably. The pulling method was by hand but the surfaces were too heavy for the strength of the rope, which made it stretch. Even with the adding of several PP elements to reduce friction it was difficult to make the surfaces move.

b) Control of Folding Angles: Evaluation – 4

Since the folding method was by having a fixed face and dragging the others as a curtain, there was no real control of the folding angles. The needed effort to pull increased the difficulty to control the folding.

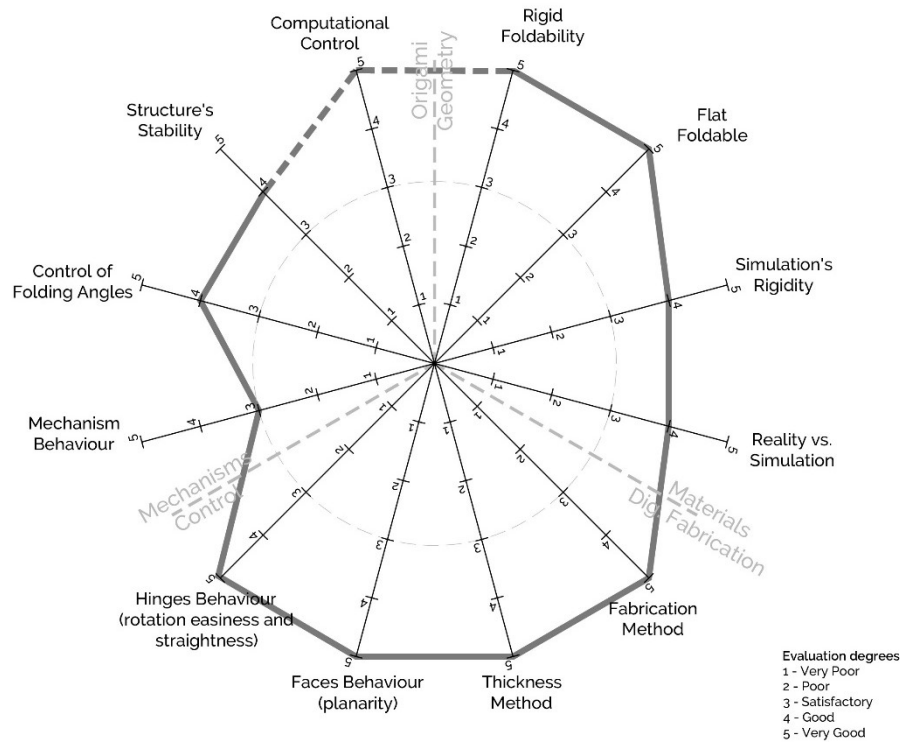
c) Stability of the Structure: Evaluation – 4

The surfaces presented good stability during the folding and unfolding motions but showed some tendency to collapse due to gravity.

d) Computational Control: Evaluation – 5

The computational control was not related to the motion of the surfaces (hence the dashed line on the spider diagram), since the motor was not used on this experiment. The intention was to have a “being” inside the surfaces that would react to their opening, in this way it worked perfectly.

In **Figure 3.109** is the global evaluation of the structure on the spider scheme. The configuration of the polygon shows a majority of criteria graded with 4 or 5, only the criterion for mechanism behaviour was graded 3. This experiment performed generally very well.



Experiment 03 – Group D

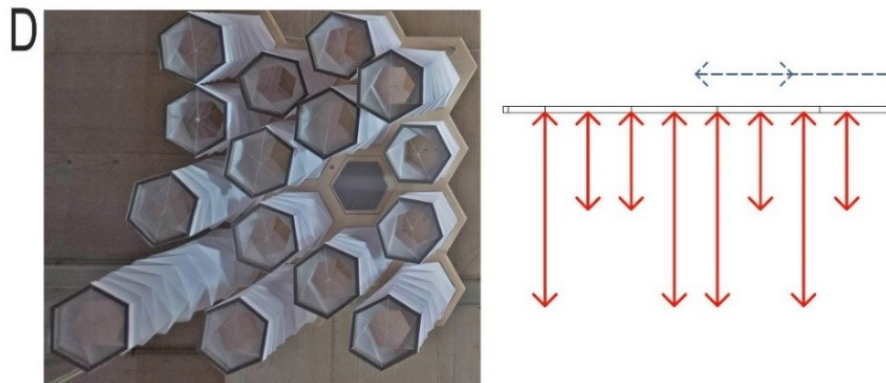


Figure 3.110.
 Group D
 Prototype and
 movement scheme

Origami Geometry:

a) Rigid Foldability: Evaluation – 5

The designed pattern was able to rigidly fold from the unfolded to the folded position.

b) Flat-Foldable: Evaluation – 5

The used CP was the Yoshimura Pattern, which only has degree 6 vertices that obey to the flat foldability rules and the pattern was able to fold flat without intersections

c) Rigidity of the Simulation: Evaluation – 4

The simulation was not based on rigid kinematics. The springs had very low elasticity, but still had it.

d) Reality vs. Simulation: Evaluation – 5

The real prototypes behaved in a similar way to the simulation, aided by the fact that the chosen material was paper, thus has almost no thickness.

Materials and Digital Fabrication:**a) Fabrication Method: Evaluation – 5**

The fabrication method of printing the CP on paper of 160g/m² worked perfectly.

b) Thickness Method: Evaluation – 5

There was no thickness method needed since the material used had almost no thickness.

c) Faces behaviour: Evaluation – 4

The faces behaved well and were planar but had no stiffness.

d) Hinges behaviour: Evaluation – 4

After the pre-creasing the hinges behaved well but had no way of restricting the movement for mountain or valley, it was the intrinsic geometry of the pattern that did this work.

Mechanisms and Control:**a) Mechanism Behaviour: Evaluation – 5**

The mechanism behaved very well. The different diameter wheels pushed and pulled the cylinders at different speeds and the passage from linear to rotational movement was very well achieved. Additionally, the use of the force of gravity through weights at the bottom part of the cylinders helped greatly with the unfolding of the surfaces.

b) Control of Folding Angles: Evaluation – 4

The folding angles were not individually controlled but the use of fixed bases at both extremes of the cylinders and the behaviour of paper showed a uniform distribution of the surface faces.

c) Stability of the Structure: Evaluation – 5

The surfaces presented very good stability during the folding and unfolding motions.

d) Computational Control: Evaluation – 5

The computational control consisted of the use of distance sensors to detect the proximity of objects and to make the actuator move accordingly, it worked very well.

In **Figure 3.111** it is possible to understand the global evaluation of the structure prototype. The configuration of the polygon shows that all criteria were graded with 4 or 5, it is the best graded experiment out of the ten presented in this section.

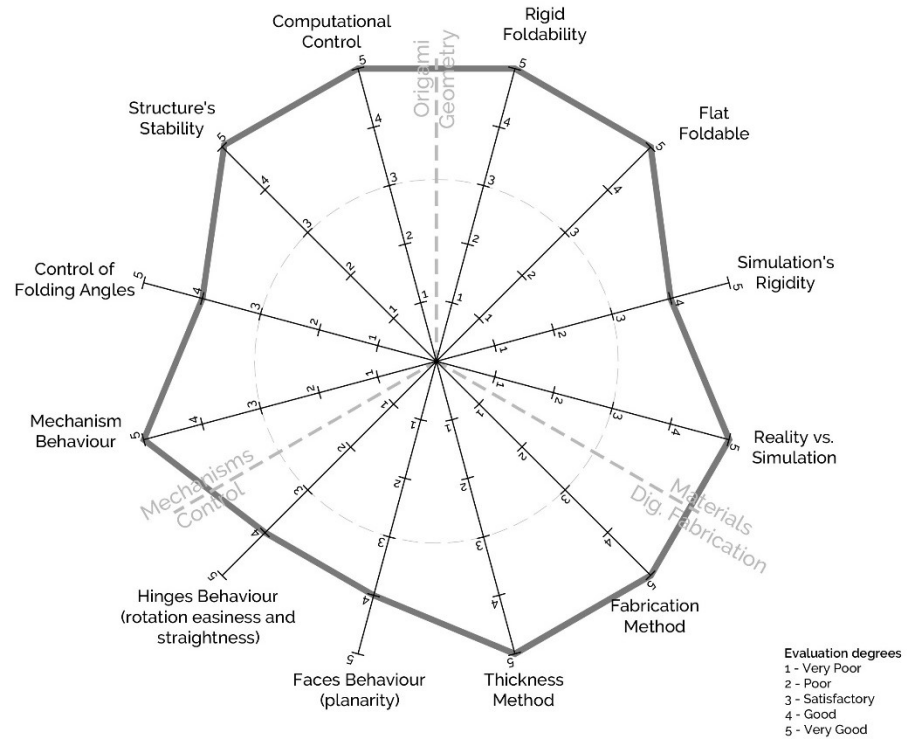


Figure 3.111.
 Summary of grades
 for the evaluation of
 Experiment 03 - D

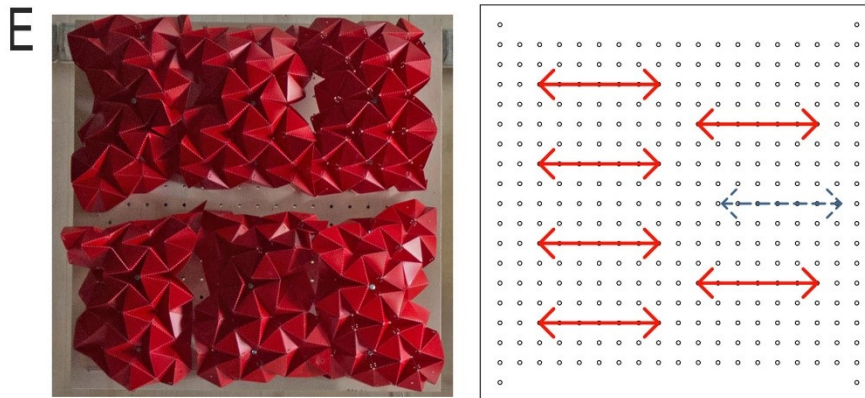
Experiment 03 – Group E

Figure 3.112.
Group E
Prototype and
movement scheme

Origami Geometry:**a) Rigid Foldability: Evaluation – 5**

The designed pattern is the Ron Resch pattern and is able to rigidly fold from the unfolded to the folded position.

b) Flat-Foldable: Evaluation – 1

The pattern is not flat foldable at all and has a compression capacity of only 66.66 %, as shown in **Section 3.3.1**.

c) Rigidity of the Simulation: Evaluation – 2

The simulation was not based on rigid kinematics, and since the simulated pattern had big dimensions with many faces the springs had to have high elasticity to allow the entire pattern to fold.

d) Reality vs. Simulation: Evaluation – 3

The constructed surface was much smaller than the one used for simulation, approximately 5 times smaller. Central pulling points were chosen to make it move in a similar way to the simulation.

Materials and Digital Fabrication:**a) Fabrication Method: Evaluation – 4**

The chosen fabrication method was laser dashing the crease lines on PP and cutting off the vertices. Then the PP was folded as paper, several times in both directions, it did not work perfectly but worked well for the specific CP and material.

b) Thickness Method: Evaluation – 4

There was no choice for a specific thickness method, regular folding was used as if it was paper, it worked well but not as well as if it was a non-thick material.

c) Faces behaviour: Evaluation – 3

The faces behaved reasonably, but due to their reduced dimension and pattern geometry this caused contradictory forces to the folding, the tendency to bend and to prevent movement was clear.

d) Hinges behaviour: Evaluation – 4

The hinges behaved well but the bending tendency of the faces affected their work negatively.

Mechanisms and Control:

a) Mechanism Behaviour: Evaluation – 3

The mechanism was roughly designed and was not able to accurately produce the desired effect of different actions by different pulling points. All points were pushed and pulled in the same manner.

b) Control of Folding Angles: Evaluation – 3

There was no individual control of the folding angles, the surface adjusted itself naturally to the pulling strength, but the inner forces caused by the specific geometry of the pattern and the material properties worked contrarily to the mechanism and intended movement.

c) Stability of the Structure: Evaluation – 3

The structure behaved reasonably in respects to its stability. The inner forces of the surface occasionally caused faces to leave their expected position, introducing some instability and unexpected behaviour.

d) Computational Control: Evaluation – 3

The computational control consisted of the use of distance sensors to detect proximity of objects and to make the actuator move accordingly, this part worked well but the impact on the surface movement was poor.

In **Figure 3.113** is the global evaluation of the structure on the spider scheme. The configuration of the polygon shows a low area with peaks. This experiment had six criteria (half of the 12) rated as 3. It behaved satisfactorily overall.

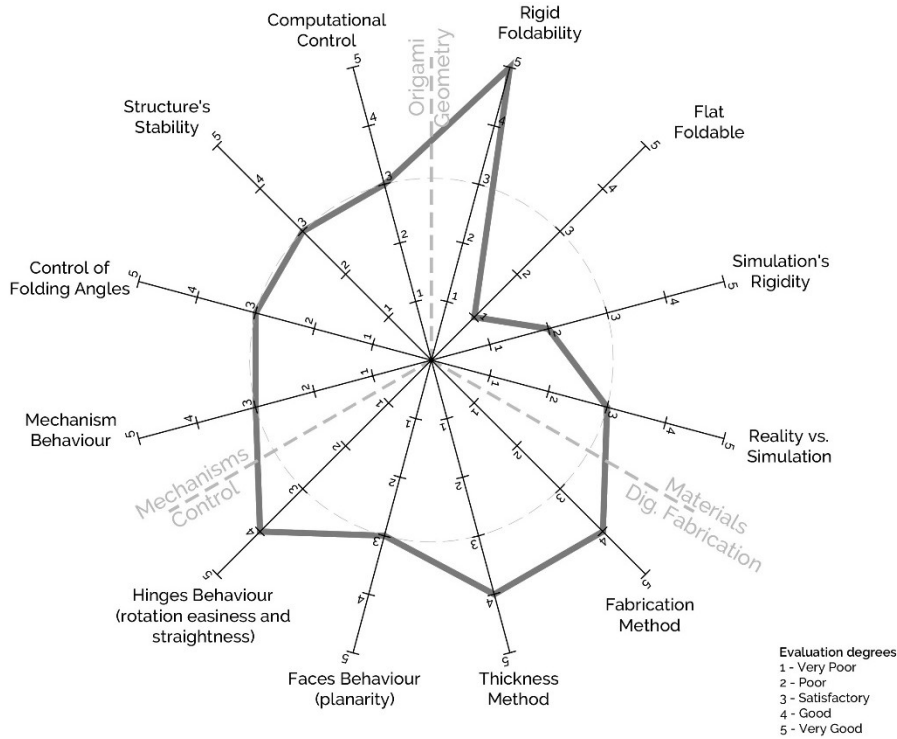


Figure 3. 113. Summary of grades for the evaluation of Experiment 03 - E

3.5.4 | Conclusions of the Experiments

From the analysed prototypes in the previous sections several conclusions were drawn, in regard to origami geometry, fabrication, materials, mechanisms and control and also the specific workflow used to develop these experiments.

In Figure 3.114 is the summary of the evaluation for every experiment as well as their area as a percentage of the area of the “aimed” dodecagon with grade 5 for every criterion.

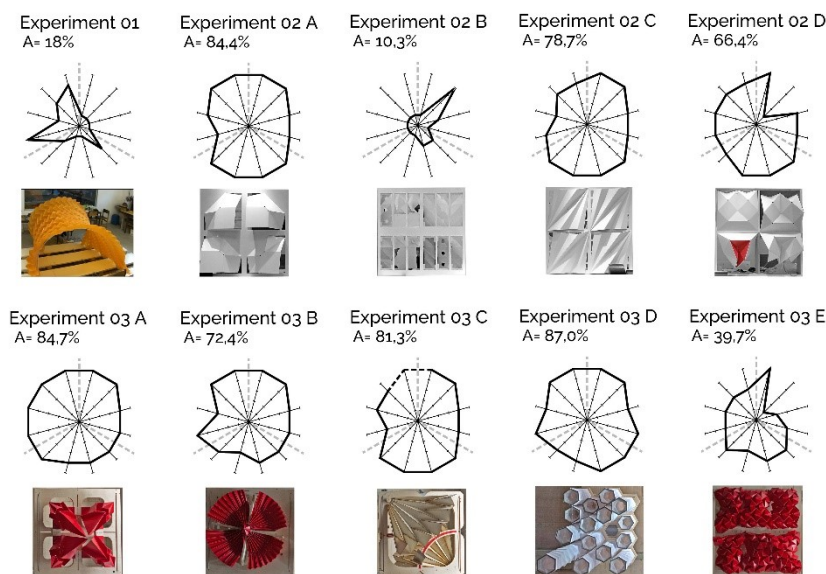


Figure 3. 114. Comparison between experiments' analysis

The best rated experiments were Experiment 03 D (87%), Experiment 03 A (84,7%) and Experiment 02 A (84,4%). There are three experiments with clear low evaluations (01, 02 B and 03 E). These experiments did not perform well in the overall experiment but were extremely important for the identification of errors and understanding of the consequences of determined choices.

Experiment 01 demonstrates that not knowing enough about CPs properties and not using reliable simulators may lead to unpredictable functioning of the constructed structure as well as contradictory inner forces and instability.

Experiment 02 B demonstrated that even if the folding simulation seems to work when the elasticity of the elements is increased, if the mechanism is not carefully designed and tested then it is probable that the final model will not work as intended, or not work at all.

Through Experiment 03 E it was possible to understand that the CPs drawing and dimensions should be equal, or at least very approximate, in both the simulation and in reality. This experiment simulated the folding with a CP five times the size, which misled its ability to behave fluidly with a smaller surface. Additionally, as well as experiment 03 E, the mechanism was not carefully designed and tested before construction.

Some more general considerations can be made in relation to the whole group of experiments. From the developed prototypes it was possible to verify that the fixed points on a kinetic structure can be very important for the behaviour of the surfaces and capacity of compression, but it is also possible to construct them without any fixed points. It can be important to control the individual folding angles, but if the surface has a small number of faces arranged with symmetry, this control gets easier. The geometry of the pattern, the material used and the force of the motors used are also key factors for the range of compression the surfaces can undertake, which becomes clear simply by comparing Experiment 02 and Experiment 03, since the first used small step motors, and the second used a linear actuator with great strength.

From the developed prototypes it was also possible to compare the patterns' ability to fold flat in the simulations and in reality. The real capability of compression differs from the folding simulations because these simulations were not kinematic and did not consider the internal forces created by the chosen material in the area of the creases or the real strength of the motors. With regard to materials it was observed that, when using PP, the patterns with bigger faces behaved better than the patterns with smaller faces, possibly because this material has the tendency to bend due to internal forces

generated in the areas near the creases and with bigger faces this effect gets softened.

Using the laser machine to engrave the creases directly on the PP proved to be a satisfactory way of making rigid origami foldable surfaces if the vertices are cut away. The elimination of a small area in turn of the vertices reduces the tension in that area and allows the faces and creases (hinges) to behave more similarly to the kinematic models.

With regard to the two ways of engraving the creases on PP with the laser cutting machine, the “engraving on both sides” method proved to be more efficient than the “dashed lines” method because the first one removes some material over the entire crease, while the dashed lines method leads to “crushing” on the non-dashed parts. The fact that the creases are engraved along their entire length and until half the thickness of the material, makes the folding more natural and creates less “crushing” of the material under the crease lines and so inhibits the folding less.

The method used in Experiment 03 C to put together the plywood faces by stitching them with nylon thread also proved to be an efficient way of making these surfaces fold, and their behaviour and strength as hinges worked very well for the dimensions and thickness of those surfaces.

The method that proved to work best in all experiments in relation to the similarity of kinematic behaviour, and in respect to the zero-thickness surface was undoubtedly the creation of faces with rigid and stiff materials, such as plywood or PVC, and making the hinges through another method. For the presented scales duct tape or nylon stitching were very good ways of creating hinges.

Concerning the Thickness Method, the most successful was the Axis Shift Method, not to mention the method used in Experiment 03 D, which was not a “method” at all since the used material was paper. Unfortunately, it would not be possible to use paper every time, it would depend on the scale of the intended structure.

In relation to the mechanism and surface movement the experiments behaved generally well. The importance of testing the mechanism on small scale models was very clear however, so that cases such as Experiments 02 B and 03 E could be prevented.

Another important issue was observed; every surface started its folding in a slightly folded state. It seems to be a question to be attentive to in future experiments since this can aid the movement of the surfaces, otherwise the motors would require tremendous strength in order to make the surfaces leave the completely unfolded state towards a folded one. The addition of friction-

reducing elements on rails and similar can be also an important aspect to be aware of. In the case of prototype C, the addition of PP on the rails was a clever way to diminish the friction and allow the surface to slide in a smoother way.

The computational control behaved very well in every experiment, maybe because a simple control was used with only one input element, except for Experiment 01 where three input elements were used. In fact, the input elements were the ones that worked in the worst way, none of the sensors resisted to this day, still they could be easily substituted, and the systems would continue to function acceptably.

From this information it is possible to infer that simple control may work well for complex structures if the input element, the programming and the mechanism are well adjusted to each other.

From the results of these experiments and workflows followed became clear that a workflow for the development of these type of structures should have more detailed steps for all of the intervening areas. It should be more demanding in respect to the rigid kinematics of the simulations, as well as to the experimentation on simplified versions of the mechanisms on smaller scales than the one intended for construction.

It should also have more evaluation steps in order to allow for early problem solving before reaching the construction of the final structure which becomes even more important when increasing the scale of the structures and if they are expected to shelter people.

In the next chapter such a workflow will be presented in a detailed manner and will be used for the construction of the final structure as the main objective of this thesis and a Proof-of-concept prototype. This will then be able to validate the Thesis methodology and to be an experimented contribution to the design of kinetic structures, based on rigidly and flat folding origami surfaces to be used in architecture.

**04 | WORKFLOW AND KOS
PROOF-OF-CONCEPT
PROTOTYPE**

04 | Workflow and KOS Proof-of-Concept Prototype

This chapter intends to present a detailed description of the main contribution of the research, namely the developed workflow to achieve Kinetic Origami Surfaces (KOS). The methodology is tested through the construction of the Proof-of-Concept prototype that uses pantographic systems as mechanisms. Chapter 04 intends to contain the knowledge constructed along the last years and to be a natural consequence of the last chapters. From the state-of-the-art, the analysis, conclusions and the experiments made, along with their methodology and results, a very specific workflow was generated to be of aid for other designers. The workflow aims to create a comprehensive methodology with individual steps for each matter involved in the design process and construction of a rigidly folding origami surface to be used as a computationally controlled kinetic element for architecture.

The next sections will describe the process for conceptualization, dimensioning, kinematic simulation, structural evaluation, construction and implementation of a structure through the described workflow. In reality, workflow and experiment, had a reciprocal relationship, where each one helped to frame and define the other.

After the justified description of the workflow in **Section 4.1**, a thorough explanation of the construction of the physical prototype will be made in **Section 4.2**.

4.1 | Proposed Workflow

The proposed workflow incorporates steps for every main theme under research, it was developed from the workflows presented for experiments 01, 02 and 03 but is much more detailed and has more evaluation points. From the previously described workflows it was realized that more detailed steps and more critique points could have helped to prevent problems and generate better functioning structures. Additionally, the workflow that will now be presented aims at being used for real scale structures, much heavier than the ones presented before and likely to be used with people inside or close to them, so there must be a bigger concern with safety issues and prediction of the structure's behaviour, hence the importance of more detailed steps and evaluation points.

The proposed workflow has 17 individual steps and four main evaluation points, these allow to go back to previous steps, correct the issues, and then continue the design of the kinetic structure.

The process could be graphically described as shown in **Figure 4.1**.

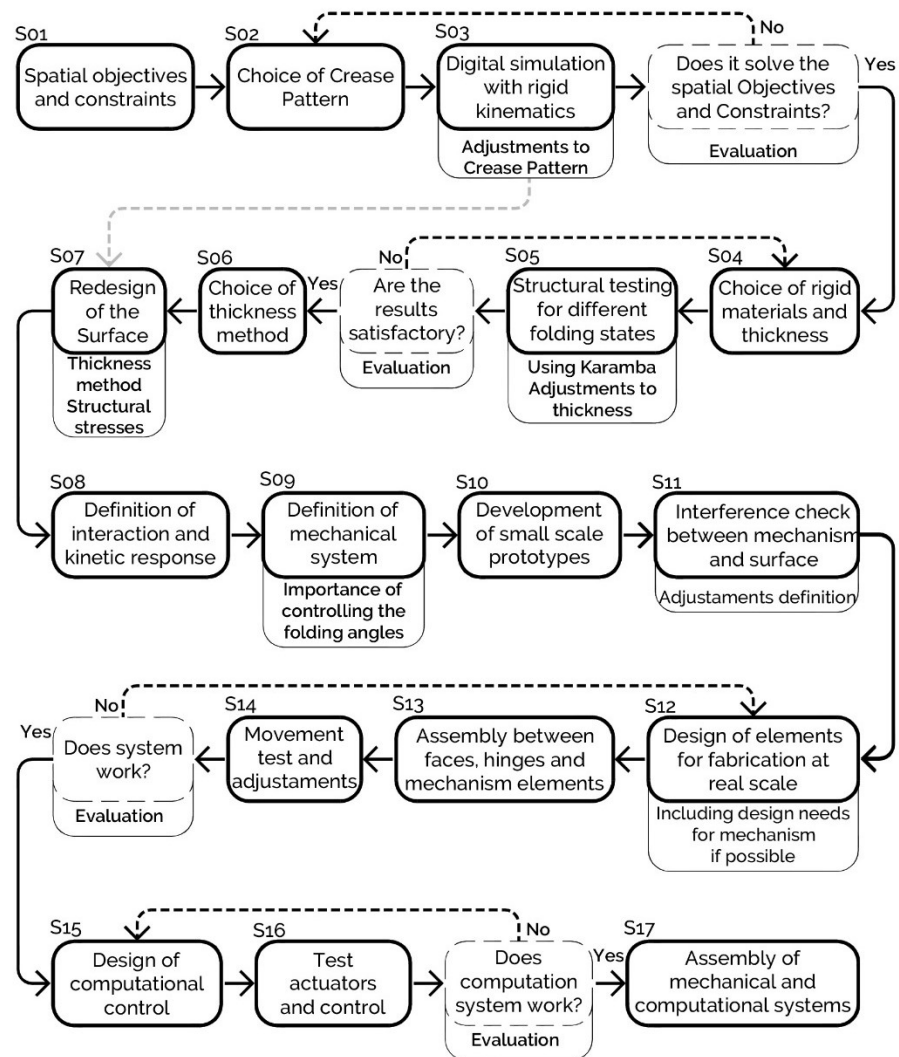


Figure 4.1.
Proposed Workflow

The proposed workflow starts with the assessment of the **Spatial Objectives and Constraints**, just as in the workflows described for experiments 01, 02 and 03. This step consists of two main parameters, the analysis of the physical space where the KOS is to be implemented and the function it will serve. The first parameter can be a very direct physical analysis of the space where the surface will be established, such as the unobstructed space where it will move, the configuration of that space, the possible locations for attachment and support points, for example. The second parameter consists of the function of the surface and its formal intentions. In order to design a rigidly folding kinetic surface there is the need to know the purpose of that surface, the formal, geometric, objectives that is, the concept behind the structure to design. For the definition of the formal objectives for the surface it is also important to understand if it will be exposed to the natural elements, like sun, rain, snow

and wind since the geometry of the surface can aid in solving such matters or otherwise work against them.

In the **second step** the crease pattern for the surface is chosen from tables presented in **Section 3.3.1**. The tables comprehend the tessellations defended as pertinent to be used in architectural elements subdivided into families along with their compliance with the rules for rigid and flat-foldability and the geometries into which they fold, so to choose the pattern that may better respond to the aims and restrictions determined in the first step.

From the choice of the pattern the folding simulators presented in **Section 3.3.2** can be used for degree-4 and degree-6 CPs, if the chosen pattern is included on the cluster foldable by the simulators.

These simulators are intended to aid the designer in the understanding of the kinematic behaviour of the structure, its maximum and minimum folding stages, as well as all of the in-between. Moreover, the simulation can be used to place the structure on a three-dimensional model of the actual place where it will be located and evaluate for collision issues. The placement of the simulation on a model can also help to determine the paths undertaken by specific vertices, creases or faces which can be of service for the mechanical system. Finally, the simulators are intended to allow for adjustments to the pattern, to optimize its geometry for the specific final purpose, and to establish if it would be desirable to use the full possible range of motion or if the use of a specific part of the full range would be more suitable.

The next step is an evaluation point, where the designer must evaluate if the generated surface corresponds to the initially defined objectives and existing constraints. If the answer is positive then it is possible to proceed to the next step, if it is negative then it would be necessary to retreat to the second step and choose a better fitting surface, or maintain it but redefine its crease pattern, by altering its dimensions, metrically or by number of faces, and/or by changing the geometric configuration of the faces, and then follow the subsequent steps again.

When a positive answer is reached on the first evaluation point, the user should decide on the material to be used for the construction of the faces of the rigidly folding structure. These materials, as explained in **Section 3.4**, would ideally be metal, wood, or wood-based materials that are the result of controlled production such as MDF or Plywood, since they have mechanic properties in accordance to the needs of rigidly folding surfaces, namely an high Young's Modulus and good resistance to bending, tension and compression. The decision on the type of material should also be influenced by the function of the surface, how it will be used and where, that is, indoors

or outdoors. From the decision on the type of material, the geometry of the surface generated in the folding simulator must be subjected to a structural evaluation.

Since, within Grasshopper plugins, a reliable structural evaluator that would allow for testing a moving structure was not found, the approach used by the research was to create at least three folding states of the surface, and test them individually on Karamba3D. Karamba3D is a structural simulator that uses finite element analysis (FEA) and allows to obtain the response of three-dimensional beams or shell structures under arbitrary loads (Preisinger, 2013). It is generally very well accepted for structural evaluation inside the Grasshopper community.

The rigidly folding origami structures would be tested as shell structures where the thickness of the shell can be altered directly on Karamba3D and the type of material can be chosen from the simulator library, which includes its mechanical properties, or can be manually set by the user.

The strategy of using static stages of the foldable surface may not be considered to be completely accurate, but if the mechanical system is able to control the generality of the folding angles and to lock the structure in specific stages of the folding, then the structure would actually behave as a shell structure (Lebée, 2015).

After the structural evaluation step (**Step 05**) there is the need to critically measure the results and decide if the material chosen and corresponding thickness are a good option for the structure in development. If not, the thickness of the material should be altered, or an alternative found.

When the obtained results are satisfactory it is possible to move to **Step 06** and choose the thickness method, which would be a choice between ASM or the TPM, since these two seem to be the most appropriate to use on large scale structures that act as surfaces with many faces, and for which is crucial the maintenance of the rigid kinematics present in the zero-thickness CP, as explained in **Section 3.3.3**.

In **Step 07** of the workflow, a first redesign of the surface is proposed. Primarily based on the geometry developed in the rigid kinematic simulation but altered with consideration for the thickness of the material and the structural evaluation, which may allow for the subtraction of parts of the faces in order to make it lighter.

Then comes the step where the type of interaction with the surface should be settled in order to determine the movements it will be able to make and use that information for the design of the mechanical system. When creating the mechanical system must be decided about the importance of controlling the

generality of the folding angles or if the intention would be to use a “Curtain” kind of movement.

At this point it is proposed to create small scale prototypes (**Step 10**) that reproduce the geometry of the surface as well as the mechanisms that are intended to be used. Here, for the second time, it is possible to redesign the surface and include the needs for the mechanism in the global design, if relevant.

Step 11 consists of the evaluation of the small-scale prototypes through critical observation for movement, mechanism appropriateness, the chosen thickness method, and the existence of physical interferences between surface and mechanism.

From the critical evaluation of Step 11 adjustments should be made for the design of the surface at the final scale. Issues such as the placing of actuators within the structure, if this is the case, dimension of mechanism elements and the time when they will be implemented in the structure, must be seriously considered in order to facilitate the construction and prevent the need to manually alter the structure after fabrication, that should happen in **Step 12**.

When all the elements are ready, **Step 13** is dedicated to the assembly of faces, hinges and mechanical elements, disregarding for now the actuators. In the case of origami folding surfaces, there must be extra care taken when assembling the individual faces together, since any misalignment can seriously alter the expected movement and even cause the rupture of faces and/or hinges.

This step must be carefully thought through. Before starting the assembling there should be an exercise of determining which piece goes where and when, because probably there will be pieces that will need to be located in places difficult to access, hence they should be assembled when it is easy to reach those locations, whenever possible.

In **Step 14** the whole constructed system should be tested for movement, without the actuators, if possible. At this step it is very important to open and close the structure at least a few times to check for movement fluidity, if the elements have good friction, if there are any elements that are not working well or if any are causing unexpected stresses. This leads to another evaluation point that validates if the system really works, if it needs small adjustments or if Step 12 should be reassessed and the structure redesigned and digitally fabricated again.

In **Step 15** the computational control can finally be prepared. That is the relation between the inputs received and the corresponding movement response. At this step the inputs can be virtually anything, as long as the

response is in accordance with the movements the structure can perform when actuated through specific motors and their particular behaviour and properties. When designing the control, it is important to understand the maximum and minimum positions the structure will undertake, the velocities allowed for the actuators and their strength along with the weight of the structure and internal forces. This understanding is particularly important when designing large scale structures.

In **Step 16** it is recommended to test the input source and the actuators separately from the structure. Only when the computational system is satisfactorily adjusted should it be implemented into the structure, this means testing the velocity of each actuator and response to the controlling program, comparing the actuators in relation to one another and to the particular performance storyboard. The reason for this particular care is that, on a large scale rigid origami folding structure, it is probable that several actuators will be needed to work together, and since the whole structure is continuous and has a rigid kinematic, if there is no synchronicity and/or continuity in their actions, the actuators can break the structure, or be broken by it, due to the structure's internal forces.

The last evaluation point regards the accuracy of the computational setup, only when it is well tuned should it be implemented into the structure. If any part of the system is not functioning correctly the workflow proposes returning to step 15 and redesigning the computational control.

When the last evaluation point reaches a positive answer, the final step (**Step 17**) is achieved, which allows for the final assembly between the computational control and the mechanism, pre-set on the structure.

In the step 17 the KOS is put in motion, it is the ultimate test.

4.2 | Prototype Development

The next sections describe the application of the proposed workflow with the exact step by step, on the construction of the KOS PoC prototype. This section includes the description of problems and corrections that were found during the construction process which, in turn, helped with the definition of the workflow.

Some steps are directly correlated, these will be described in the same section in order to better explain the implications one had on the other.

The following sections describe the KOS PoC development and also include critical analysis of each specific step and its implication on the structure in construction and on subsequent steps.

The section ends with the evaluation of the KOS PoC prototype through a spider scheme with the same criteria as those used for experiments 01, 02 and 03.

4.2.1 | Spatial Objectives and Constraints - Step 01

Step 01 is the first of the workflow (**Figure 4.2**) and consists of two parameters, the analysis of the physical space where the KOS is to be implemented and the function it will serve.

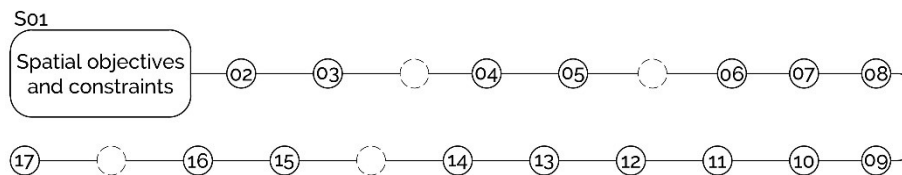


Figure 4. 2.
Overview of the workflow and location of step 01

For the KOS PoC there is no real space for implementation, so a generic planar space free of obstacles was supposed. It was considered however that, during construction, the surface would occupy an area at least equal to the area of the unfolded surface thus, it would be important to have a space for construction where the surface would have enough space to be unfolded as well as completely folded and to have enough free space around it for manipulation. Other than that, in this particular case, there are no other restraints relating to the first parameter, the analysis of the physical space.

With regard to the second parameter, the function of the kinetic surface, the formal objective is to use a vaulted structure, with single or double curvature. It is intended to create a surface that can be, at the same time, wall and roof, and that can be used while in movement and when static.

As a geometric concept, it was intended to try a symmetric pattern that is not completely regular, that is, the faces should not be all equal to one another in order to explore more complex geometries.

The aim of this project was also to create a structure that could support itself through the folding without additional structures and try to avoid the “curtain type” of movement, since it was so intensively tested in the first three experiments. This way is believed to add to the contribution for the study of crease patterns, mechanisms and movements investigated by this thesis.

4.2.2 | Crease Pattern and Digital Simulation – Steps 02 and 03

From the geometrical intentions designated by the first step, the workflow then has a step for the choice of the CP followed by a rigid kinematic simulation and an evaluation point, as **Figure 4.3** demonstrates.

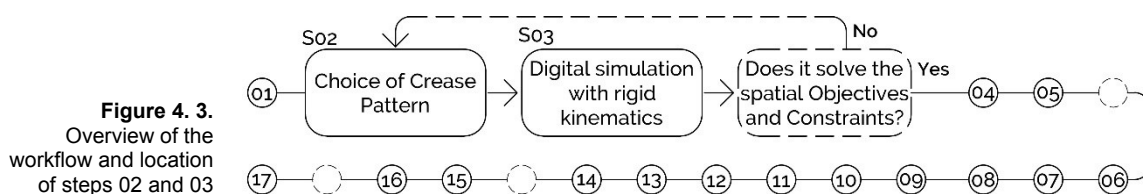


Figure 4.3.
 Overview of the workflow and location of steps 02 and 03

At the second step were reviewed the tables presented in **Section 3.3.1** for CPs with degree-4 and degree-6 vertices and chosen the Yoshimura pattern (**Figure 4.4**).

From the tables, all the tessellations that assume “folding on the plane” configurations are disregarded, since the determined functional objectives are to have a self-supporting vaulted structure.

The patterns with degree-4 vertices that fold into single curvature geometries but that have faces tucking inside other faces, such as the irregular Miura, the chicken wire or the quadrilateral meshed pattern, were also disregarded due to the probability of creating too much stresses around the vertices when subjected to a thickness method, as described in **Section 3.3.3**. The same reasoning was applied to the degree-6 table and so patterns such as the Kresling and the Fujimoto and Nishiwaki were also disregarded for the KOS PoC structure.

The degree-6 crease patterns that fold into single curvature geometries but that do not create a vaulted structure during all the folding motion, were also overlooked. These patterns may have some folding ranges that correspond to vaulted structures but the “vault” changes into other types of geometries during motion. Such patterns would be the double helicoidal, symmetric

helicoidals and whirlpool spiral, which get twisted during motion and consequently alter the supporting vertices or faces. These patterns change the vaulted-like configuration while folding, or twist around themselves, thus making them unsuitable to be used as a self-supporting vaulted structure.

Degree 4 Tessellations

Degree 6 Tessellations


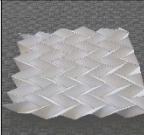



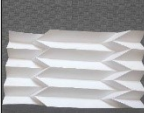
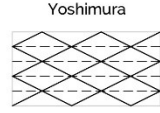


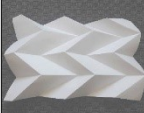
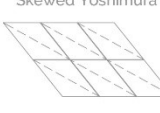



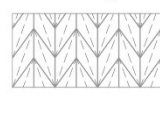

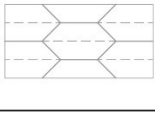

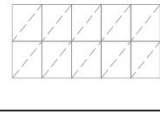
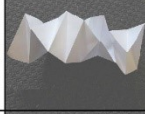


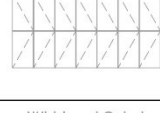
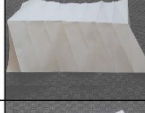



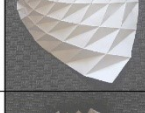


Crease Pattern	Folding State	Folds Along	Crease Pattern	Folding State	Folds Along
Miura 		Plane	Radial Fujimoto and Nishiwaki 		Plane
Stretched Miura 		Plane	Yoshimura 		Single Curvature
Irregular Miura 		Single Curvature	Skewed Yoshimura 		Single Curvature
MARS 		Plane	Kresling 		Single Curvature
Chicken Wire 		Single Curvature	Double Helicoidal 		Single Curvature
Huffman Grid 		Single Curvature	Symmetric Helicoidals 		Single Curvature
Quadrilateral Meshed Pattern 		Single Curvature	Whirlpool Spiral 		Single Curvature
			Fujimoto and Nishiwaki 		Double Curvature

Figure 4. 4.
Choice for CP - Step 02

At this point the remaining patterns would be the Yoshimura and the Skewed Yoshimura. The Skewed Yoshimura was not chosen due to the small number of supporting points and their asymmetry when touching the ground plane, which seemed to be a possible cause for instability in an heavy moving structure.

After the reasoning and dismissing criteria, only the Yoshimura Pattern was left as a possibility for the structure to be used for the KOS PoC.

The consequent step is the third one whereby the Yoshimura pattern was developed and tested by the degree-6 simulator.

First a regular CP was tested, composed of symmetric triangles with a 2.0m base and 0.5m height. In **Figure 4.5** the regular Yoshimura CP is depicted in 5 folding stages retrieved from the degree-6 simulator, at 0°, 15°, 30°, 46.3° and 56.95°. The faces that are represented in a vanished way are the ones that are generated by the simulator, due to the method of using sets of base faces, but that would not be considered if the pattern was to be used for construction so the attachment points to the ground plane could be aligned and consequently work better in regard to the stability of the structure.

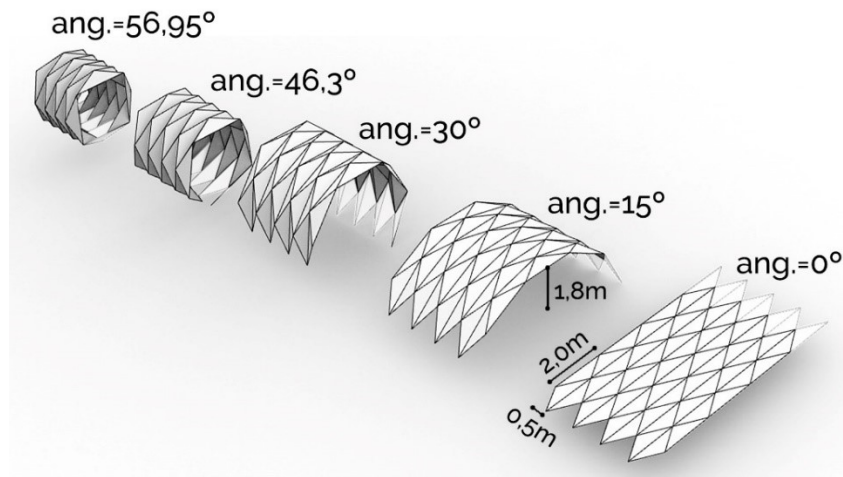


Figure 4. 5.
 First Crease Pattern
 experiment for KOS
 PoC using the
 degree-6 simulator –
 Step 03

At first this pattern seemed a good option since it allowed for a generous covered area and, from only 15° of folding it already had a 1,8m free height inside. This would mean that from this folding angle it could be used by people, but around folding angle 56,95° the structure started to intersect itself.

The early collision between faces generated a negative answer for the first evaluation step since this would make it always be very far from flat-foldability, and so the pattern was redesigned on the simulator. It was tested a pattern with slightly smaller faces and intentionally non-similar triangles (**Figure 4.6**).

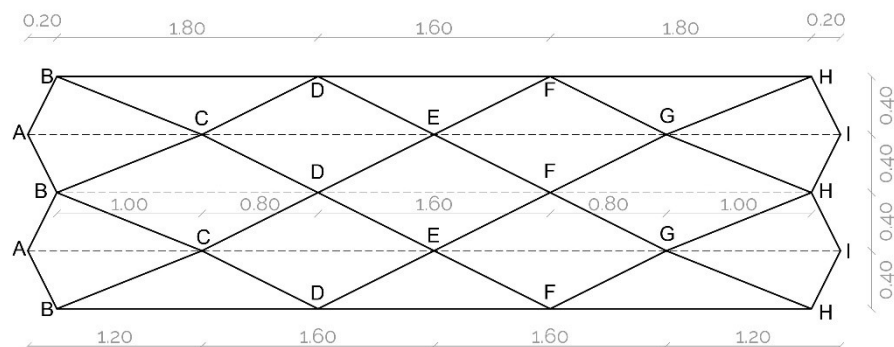


Figure 4. 6.
 Crease Pattern for
 KOS PoC

The non-similar triangles are expected to help the structure rise quicker above the 1,8m free height and to have less acute angles when touching the ground. The design of faces **ABC** and **GHI** are intended to aid with the self-support objective and, at the same time, provide a more irregular CP for testing. As a consequence, the new proposed pattern is irregular but intentionally symmetric in respect to the line defined by vertices **E**, to prevent stability issues.

This pattern reaches the internal free height of 1,8m when the folding angle is 35° and at folding angle 76° the vertices **A** and **I** get coincident, as shown in **Figure 4.7**. From the demonstrated folding states this pattern seems to be usable by people as a kinetic rigidly folding surface for the folding range between 35° and 76° of folding.

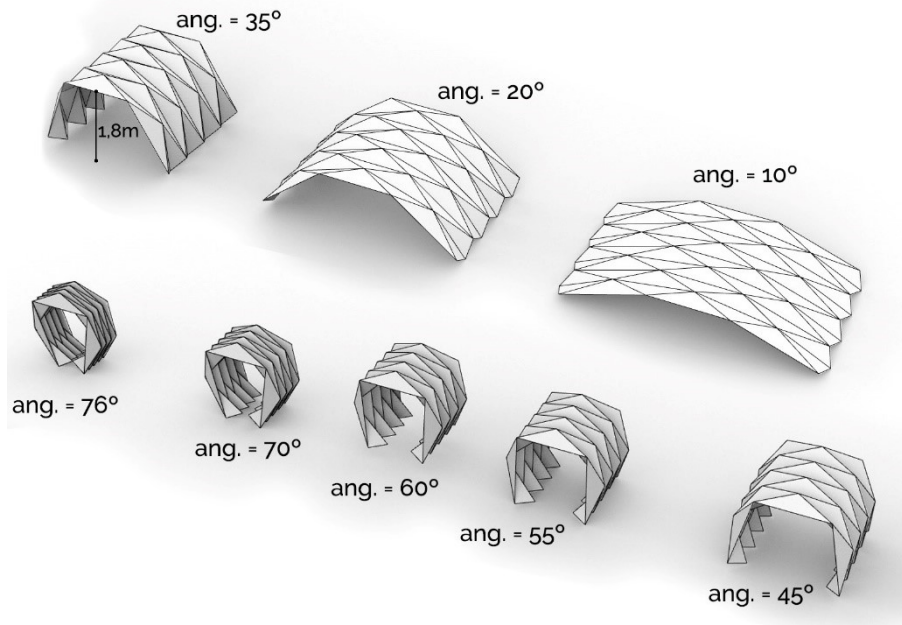


Figure 4.7. Rigidly folding states simulated for KOS PoC using the degree-6 simulator

The presented CP design for the KOS PoC surface and its rigidly folding kinematics reached a positive answer at the first evaluation point. The CP is capable of answering to the initial spatial objectives and constraints of being a vaulted structure, with single curvature to be used when static or while in motion for the folding range between 35° and 76° . The reached CP is symmetric in relation to the line defined by vertices **E**, but the faces are not similar to each other. The designed CP has four distinct faces to allow for the exploration of more complex geometries, as determined at step 01.

4.2.3 | Rigid Materials, Thickness and Structural Testing – Steps 04 and 05

Step 04 of the proposed workflow is related to the choice of materials to be used when developing a rigidly folding origami surface. Step 05 relates to the structural testing of a surface created with the CP determined by Step 03 and the materials chosen at Step 04 (**Figure 4.8**).

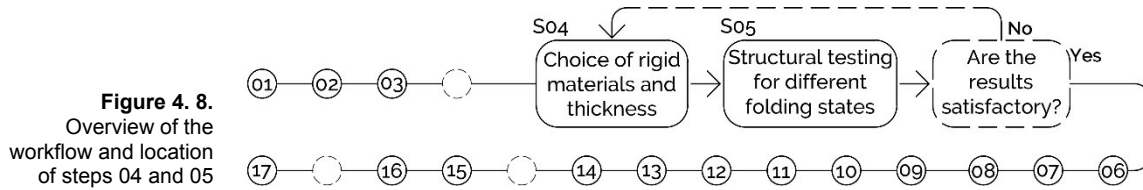


Figure 4.8.
 Overview of the workflow and location of steps 04 and 05

The key aspects that a designer should be attentive to at these particular steps are the mechanic properties of the materials chosen for the faces and hinges and the states of folding to use for structural testing.

As stated in **Section 3.4**, the material chosen for the faces must assure their rigidity by having a high Young’s Modulus and must also be resistant to bending, tension and compression. The hinges should be made of a material that guarantees their straightness throughout folding and the continuous connection between faces.

For the KOS PoC the use of an association of materials is attempted that can represent the intended behaviour for faces and hinges. MDF was chosen for the faces of the structure, due to their mechanic properties and workability on the available CNC milling machine. Metallic piano hinges were used, since they can be cut into particular measures and can continuously connect the two faces. By using piano hinges was intended to have a continuous axis between faces, to prevent problems that could be raised by the use of several individual revolute joints and the inherent possibility of misalignment between the various axis. This way was intended to enable the structure to behave closely to the kinematic simulation and prevent errors from discontinuity between the parts.

Since the range of motion determined at Step 03 is from 35° to 76° three folding states were set to be tested through Karamba3D at 35°, 55° and 76° fold angles.

The folding states were chosen for particular reasons, the beginning and end of the folding range, and an intermediary angle were creases **AB** and **HI** are almost at the horizontal plane. Around the 55° folding angle the support points of the structure change from vertices **A** and **I** to vertices **B** and **H**.

Each state was “baked” in Grasshopper and transformed into a mesh in Rhino which was then interpreted by Karamba3D as a shell. For the material of the shell a wood derivate was set with mechanic properties of MDF and thickness of 24mm. The model analysed on Karamba3D represents a static shell and not a kinetic one but allows to understand the kind and magnitude of stresses on the surface in each folding state. Depending on the chosen mechanism the model can be very close to reality, if the mechanism allows for the locking of the structure.

In the Karamba 3D simulation the only considered force was gravity, that is the structure’s own weight, since the KOS PoC prototype was constructed in a controlled environment, without the subjection to other forces when static. As initial support points were considered the vertices **A** and **I**, the final support points are vertices **B** and **H**. The support points can be seen in the following figures associated to a symbol of the XYZ axis with a circle around them, which means that Karamba3D considers them as support points fixed to the ground and unable to move or rotate.

Through Karamba3D three main parameters were accessed for stresses on structures, the Van Mises Stresses, the Utilization and the Displacement Parameters.

The **Van Mises Stresses** determine which areas are more likely to bend (until fracture) and how much, through coloured graphics that allow for magnitude visualization (Preisinger, 2018). **Figures 4.9, 4.10** and **4.11** demonstrate the analysis of the Van Mises Stresses on the surface on three folding states, at 35°, 55° and 76° folding angles.

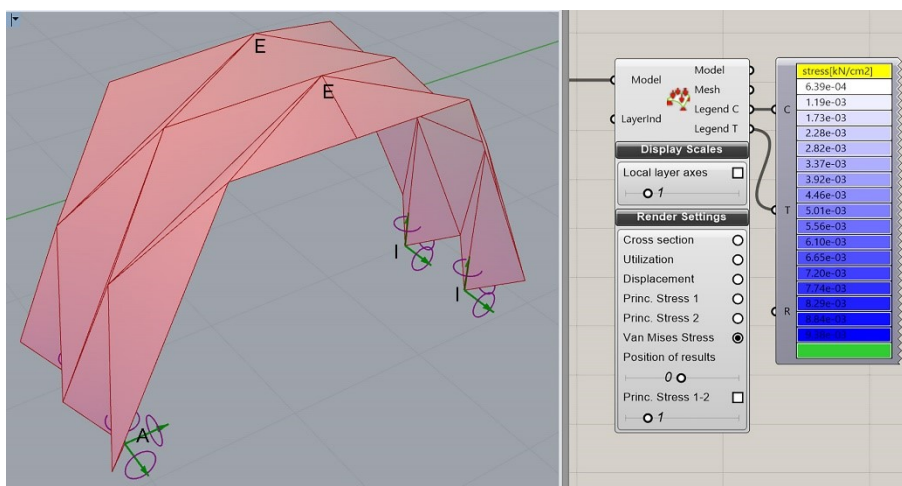


Figure 4. 9.
Van Mises Stresses
for KOS PoC 35°
folding angle

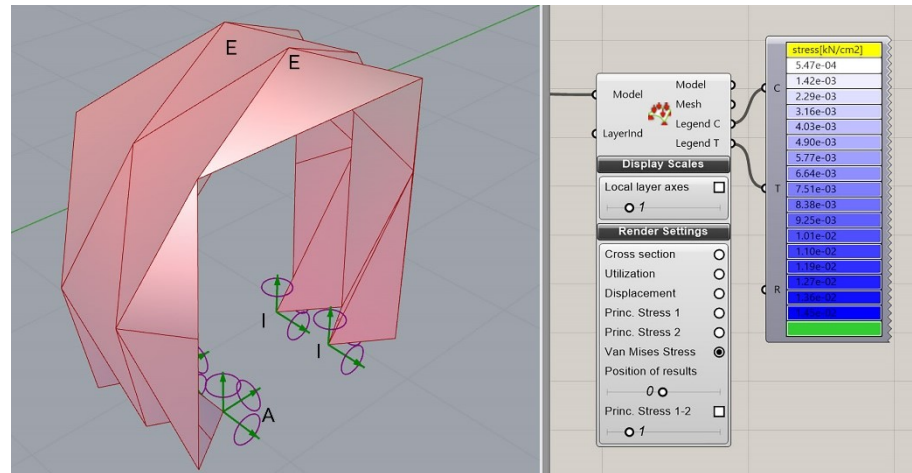


Figure 4.10.
 Van Mises Stresses
 for KOS PoC 55°
 folding angle

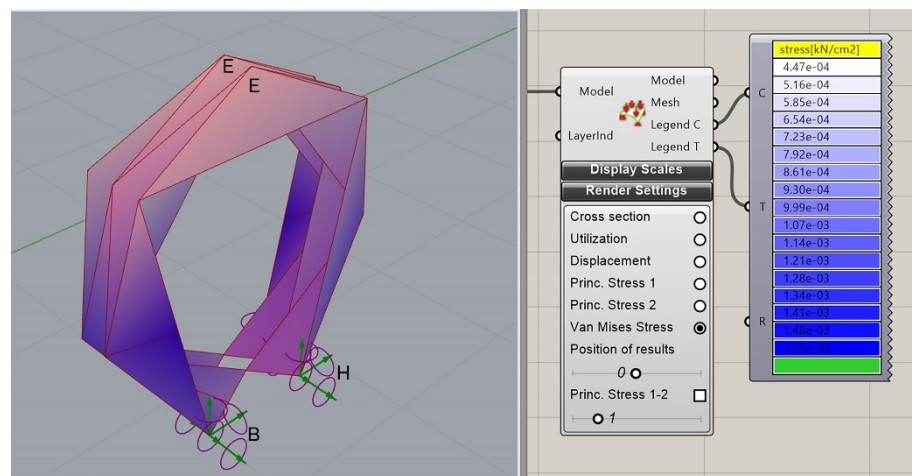


Figure 4.11.
 Van Mises Stresses
 for KOS PoC 76°
 folding angle

From the Karamba3D evaluation for the Van Mises Stresses it is possible to understand that the values are generally low, thus meaning that the structure and its geometry, when built with 24mm MDF and only subjected to gravity, is not very likely to bend, let alone fracture.

At the 76° folding angle state the vertices **B** and **H** would be the ones under biggest tension since they are now the support points, followed by vertices **C** and **G**, even so, the stresses seem to concentrate around vertices and hinges and to get dissipated at the centre of the faces.

For the 35° and 55° folding angle states, it is possible to observe that only the vertices **A** and **I** would be subjected to higher stresses but at a low value.

This means that the structure is likely to behave generally well with respect to bending. Nevertheless, it seems important to pay special attention to the 76° folding angle.

The **Utilization Output** refers to the stability of the structure and is calculated as the ratio between the yield stress (the point beyond which the material leaves the elastic mode and breaks) of the specific material and its maximum Van Mises Stress (Preisinger, 2018).

Graphically, this parameter demonstrates, by colouring, the areas of the shell structure that are at work and how much, in terms of the maximum stress capacity of the material. The red areas (negative values) correspond to compression stresses and the blue ones (positive values) relate to tension stresses (Figures 4.12, 4.13 and 4.14).

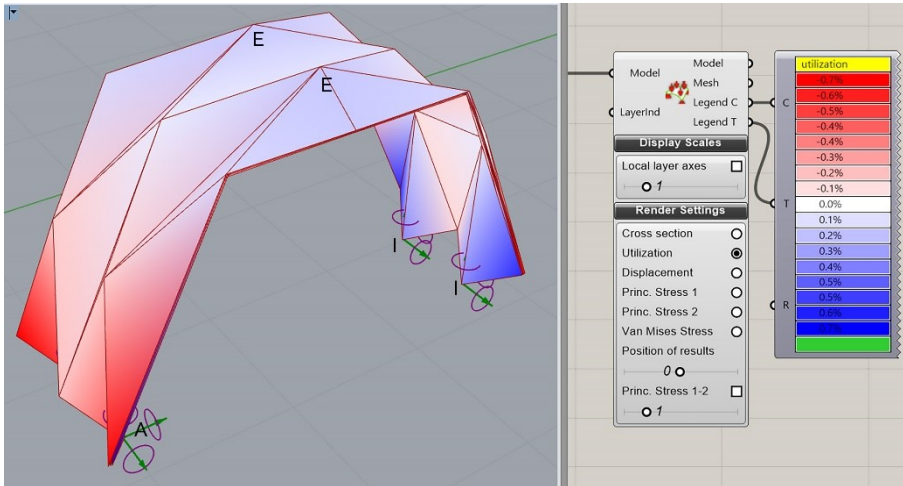


Figure 4. 12.
Utilization for KOS
PoC 35° folding angle

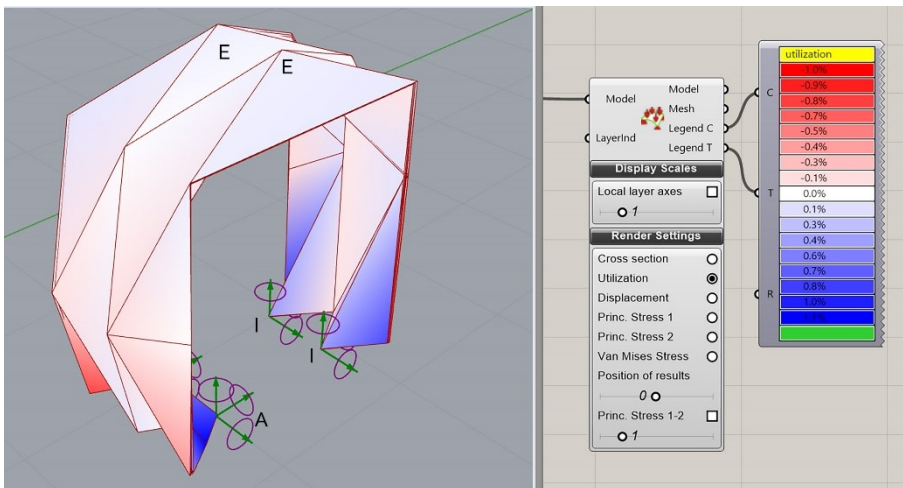


Figure 4. 13.
Utilization for KOS
PoC 55° folding angle

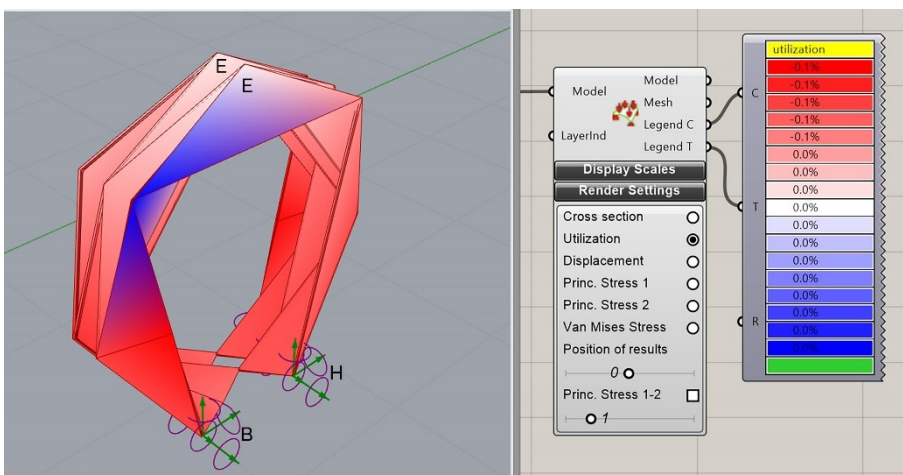


Figure 4. 14.
Utilization for KOS
PoC 76° folding angle

From the Utilization analysis it can be concluded that the structure is always working under tension and compression. The outside face of the shell tends to be in compression and the inside face tends to be in tension. Generally, the stresses get higher at the most folded state, at the 76° fold angle.

At the 35° and 55° folding angles the tension and compression stresses are more clearly visible on the faces directly related to the supporting points. In these areas the compression stresses on the outside part of the faces and the tensions on the inside part of the same faces are clearly visible. Additionally, it is also perceivable that, as in the Van Mises Stresses, these get more concentrated on the lower faces and around vertices and hinges, not so much at the centre of faces.

The **Displacement Parameter** shows the dislocation (rotation and translation) of each part of the shell structure under given loads (Preisinger, 2018) which, in this particular case, is only gravity that is being considered to act on the structure.

Figures 4.15, 4.16 and 4.17 show the Karamba3D analysis for the Displacement of the KOS PoC.

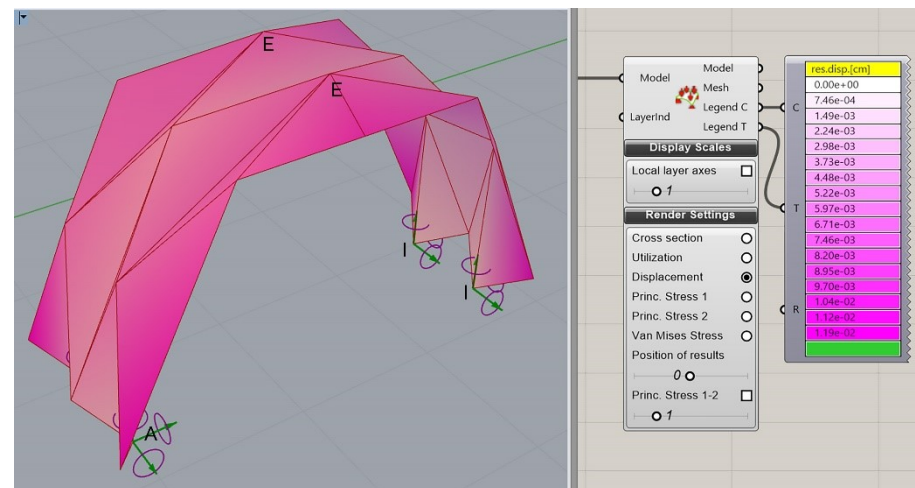


Figure 4. 15.
 Displacement for
 KOS PoC 35°
 angle

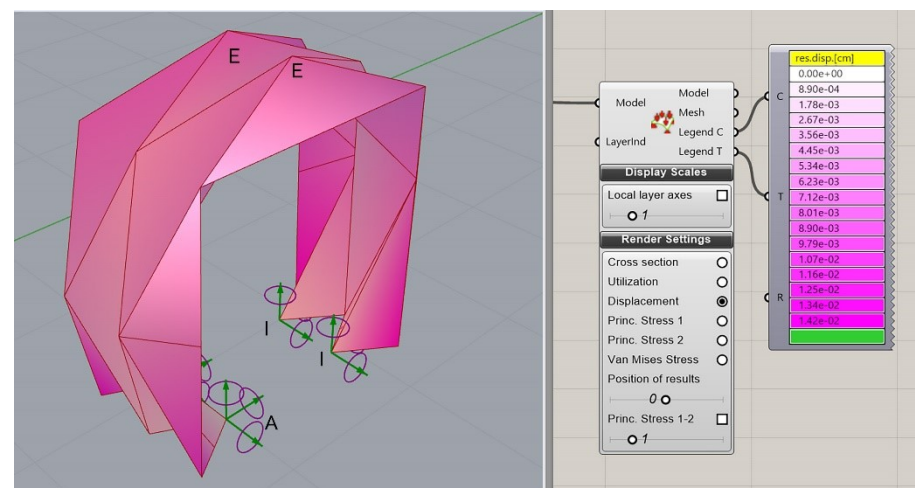


Figure 4. 16.
 Displacement for
 KOS PoC 55°
 angle

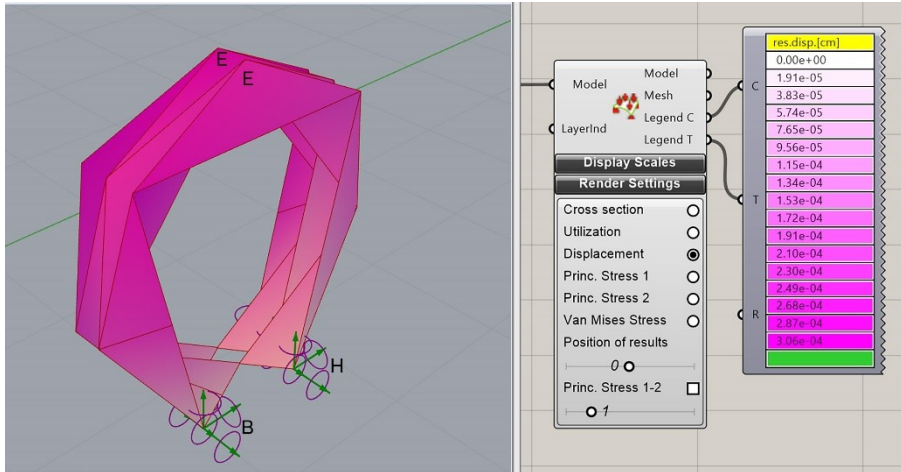


Figure 4. 17.
Displacement for KOS PoC 76° folding angle

From the last three images it becomes clear that the central area of the shell and the supporting points are the most unlikely to move under gravity load. The areas most affected by displacement would be the external boundaries, but even those would be subjected to small displacement values.

The results retrieved from Karamba3D for the Van Mises Stresses, Utilization and Displacement were satisfactory. It seems that there are no issues for major concerns in regard to the behaviour of the structure to bending, tension, compression and displacement. Nevertheless, the most folded state is clearly the one subjected to higher stresses and that should be considered when the structure is in motion.

From the pattern design and structural results retrieved at steps 04 and 05 it is possible to move forward for the next steps of the workflow.

4.2.4 | Thickness Method and Redesign - Steps 06 and 07

Steps 06 and 07 are the beginning of the physical construction of the KOS PoC as a consequence of the results retrieved from previous steps, **Figure 4.18.**

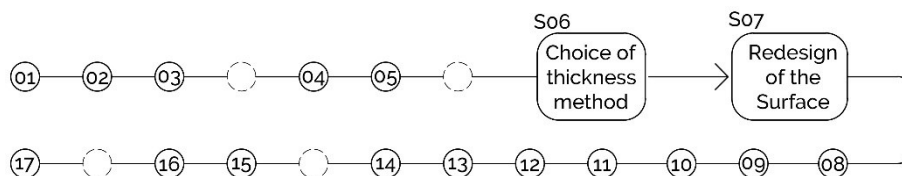


Figure 4. 18.
Overview of the workflow and location of steps 06 and 07

Step 06 relates to the choice of the thickness method to be used on thick origami surfaces. In **Section 3.3.3** the existing thickness methods for origami surfaces were described and analysed. It seems that the most suitable for the Yoshimura pattern would be the ASM. Due to the particular properties of the

CP, the triangle like faces and their disposition around the vertices and along parallel lines, it is able to achieve a perfect separation between mountain and valley hinges, hence this type of pattern does not generate tucking faces. Nevertheless, to the fact that on each vertex meet six faces must be paid attention to, as well as that they are connected by one vertex and that the Yoshimura pattern has an arrangement of MMVMMV. This leads to a case where the thickness of the faces causes the separation between two opposite faces on the vertex where they meet, as demonstrated in **Figure 4.19**.

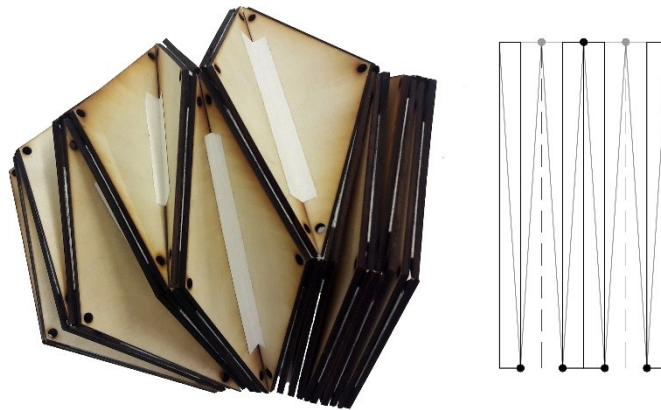


Figure 4.19.
 Displacement of faces
 on an MMVMMV
 vertex of a thick
 surface

The separation between opposite faces does not bring any particularly difficult issue in regard to the utilization of the ASM, but it might bring problems depending on the mechanism used to make the structure move, hence must be flagged as a potential issue.

In respect to the redesign of the surface after the structural analysis, it seems possible to use the crease pattern settled in Steps 02 and 03 and define areas around the centroids of the faces to be subtracted thus making the surface lighter, but without compromising its structural behaviour.

From the structural analysis was observed that the areas where there is less work from the examined types of stresses were the central parts of the faces, so these were subtracted for the final prototype, **Figure 4.20**.

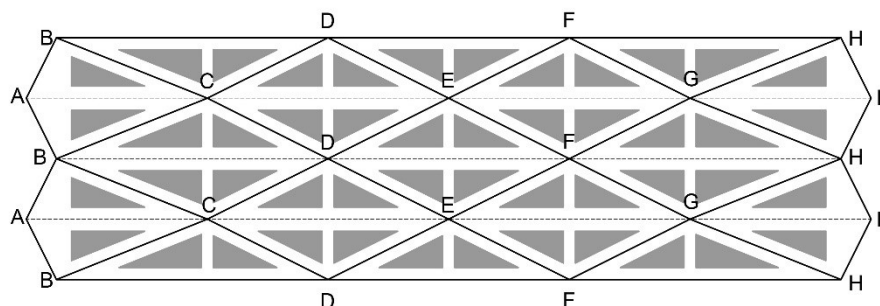


Figure 4.20.
 Redesign of the
 Surface, Step07

The subtraction generates a framed type of face but with large enough dimensions to still allow the faces to be strictly rigid. Around vertices **A, B, H** and **I** a larger area on the faces was left as reinforcement, since these are the

vertices subjected to higher stresses, as can be recognized from the Karamba3D simulation. These vertices correspond to the attachment to the ground points and will bear the entire weight of the structure. A reinforcement line was also maintained on the interior of the faces, which corresponds to the triangles height line, to prevent any type of bending within the faces. Through the subtraction of the superfluous areas was possible to reduce the structure's area, and consequently its weight, by 27%, which is believed to help the structure's motion and reduce the effort for the actuators.

4.2.5 | Interaction and Kinetic Response - Step 08

Step 08 covers the establishment of the desired interaction and the possibilities for movement of the surface that were perceived in the previous steps and from which it will be possible to move forward to Step 09 and establish the mechanical system that will be used, **Figure 4.21**.

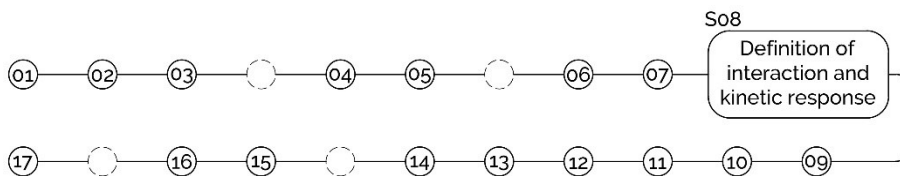


Figure 4. 21. Overview of the workflow and location of step 08

The motion of the Yoshimura pattern can be described as a cylinder that deploys and contracts in the sense of its axis as demonstrated in **Section 3.3.1**. On the case of the CP for KOS PoC, the motion implies the distancing between vertices **A** and **I** and on the free height inside the structure, **Figure 4.22**.

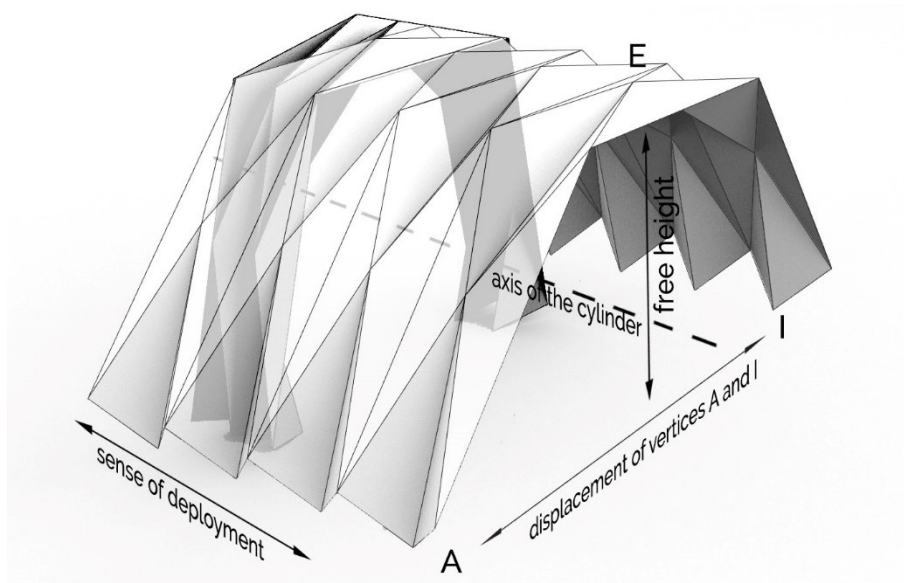


Figure 4. 22. Movement and its implications on KOS PoC

As settled at Step 03, the pattern determined for KOS PoC is usable for the range between 35° and 76° of the folding. To understand the type of motion response that the KOS PoC may have, and its relation to the received inputs it is necessary to comprehend how the variables of height and covered area change during motion. The reason for this understanding is that if the behaviour of a kinetic structure is well-known, predictable and controllable, the interaction can be anything, as long as the inputs provoke the possible responses of the structure.

For the specific case of the KOS PoC were set six folding states of one column of the CP and their covered area and free height measured, as shown in **Figure 4.23** and **Table 4.1**.

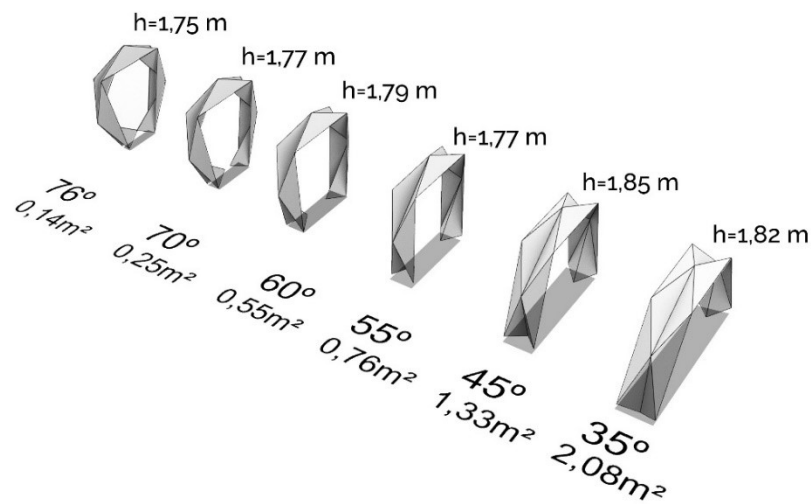


Figure 4. 23.
 Area and free height
 changing values for
 motion range between
 35° and 76°

Table 4. 1.
 Values for area and
 free height for the
 folding states

folding	area	height
35°	2,08 m ²	1,82 m
45°	1,33 m ²	1,85 m
55°	0,76 m ²	1,77 m

folding	area	height
60°	0,55 m ²	1,79 m
70°	0,25 m ²	1,77 m
76°	0,24 m ²	1,75 m

Through the analysis of the parameters of area and height for the base faces it is possible to multiply them per the number of columns that compose the CP of a constructed structure and use them for the mapping between input and response.

In a structure that is intended to be used by people, shelter them as its form changes, a possible example for interaction could be reading the number of people approaching the structure through sensors able to read distances and number of “objects”, giving a determined area per person (1,0 m² for example), and making the structure deploy or contract until the sum of individual areas is reached.

4.2.6 | Mechanical System - Step 09

Step 09 of the proposed workflow was created to resolve the mechanical system that can put the structure in motion as determined in step 08 (Figure 4.24). The guideline to be followed for this particular step is the congruence between mechanism and desired motion established in the previous one.

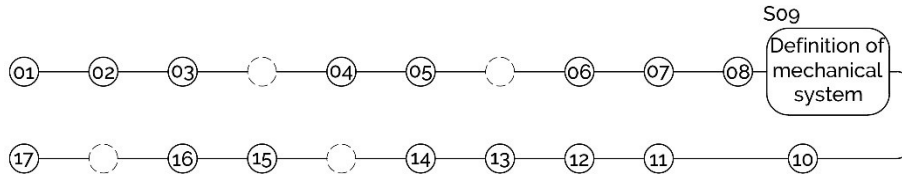


Figure 4. 24. Overview of the workflow and location of step 09

The intended motion for the KOS PoC is a linear motion in the direction of the axis of the cylinder defined by the surface and the preservation of the rigid kinematics simulated at step 03. For those purposes it is necessary to create a mechanism that is able to control every folding angle. From the mechanisms described in Section 3.2, and summarized in Table 4.2, were chosen the straight translational pantographic linkages.

Category	Simple Mechanisms			
Subcategory	Open or closed circuits of: Ropes, Belts or Cables on Pulleys or Toothed Wheels 	Translational Bearings 	Rotary Bearings 	Hinges
Category	Linkages			
Subcategory	Non-Pantographic Linkages 	Pantographic		
		Straight Translational 	Straight Polar 	Angulated
Category	Smart Materials as Mechanisms			Pressure as Mechanism
Subcategory	Hygroscopic 	Shape Memory Alloys + 0 - 	Programmable Matter 	Flexible Materials (includes Pneumatics)

Table 4. 2. Summary of mechanisms described in Section 3.2

As described in Section 2.1.2, through the contributions of You and Chen (2012), Edmondson *et al.* (2015), Bowen *et al.* (2013), Dureisseix (2012) and Zhang *et al.* (2015), a rigidly folding origami tessellation is a set of spherical mechanisms that can be organized in an open chain or a network. On the case of the proposed irregular Yoshimura CP each spherical mechanism has

six rigid panels (faces) attached by revolute joints (hinges) concurrent at each vertex and all spherical mechanisms (vertices) are organized on a closed network.

As Lang (2018) defends, the Yoshimura pattern has multiple Degrees of Freedom, even though each vertex has only two DoF (instead of the typical three) when it is inserted in a periodic network (Lang, 2018).

This means that the Yoshimura pattern can be quite uncontrollable if the folding angles of the multiple faces are not congruent. To prevent this issue and to recreate the intended motion is proposed the use of a pantographic system, able to introduce synchronicity on folding.

Kinematically both mechanisms, pantographs and rigid origami, are similar, they are both rigid and while origami is made of rigid faces with straight revolute joints, pantographs are made of rigid bars with revolute joints, so the relative motions they allow can be compared and put to work together as long as they are accurately placed. For the KOS PoC are proposed four specific lines represented in **Figure 4.25**.

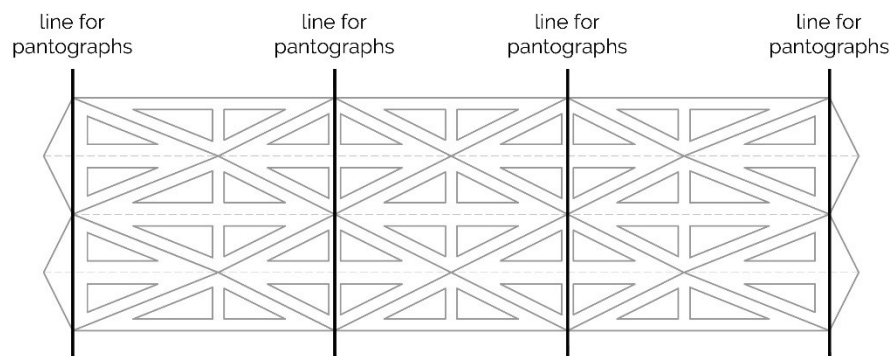


Figure 4. 25.
Lines of similar
movement between
CP and Pantographs

The lines of pantographs must be connected to the rigidly folding origami surface on the specific lines where motion is the same. In the case of the general Yoshimura pattern it means that they must be placed on perpendicular lines to the valley folds and in such a way that their revolute joints coincide with the origami creases and/or vertices.

The pantographs can be additionally useful since they enable the possibility of locking an entire line of the surface on any step of the folding. If the pantographic system is strictly connected to the surface, when the system is locked it also locks the surface since it creates a continuity within the whole system, due to the connection between its rigid bars, and obliges to reciprocity on an aligned set of faces.

By using these two systems together is believed to be possible to accurately control the folding angles of the individual faces on a vaulted structure and

produce a non “Curtain Type” of movement. The pantographs work on parallel lines and the remaining faces of the surface guarantee the connection between each pantographic line and the vaulted geometry. It is intended to demonstrate that by using the rigidly folding origami surface along with the pantographs is possible to produce a stable moving structure that can behave as a static one when the pantographic mechanism is locked.

4.2.7 | Small-Scale Prototypes for Testing - Steps 10 and 11

Steps 10 and 11 are meant to test the options that were made in the previous steps regarding the design of the CP, the choice for the thickness method and the mechanism through diverse scale prototypes, prior to the engagement on Step 12 (Figure 4.26).

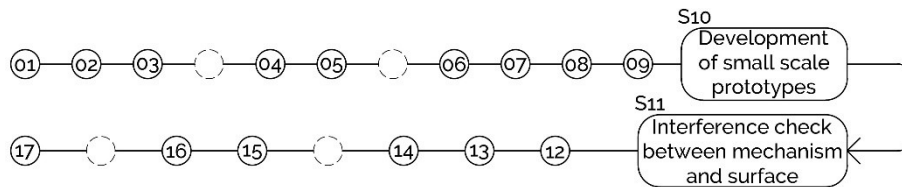


Figure 4. 26. Overview of the workflow and location of steps 10 and 11

For the KOS PoC three prototypes were developed, A, B and C, to better understand the behaviour of the proposed irregular Yoshimura pattern while folding and the demands for the pantographic system.

The first model was done at the beginning of the development of the KOS PoC when the final CP was not yet reached so it has no scale in relation to the final prototype but allowed to draw general conclusions regarding the mechanism and thickness of the surface.

Prototype A was done with a regular Yoshimura pattern, on a paper surface with two pantographic systems parallel to the axis of the “cylinder” and another system on the other sense that intended to connect the first two. **Figure 4.27** shows prototype A on three states of the folding, each state on a top and frontal views.

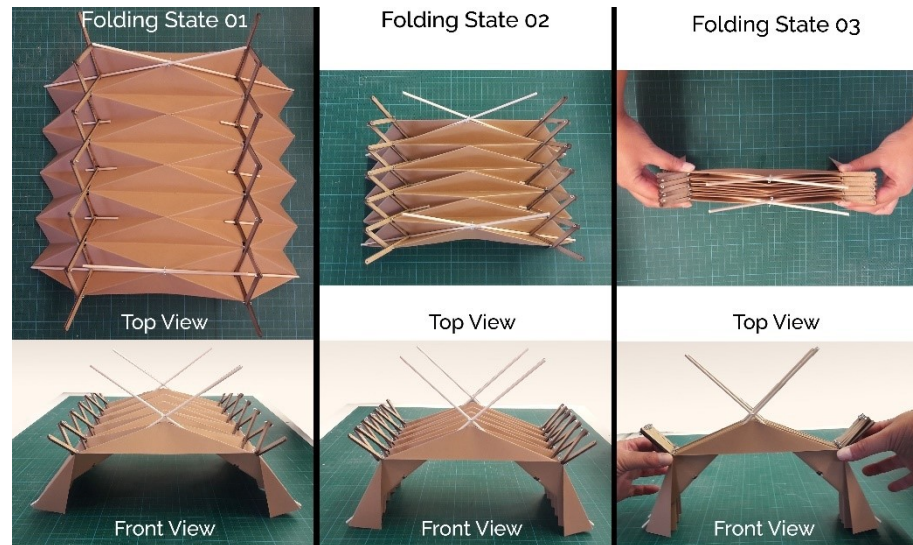


Figure 4. 27.
 prototype A folding
 states

From prototype A was possible to understand that the pantographic lines, parallel to the axis, worked as the origami surface if the vertices were cut away from the surface. By cutting off the vertices was possible to introduce the pantographs joints as well as the corresponding space on the creases, so geometric coincidence was achieved.

It also allowed to verify that the pantographs on the opposite sense had no impact on movement, maybe they could have some impact on the stability of the structure, but it was not obvious through observation. These were composed by only one SLE that, if not connected to other elements, did just the same as the origami creases and so were found to be redundant and were dismissed.

This model proved to work well when manipulated but it was also possible to observe that the faces bent, they were not planar at all times so the control of the structure was almost entirely on the pantographic system.

Prototype B was constructed at 1:10 scale of the final KOS PoC and made in 5mm plywood. On this prototype was tested the use of rigid faces and the inclusion of the pantographic system as part of the faces. **Figure 4.28** demonstrates the pieces design that were cut at the laser cutter.

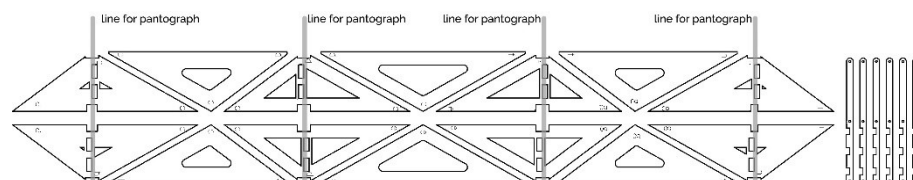


Figure 4. 28.
 prototype B
 fabrication pieces

The faces were drawn considering the exact place for the insertion of the pantographic systems, four lines for pantographs, and the vertices and crease

spaces that had to be cut so there was geometric coincidence between the revolute joints of both systems.

The hinges were created with strong duct tape placed on the corresponding side for the valley folds as shown in **Figure 4.29**, which displays also the assembling between base faces and the pantographic systems.

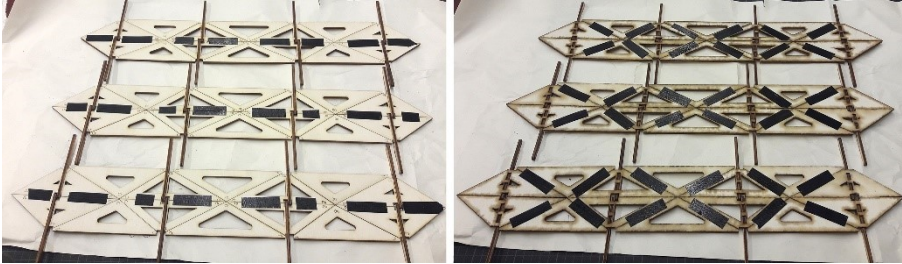


Figure 4.29.
prototype B
assembling of base
faces, pantographic
system and hinges

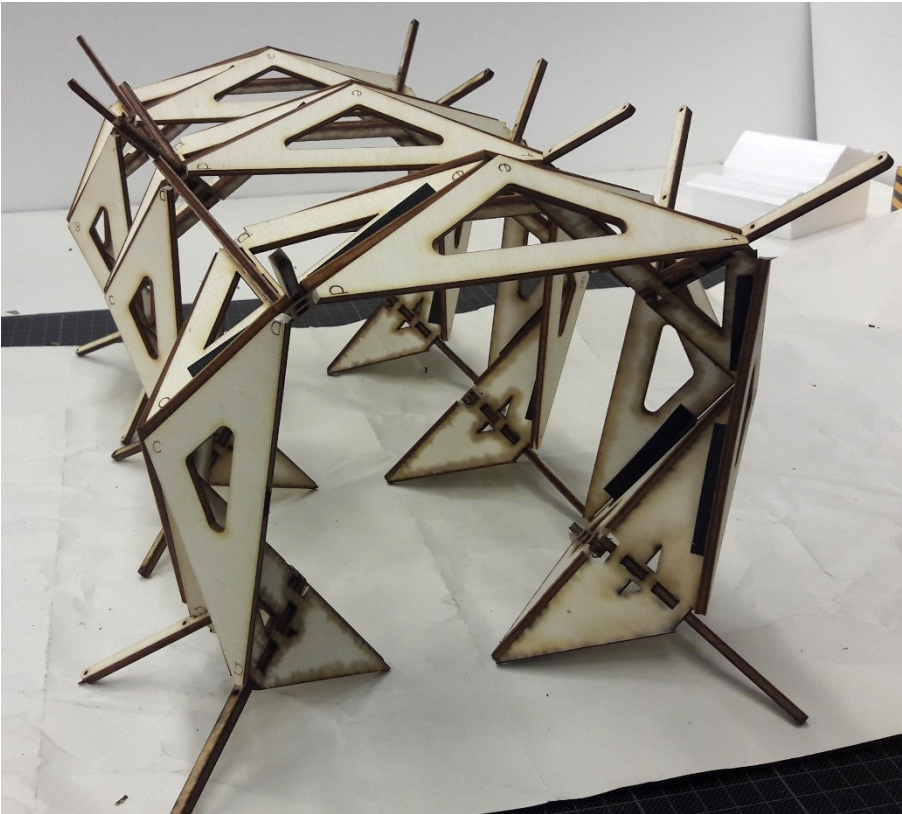


Figure 4.30.
prototype B folded
columns

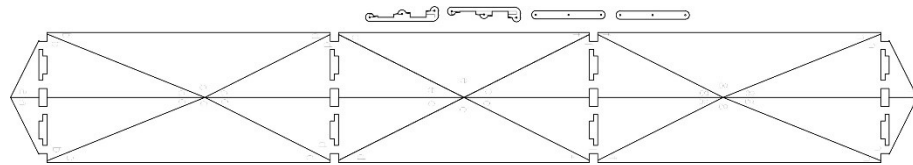


Figure 4.31.
prototype B detail of a
folded vertex

On prototype B were observed two limitations of the design. The pantographic elements projected themselves to far on the outside of the structure which created implications on the movement of the structure. In the middle of the folding process the structure was caused to leave the ground plane thus starting to be supported by the pantographs instead of the ground plane vertices, as seen in **Figure 4.30**. The other limitation was that, even though the pantographic system was similar to the one used in prototype A, the thickness of the material did not allow the faces of the degree-6 vertex to meet and reach a planar state (**Figure 4.31**), because the pantographs were designed without consideration for the position of the zero-thickness tessellation, or the “joint plane” as nominated by Edmondson *et al.* (2015).

Prototype C was created to correct the limitations found on the previous models. This prototype intended to be the final test for the KOS PoC, so several issues were addressed on its design. It was made at scale 1:5 so the thickness of the plywood (5mm) would be closer to the 24mm intended for the surface that was tested on Karamba3D. It was fabricated with the final CP and the pantographic system and its connection to the faces were completely redesigned as depicted in **Figure 4.32**.

Figure 4.32.
 prototype C pieces
 for fabrication



In what regards the design of the pantographic system, was tested if was possible to make each rigid bar correspond completely to the width of the face, so the pantograph would not project itself out of the structure. Besides solving the intersection with the ground issue, this design option allowed also to achieve a more beautiful final design by letting the origami surface really be the central actor once the pantograph gets “hidden” within the overall design instead of projecting itself to outside of the surface.



Figure 4.33.
 prototype C folding
 states for Scissor
 Elements design

Figure 4.33 demonstrates where would lay the origami zero thickness surface, which is coincident with the pantographic system. The zero-thickness surface is like an imaginary surface, called by Edmondson *et al.* (2015) as the “joint plane”, that is not completely coincident with the thick faces, but the kinematics of the entire structure is preserved and is congruent with the scissor-like system, in the same manner of the work developed by Edmondson *et al.* (2015) and referred in **Section 2.2.2**.

From the exemplified unfolded and folded states were drawn the pantographic bars. The bars have holes for the revolute joints consistent with the previously exemplified folding states and in such a way that would allow to attach one of each SLE set to one face and letting the other free for rotation and attachment to the next SLE. The design detail of each bar of the SLEs and the attachment space on the faces is presented in **Figure 4.34**.

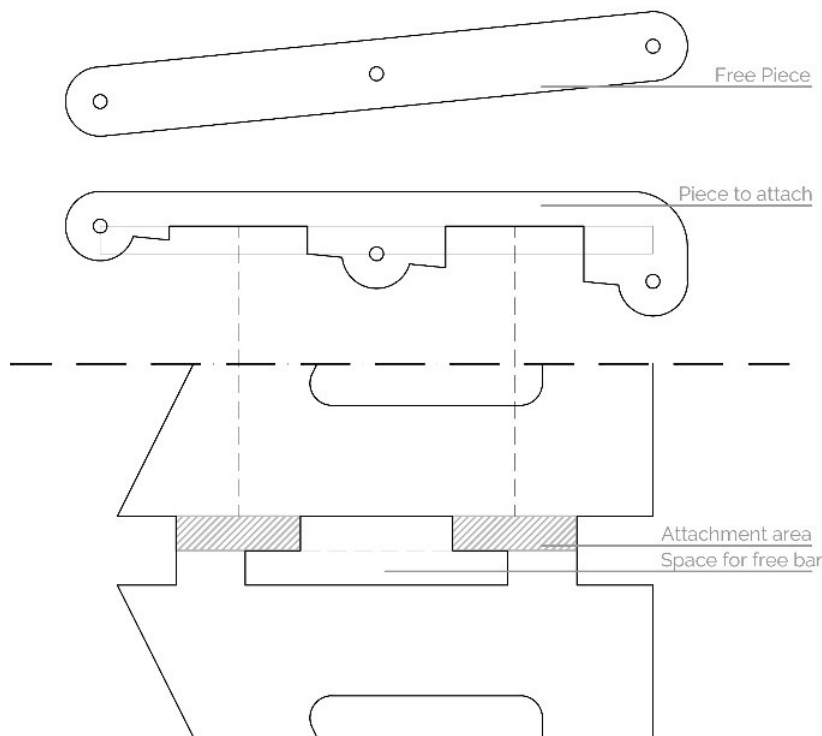


Figure 4. 34.
prototype B
pantograph design
and scheme
attachment to faces

This design allows to have a pantograph system that is half the size of the one used on prototype B, which was the objective, but arose another issue. The space for the free bar must be subtracted to the face which limits the rotation it is allowed to do since, at some point, there will be a collision between the free bar and the face.

Figure 4.35 demonstrates the maximum and minimum folding states of the surface when made with a 24mm thick material and with the specific pantograph design.

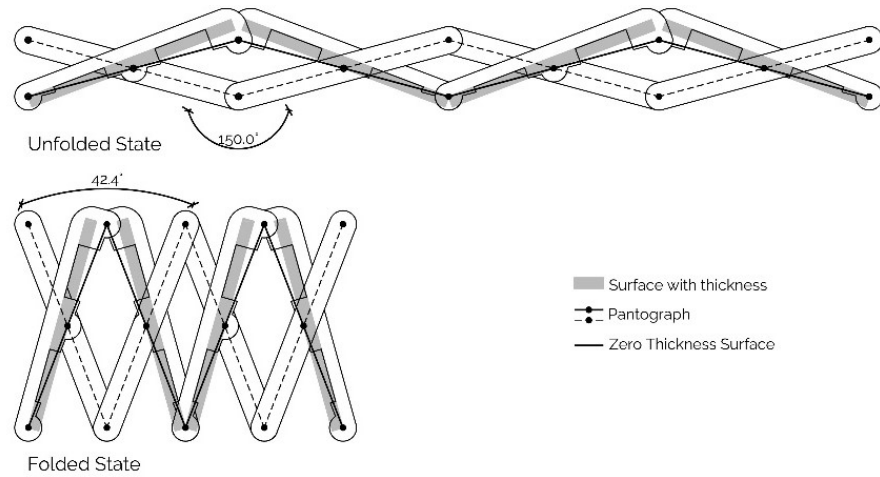


Figure 4.35.
 Maximum and
 minimum folding
 states with new
 Scissor Elements

The intersection between faces and free bars is not a problematic limitation since the folding range of the surface goes from 35° to 76° folding angles. As demonstrated in **Figure 4.36**, when the folding angle is 35° the angle between the top faces is 110°, when it is 70° the angle between the top faces is 40° and when the folding angle is 76° the angle between the faces is 28°.

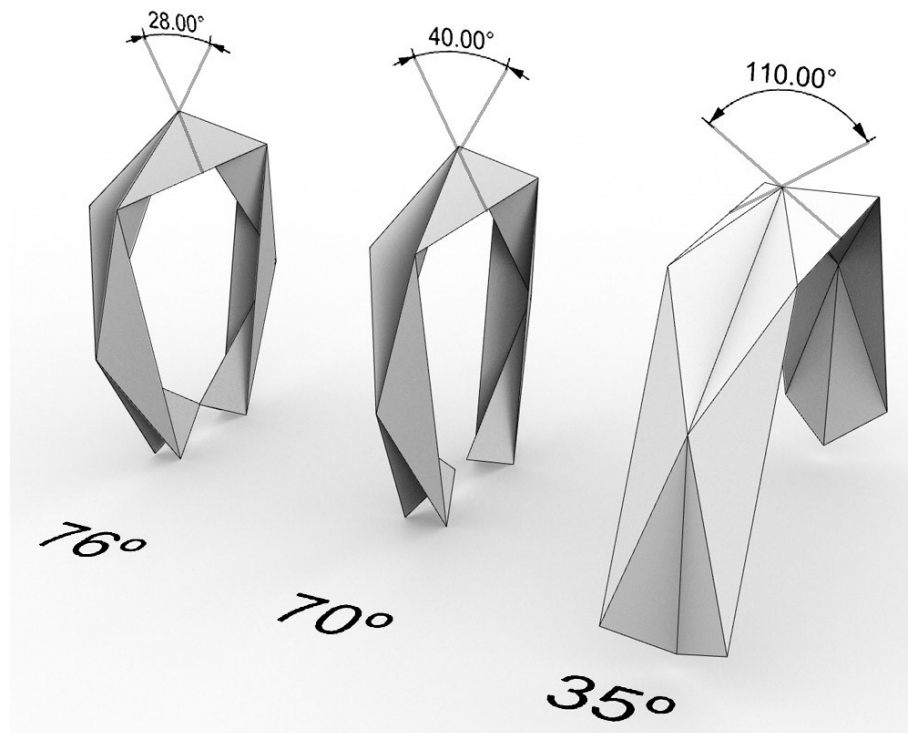


Figure 4.36.
 Relation between
 folding angles and
 faces angles

With the proposed pantographic design, the surface can be used from the 35° folding angle until the 70° folding angle. The fact that it cannot be used from 70° to 76° does not seem to be limitative for its utilization, since this range corresponds to great proximity between the extremes of the surface.

Therefore, from prototype C the range of motion of the KOS PoC was resettled from 35° to 70° folding angles.

After the redesign of the pantographic system, prototype C was constructed at scale 1:5 in 5mm plywood and the hinges were made similarly to prototype B but that were stapled to the faces to make them work more closely to the kinematic model, as shown on **Figures 4.37** and **4.38**.

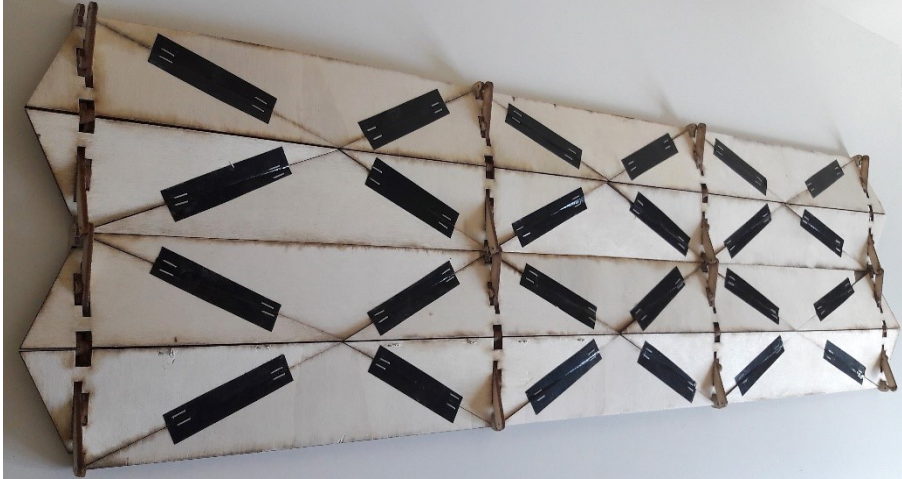


Figure 4.37.
Prototype C
Assembling



Figure 4.38.
Prototype C
Assembling

Prototype C demonstrated that the redesign of the pantographs worked in consonance with the rigid origami surface and gave also important tips on the closing of the scissor system, which can only be done after every SLE is placed on the surface and is easier if done with the surface on the fully folded position. This prototype permitted also to verify that the duct tape hinges do not work well on such scale, even after the stapling they had the tendency to detach from the faces. **Figure 4.39** demonstrates two folded states of the prototype C.

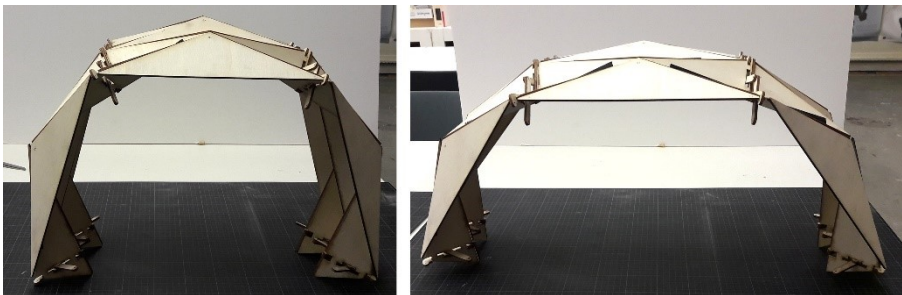
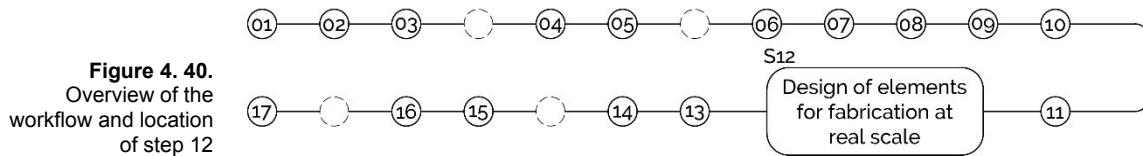


Figure 4.39.
Prototype C folded
states

4.2.8 | Design for Fabrication – Step 12

Step 12 of the proposed workflow concerns the fabrication of the kinetic origami surface at real scale and should consider the chosen materials from the structural simulation, the thickness method most appropriate for the CP as well as the design of the surface settled at step 07 and the conclusions reached through the small-scale models (**Figure 4.40**).



For the specific case of the KOS PoC the material to be used for the faces is MDF in 24mm thick panels. MDF is a wood base material with mechanic properties similar to the ones used on the Karamba3D simulation.

The 24mm MDF panels are very heavy and difficult to manipulate and assemble for the 1:1 scale. Therefore, the scale was decreased, and the KOS PoC final prototype was tested at 1:2 scale in 12mm thick grey MDF. From the 1:2 scale prototype will be drawn conclusions consistent with a 1:1 scale prototype since they have close dimensions and every element is scaled accordingly.

The chosen thickness method is the ASM and the design of the faces correspond to the CP settled at step 07 with the correspondent subtraction areas and added rounded corners at vertices A and I, to help on the support change through motion. For the pantographic system was initially tested its fabrication also with 12mm thick MDF and their design corresponds to the one determined through the small-scale prototypes. The final design for each piece is depicted in **Figure 4.41**.

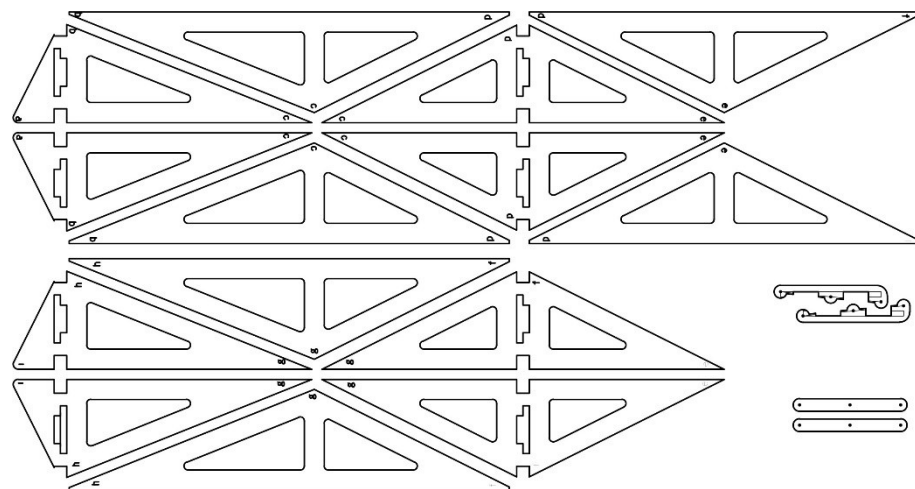


Figure 4.41.
Pieces for fabrication for the final prototype

The fabrication of the pieces was made at a CNC milling machine through a simple cut on Z direction that created every individual face, the subtraction areas to make the final surface lighter and the spaces to insert the pantographic system as seen in **Figure 4.42**.



Figure 4. 42.
Faces for the final prototype

When designing the faces for the CNC milling machine was not considered space for the screws and bolts that would make the revolute joints, neither the 2mm low relief for the insertion of the piano hinges. These improvements had to be made after fabrication (**Figure 4.43**) by hand. If foreseen, these issues could have been considered on the design of the faces for fabrication and easily done by the CNC milling machine. In what respects the low reliefs for the placement of the hinges, the surface would have to be turned at the CNC milling machine, since the hinges only get placed on the valley side creases.

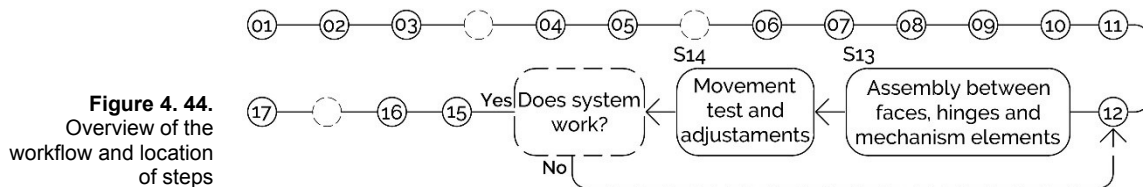


Figure 4. 43.
Voids for screws and bolts and low relief for piano hinges

When all faces and pantographic bars were fabricated, sanded and improved was possible to move to the next step of the proposed workflow.

4.2.9 | Assembly and Testing – Steps 13 and 14

Steps 13 and 14 are related to the assembly of the system composed by surface and mechanism and the initial tests for the motion of the structure. It is only possible to move to the following steps when the evaluation point reaches a positive answer (**Figure 4.44**).



For the KOS PoC, after the fabrication of faces and scissor elements, were attached the metallic piano hinges along the 2mm low relief areas for the valley folds (**Figure 4.45**).

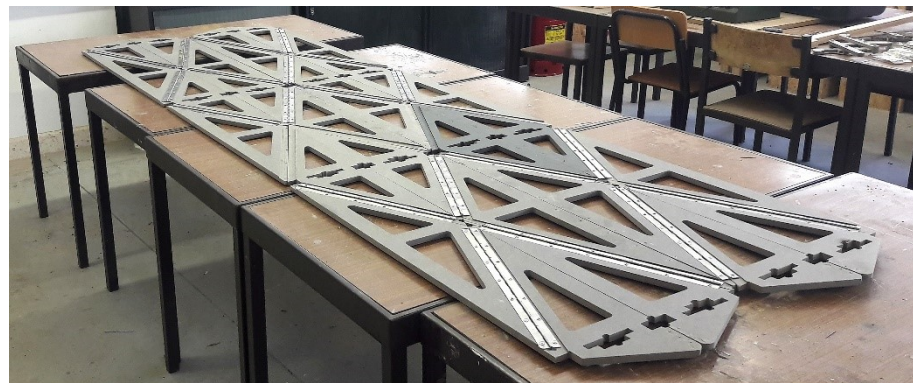


Figure 4.45.
Faces attached through piano hinges

When attaching the piano hinges, particular attention was paid to the alignment between faces, which were held together by fixing clamps while putting the screws. The alignment between faces is a critical issue since, if not made correctly, may compromise the expected rigid motion.

After the hinges were placed started the assembly of the pantograph systems. These must not be closed before folding, partially or completely, the structure, otherwise they will lock motion and make impossible to depart from the unfolded state (**Figures 4.46 and 4.47**).



Figure 4.46.
Assembly of pantograph system



Figure 4.47.
Assembly of
pantograph system

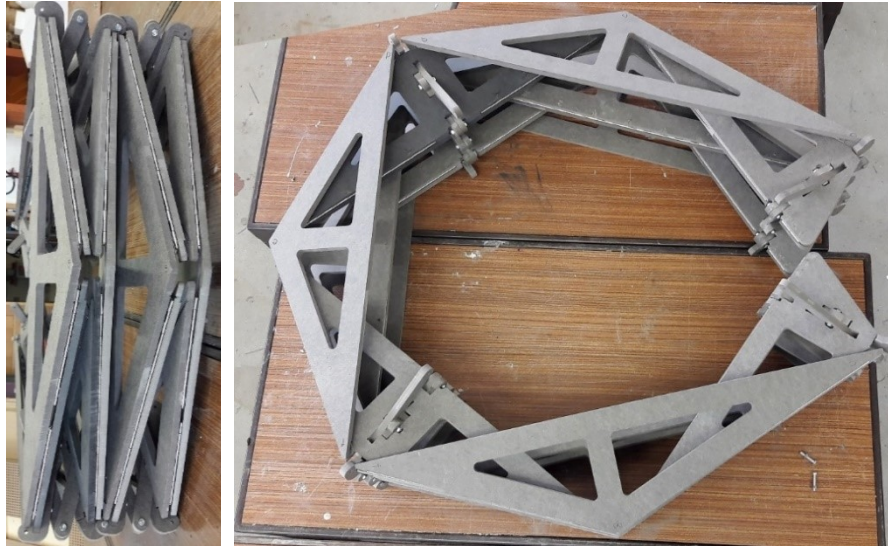


Figure 4.48.
Closed structure, two
views

After the assembly between faces, hinges and pantographs the structure was put into the most folded position (**Figure 4.48**), and the individual SLEs were joined by metallic axis. Consequently, was tested the folding motion of the surface and its ability to support itself on different folding states as can be seen in **Figure 4.49**.

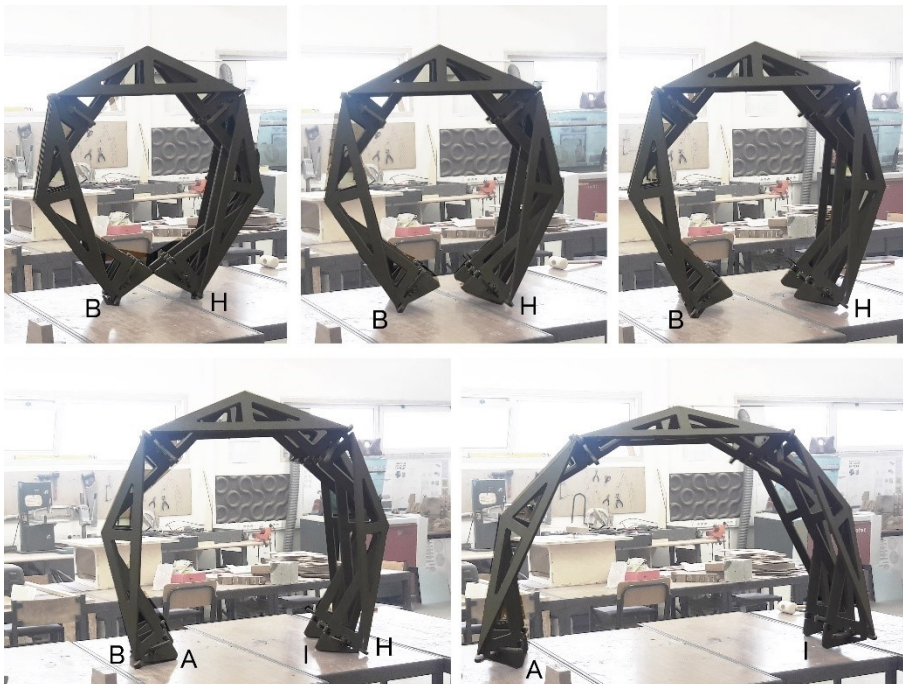


Figure 4.49.
Movement tests

Until this point the system was having a very satisfactory behaviour because the probable problems were positively prevented, the structure opened and closed as simulated and had the ability of sustaining it-self on static positions. Then was tested the continuous motion from the unfolded to the completely folded positions. It was observed that the passage from the support points **A** and **I** to the support points **B** and **H** could bring some problems for the actuation step since the passage could not be done smoothly. Additionally, the bottom SLEs touched the ground on the most folded positions causing visible stresses on the attachment areas.

These scissor elements were initially glued to the faces with carpenter's glue, but when testing the surface some started to detach from the faces and as a precaution was decided to screw them to the faces. The action of screwing the SLEs to the faces on the perpendicular sense to the MDF surface was not a good choice, it caused the definite collapse of some pieces (**Figure 4.50**).

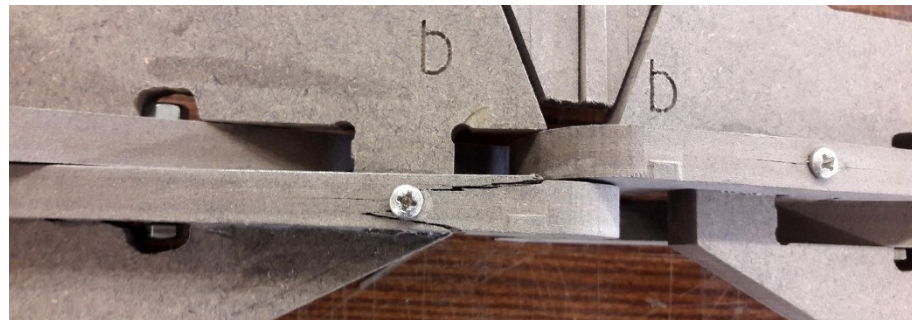


Figure 4. 50.
SLE collapse

From this point was tried to make an alteration to the bottom faces of the surface. It was created an MDF round “foot” for the faces that touched the ground plane, with the objective of putting the lower SLEs away from the ground and at the same time facilitate the change between the support vertices (**Figure 4.51**).

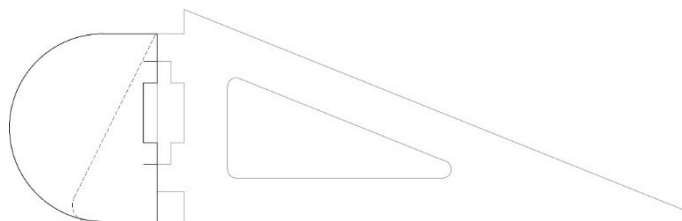


Figure 4. 51.
Round foot for
ground supporting

The pantographic elements were redone in plywood, that was expected to behave better than the MDF when screwed to the faces. At this point was also included on the design of the pantographic bars the points for attachment of the actuators. The available motors were linear actuators similar to the ones used on experiment 03.

The first option was to place the motors on the unit lines of each scissor system on the inside part of the structure, but this would mean that they would be obstacles to the passage of people. Another option would be to use the

unit lines but position the motors on the outside part of the structure which, only empirically, seemed to be a possible source for difficult issues in terms of stability of the whole system. By having the motors placed on the outside part of the structure the result would be like having dancing weights on the top of a moving structure thus generating additional forces with unpredicted outcomes.

Once discarded the placement of the motors on the unit lines was tested the possibility of aligning the motors with the main directions for movement and attached directly to each pantographic system. Since each motor can only run a course of 31,5 cm were chosen two points on the scissor systems, on the interior of the surface to attach the fixed point of the motor on the second element and the moving point on the extreme. The open and closed positions of the pantographs and their relationship with the motors are shown on **Figure 4.52**. The final design of the pantographic elements is directly related with the positioning of the actuators (**Figure 4.53**).

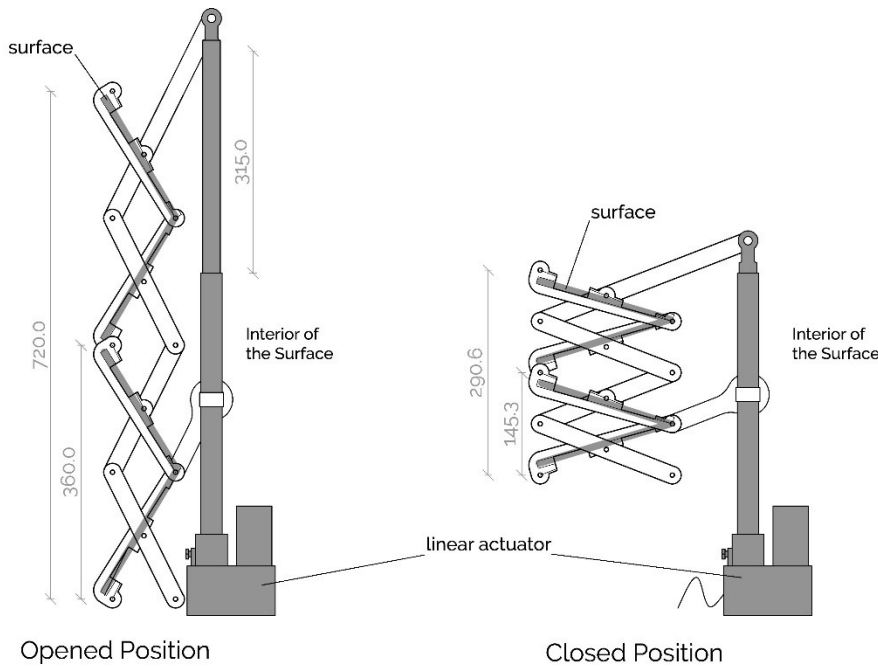


Figure 4. 52.
Actuator's open and closed positions



Figure 4. 53.
Final pantograph pieces

In **Figure 4.54** is shown a detail of the assembly for the final structure including the described adjustments namely, the round foot for the support points and the scissor system replacement. Substituting the scissor systems while the structure was completely constructed was not an easy endeavour due to the difficult access to some points and to the need to have it slightly folded for some operations.



Figure 4.54.
 Adjustments to the structure

The structure was then resubjected to the movement tests and passed on the evaluation point. The whole system demonstrated a good behaviour regarding motion and the pieces that compose the whole system, therefore was possible to proceed to the next step on the workflow.

4.2.10 | Computational Control and Actuators – Steps 15 and 16

Steps 15 and 16 of the proposed workflow respect the implementation of the computational system for actuation of the structure before the final assembly step and after the construction of the structure (**Figure 4.55**).

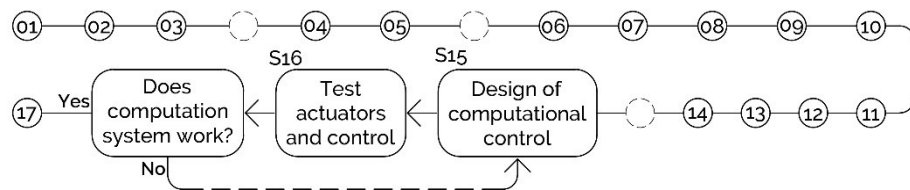


Figure 4.55.
 Overview of the workflow and location of steps 15 and 16

At this step the designer should be particularly attentive to the type of interaction established in step 08 and the intended response by the structure. The response must agree with the expansion and contraction that the surface is able to perform when moved through the specific mechanism, determined at step 09. Furthermore, the designer should experiment the entire input-output system, with special care to the test of the actuators, before passing on to the final step.

For the KOS PoC, at these steps, a very simple program was designed to put the actuators in motion. No particular kind of interaction was created since the structure could react to anything, as long as the system works.

The actuators would start opening at the same time and velocity until they reach the total course (31,5cm), wait 45 seconds and then start to close all together and wait 45 seconds until opening again. This way was expected to be possible to run several opening and closing courses to test the structure's motion and have enough time to rearrange the structure, shut it down if necessary, during the 45 second waiting.

The actuators were tested and adjusted several times for velocity and synchronicity by putting all of them aligned and moving at the same time. In order to evaluate their ability to move and stop, the actuators were switched on and off and forced by hand. At this last evaluation step the actuators proved to be well synchronized and to have enough strength to resist to the pushing, leading to believe that they would be able to be strong enough to maintain the surface locked. So, since the structure passed the last evaluation point it was possible to start the final assembly.

For the attachment of the actuators to the pantographic system and consequently the surface, it was tried to distribute the weight by placing the motors with the bottom part on opposite directions, as seen in **Figure 4.56**. It is expected that this positioning allows to prevent for instability within the structure when in motion.

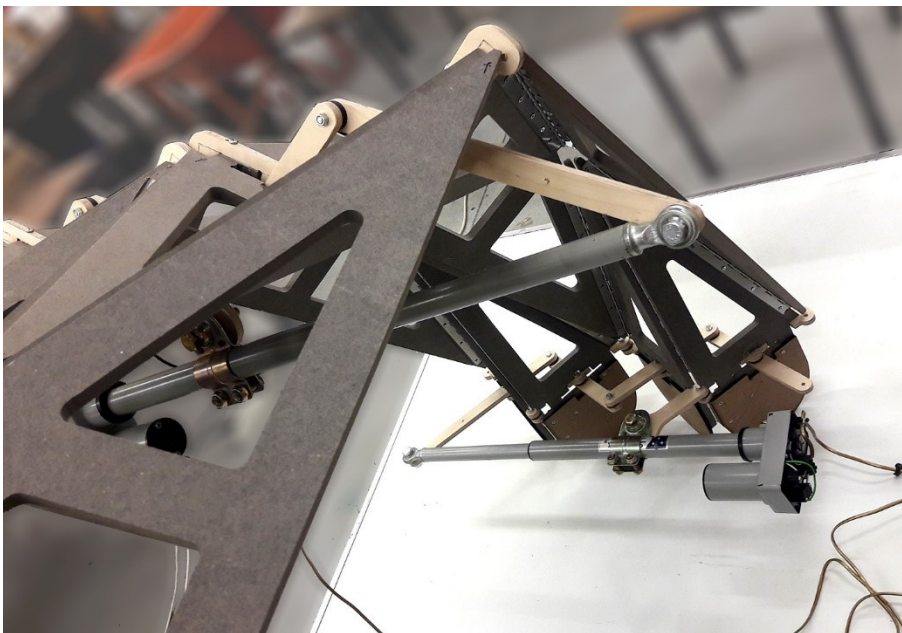
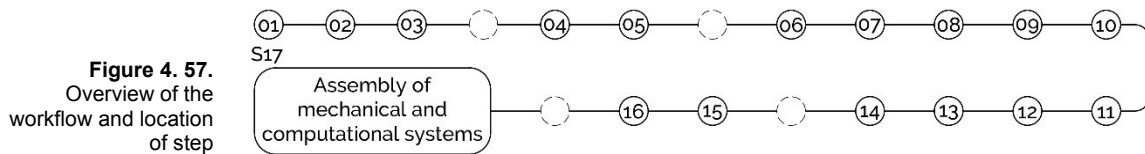


Figure 4. 56.
Positioning of the
actuators on the
structure

4.2.11 | Final Assembly – Step 17

Step 17 is the final step of the workflow. It concerns the last assembly between every system in action, the origami surface, the mechanism and the computational system. If the structure behaves well at this point it is ready for use (**Figure 4.57**).



With the surface and pantographic systems assembled, from step 14, the actuators were attached to the pantographs and the entire KOS PoC was first tested in a suspended position.

The two extreme points of the central crease were chosen to attach the structure to the ceiling (white arrows on **Figure 4.58**). These were the elected points since they are the highest central points of the KOS PoC in relation to which can be determined the symmetry of the structure and of movement. This way was intended to test if the rigid kinematic of the structure was analogous to the simulations made at step 03.

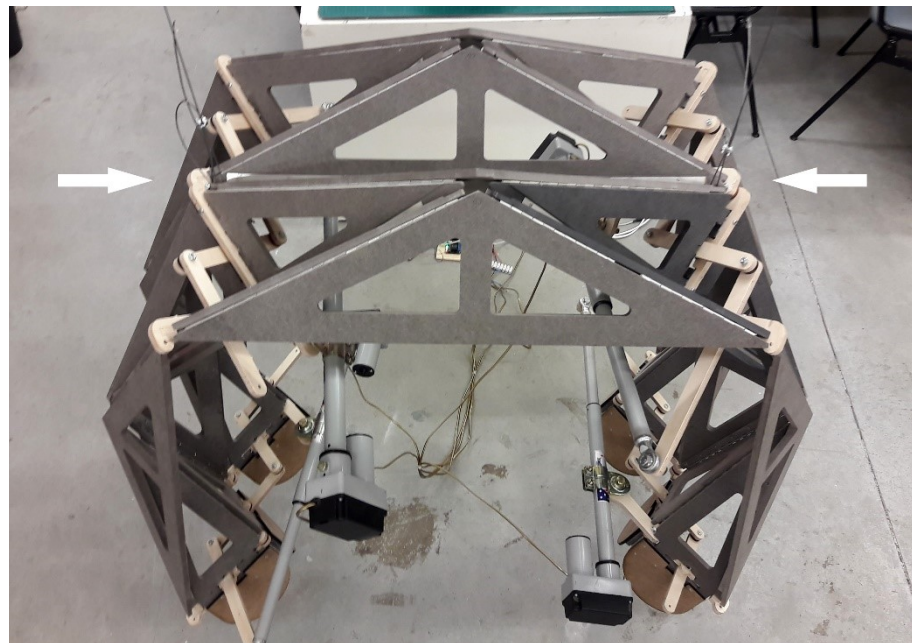


Figure 4.58.
Suspended Structure

From the test was observed that the motion of the structure was similar to the rigid kinematics simulations (film available at cutt.ly/FilipaOsorio_KOS).

During four courses for folding and unfolding the surface was also tested the ability of the motors to maintain the locking of the surface. The structure demonstrated a motion analogous to the kinematic simulation, the path taken by the faces was the same, the angles between faces progressed regularly within the entire surface, and the motors proved to be well tuned and strong to maintain the structure in a locked mode along with the pantographic systems.

At this point was finally set the test for the movement of the structure when supported on the ground. The structure performed satisfactorily two folding-unfolding courses (**Figure 4.59**) but was necessary to readjust the alignment between support points during the 45 second waiting period.

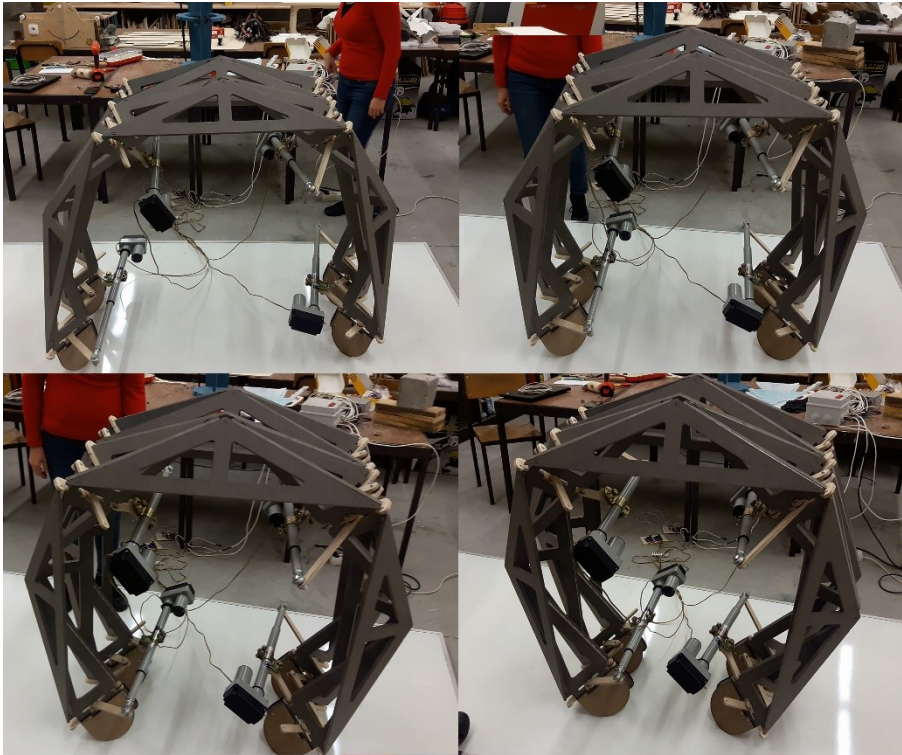


Figure 4. 59.
Movement tests
Supported on the
ground Structure

At the third course the misalignment between support points caused a torsion on the surface (**Figure 4.60**). The torsion lead to the break of two bars of the pantographs (**Figure 4.61**). The pantographs that broke are on the same side of the structure (right side on Figure 4.60) and the pieces were the same on both pantographs it was the pieces that hold the heaviest part of the actuators.

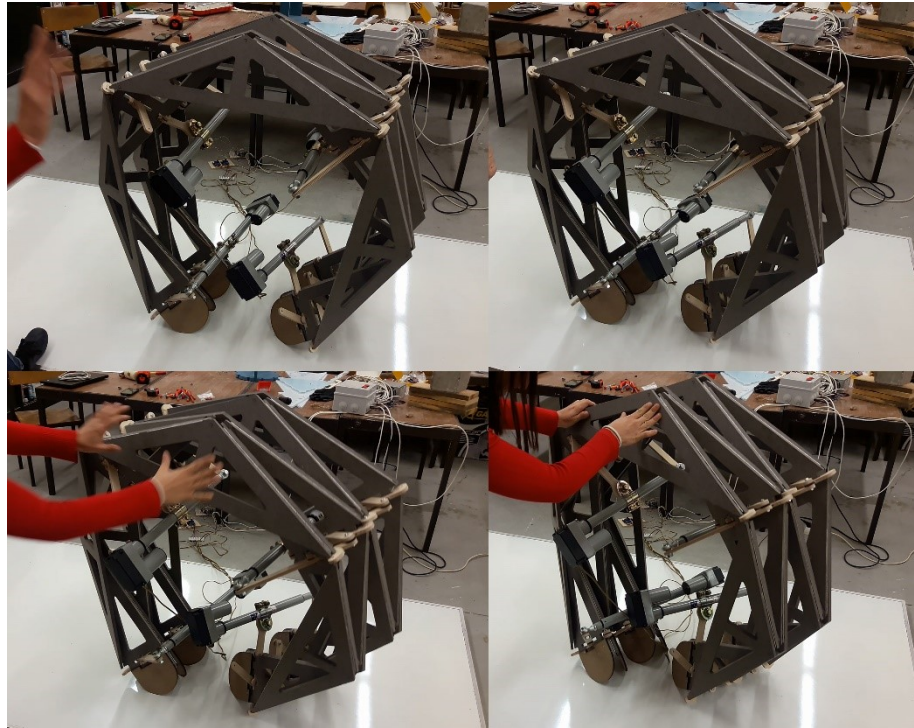


Figure 4. 60.
Supported Structure,
breaking point

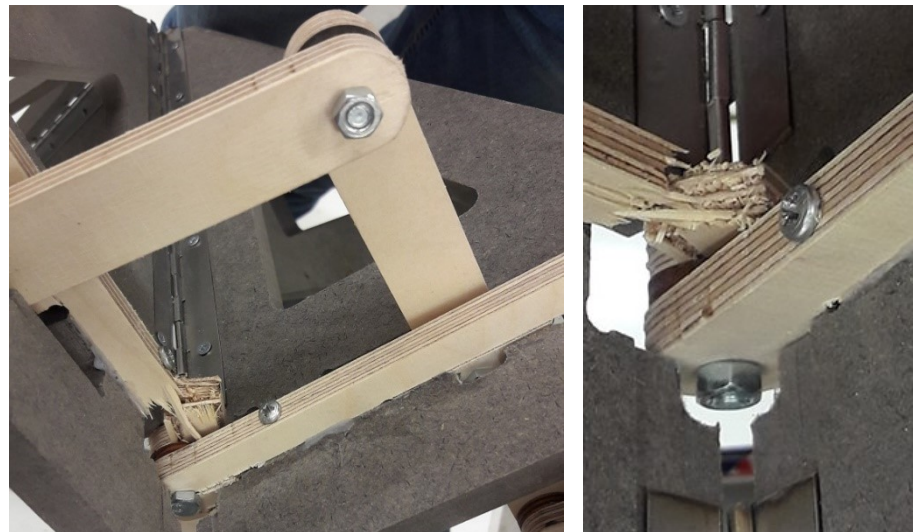


Figure 4. 61.
Broken bars of the
pantographs

The next section of the thesis will present the evaluation relating to the utilization of the workflow for the KOS PoC construction as well as the results retrieved for each of the main parameters under evaluation.

4.3 | Evaluation and Results

The construction of the KOS PoC allowed to evolve on the knowledge about CPs, mechanisms and movements investigated by this thesis. For its construction was followed the proposed step-by-step workflow which permitted to generate a functioning prototype that strictly followed the rules to achieve a rigidly folding origami tessellation, able to be used as kinetic structure for architecture, through a mechanism that allows to control the generality of the folding angles.

Next will be presented the detailed evaluation for each of the parameters used in **Section 3.5** for the evaluation of experiments 01, 02 and 03. These parameters relate to the three main areas present on the development of rigid origami surfaces to be used for kinetic architecture which are origami geometry, materials and digital fabrication and mechanisms and control.

Origami Geometry:

a) Rigid Foldability: Evaluation – 5

The designed pattern was achieved through the analysis of the tables for degree-4 and degree-6 for rigid and flat-foldable patterns which lead to the choice of the Yoshimura pattern. This pattern responds to the objectives set at the first step of the workflow that determined the use of a vaulted structure.

Through the simulator was redesigned the CP into an irregular Yoshimura pattern that can rigidly fold from the unfolded to the folded position thus achieving the highest grade possible for this parameter.

b) Flat-Foldable: Evaluation – 4

The used CP cannot achieve a completely flat-folded position due to the intersection between the bottom faces from the 76° folding angle. This means that the designed pattern cannot perform only the last 14° of folding of the 90° range. If the pattern was slightly changed it would be able to perform the entire folding, thus the grade 4.

c) Simulation's Rigidity: Evaluation – 5

The simulation is based in rigid kinematics achieved through exact geometric relations. The geometric relations were created through non changing dimensions from the unfolded pattern thus no elasticity was allowed for the dimensions of creases or faces, therefore the highest possible grade at this parameter.

d) Reality vs. Simulation: Evaluation – 5

The KOS PoC made through the ASM and with 12mm thick MDF was able to follow a folding path similar to the one generated by the rigid kinematic simulation. The analogous behaviour between reality and simulation guaranteed a 5 grade at this parameter.

Materials and Digital Fabrication:

a) Fabrication Method: Evaluation – 4

The fabrication method of cutting the individual faces through the CNC milling machine from 12mm thick MDF worked well and allowed to include several of the needs for the attachment to the mechanic system. The used material proved to be easily worked at the CNC milling machine as well as being a good fit for the needed rigidity of the faces. The design of the framed faces allowed for rigidity and inclusively for space to the adjustments made during the workflow.

The fabrication method for the mechanic system did not work so well. The design of the pantographic bars was well achieved, and they fit perfectly the intended places for implementation. In what regards rigid kinematics they also worked well and were able to easily be put in motion through the actuators. Nevertheless, the chosen material, first MDF and then plywood, did not behave properly, therefore two bars broke at the end of the movement test.

On the overall, this parameter receives an evaluation of 4.

b) Thickness Method: Evaluation – 5

The used thickness method was the ASM. This method demonstrated to be a good choice to be used on a degree-6 CP. It provokes the shift of the original rigidly folding surface turning it into an imaginary surface but guarantees the maintenance of the rigid kinematics of the entire system. Hence the best possible grade.

c) Faces behaviour: Evaluation – 5

The faces demonstrated to be able to maintain their integrity, rigidity and planarity throughout the construction process as well as during the various movement tests that the structure was subjected to. The areas that were subtracted to make the structure lighter, and the resulting frame, proved to be a well-functioning design that did not compromise the behaviour of each face. The faces maintained their planarity throughout the folding process without stretching, bending or collapsing. Therefore, this parameter achieved the grade 5.

d) Hinges behaviour: Evaluation – 5

The hinges were made with metallic piano hinges. These were placed along the entire low-relief areas between faces, this way guaranteeing the continuity of the rotation axis as well as the alignment between consecutive faces. Throughout the developed tests the hinges maintained their straightness, fluidity in rotation and good attachment to the faces. Through the good performance of the hinges, along with the planarity of faces, the system was able to behave as the rigid kinematic simulation, thus this parameter was also graded 5.

Mechanisms and Control:**a) Mechanism Behaviour: Evaluation – 4**

From the possible mechanisms to be used in kinetic structures was tried a rigid linkage mechanism through straight translational pantographic links due to the similar rigid kinematics in respect to rigidly folding origami surfaces. Four pantographs were developed and placed at specific lines of the surface with one bar of each SLE connected to the face and another bar free for rotation.

The mechanism proved to function correctly and be able to follow the rigid motion of the surface and additionally introduce synchronicity on the folding and a way of locking the movement on specific folding stages. Nevertheless, two bars broke during the tests conducted while the structure was supported on the ground. They broke because of the lack of resistance of the plywood used to create the pantograph bars and because of a torsion within the structure, that was not in accordance with the natural movement of the pantograph. For the material reason alone, the mechanism received a grade of 4 instead of 5.

b) Control of Folding Angles: Evaluation – 5

Through the developed pantograph mechanism, the attachment to the faces along specific lines and the combined work of each of the four pantographs was achieved an overall control of the folding angles of the rigidly folding origami surface. During the motion tests the surface proved to deploy and contract in a consistent way within all of the angles between faces. The control of the folding angles was very well achieved and no “curtain type” of movement was created, as determined at the first step of the workflow, therefore this parameter had an evaluation of 5.

c) Structure's Stability: Evaluation – 3

The rigid origami surface presented very good stability during the folding and unfolding tests while in a suspended mode. When the structure was tested on a supported on the ground situation its stability was less than satisfactory. The fact that there were not any fixed supporting points neither anything that would guarantee the alignment between the two extremes of the surface lead to a situation where the surface lost the movement symmetry and so was free to rotate around itself causing a torsion and losing stability.

This was the lowest graded parameter, with an evaluation of 3.

d) Computational Control: Evaluation – 5

The computational control consisted of a simple program that set the four linear actuators to start opening at the same time until reaching the end of their courses, wait 45 seconds and then initiate closure altogether. These could be set off at any time and were able to guarantee the locked motion of the structure.

The computational control worked well on every tested course and the actuators maintained the same velocity and synchronicity every time, hence the computational control parameter was graded 5.

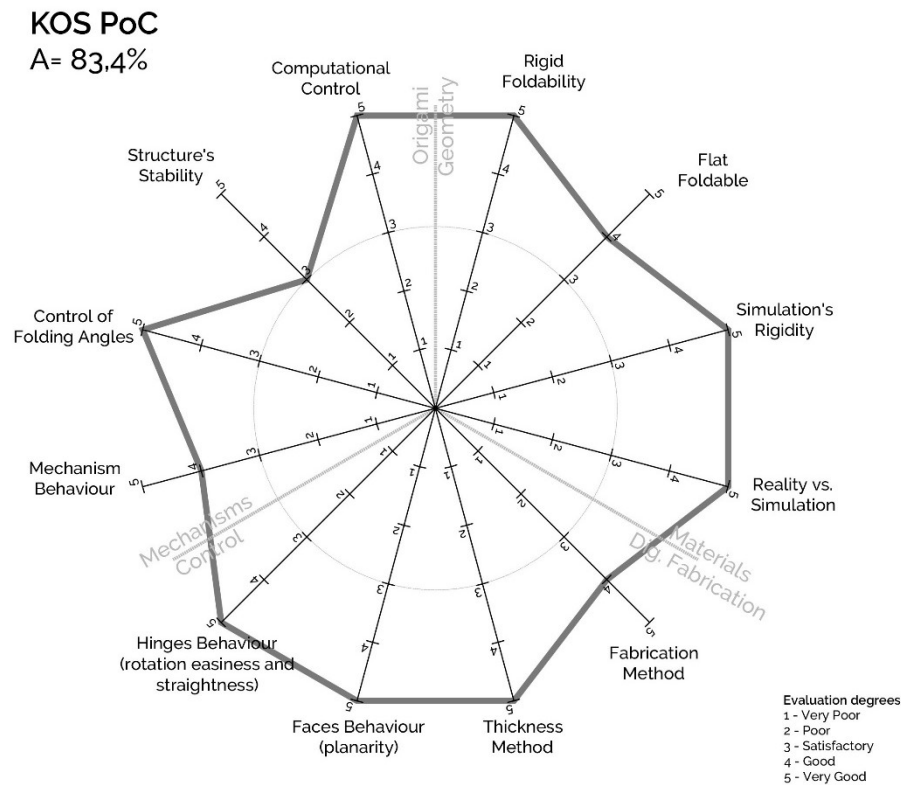


Figure 4. 62.
 Spider Scheme for
 KOS PoC prototype

From **Figure 4.62** it is possible to observe the overall evaluation of the KOS PoC. Out of the twelve parameters under evaluation it received a 5 grade on 8 of them, a 4 grade on three parameters and a 3 grade on one parameter.

The polygon that the grades generate on the scheme has a generous area, 83,4% of a dodecagon with radius value 5.

By observing the scheme, it can be concluded that the KOS PoC was generally well achieved. Nevertheless, it presents some limitations, mainly regarding the stability of the structure. If this specific limitation was corrected, for example by rails that would guarantee the alignment between the opposite supporting vertices, maybe the KOS PoC could have a better evaluation on the “structure’s stability” parameter. If there were not stability issues the torsion could be prevented and also the breaking of the pantograph bars, which would lead to a better result in the “fabrication method” and “mechanism behaviour” parameters.

When comparing the evaluation results of the KOS PoC with the previously developed experiments, whose schemes were presented in **Figure 3.114**, is possible to notice that its results are close to the best rated ones, which were experiment 02 A and 03 D. Even though the results are close, the KOS PoC brings important developments to the knowledge achieved through the former experiments. The KOS PoC is done at a larger scale with thicker materials than the ones used at experiment 03 D and with a larger tessellation than the one used for experiment 02 A.

With respect to the following of the proposed workflow, from the KOS PoC was proven that it can be of great aid for the conceptualization and construction of this type of kinetic surfaces. The workflow is based on a consequent process that allows to predict probable issues and return to previous steps for adjustments after specific evaluation points. The possibility of returning to previous steps and correcting issues was important for the development of the KOS PoC and especially used for the CP design and for the mechanism establishment. The models at small scale have proven to be a very important step inside the workflow. For the KOS PoC several corrections were made because of the tests made with these models.

From the step-by-step workflow was created a kinetic rigidly folding surface based on rigid kinematics that were preserved from simulation to construction. Every required step to achieve the KOS PoC was present at the workflow including steps for fabrication, mechanism development and computational control.

05 | CONCLUSIONS AND FUTURE WORK

05 | Conclusions and Future Work

This chapter makes a general review of the process followed by this thesis and the conclusions achieved. It starts with the motivations and proposed contributions presented in **Chapter 01**, and continues with the research development, used methodology and the conclusions that allowed to reach those contributions.

The chapter ends with proposals for progress in the developed research through a section for future work.

5.1 | Conclusions

As described in Chapter 01, this research is the result of three particular motivations. One of them is the opportunity to produce a practical contribution to the existing options within kinetic architecture for the creation of reconfigurable spaces through specific means, rigidly folding origami surfaces with regular CPs. Another purpose of the thesis is to explore the possibility of using digital tools for the form-finding process when using regular origami tessellations as surfaces for kinetic architecture. The final motivator of this research is the possibility of developing a multidisciplinary methodology containing every required step to guide designers through the design and construction process to achieve rigidly folding thick origami surfaces.

From the motivations that guided the thesis, five practical and theoretical contributions are proposed and summarised below:

Contribution 1 – Practical contribution that consists of the development of a multidisciplinary workflow through in practice demonstration. The developed workflow is intended to be used as a tool for other designers to create functional kinetic surfaces by using rigidly folding origami tessellations able to reconfigure themselves through movement.

Contribution 2 – Theoretical contribution that demonstrates that rigidly folding origami surfaces can have a distinct category within an updated kinetic architecture taxonomy. This contribution is intended to be further developed by determining the distinction between kinetic structures for architecture and the demountable/transportable structures, and by producing an additional classification for these types of structures.

Contribution 3 – Contribution that may be subdivided in two parts, one theoretical and the other practical. The theoretical part deals with the characterization of CPs that are suitable to be used in architecture. The characterization is made through analysis of the geometry of the CPs and forms into which they fold leading to a proposed establishment of CP families. The practical part of Contribution 03 consists of the elaboration of two rigid kinematic simulators for some of the previously defined CP families for degree-4 and degree-6 vertices. The provided simulators are intended to be a tool for designers by allowing them to easily use eight CPs of degree-4 and degree-6, adjust them at any stage of the folding process, as well as assessing its kinematics and exporting the generated model for structural analysis simulation or 3D modelling implementation.

Contribution 4 – Practical contribution through experimentation with geometries, materials, simulations, mechanisms and actuation in practical case studies at different scales. The case studies are developed by multidisciplinary teams and use different methodologies. The case studies are evaluated through demonstration and analysis in regard to the workflow used and specific criteria similar to each experiment. Through the process of demonstration, analysis and evaluation several conclusions are reached and inputs to aid in the development of succeeding experiments.

Contribution 5 – Practical contribution that demonstrates the applicability and the benefits of using pantograph systems fixed on specific lines of the rigidly folding surfaces. Rigidly folding origami and pantograph systems have similar kinematics and the pantographs provide the ability to control the folding angles of the surface, introduce synchronicity in the folding of the system and to lock the structure at any folding point.

In order to reach the proposed contributions this thesis focuses the research on four main areas: kinetic architecture, origami geometry, materials and digital fabrication and mechanisms and control.

So as to understand the current state-of-the-art on kinetic architecture and the possibility of placing these specific types of kinetic structures, the definitions found to have been the most relevant over the last 45 years have been studied. From the analysis of the work developed by the authors it is proven that the four most used criteria are the structural aspects, application, type of material and type of movement. It was also demonstrated that Merchant (1987), Hanaor and Levy (2001, 2009), Pellegrino (2001), Stevenson (2011),

Del Grosso and Basso (2013) and Rivas Adrover (2015) already considered rigid origami folding surfaces as a specific type of kinetic structures.

Within the analysed definitions this thesis proposes a distinction between demountable/transportable structures and kinetic structures. It is argued that the moment when movement takes place is an important factor that distinguishes the two types of structures. Nevertheless, it is acknowledged that both have similarities in their structural aspects and mechanisms. As a result, two general classifications are proposed, one for the demountable/transportable structures and another one for kinetic architecture. The proposed classifications are built from the work developed by the set of authors referred to and use the structural aspects criterion along with its close relationship to the criteria of type of materials and type of movement. The proposed classifications include every type of known structure, even the most recent ones, and have two main branches relating to the structural aspects, one for rigid components and another for deformable components as described in **Section 3.1.2**.

The validity of each branch of the taxonomy is demonstrated by the work of the reviewed authors and also by the establishment of a direct relationship between each branch and existing examples (**Table 3.1**). In **Section 2.1.2** the Ways and Means are established for kinetic architecture through the work of the revised authors. This thesis supports the use of the definition of Ways by Schumacher *et al.* (2010), which relates directly to the types of movement, and the Means by the same author along with the contributions of Fox. Regarding the Means subject, a thorough review has been made of existing mechanisms for kinetic architecture, with an emphasis on the determination of origami as a specific type of mechanism. From the analysis of the reviewed means the establishment of a link between the proposed kinetic architecture taxonomy categories and the type of movement and mechanisms is proposed (**Tables 3.3 and 3.4**)

Within the taxonomy the pertinence of a particular branch for rigid folding origami is proven since, besides the structural aspects, it has also a particular kinematics that justifies its individuality (**Section 3.3**) by being an open chain or a network of connected spherical mechanisms.

In **Section 2.2** the state-of-the-art on the geometry of origami that is considered most relevant for kinetic architecture is reviewed, as well as the existing simulators. Within the reviewed work is a description of the Huzita-Justin axioms, the rules for rigid foldability and existing strategies to transform non-rigidly folding vertices. This section also includes an explanation of the rules for flat-foldability, the Kawasaki-Justin and Maekawa-Justin theorems,

the Big-Little-Big Lemma, as well as strategies to turn non-flat foldable vertices into flat foldable. Subsequently the non-crossing conditions are designated and the strategies to test for collisions in a CP. In **Section 2.2** a review is also made of the utilization of rigidly folding origami in architecture and it is demonstrated that large tessellations are less used than modules which have a small amount of faces and centralized motion.

It is the aim of this thesis to positively argue the utilization of rigidly foldable regular CPs to be used in architecture. From the described rules and an extensive bibliographic review relating to origami tessellations, in **Section 3.2** a *Corpus* of regular and rigidly folding tessellations to be used specifically in architecture is established.

It is suggested that the *Corpus* can be divided into three families regarding their vertices degree, degree-2, degree-4 and degree-6 CPs and is demonstrated that each of the families and the identity of the vertices results in specific geometric properties and forms into which the patterns fold.

The analysis of the *Corpus* of tessellations follows a process that departs from the establishment of a set of base faces within each CP, as done by Miura (2002), Halloran (2009), Klett (2011) and Gardiner (2018). It is argued that from the base faces it is possible to evaluate the local behaviour of a tessellation and then replicate it to compose the entire tessellation and understand its global behaviour. Subsequently the three groups that compose the *Corpus* of regular tessellations to be used in architecture as kinetic folding surfaces are analysed. The CPs are systematically analysed regarding the accomplishment of the rules for rigid and flat foldability, for non-intersection and the geometries each one tends to undertake while folding as well as the relation of the geometries and the identity of the vertices that constitute the tessellation.

While analysing the tessellations throughout **Section 3.3.1** general conclusions are presented in respect to each family of CPs at the same time that particular conclusions are drawn concerning individual patterns. The information retrieved from this analysis is systematized into five tables, **Table 3.7** for degree-2 CPs, **Tables 3.9** and **3.10** for degree-4 CPs and **Tables 3.13** and **3.14** for degree-6 CPs. The provided tables resume the geometric conclusions about the studied CPs for kinetic architecture and are intended to be helpful for the design community.

From the analysis of the proposed CPs the thesis moves on to the use of origami tessellations with thickness. As argued by several authors and this research, the use of origami tessellations in architecture cannot be done with zero-thickness materials. By thickening an origami tessellation several

geometric problems may be created as well as implications regarding the rigid kinematics of the surface. In this way the known existing methods to thicken origami surfaces are presented along with several examples, in different contexts and for diverse purposes, developed by other authors. These methods are tested via the executed experiments and conclusions relating to each one presented. These conclusions regard especially the thickening of origami surfaces for architectural application

In order to conclude the state-of-the-art on origami geometry a review is made of the available digital tools for origami folding simulation. The simulators found are grouped regarding their purpose, the degree of liberty for a user to change the pattern to fold and also the feedback they can provide concerning the folding process. It is argued by this thesis that the existing simulators are not sufficiently developed to be of real aid to the designers since they are restrictive in terms of CP adjustments or in terms of the visualization and evaluation of the folding process and, consequently, the kinematics of the surface.

This thesis proposes the use of the two developed simulators (**Section 3.3.2**) as an addition to the existing simulators. The proposed simulators follow a general methodology (**Figure 3.27**) that may be used for the development of other similar Grasshopper definitions for the rigid kinematic simulation of regular origami tessellations.

Each of the provided simulators is able to fold a cluster of patterns from the family of degree-4 or degree-6 vertices, it starts by rigidly folding a set of base faces that can be adjusted in order to reproduce each pattern of the cluster. The folding of the base faces is strictly geometric to guarantee the rigidity of the simulation and the Grasshopper definition is constructed in a way that assures that the theorems and rules described in the origami geometry state-of-the-art are followed.

The first simulator developed provides the possibility of folding a cluster of degree-4 CPs, namely the Miura, stretched Miura, irregular Miura and quadrilateral meshed pattern. The second simulator allows a user to rigidly fold a cluster of degree-6 tessellations, particularly the regular Yoshimura, irregular Yoshimura, skewed Yoshimura and double helicoidal patterns.

Each of the proposed simulators allows to create a wide tessellation through vectorial copies of the base faces at the same time that it permits to change the geometry of the base faces at any stage of the folding process. This way is provided a useful tool for designers to easily test some rigidly folding origami patterns, alter the geometry for specific optimization, understand the paths followed by each part of the surface during motion, the possibility of collisions

with other objects and to export the geometry to three-dimensional models of sites and/or to structural simulators.

In **Section 3.5** the constructed experiments that facilitated the testing of workflows from concept to fabrication are described. Through these experiments diverse CPs, scales of surfaces, simulation methods were explored as well as diverse materials, digital fabrication tools and thickness methods. The conduction of such experiments, their evaluation and the related conclusions, allowed to refine the workflow proposed by this thesis. The experiments were developed by multidisciplinary teams at different stages of this research which allowed to go deeper into the extracted knowledge from each one. Each experiment was evaluated regarding the workflow followed for its development and twelve criteria relating to origami geometry and simulation, materials and digital fabrication and mechanisms and control. The evaluation of each experiment and the comparative analysis of all the experiments that followed, helped shaping the final workflow and the KOS PoC prototype at the same time that they provided specific inputs for the decision-making process in regard to origami geometry, simulation, materials, digital fabrication and control.

Through the experiments it was also possible to prove that the architect can, in fact, be the central player in a multidisciplinary workflow for the development of rigidly folding origami surfaces to be used in architecture but he should not be the only player. It is the multidisciplinary and teamwork that is the key to achieve well-functioning kinetic structures. These are complex structures and their development demands for knowledge in specific areas. The development is better achieved through multidisciplinary teams.

The proposed workflow is composed of seventeen individual steps with specific parameters to follow and four evaluation points. The steps intend to guarantee a logical sequence between the areas at play, namely conceptual intentions, origami geometry, rigid kinematics simulation, choice of materials, thickness methods and mechanisms and also, actuation and control. Aside from the four evaluation points present at specific positions within the workflow are also included steps for testing through small scale models and structural evaluation and steps for adjustments to the CP and to the chosen materials. The presented workflow is tested, and its validity proven through the construction of the KOS PoC prototype.

The KOS PoC prototype is formalized with an irregular Yoshimura pattern that was defined, simulated and adjusted through the utilization of the degree-6 simulator for rigid kinematics. The pattern has proven to be rigidly foldable but not flat-foldable due to the intersection between some faces from the 76°

folding angle. The construction of the KOS PoC used the ASM applied to 12mm thick MDF and its behaviour while folding was analogous to the simulated folding. The digital fabrication method used proved to be suitable for the transformation of the MDF and was able to produce rigorous pieces that were easily set together and materialized the kinematic simulation. The redesign of the faces, set by the step for structural evaluation from Karamba3D, allowed for the transformation of the continuous faces into lighter framed faces, that have proven to maintain the demands for rigidly folding origami surfaces, since no deformations were observed, and the faces maintained their planarity and integrity at all times. The materialization of the creases through metallic piano hinges was able to recreate the continuity of the rotation axis between faces and the hinges maintained their straightness, ability to connect consecutive faces and fluidity of rotation. In regard to the digital fabrication of the pantographic system the results were not satisfactory, since two pieces broke due to an expected torsion on the origami surface and lack of resistance of the plywood.

The utilization of pantographic systems connected to the rigidly folding origami surface along specific lines has demonstrated to be able to recreate the rigid motion simulated on the degree-6 folding simulator and introduce synchronicity in the folding process, as well as to lock the folding surface and to allow for control of the folding angles, thus inhibiting the “curtain” type of movement.

The stability of the structure when supported on the ground was not successfully achieved. Without fixed points and/or rails that would guide the surface it was too vulnerable to non-simulated forces, such as the weight of the motors in combination with movement. These forces that were not predicted during the structural simulation were the reason for the torsion that ultimately caused the collapsing of two pantograph bars.

In conclusion, the KOS PoC developed through the proposed workflow has demonstrated that the workflow allows for the generation of rigidly folding origami surfaces, with thickness and actuated through computational control via a step-by-step methodology. Nevertheless, it still has space for improvement as will be outlined in detail in the next section.

The thesis has reached the proposed contributions determined in Chapter 01. It has concluded theoretical and practical contributions for the architecture community specifically for kinetic architecture and the utilization of rigidly folding origami surfaces through a directed workflow, as have not been done before. The present research has positively contributed for the establishment of kinetic architecture typologies in line with the evolution of this matter since

the 70's through an up to date review and consequent classification of every class for kinetic architecture that places rigidly folding origami in a specific one.

From the contributions of this research may be possible to develop a new type of kinetic architectural elements able to generate spaces reconfigurable through motion that can better serve the society in which are inserted. For the development of these spaces this thesis provides insight in origami geometry and foldability, mechanisms, materials and digital fabrication along with tools for parametric simulations for rigidly folding origami surfaces and a comprehensive workflow to guide the designer through the process from concept to construction.

5.2 | Future Work

Although this research has demonstrated to have successfully contributed to the current state of kinetic architecture and the utilization of rigidly folding origami surfaces, the developed work has still space for improvement and evolution. In this way some lines of investigation can be proposed to allow for further development.

In regard to the developed **workflow** it is considered that the step for structural analysis could be improved if it was possible to have a structural simulator able to introduce movement in the structure, as well as fixed points and elements that would constrain the movement, such as rails, for example, instead of testing only static stages. It would also be interesting to make it closer to reality by introducing the weight of actuators and the forces they bring into the structural simulation. In this case the structural simulator and the kinematic simulator could be fused in one and be an even powerful tool for designers to test every specificity of rigidly folding origami surfaces. By connecting both simulators maybe it would be possible to introduce the thickness of the faces and propose areas to subtract from the results retrieved from the structural analysis. In this way a redesign version of the unfolded CP could be made, including areas to subtract, to directly inform the digital fabrication process.

Regarding specifically the rigid kinematics **folding simulators**, these could be improved in many ways. It would be important to make them more general and extend the CPs to fold. It would be interesting to find a way of having only one simulator for every CP family and extend the foldable patterns. Another line of improvement could be the introduction of irregular tessellations folding.

The possibility of introducing obstacles and different ways of support and to make the surfaces fold considering these elements could be an important contribution to the utilization of these surfaces applied to kinetic architecture. The simulators could also have an option of generating curves of the motion carried out by specific elements during folding, this way these lines could be used for the establishment of paths that could be of service in the determination of the mechanical system.

Regarding specifically the construction of the **KOS PoC** a line to follow could be the development of other versions in other materials, such as metal. It could bring about important conclusions to test the framed faces in rectangular section tubes, in aluminium for example, as well as the pantographic systems. In the development of the KOS PoC the materialization of the pantographic elements in plywood was not a good choice, maybe in metal they would have had a better behaviour

Regarding the digital fabrication process maybe a system could be developed to create the hinges directly on to the faces, thus reducing the probability of misalignments between faces and the folding accuracy of the entire system by making it a unified system, closer to the behaviour found on paper models.

REFERENCES

References

- ABEL, Z.; Cantarella, J.; Demaine, E.; Eppstein, D.; Hull, T.; Ku, J.; Lang, R.; Tachi, T.; Rigid Origami Vertices: Conditions and Forcing Sets, in *Journal of Computational Geometry*, pp. 171-184, 2016.
- ADDINGTON, M.; Schodek, D.; *Smart Materials and New Technologies - For the architecture and design professions*, Architectural Press, 2005.
- AHLQUIST, S.; Menges, A.: *Computational Design Thinking: Computation Design Thinking*, in *Architectural Design Reader, Computational Design Thinking*, 2011
- AKGUN, Y.; Charis J.; Gantes, C.; Sobekd, W.; Korkmaz, K.; Kalochairetis, K.; A novel adaptive spatial scissor-hinge structural mechanism for convertible roofs, in *Engineering Structures*, 33, pp. 1365–1376, 2011.
- ALPERIN, R.; Lang, R.; One-, Two-, and Multi-Fold Origami Axioms in *Origami4 - Fourth International Meeting of Origami Science, Mathematics, and Education*, pp. 371-394, A. K. Peters, 2009.
- ASHBY, M.; *Materials Selection in Mechanical Design*, Elsevier, 2005 (3rd Edition).
- AZUMA, H.; On the Fish Base Crease Pattern and Its Flat Foldable Property in *Origami4 - Fourth International Meeting of Origami Science, Mathematics, and Education*, pp. 417-428, A. K. Peters, 2009.
- BALKCOM, D.; Demaine, E.; Demaine, M.; Ochsendorf, J.; You, Z.; *Folding Paper Shopping Bags* in *Origami4 - Fourth International Meeting of Origami Science, Mathematics, and Education*, pp. 315-333, A. K. Peters, 2009.
- BARRETO, P. T.; *Lines Meeting on a Surface - The Mars Paperfolding* in *Origami Science and Art, Proceedings of the Second International Meeting of Origami Science and Scientific Origami*, pp. 343-360, Tokyo Seian University of Art and Design, 1994.
- BATEMAN, A.; *Computer Tools and Algorithms for Origami Tessellation Design*, in *Origami3 - Third International Meeting of Origami Science, Mathematics, and Education*, pp. 121-127, A. K. Peters, 2002.
- BERN, M.; Demaine, E.; Eppstein, D.; Hayes, B.; A Disk-Packing Algorithm for an Origami Magic Trick. in *Origami3 - Third International Meeting of*

- Origami Science, Mathematics, and Education, pp. 17-28, A. K. Peters, 2002.
- BERN, M.; Hayes, B.; *The Complexity of Flat Origami*, in Proceedings of the 7th ACM-SIAM Symposium on Discrete Algorithms, New York/Philadelphia, pp. 175–183, 1996.
- BOWEN, L.; Grames, C.; Magleby, S.; Howell, L.; Lang, R.; A Classification of Action Origami as Systems of Spherical Mechanisms, in Journal of Mechanical Design, Vol. 135, Issue 11, ASME, 2013.
- BRITT, A.; Lalvani, H.; Symmetry as a Basis for Morphological Analysis and Generation of NASA-Type Cubic Deployables, in IUTAM-IASS Symposium on Deployable Structures: Theory and Applications. Solid Mechanics and Its Applications, vol 80, pp.45-54, Springer, 2000.
- BURRY, M.; Burry, J.; Prototyping for Architects, Thames & Hudson, 2016
- CACHIM, P.; Construções em Madeira - a Madeira como Material de Construção, Publindústria, 2007.
- CASALE, A.; Valenti, G. M.; Architettura delle Superfici Piegate: le Geometrie che Muovono gli Origami, Nuovi Quaderni di Applicazioni della Geometria Descrittiva, Edizioni Kappa, 2012
- CASALE, A.; Valenti, G. M.; Calvano, M.; From Origami to Folded Surfaces: Representing Moving Forms, in the 17th International Conference on Geometry and Graphics, pp. 0-11, 2016
- CHENG, H. Y.; A General Method of Drawing Biplanar Crease Patterns, in Origami5 - Fifth International Meeting of Origami Science, Mathematics, and Education, pp. 421-435, A K Peters/CRC Press, 2011.
- DE LAS PEÑAS, M. L. A. N.; Taganap, E. C.; Rapanut, T. A.; Color Symmetry Approach to the Construction of Crystallographic Flat Origami, in Origami 6 - Sixth International Meeting on Origami Science, Mathematics, and Education, I: Mathematics, pp. 11-20, American Mathematical Society, 2015.
- DE RUYSSER, T.; Wearable Metal Origami, in Origami 6 - Sixth International Meeting on Origami Science, Mathematics, and Education, II: Technology, Art, Education, pp. 613-624, American Mathematical Society, 2015.

- DE TEMMERMAN, N.; Alegria Mira, L.; Vergauwen, A.; Hendrickx, H.; De Wilde, W. P.; Transformable Structures in Architectural Engineering, in High Performance Structure and Materials VI, pp. 457-468, WIT Press, 2012.
- DEL GROSSO, A. E.; Basso, P.; Deployable Structures, in Advances in Science and Technology Vol. 83 pp 122-131, Trans Tech Publications, 2013.
- DEMAINE, E.; Demaine, M.; Hart, V.; Price, G.; Tachi, T.; (Non)existence of Pleated Folds: How Paper Folds Between Creases, in Graphs and Combinatorics, Vol. 27, 3, pp. 377-397, Springer Japan, 2011 (a).
- DEMAINE, E.; Demaine, M.; Huffman, D.; Koschitz, D.; Tachi, T.; Conic Crease Patterns with Reflecting Rule Lines, in Origami 7, Seventh International Meeting on Origami in Science, Mathematics, and Education, Vol.2: Mathematics, pp. 573-589, Tarquin Group, 2018.
- DEMAINE, E.; Demaine, M.; Koschitz, D.; Reconstructing David Huffman's Legacy in Curved-Crease Folding, in Origami5 - Fifth International Meeting of Origami Science, Mathematics, and Education, pp. 39-52, A K Peters/CRC Press, 2011 (b).
- DEMAINE, E.; Demaine, M.; Koschitz, D.; Tachi, T.; A Review on Curved Creases in Art, Design and Mathematics, in Symmetry: Culture and Science, Vol. 26, No. 2, pp. 145-161, 2015
- DEMAINE, E.; Demaine, M.; Recent Results in Computational Origami, in Origami3 - Third International Meeting of Origami Science, Mathematics, and Education, pp. 3-16, A. K. Peters, 2002.
- DEMAINE, E.; O'Rourke, J.; Geometric Folding Algorithms: Linkages, Origami, Polyhedra, Cambridge University Press, 2007.
- DUREISSEIX, D.; An Overview of Mechanisms and Patterns with Origami, in International Journal of Space Structures, Multi-Science Publishing, 27 (1), pp.1-14, 2012.
- EDMONDSON, B.; Lang, R.; Morgan, M.; Magleby, S.; Howell, L.; Thick Rigidly Foldable Structures Realized by an Offset Panel Technique, in Origami 6 - Sixth International Meeting on Origami Science, Mathematics, and Education, I: Mathematics, pp. 149-161, American Mathematical Society, 2015.

- EL RAZAZ, Z.; Sustainable vision of kinetic architecture, in *Journal of Building Appraisal* Vol. 5, 4, pp. 341–356, Macmillan Publishers, 2010.
- ENGEL, H.; *Sistemas Estruturais*; Editorial Gustavo Gili, 2001.
- ESCRIG, F.; Valcarcel, J.; *Geometry of Expandable Space Structures*, *International Journal of Space Structures*, Vol.8 No. 1/2, pp. 71-84, 1993.
- EVANS, T.; Lang, R.; Magleby, S.; Howell, L.; *Rigidly Foldable Origami Gadgets and Tessellations*, *R. Soc. open sci.*2: 150067, 2015 (a).
- EVANS, T.; Lang, R.; Magleby, S.; Howell, L.; *Rigidly Foldable Origami Twists in Origami 6 - Sixth International Meeting on Origami Science, Mathematics, and Education, I: Mathematics*, pp. 119-130, American Mathematical Society, 2015 (b).
- FASTAG, J.; *eGami: Virtual Paperfolding and Diagramming Software*, in *Origami4 - Fourth International Meeting of Origami Science, Mathematics, and Education*, pp. 273-283, A. K. Peters, 2009
- FENCI, G.; Currie, N.; *Deployable structures classification: A review*. *International Journal of Space Structures*. 2017. Vol. 32, no. 2, pp. 112–130, 2017.
- FOX, M.; *Bio Robotic Architecture*, in *Building Dynamics: Exploring Architecture of Change*, pp.161-176, Routledge, 2015.
- FOX, M.; Kemp, M.; *Interactive Architecture*, New York, Princeton Architectural Press, 2009.
- FOX, M.; Yeh, B.; *Intelligent Kinetic Systems in Architecture*, in *1st International Workshop on Managing Interactions in Smart Environments (MANSE'99)*, pp. 91-103, Dublin, Springer, London, 2000.
- FOX, M.; *Kinetic Architectural Systems Design*, in Kronenburg, R., *Transportable Environments 2*, pp. 163-186, Spon Press, London, 2003.
- FUJIMOTO, S.; Nishiwaki, M.; *Sozo Suru Origami Asobi e no Shotai (Invitation to Creative Playing with Origami, in Japanese)*. Osaka, Japan: Asahi Culture Center, 1982.
- FUSE, T.; *Spiral: Origami, Art, Design*, Viereck Verlag, 2012

- GARDINER, M.; A Brief History of Oribotics, in Origami4 - Fourth International Meeting of Origami Science, Mathematics, and Education, pp. 51-60, A. K. Peters, 2009.
- GARDINER, M.; Oribotics: The Future Unfolds, in Origami5 - Fifth International Meeting of Origami Science, Mathematics, and Education, pp. 127-137, A K Peters/CRC Press, 2011.
- GARDINER, M.; PhD Thesis; ORI*: On the Aesthetics of Folding and Technology, University of Newcastle, Australia, 2018.
- GJERDE.E.; Origami Tessellations: Awe-Inspiring Geometric Designs. AK Peters Ltd., 2008.
- GRAY, S.; Zeichner, N. J.; Yim, M.; Kumar, V.; A Simulator for Origami-Inspired Self-Reconfigurable Robots, in Origami5 - Fifth International Meeting of Origami Science, Mathematics, and Education, pp. 323-333, A K Peters/CRC Press, 2011.
- GUIMARÃES, N.; Paio, A.; Oliveira, S.; Osório, F. C.; Oliveira, M; (editors); Architecture INPLAY International Conferences Proceedings, 2016
- HALLORAN, E.; Concepts and Modelling of a Tessellated Molecule Surface in Origami4 - Fourth International Meeting of Origami Science, Mathematics, and Education, pp. 305-314, A. K. Peters, 2009.
- HANAOR, A.; Some Structural-Morphological Aspects of Deployable Structures for Space Enclosures, in An Anthology for Structural Morphology, pp. 83-108, World Scientific Publishing, 2009.
- HATORI; K.; *History of Origami in the East and the West before Interfusion*, in Origami⁵ - Fifth International Meeting of Origami Science, Mathematics, and Education, pp. 3-11, A K Peters/CRC Press, 2011.
- HAWKES, E.; An, B.; Benbernou, N. M.; Tanaka, H.; Kim, S.; Demaine, E.; Rus, D.; Wood, R. J.; Programmable Matter by Folding, in Proceedings of the National Academy of Sciences of the USA, vol.107, pp. 12441–12445, 2010.
- HENRIQUES, G. C.; TetraScript: A Responsive Pavilion, From Generative Design to Automation, in International Journal of Architectural Computing, Built Environment, Architectural Theory and Computer Aided Architectural Design, Issue 1, Vol. 10, pp. 87-104, Multi Science Publishing, 2012

- HOBBERMAN, C.; Company Profile and Selected Works: 1990 – 2012, 2012
(www.hoberman.com).
- HOBBERMAN, C.; Radial expansion/retraction truss structures, US Patent No.
5,024,031, 1991.
- HOBBERMAN, C.; Reversibly Expandable Three-Dimensional Structure, US
Patent No. 4,780,344, 1988.
- HOBBERMAN, C.; Transformable: Building Structures that Change
Themselves, in Building Dynamics: Exploring Architecture of Change,
pp.101-126, Routledge, 2015.
- HULL, T.; Coloring Connections with Counting Mountain-Valley Assignments,
in Origami 6 - Sixth International Meeting on Origami Science,
Mathematics, and Education, I: Mathematics, pp. 3-10, American
Mathematical Society, 2015.
- HULL, T.; Project Origami: Activities for Exploring Mathematics, CRC Press,
Taylor and Francis Group, 2013.
- HULL, T.; The Combinatorics of Flat Folds: A Survey, in Origami3 - Third
International Meeting of Origami Science, Mathematics, and Education,
pp. 29-38, A. K. Peters, 2002.
- IKEGAMI, U.; Fractal Crease Patterns, in Origami4 - Fourth International
Meeting of Origami Science, Mathematics, and Education, pp. 31-40,
A. K. Peters, 2009.
- JACKSON, P.; Folding Techniques for Designers: From Sheet to Form,
Laurence, King Publishing, London, 2011.
- JENSEN, F.; Pellegrino, S.; Expandable Structures formed by Hinged Plates,
in Fifth International Conference on Space Structures, University of
Surrey, 2002.
- JENSEN, F.; PhD Thesis; Concepts for Retractable Roof Structures,
University of Cambridge, 2004.
- KASSABIAN, P. E.; You, Z.; Pellegrino, S.; Retractable roof structures, in
Proceedings of the Institution of Civil Engineers, Structures 8 Buildings,
134, pp. 45- 56, 1999.

- KAWAMURA, M.; Origami with Trigonometric Functions, in Origami3 - Third International Meeting of Origami Science, Mathematics, and Education, pp. 169-178, A. K. Peters, 2002.
- KAWASAKI, T.; The Geometry of Orizuru, in Origami3 - Third International Meeting of Origami Science, Mathematics, and Education, pp. 61-73, A. K. Peters, 2002.
- KLETT, Y.; Drechsler, K.; Designing Technical Tessellations, in Origami5 - Fifth International Meeting of Origami Science, Mathematics, and Education, pp. 305-322, A K Peters/CRC Press, 2011.
- KOLAREVIC, B; Towards Architecture of Change, in Building Dynamics: Exploring Architecture of Change, pp.1-16, Routledge, 2015.
- KOLOVSKY, M.; Evgrafov, A.; Semenov, J.; Slousch, A.; Advanced Theory of Mechanisms and Machines, Springer, 2000.
- KONG, M.; Januário, P; Remeshylo-Rybchynska, O.; Paper Architecture and Parametric Design Workbook, Lviv Polytechnic Publishing House, 2015.
- KORKMAZ K.; PhD Thesis; An analytical study of the design potentials in kinetic architecture. İzmir: İzmir Institute of Technology, 2004.
- KRESLING, B.; Folded and Unfolded Nature, in Origami Science and Art, Proceedings of the Second International Meeting of Origami Science and Scientific Origami, pp. 93-108, Tokyo Seian University of Art and Design, 1997.
- KRONENBURG, R.; Flexible Architecture: Continuous and Developing, in Building Dynamics: Exploring Architecture of Change, pp.29-42, Routledge, 2015.
- KRONENBURG, R.; Portable Architecture, Elsevier/Architectural Press, 2003.
- LANG, R.; Bateman, A.; Every Spider Web has a Simple Flat Twist Tessellation, in Origami5 - Fifth International Meeting of Origami Science, Mathematics, and Education, pp. 455-473, A K Peters/CRC Press, 2011.
- LANG, R.; Demaine, E.; Facet Ordering and Crease Assignment in Uniaxial Bases in Origami4 - Fourth International Meeting of Origami Science, Mathematics, and Education, pp. 189-205, A. K. Peters, 2009.

- LANG, R.; Origami and Geometric Constructions, langorigami.com, 2010.
- LANG, R.; Origami Design Secrets: Mathematical Method for an Ancient Art, CRC Press, 2011.
- LANG, R.; Polypolyhedra in Origami, in Origami3 - Third International Meeting of Origami Science, Mathematics, and Education, pp. 153-167, A. K. Peters, 2002.
- LANG, R.; Twists, Tilings, and Tessellations - Mathematical Methods for Geometric Origami, CRC Press by Taylor & Francis Group, 2018.
- LEBÉE. A.; From Folds to Structures, a Review, in International Journal of Space Structures, 30 (2), pp. 55-74, Multi-Science Publishing, 2015.
- LI, R.; Yao, Y.; Kong, X.; A class of reconfigurable deployable platonic mechanisms, in Mechanism and Machine Theory, 105, pp. 409–427, 2016.
- MADEN, F.; Korkmaz, K.; Akgun, Y.; A Review of Planar Scissor Structural Mechanisms: Geometric Principles and Design Methods, Architectural Science Review, 54:3, pp. 246-257, Taylor and Francis Group, 2011.
- MEGAHED, N.; Understanding kinetic architecture: typology, classification, and design strategy, in Architectural Engineering and Design Management, 13:2, pp. 130-146, 2017.
- MERCHAN, C.; Deployable Structures, MSc Thesis, MIT - Massachusetts Institute of Technology, 1987
- MITANI, J.; Oripa: Origami Pattern Editor, 2005. (available at mitani.cs.tsukuba.ac.jp/pukiwiki-oripa/)
- MIURA, K.; The Application of Origami Science to Map and Atlas Design in Origami3 - Third International Meeting of Origami Science, Mathematics, and Education, pp. 137-146, A. K. Peters, 2002.
- MIURA, K.; The Science of Miura-Ori: A Review, in Origami4 - Fourth International Meeting of Origami Science, Mathematics, and Education, pp. 87-99, A. K. Peters, 2009.
- MOLONEY, J., Designing Kinetics for Architectural Facades - State change, Routledge, 2011.
- NEGROPONTE, N; The Architecture Machine: Toward a More Human Environment, The MIT Press, 1973

- OSÓRIO, F.; Paio, A.; Oliveira, S.; Kinetic Origami Surfaces, From Simulation to Fabrication, in Proceedings of the 17th International Conference, CAAD Futures 2017, Istanbul, Turkey, pp. 229-248, 2017.
- PARLAC, V.; Material as Mechanism in Agile Spaces, in Building Dynamics: Exploring Architecture of Change, pp.176-190, Routledge, 2015. (a)
- PELLEGRINO, S.; Deployable Structures in Engineering, in Deployable Structures, International Centre for Mechanical Sciences, Courses and Lectures - No. 412, pp. 1-35, Springer-Verlag Wien New York, 2001.
- PIKER, D.; Kangaroo: Form Finding with Computational Physics, Architectural Design, Vol.83 (2), pp. 136-137, 2013
- PREISINGER, C.; Karamba3D Parametric Engineering, User Manual Version 1.3.1, 2018
- PREISINGER, C.; Linking Structure and Parametric Geometry in Architectural Design, 83: pp. 110-113. doi: 10.1002/ad.1564, 2013 (Karamba 3D Software).
- RIVAS ADROVER, E.; Deployable Structures, Laurence King Publishing Ltd., United Kingdom, 2015.
- ROW, T. S.; *Geometric Exercises in Paper Folding*, Addison & Co., 1893.
- SCHÖN, D.; The Reflective Practitioner: How Professionals Think in Action, Basic Books, 1984
- SCHUMACHER, M.; Schaeffer, O.; Vogt, M.; Move: Architecture in Motion - Dynamic Components and Elements, Birkhauser, Germany, 2010.
- SCIMEMI, B.; Paper-Folding Constructions in Euclidean Geometry: An Exercise in Thrift, in Origami3 - Third International Meeting of Origami Science, Mathematics, and Education, pp. 107-117, A. K. Peters, 2002.
- SEYMOUR, K.; Burrow, D.; Avila, A.; Bateman, T.; Morgan, D.; Magleby, S.; Howell, L.; Origami-Based Deployable Ballistic Barrier, in Origami 7, Seventh International Meeting on Origami in Science, Mathematics, and Education, Vol.3: Engineering One, pp. 763-777, Tarquin Group, 2018.
- STEVENSON, C.; Morphological Principles of Kinetic Architectural Structures in Adaptive Architecture Conference, pp. 1-12, London, 2011.

- SZINGER, J.; The Foldinator Modeler and Document Generator, in Origami3 - Third International Meeting of Origami Science, Mathematics, and Education, pp. 129-135, A. K. Peters, 2002.
- TACHI, T.; 3D Origami Design Based on Tucking Molecules, in Origami4 - Fourth International Meeting of Origami Science, Mathematics, and Education, pp. 259-272, A. K. Peters, 2009 (b).
- TACHI, T.; Rigid Folding of Periodic Origami Tessellations, in Origami 6 - Sixth International Meeting on Origami Science, Mathematics, and Education, I: Mathematic, pp. 97-108, American Mathematical Society, 2015.
- TACHI, T.; Rigid-Foldable Thick Origami, in Origami5 - Fifth International Meeting of Origami Science, Mathematics, and Education, pp. 253-264, A K Peters/CRC Press, 2011.
- TACHI, T.; Simulation of Rigid Origami, in Origami4 - Fourth International Meeting of Origami Science, Mathematics, and Education, pp. 175-188, A. K. Peters, 2009 (a).
- TERZIDIS, K.; Algorithmic Architecture, Architectural Press, 2006
- TRAUTZ, M.; Kunstler, A.; Deployable Folded Plate Structures - Folding Patterns Based On 4-Fold-Mechanism Using Stiff Plates." In Proceedings of the International Association for Shell and Spatial Structures (IASS) Symposium 2009, pp. 2306-2317, Valencia, 2009.
- TSURUTA, N.; Mitani, J.; Kanamori, Y.; Fukui, Y.; A CAD System for Diagramming Origami with Prediction of Folding Processes, in Origami5 - Fifth International Meeting of Origami Science, Mathematics, and Education, pp. 335-346, A K Peters/CRC Press, 2011.
- VALCÁRCEL, J.; Escrig, F.; La Obra Arquitectónica de Emilio Pérez Piñero, Boletín Académico, Nº. 16, pp. 3-12, 1992.
- WANG, C.; Li, J. L.; You, Z.; A Kirigami-Inspired Foldable Model for Thick Panels, in Origami 7, Seventh International Meeting on Origami in Science, Mathematics, and Education, Vol.3: Engineering One, pp. 715-730, Tarquin Group, 2018.
- WANG, K; Chen, Y.; Folding a Patterned Cylinder by Rigid Origami, in Origami5 - Fifth International Meeting of Origami Science, Mathematics, and Education, pp. 265-276, A K Peters/CRC Press, 2011.

- WATANABE, N.; Kawaguchi, K.; The Method for Judging Rigid Foldability, in Origami4 - Fourth International Meeting of Origami Science, Mathematics, and Education, pp. 165-174, A. K. Peters, 2009.
- YAR, M.; Korkmaz, K.; Kiper, G.; Maden, F.; Akgün, Y.; Aktas, E.; A Novel Planar Scissor Structure Transforming Between Concave and Convex Configurations, in International Journal of Computational Methods and Experimental Measurements, Vol. 5, Issue 4, pp. 442-450, WitPress, 2017.
- YOU, Z.; Chen, Y.; Motion Structures: Deployable Structural Assemblies of Mechanisms, Spon Press, 2012.
- YOU, Z.; Kuribayashi, K.; Expandable Tubes with Negative Poisson's Ratio and their Application in Medicine, in Origami4 - Fourth International Meeting of Origami Science, Mathematics, and Education, pp. 117-127, A. K. Peters, 2009.
- YOU, Z.; Pellegrino, S.; Foldable Bar Structures, in International Journal of Solids and Structures, vol. 34, no. 15, pp. 1825–1847, 1997.
- ZEIGLER, T. R.; Collapsible self-supporting structures, US Patent No. 4,026,313, 1977.
- ZHANG, K.; Qiu, C.; Dai, J. S.; Screw Algebra and Static Modelling of Origami Inspired Mechanisms, in Origami 6 - Sixth International Meeting on Origami Science, Mathematics, and Education, I: Mathematics, pp. 139-148, American Mathematical Society, 2015.
- ZUK, W.; Clark, R.; Kinetic Architecture, Van Nostrand Reinhold, New York, 1970.

Website References

- ahr-global.com (last accessed on 30-10-2019)
- amirshahrokhi.christopherconnock.com (last accessed on 30-10-2019)
- archdaily.com/270592/ (last accessed on 30-10-2019)
- architectureinplay2016.weebly.com (last accessed on 30-10-2019)
- blumenlumen.com *or* foldhaus.com (last accessed on 30-10-2019)
- compliantmechanisms.byu.edu (last accessed on 30-10-2019)
- davidletellier.net (last accessed on 30-10-2019)
- fishtnk.com (last accessed on 30-10-2019)
- langorigami.com (last accessed on 30-10-2019)
- matthewgardiner.net *or* oribotics.net (last accessed on 30-10-2019)
- mitani.cs.tsukuba.ac.jp/oripa/ (last accessed on 30-10-2019)
- origami.c.u-tokyo.ac.jp/~tachi/software/ (last accessed on 30-10-2019)
- ottocad.net (last accessed on 2018)
- ozeloffice.com (last accessed on 30-10-2019)
- responsivekinematics.blogspot.com (last accessed on 30-10-2019)
- rvtr.com (last accessed on 30-10-2019)
- tsg.ne.jp/TT/ (last accessed on 30-10-2019)

Film References

- GOULD, V.; Documentary: Between the Folds, PBS Independent Lens, Green Fuse Films, Kanopy Streaming, PBS, 2009.
- HOLT, S.; Vives, F., X.; Bamas, A.; Wolff, M.; Bartlmae, E.; The Origami Revolution: Discover How Scientists Are Using Origami to Transform Our World, PBS, 2017
- RESCH, R.; Armstrong, E.; The Paper and Stick Film – Works from 1960-1966, Salt Lake City, UT: Resch Films, 1992

ANNEXES

Annex I

Algorithm for rigidly folding of Degree-4 Crease Patterns

Relation between Clusters

Available at cutt.ly/FilipaOsorio_KOS

Control

Step 01

Vx = Bx = Dx ?
Toggle True

Points B and D x coordinate if different from Vx
Dx:

Point D y coordinate
Dy = Vy slider:

Point B y coordinate
By = Vy + slider:

Point V coordinates
Vx:
Vy:

Point A x coordinate
Ax:

Point A y coordinate
Ay:

Point AB y coordinate
Ay:

Number of Columns
Count:

Number of lines
Count:

Folding to 90°
Folding:

Step 02


Step 04

Step 03

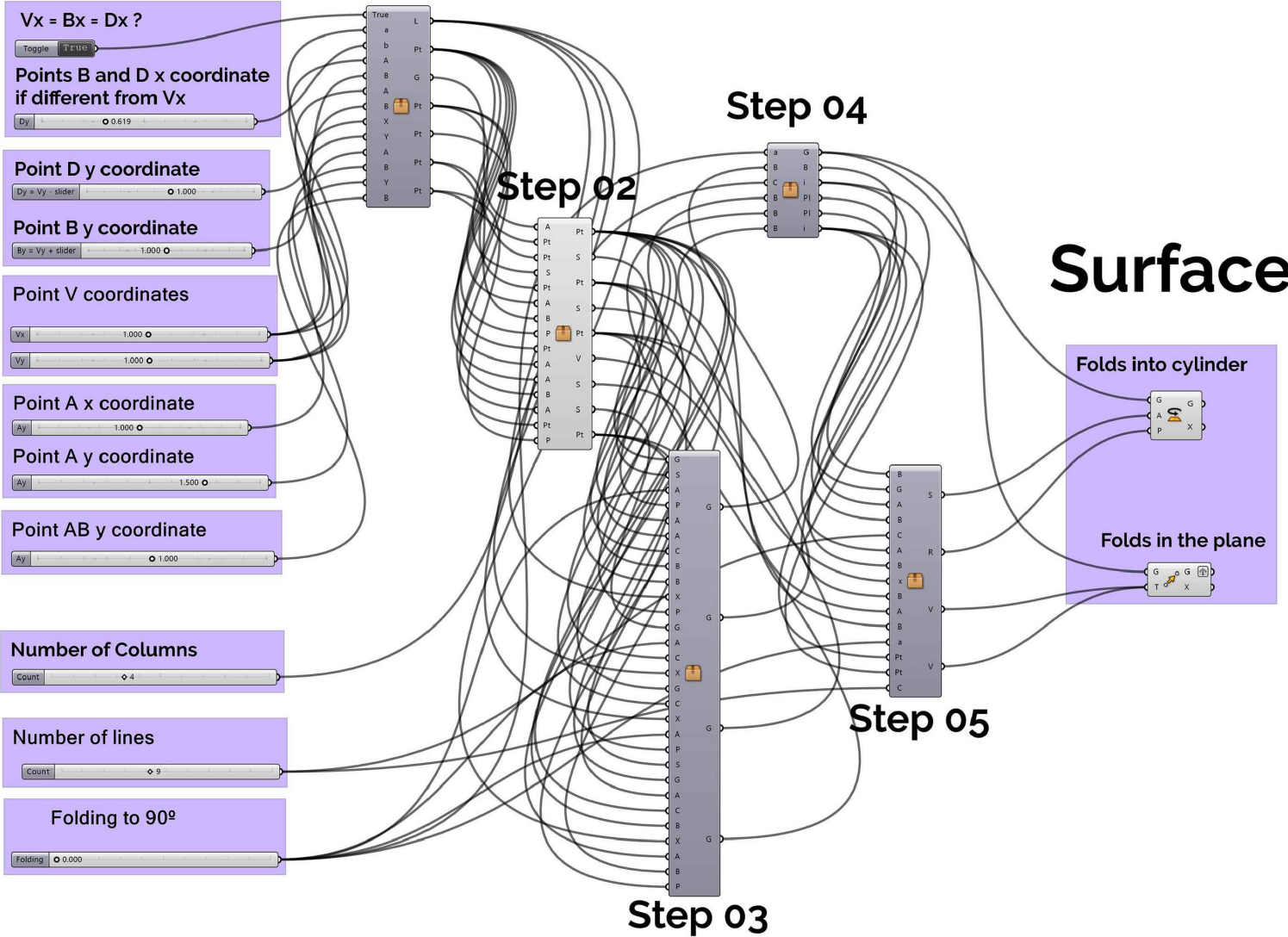

Step 05

Surface

Folds into cylinder



Folds in the plane



Control

Vx = Bx = Dx ?

Points B and D x coordinate if different from Vx

Point D y coordinate

Point B y coordinate

Point V coordinates

Point A x coordinate

Point A y coordinate

Point AB y coordinate

Number of Columns

Number of lines

Folding to 90°

Step 01

Crease b

Point B

Point D

Crease d

Point A

Crease a

Point AB

Point V

Point V

Step 02

Summary of Points

Point CD

Point V

Point A

Point AB

Point D

Point B

Point BC

Point C

Point DA

Point V

Point Ax

Point V

Point V

Point V

Point V

Point V

Point V

Point V

Point V

Point V

Point V

Point V

Point V

Point V

Point V

Point V

Point V

Point V

Point V

Point V

Point V

Point V

Point V

Point V

Point V

Point V

Point V

Point V

Point V

Point V

Point V

Point V

Point V

Point V

Point V

Point V

Point V

Point V

Point V

Point V

Point V

Point V

Point V

Point V

Point V

Point V

Point V

Point V

Point V

Point V

Point V

Point V

Point V

Point V

Point V

Point V

Point V

Point V

Point V

Point V

Point V

Point V

Point V

Point V

Point V

Point V

Point V

Point V

Point V

Point V

Point V

Point V

Point V

Point V

Point V

Point V

Point V

Point V

Point V

Point V

Point V

Point V

Point V

Point V

Point V

Point V

Point V

Point V

Point V

Point V

Point V

Point V

Point V

Point V

Point V

Point V

Point V

Point V

Point V

Point V

Point V

Point V

Point V

Point V

Point V

Point V

Point V

Point V

Point V

Point V

Point V

Point V

Point V

Point V

Point V

Point V

Point V

Point V

Point V

Point V

Point V

Point V

Point V

Point V

Point V

Point V

Point V

Point V

Point V

Point V

Point V

Point V

Point V

Point V

Point V

Point V

Point V

Point V

Point V

Point V

Point V

Point V

Point V

Point V

Point V

Point V

Point V

Point V

Point V

Point V

Point V

Point V

Point V

Point V

Point V

Point V

Point V

Point V

Point V

Point V

Point V

Point V

Point V

Point V

Point V

Point V

Point V

Point V

Point V

Point V

Point V

Point V

Point V

Point V

Point V

Point V

Point V

Point V

Point V

Point V

Point V

Point V

Point V

Point V

Point V

Point V

Point V

Point V

Point V

Point V

Point V

Point V

Point V

Point V

Point V

Point V

Point V

Point V

Point V

Point V

Point V

Point V

Point V

Point V

Point V

Point V

Point V

Point V

Point V

Point V

Point V

Point V

Point V

Point V

Point V

Point V

Point V

Point V

Point V

Point V

Point V

Point V

Point V

Point V

Point V

Point V

Point V

Point V

Point V

Point V

Point V

Point V

Point V

Point V

Point V

Point V

Point V

Point V

Point V

Point V

Point V

Point V

Point V

Point V

Point V

Point V

Point V

Point V

Point V

Point V

Point V

Point V

Point V

Point V

Point V

Point V

Point V

Point V

Point V

Point V

Point V

Point V

Point V

Point V

Point V

Point V

Point V

Point V

Point V

Point V

Point V

Point V

Point V

Point V

Point V

Point V

Point V

Point V

Point V

Point V

Point V

Point V

Point V

Point V

Point V

Point V

Point V

Point V

Point V

Point V

Point V

Point V

Point V

Point V

Point V

Point V

Annex II

Algorithm for rigidly folding of Degree-6 Crease Patterns

Relation between Clusters

Available at cutt.ly/FilipaOsorio_KOS

Control

Decision between Skewed Yoshimura and Double Helicoidal

Double Helicoidal?

Yes No

Point A x coordinate

Point B y coordinate

Length

Columns

Irregular Yoshimura

Point C y coordinate

Point D y coordinate

Point E y coordinate

Point F y coordinate

Point G y coordinate

Point H y coordinate

Point I y coordinate

Skewed Yoshimura or Double Helicoidal

Base Faces for Double Helicoidal or Skewed Yoshimura

CP and Folding Double Helicoidal or Skewed Yoshimura

Points for Double Helicoidal or Skewed Yoshimura

Regular Yoshimura

FOLDING Set of base faces

SURFACE

Points for Regular Yoshimura

Irregular Yoshimura

FOLDING First set of base faces

FOLDING Second set of base faces

Surface

FOLDING Third set of base faces

FOLDING Fourth set of base faces

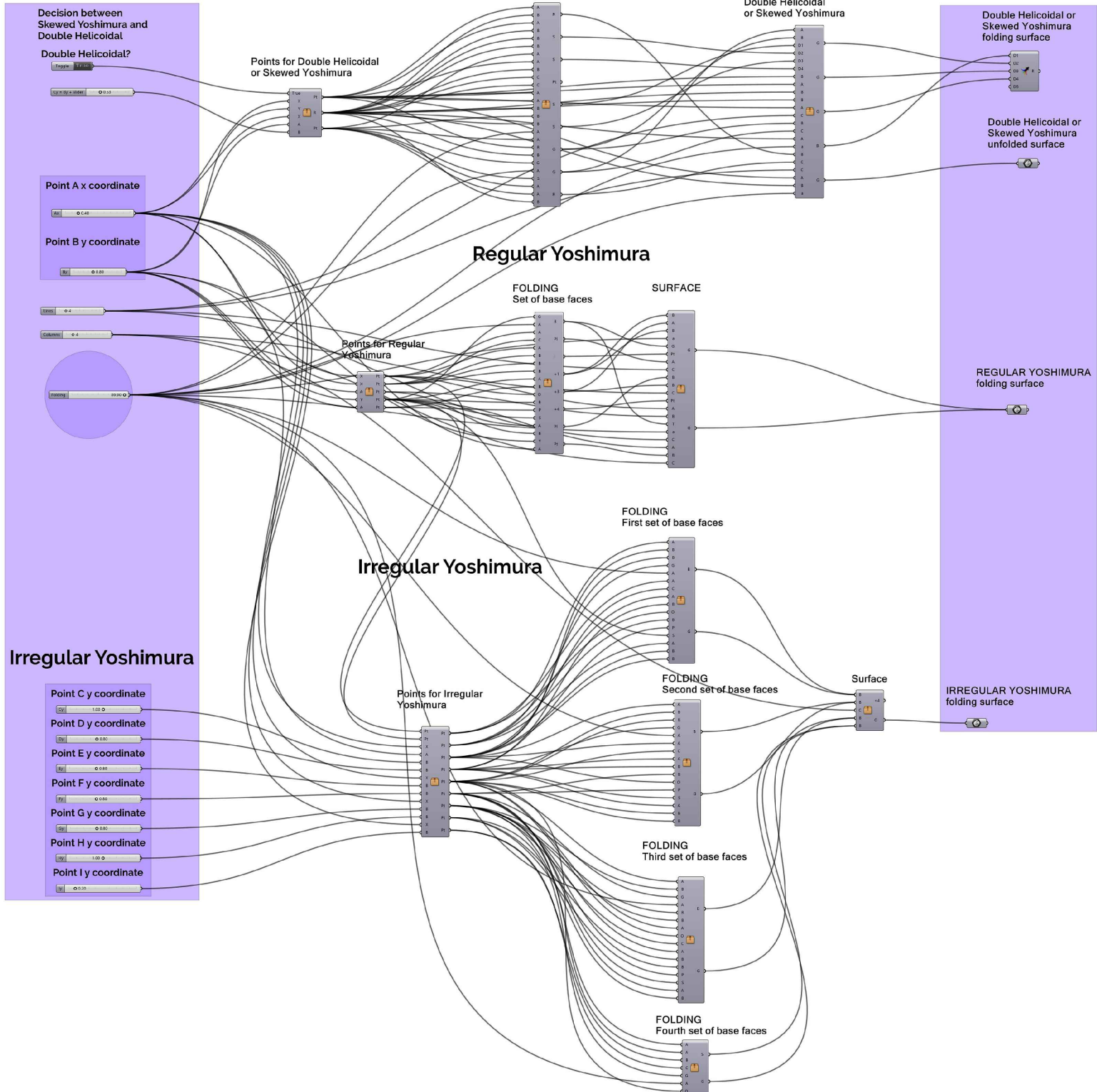
Surfaces

Double Helicoidal or Skewed Yoshimura folding surface

Double Helicoidal or Skewed Yoshimura unfolded surface

REGULAR YOSHIMURA folding surface

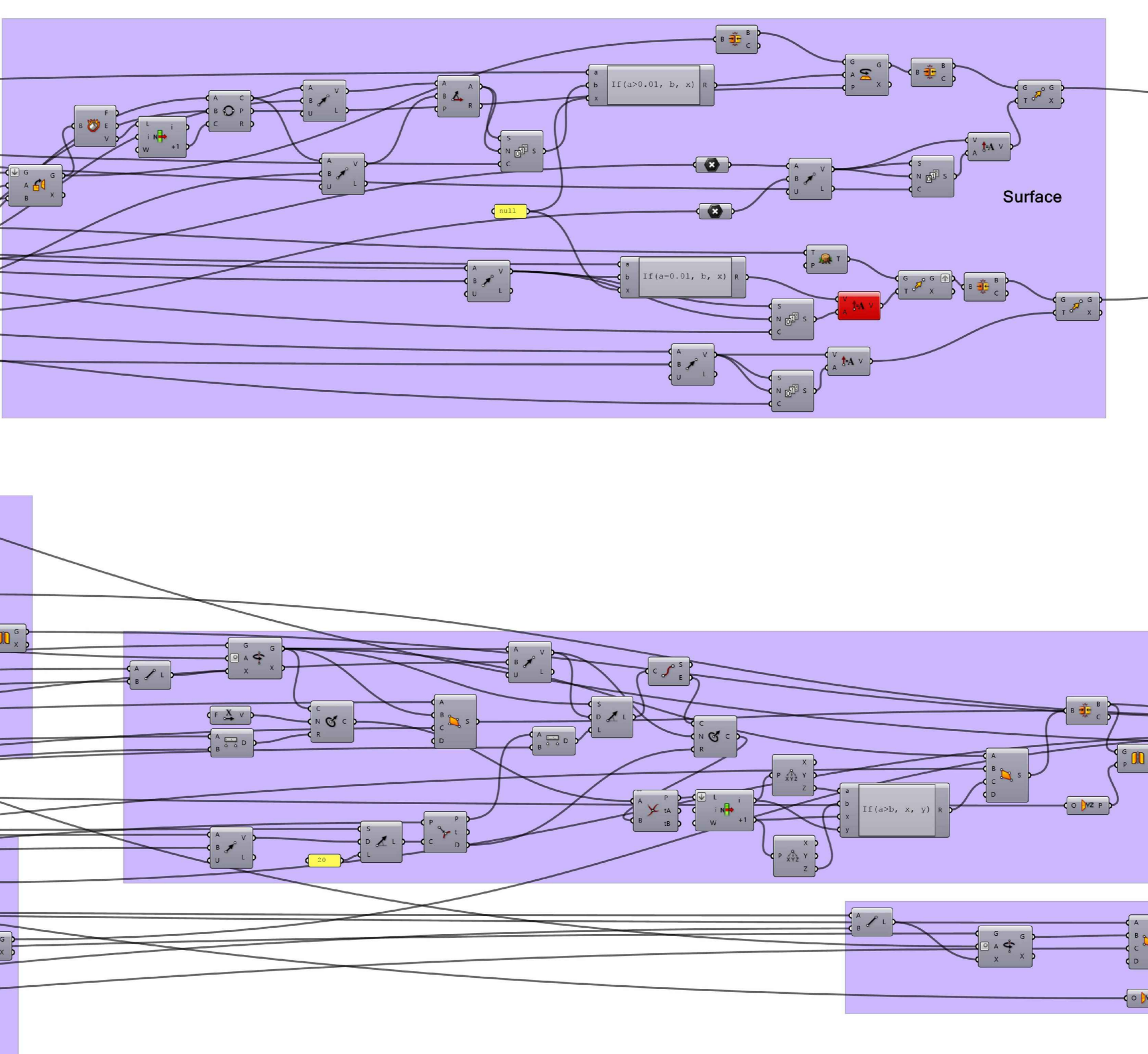
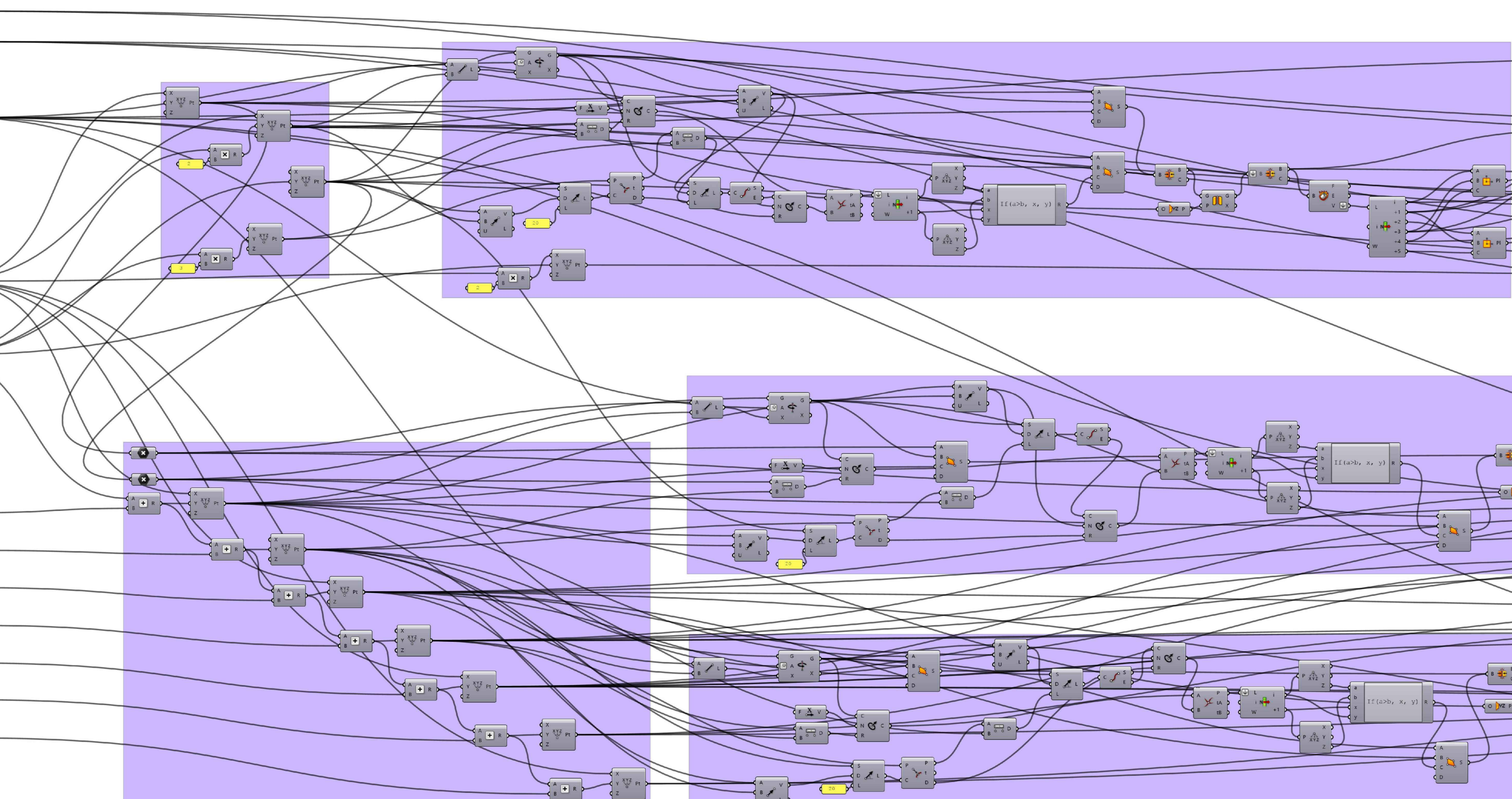
IRREGULAR YOSHIMURA folding surface



Control

Filipa C. Osório
Origami Surfaces for Kinetic Architecture

Lines: 0.4
Columns: 0.4
Folding: 0.00
W1: 0.60
W2: 0.80
L1: 1.00
L2: 0.80
L3: 0.60
L4: 0.40
L5: 0.20
L6: 1.00
L7: 0.80



Surfaces

Regular Yoshimura
Irregular Yoshimura

Annex II

Algorithm for rigidly folding of Degree-6 Crease Patterns
Extended algorithm for Regular and Irregular Yoshimura
Available at cutt.ly/FilipaOsorio_KOS

Annex II
Algorithm for rigidly folding of Degree-6 Crease Patterns
Extended algorithm for Regular and Irregular Yoshimura

Control

Decision between Skewed Yoshimura and Double Helicoidal

Double Helicoidal?

Point A x coordinate

Point B y coordinate

Layer

Folding

Skewed Yoshimura or Double Helicoidal

Points for Double Helicoidal or Skewed Yoshimura

Point A

Point B

Point C

Base Faces for Double Helicoidal or Skewed Yoshimura

Vector AC

Crease ac

Crease bc

Crease ab

Crease AB

Vector BA

Point D Before rotation

Point D' Before rotation

Point B' After Rotation

Point B Before Rotation

Point D After Rotation

Point B After Rotation

Circle 02

Circle 01

Face AB'C

Face ACB

Circle 02'

Point D' After Rotation

CP and Folding for Double Helicoidal or Skewed Yoshimura

Surface

Plane BAB'

Plane DCD'

Base Faces 1st set

Angle between base faces

First B → B'

Iteration

Compound Transformations Rotate + Move

First column when folding angle > 0

Tessellation when folding angle = 0

Surfaces

Double Helicoidal or Skewed Yoshimura folding surface

Double Helicoidal or Skewed Yoshimura unfolded surface

